

FABRICATION OF A SILICON SINGLE ELECTRON TRANSISTOR

by

SHARUKH CHINYOY

Presented to the Faculty of the Graduate School of
The University of Texas at Arlington in Partial Fulfillment
of the Requirements
for the Degree of

MASTER OF SCIENCE IN ELECTRICAL ENGINEERING

THE UNIVERSITY OF TEXAS AT ARLINGTON

August 2007

Copyright © by Sharukh Chinoy 2007

All Rights Reserved

ACKNOWLEDGEMENTS

I would like to express my utmost appreciation to my supervising professor Dr. Wiley P. Kirk who considered me as a worthy candidate to work on this research subject. His continuous support and guidance has enthused me throughout the tenure of my research. The freedom I experienced under his supervision was unparalleled.

I would also like to extend my gratitude to Dr. Donald Butler and Dr. Weidong Zhou who were kind enough to be an affiliate of my defense committee.

I also benefited from the cleanroom expertise of Dr. Kevin Clark and Eduardo Maldonado. They took an active interest in the progress made and also provided a reflective membrane to bounce off my thoughts.

This thesis would not have been possible without my family; their constant encouragement, love and blessings, have been instrumental in providing a mental buttress. I would like to dedicate this thesis to my father Mr. Roomy Chinoy, it is because of his noble sacrifices, I am where I am today.

July 12, 2007

ABSTRACT

FABRICATION OF A SILICON SINGLE ELECTRON TRANSISTOR

Sharukh Roomy Chinoy, M.S.

The University of Texas at Arlington, 2007

Supervising Professor: Dr. Wiley P. Kirk

Single electronics has bright prospects because of its high scalability. The single electron transistor (SET) which utilizes these principles could replace the current workhorse of the industry, the MOSFET.

The SET is plagued with limitations such as, a low operating temperature, background charge issues, a low voltage gain and high output impedance. The current generation SET devices have overcome most of the aforementioned issues but use highly complicated fabrication techniques.

Electron beam lithography was used to pattern device structures on silicon-on-insulator (SOI) wafers with a hydrogen silsesquioxane (HSQ) system being the resist. The silicon was then etched using HSQ as the mask in a deep reactive ion etcher with SF₆ and O₂ gasses.

Experimentation was also carried out on other electron beam resists namely UVN30 and PMMA; these were incompatible with my fabrication technique due to their resolution capability and etch resistance respectively.

TABLE OF CONTENTS

ACKNOWLEDGEMENTS.....	iii
ABSTRACT	iv
LIST OF ILLUSTRATIONS.....	ix
LIST OF TABLES.....	xvi
Chapter	
1. INTRODUCTION.....	1
1.1 Single electronics.....	1
1.1.1 Charging energy.....	2
1.1.2 Tunneling.....	3
1.1.3 Quantization of energy in an atom.....	6
1.2 The single electron box.....	6
2. THE SINGLE ELECTRON TRANSISTOR.....	9
2.1 Working principles of an SET	9
2.1.1 Electron addition energy.....	16
2.2 Limitations of the SET	18
3. FABRICATION OF THE SET	20
3.1 Wafer specifications.....	21
3.2 E-beam lithography and e-beam resists	22

3.2.1 Electron beam lithography.....	22
3.2.2 Scanning electron microscope	23
3.2.3 Nanometer Pattern Generation System.....	25
3.2.4 Electron beam lithography equipment.....	29
3.2.5 Electron beam resists	30
3.3 Reactive Ion Etching.....	37
4. RESULTS AND DISCUSSION.....	39
4.1 The first generation of DesignCAD patterns	39
4.2 The first test.....	43
4.3 UVN30 and PMMA tests.....	46
4.4 HSQ tests.....	82
4.5 The new pattern.....	119
5. CONCLUSION.....	150
5.1 Summary.....	150
5.2 Future work.....	152
 Appendix	
A. UVN30 RECEIPES	155
B. PMMA RECEIPES	185
C. HSQ RECEIPES	218
D. ETCHING RECEIPES	296

REFERENCES	306
BIOGRAPHICAL INFORMATION.....	310

LIST OF ILLUSTRATIONS

Figure	Page
1.1	Conducting island (a) before and (b) after addition of an electron 3
1.2	Two conductors separated by a tunnel barrier 4
1.3	Tunneling of an electron 5
1.4	Diagrammatic representation of a single electron box..... 6
1.5	The effect of the electric field exerted by the gate 6
1.6	The Coulomb staircase 8
2.1	Drain conductance vs. gate voltage graph..... 10
2.2	The differential conductance of an SET as a function of the source-drain plotted voltage and gate voltage. The gray areas indicates the Coulomb blockade region..... 13
2.3	Differential conductance plotted in the color scale as a function of V_{ds} and V_g 15
2.4	Electron addition energy calculated for a small conducting spherical island using a simple model..... 17
3.1	A typical Run file 26
3.2	Connection diagram of the NPGS and the SEM system..... 30
3.3	IR spectra of HSQ (a) before and (b) after e-beam exposure..... 32
3.4	SEM images of an HSQ line (a) after development (b) after a chlorine plasma ECR etch without oxygen treatment (c) after being treated with oxygen plasma and a chlorine plasma ECR etch..... 34
3.5	IR spectrum of HSQ after oxygen plasma treatment..... 35

3.6	Spin speed versus thickness graph for XR-1541. Thickness is in Angstroms.....	36
4.1	The wheel pattern.....	40
4.2	The DesignCAD pattern file.....	41
4.3	A diagrammatic representation of the designed SET structure.....	42
4.4	The 50 micron pad after development using UVN30 as the resist.....	43
4.5	The wheel pattern after development using UVN30 as the resist.....	44
4.6	A line of the wheel pattern after development using UVN30 as the resist.....	45
4.7	The SET pattern after development using UVN30 as a resist.....	46
4.8	The 50 micron pad after development using UVN30 as the resist.....	47
4.9	The SET pattern after development using UVN30 as the resist.....	48
4.10	The SET structure after development exposed at the lowest dose using UVN30 as a resist.....	49
4.11	The SET structure after development imaged at a 60 ⁰ tilt using UVN30 as a resist.....	50
4.12	The SET structure after development exposed at the highest dose using UVN30 as a resist.....	51
4.13	A SET pattern after development exposed at the lowest dose using PMMA as the resist.....	52
4.14	A SET pattern after development exposed at a moderate dose using PMMA as a resist.....	53
4.15	A SET pattern after development exposed at the highest dose using PMMA as a resist.....	54
4.16	The array of SET structures after development using PMMA as a resist.....	55

4.17	The SET array and the 50 micron pad after development using UVN30 as the resist	56
4.18	A SET structure exposed after development exposed at the lowest dose using UVN30 as the resist.....	57
4.19	The central part of a SET structure exposed after development exposed at the lowest dose using UVN30 as the resist.....	58
4.20	The 50 micron pad after development using UVN30 as a resist.....	59
4.21	The SET structures after development using UVN30 as a resist	60
4.22	The whole pattern of the run file after development using UVN30 as a resist.....	61
4.23	The array of SET structures in UVN30.....	62
4.24	The SET structure after development exposed at the lowest dose using UVN30 as a resist.....	63
4.25	The SET structure after development exposed at the highest dose using UVN30 as a resist.....	64
4.26	The array of wheels after development using UVN30 as a resist	65
4.27	The SET array after development using UVN30 as a resist	66
4.28	The SET structure after development exposed at the highest dose using UVN30 as a resist.....	67
4.29	The fingers of a SET structure after development using PMMA as a resist indicate that the dose was enough for defining the fingers but not the islands	68
4.30	The fingers of a SET structure after development using PMMA as a resist exposed with a slightly higher dose than the one above.....	69
4.31	The central part of a SET structure after development exposed at the second lowest dose using PMMA as a resist.....	70
4.32	The central part of a SET structure after development exposed	

	at the highest dose using PMMA as a resist.....	71
4.33	The pad of a SET structure after development using PMMA as a resist.	72
4.34	The central part of a SET structure after development exposed at 40nC/cm using PMMA as a resist.....	73
4.35	The central part of a SET structure after development using PMMA as a resist	74
4.36	The edge of a wheel after development using PMMA as a resist. It indicates the best resolution possible with PMMA.....	75
4.37	The 50 micron silicon pad left after aluminum removal.....	77
4.38	The sidewall of the 50 micron pad after aluminum removal	78
4.39	EDX of the top of the pad after RIE and aluminum etch.....	79
4.40	EDX of sidewall after RIE and aluminum etch.....	80
4.41	The SET array after RIE with UVN30 acting as an etch mask.....	81
4.42	The central part of a SET structure after RIE using UVN30 as an etch mask.....	82
4.43	The SET array after development using HSQ as a resist	83
4.44	The SET structure after development exposed at the lowest dose using HSQ as a resist	84
4.45	The SET structure after development exposed at the highest dose using HSQ as a resist.....	85
4.46	The SET array at a 60° tilt after RIE using HSQ as etch mask.....	86
4.47	The SET array from the first HSQ wafer with the brightness and contrast adjusted	87
4.48	The SET structures at a 60° tilt after RIE using Al and HSQ as etch masks.....	88
4.49	The SET structure after RIE using HSQ as an etch mask.....	89

4.50	The SET array after development using HSQ as a resist	91
4.51	The SET structure after development exposed at the lowest dose using HSQ as a resist	92
4.52	AFM image of the SET structure after thermal curing using HSQ as a resist	94
4.53	The central part of an SET structure after thermal curing using HSQ as a resist.....	95
4.54	Height measurement for a pad after thermal curing.....	96
4.55	The SET structure after development and curing using HSQ as a resist.....	99
4.56	Height measurement for the SET structure shown above.....	100
4.57	An SEM image of the wheel pattern after development and curing employing HSQ as a resist.....	101
4.58	Height measurement of the SET structure after the etch	102
4.59	A 3D view of the SET structure and its surrounding area	103
4.60	Height measurement of the SET structure after a 15 second buffered oxide etch	104
4.61	Height measurement of the SET structure after an additional 15 second buffered oxide etch.....	105
4.62	Side view of the SET array after the additional 15 second buffered oxide etch.....	106
4.63	Schematic of the steps for the bilayer resist approach	107
4.64	The SET array after the SF ₆ etch employing HSQ as an etch mask	108
4.65	The SET structure after the SF ₆ etch employing HSQ as an etch mask.....	109
4.66	Another SET structure after the SF ₆ etch employing HSQ	

	as an etch mask.....	110
4.67	The 50 micron pad imaged at a 45° tilt after the SF ₆ etch.....	111
4.68	The SET structure imaged at a 45° tilt after the SF ₆ etch.....	112
4.69	AFM image of the SET array after the SF ₆ etch	113
4.70	The height profile for the finger and island part of a SET structure in HSQ after the SF ₆ etch	114
4.71	The SET array after the CF ₄ etch	115
4.72	Height measurement of the SET structure after the buffered oxide etch.....	116
4.73	The SET structure after the buffered oxide etch.....	117
4.74	The SET structure after the buffered oxide etch imaged with the InLens detector.....	118
4.75	A diagrammatic representation of the new SET design.....	119
4.76	The design file of the new pattern.....	120
4.77	A zoomed in view of the design file displaying the islands.....	121
4.78	The SET structure after development using HSQ as a resist.....	122
4.79	The SET structure after development using HSQ as a resist	123
4.80	The SET structure after development in which the fingers and islands were exposed to an electron dose of 50 μC/cm ²	125
4.81	The SET structure after development which was given a dose of 200 μC/cm ²	126
4.82	The SET structure after development which was given a dose of 600 μC/cm ²	127
4.83	The central part of an SET structure after development which was exposed with a dose of 600 μC/cm ²	128
4.84	The SET structure after development which was exposed with	

	a dose of 2000 $\mu\text{C}/\text{cm}^2$	129
4.85	The central part of the SET structure after development which was exposed with a dose of 2000 $\mu\text{C}/\text{cm}^2$	130
4.86	The pads of a SET structure after development which were exposed with a dose of 300 $\mu\text{C}/\text{cm}^2$	131
4.87	The central part of the SET structure after development exposed with a dose of 500 $\mu\text{C}/\text{cm}^2$	133
4.88	The central part of a SET structure after development	134
4.89	The width of a finger of an SET structure after development.....	135
4.90	Width and length of the first tapered part of the finger after development.....	136
4.91	Width of the second tapered part of the finger after development.....	137
4.92	The SET structure after development with the dose for the islands altered to form constrictions.....	139
4.93	Profile for the top pad of the SET structure #1 after development	140
4.94	Profile of the bottom pad of the SET structure #5 after development	141
4.95	Profile for the top pad of the SET structure #1 after baking	142
4.96	Profile for the bottom pad of the SET structure #5 after baking.....	143
4.97	Profile for the top pad of the SET structure #1 after the first etch	144
4.98	Profile for the bottom pad of the SET structure #5 after the first etch.....	145
4.99	Profile for the top pad of the SET structure #5 after the second etch	146
4.100	Profile for the bottom pad of the SET structure #5 after the second etch.....	147
4.101	Profile of the carrier wafer after a 125 second etch.....	149

LIST OF TABLES

Table	Page
5.1 Pros and Cons of different resists used	151

CHAPTER 1

INTRODUCTION

1.1 Single electronics

The field effect devices that dominate the industry today might need to be replaced in the near future. The FET devices used in the commercial CMOS circuits are approaching gate lengths where further increases in their switching speeds might not be possible. Controlling charges within the channel and development of new materials to capacitively couple the gate structures are other issues hindering the progress. The observation of Moore's law [1] which in its simplest form states that the number of transistors per square centimeter will double every twelve to eighteen months for silicon based circuitry. To keep the law valid by 2010 a transistors dimension will be on the scale of 10 nanometers.

Commercial CMOS devices still fall under the regime of classical physics. The operating principles of these devices still remain intact despite the extensive miniaturization. Quantum physics' main principle is treating matter with a dual nature approach. Depending on experimental conditions particles are observed to behave in a discrete fashion or exhibit wave like properties. When the device dimensions, signal energy and signal charge approach the size of an atom, the energy of one photon and the charge of one electron respectively we should treat the device with a quantum mechanical approach and quantum phenomena will dominate the operation of the device. Application and manipulation of these principles to fabricate electronic devices

would certainly be beneficial. A majority of the devices utilizing quantum effects hold promise and occupy less chip area resulting in greater packing density than modern day MOSFET's. To keep Moore's Law applicable for another fifteen years, employment of these devices will be necessary, in my opinion.

Single electrons were first manipulated in very original experiments conducted as early as the beginning of the twentieth century but the implementation of those principles to fabricate a solid state circuit was not until the 1980's. This can be attributed to lack of the required nanofabrication techniques.

1.1.1 Charging energy

The charging energy arises from the way simple concept we have learnt before in the case of capacitors. I will now explain why it pertains to the topic of single electronics. Consider a very small spherical conductor to be neutral in an electronic sense i.e. it has an equal number of protons and electrons in the crystal lattice. Ideally the conductor will not exert any electrical field outside its volume. If an external force F were to bring in another electron in the vicinity of the conductor and this force was enough to add the electron to the balanced system that existed within the conductor the charge of the conductor will certainly change. Initially the charge of the conductor Q was zero but now its $-e$ which is the charge of an electron and $e = 1.6 \times 10^{-19}$ Coulomb. This will result in the conductor exerting a field that will repel further addition of electrons to the conductor.

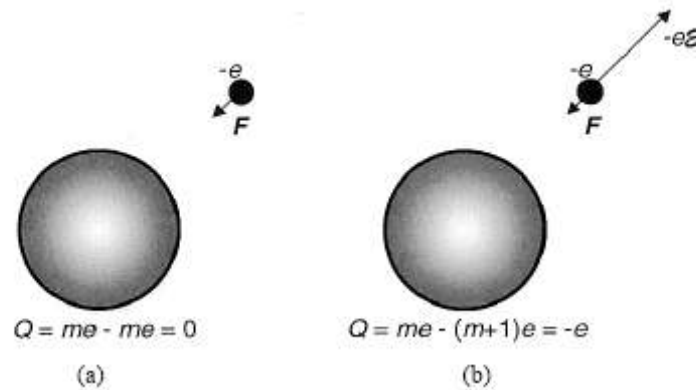


Fig 1.1 Conducting island (a) before and (b) after the addition of a single electron [2]

The charging energy associated with this addition is given by

$$E_c = e^2/C$$

where C is total capacitance of the island. When considering a two electrode system the above expression is obtained by integrating the area over a straight line, making the charging energy equivalent to $e^2/2C$. This charging energy is an accurate measure of this effect rather than the electric field. This proves that it is possible to manipulate a single electron.

1.1.2. Tunneling

Quantum mechanics plays an essential role in understanding of the tunneling phenomenon. The continuous nonzero solution of Schrödinger's wave equation entails a particle to penetrate classically forbidden regions. Consider a barrier separating two conductors, the principles of classical physics forbid the transmission of a particle from one electrode to the other through the barrier. Quantum physics on the other hand

predicts a possibility of the particle tunneling through the barrier if the barrier is finite in height and real space.

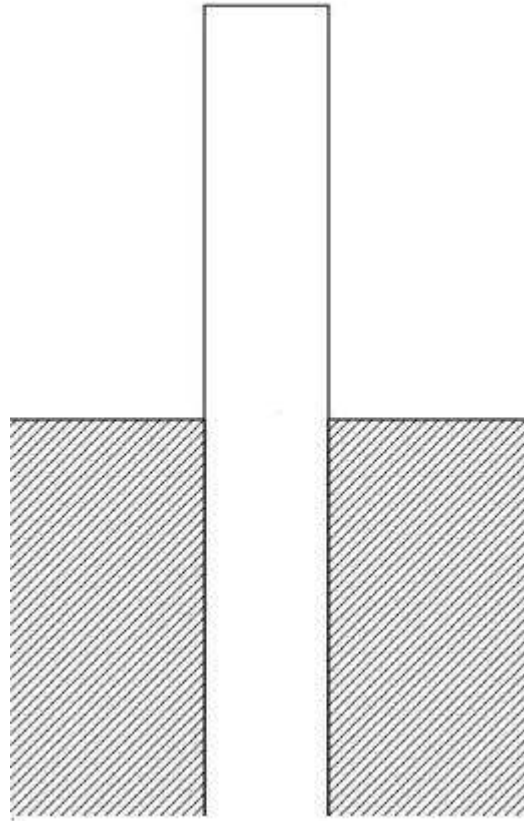


Fig 1.2 Two conductors separated by a tunnel barrier

The figure above represents a tunnel barrier with a conductor on either side (hatched line regions). Consider there be an electron on the left conductor, classically it would be impermissible for that electron to reach the right conductor but the solution to Schrödinger's equation provides a probability for tunneling. If a voltage were to be applied across the conductors a current could flow. The mechanism responsible for this is as follows; the Fermi level of the left conductor would be raised above that of the

right conductor and the electron on the left conductor tunneling through would result in easing out the energy balance thus making the tunneling event preferable. After reaching the right conductor the electron will follow to dissipate its energy bringing it closer to the Fermi level of the right electrode.

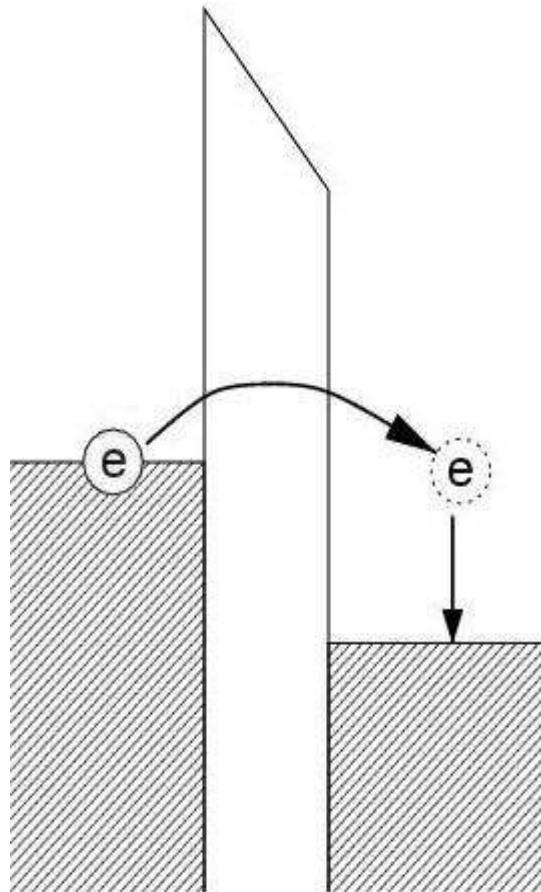


Fig 1.3 Tunneling of an electron

Esaki [3] was the first one to provide experimental evidence of tunneling. The tunnel diode set the ball rolling for research in the field of tunneling and other similar mesoscopic phenomena.

1.1.3. Quantization of energy in an atom

Bohrs atomic model was the first one to take into consideration that the electrostatic forces were responsible for the attractive and repulsive forces that aided the electrons to maintain strict orbits around the nucleus. The Bohrs model provided a simplistic picture of the hydrogen atom. The main postulates on which the model rested were that electrons traveled around the nucleus and their momentum was quantized in only certain allowed orbits and electrons did not lose their energy so the orbits were maintained. The Bohr model is adequate to explain one-electron systems. Revisions have been made to the model since. Inclusions of postulates like that which describes the relation of allowed orbits and the quantized values of the angular momentum provide a more accurate picture of the system. The Bohr model was then used to calculate the lowest energy level in a hydrogen atom and the equation which gives us energy in an orbit using the principal quantum number. The principal quantum number can take integer values only, hence the energy is quantized.

1.2 The single electron box

Understanding the principle of operation of the single electron box is essential before attempting to conquer the intricacies of the single electron transistor. It is a simple device consisting of very small conductor (the island) connected to a larger electrode which has an abundance of electrons (the source electrode) through a tunnel barrier. Another electrode (the gate) is capacitively coupled to the island. The insulation barrier between the gate and the island is much thicker and tunneling is not permitted.

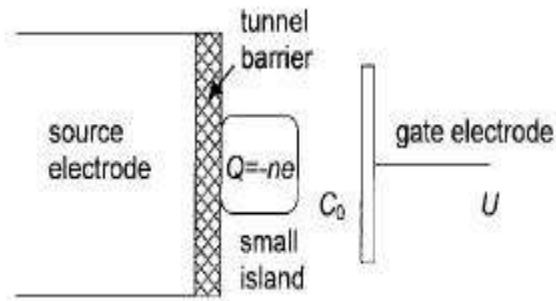


Fig 1.4 Diagrammatic representation of a single electron box [2]

The island being very small has a fixed number of electrons to begin with. The gate electrode is used to exert a field which will affect the charge distribution within the island.

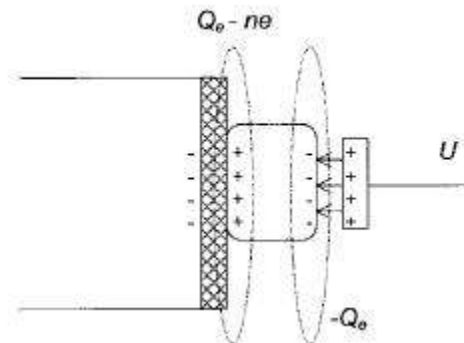


Fig 1.5 The effect of the electric field exerted by the gate [2]

Now if this field is strong enough it would cause electrons which are plentiful on the source to tunnel through onto the island and this would change the electrostatics of the island completely. This extra electron would create a force which could repulse another electron to tunnel through until the external field the one exerted by the gate can overcome it. A graph of the charge of the island against the external charge is step like. The discreteness of the transfer of electrons through the barrier gives the staircase like appearance. The charging energy as explained before is responsible for this. The

external field must be raised over the charging energy to add a single electron each time. Since this is a one electrode system the voltage of the gate needs to be incremented by e/C_g where C_g is the island-gate capacitance. The phenomenon that prevents continuous addition of electrons to the island is called the Coulomb blockade and the step like observations are termed as the Coulomb staircase.

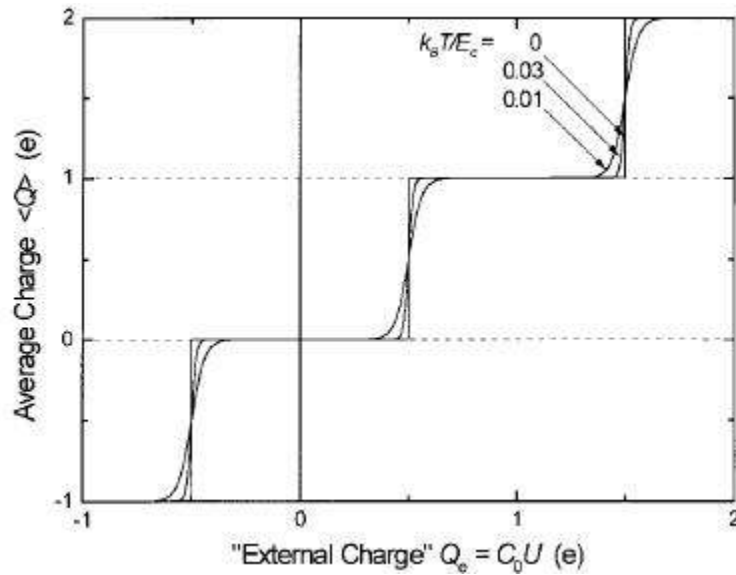


Fig 1.6 The coulomb staircase [2]

The limitations of this device are that at high temperatures the staircase is suppressed. The device also cannot be used for information storage since the number of electrons on the island are a function of the gate voltage hence it has no internal memory as such.

CHAPTER 2

THE SINGLE ELECTRON TRANSISTOR

The easiest way to define a single electron transistor would be to call it a transistor that turns on and off again for every event when a single electron is added to it. It is a transistor where the electrons are confined to an island having a very small volume and the island is connected to two electrodes through thin tunnel barriers and capacitively coupled to a gate electrode. There is no tunneling through the material insulating the gate and the island since it is much thicker. There have been various novel methods to fabricate different structures and patterns that exhibit SET like behavior.

2.1 Working principles of an SET

There are various models out there that use a ton of equations which could be used to explain how the SET functions, but I prefer a simple and uncomplicated approach involving only a few basic equations.

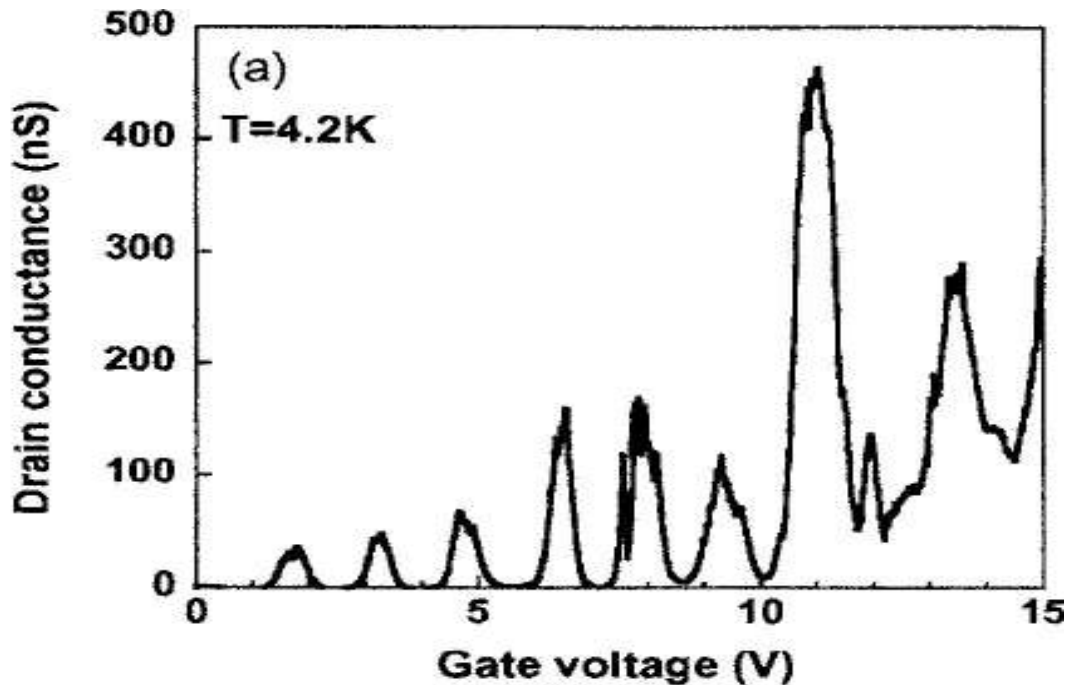


Fig 2.1 Drain conductance vs. gate voltage graph [4]

The figure above is a plot for the conductance of a device against the gate voltage applied. The experimental setup for this would be as follows; connect the drain source with a small DC voltage source V_{ds} keeping the voltage low enough so that the current is proportional to it. It is observed that the conductance of the device changes by large magnitudes periodically. This is quite similar to our observation in the simple single electron box but here we are comparing the so called channel (source - tunneling barrier - island - tunneling barrier - drain) conduction instead of the charge on the island. Clearly there is conduction oscillation observed here and this is termed the periodic Coulomb oscillation phenomenon. A calculation of the capacitance between the island and the gate proves that on every occasion the amount of voltage between two peaks is exactly that needed to add an electron onto the island. Now it is much

easier to understand why this device can be called a single electron transistor since the transistor can be turned from an off to an on state by the addition of the single electron to the island. It could also be termed a single electron tunneling transistor since the island is confined on either side by tunnel barriers.

Consider an island with n electrons to begin with. For a current to flow when there is a reasonable V_{ds} and V_g supplied would mean that number of electrons on the island must vary from n and $n+1$. Let $E(n)$ and $E(n+1)$ be the total electrostatic energies of the island when the island contains n and $n+1$ electrons respectively. If the gate were the only electrode influencing the entire energy change on the island then by multiplying V_g with e at the point where the n^{th} peak appeared on the above figure would equate the difference in the energies of the $(n+1)^{\text{th}}$ state and the n^{th} state. This is not the case though as the capacitance of the whole device plays a role. The simplest equation that could be derived from the discussion above is

$$\alpha e V_g = E(n+1) - E(n) + \text{constant}$$

where $\alpha = C_g/C_T$ is the ratio of the gate capacitance to the total capacitance of the island. The total capacitance includes the gate capacitance, the capacitance of the tunnel barriers any stray capacitance of the island too. I shall now move to a more complicated approach to explain how to predict the n^{th} peak on the graph.

Consider the Coulomb blockade model, the island could be considered to be a metal particle with a number of electrons trapped on it. The particle is considered to be electro neutral in the beginning. For a charge of Q to be added to the particle the energy of $Q^2/2C_T$ would have to be supplied. Now substituting Q by $-ne$ in equation

above will result with a condition where the peak positions being equally spaced at intervals of e/C_g in the gate voltage. Hence $\Delta V_g = e/C_g$. Charge quantization is responsible for this

The concept of charge quantization can be easily understood. The charge in a large conductor is not quantized since the wavefunctions of the electrons extend over long distances but if you were to localize electrons to a small volume restrict their transmission out of the volume, their charge will be quantized. If you consider the energy to add a charge of Q would be $E(Q) = Q^2/2C_T$ means that the energy is a parabolic function of Q . The parabola would have minima at Q_0 (the charge that minimizes the energy). If the charge was not quantized we could vary V_g to select any value of Q_0 . This is not true as only discrete values of E are possible. For the state $Q_0 = -ne$ i.e. when n , an integer number of electrons minimizes E an energy gap results due to Coulomb interaction. An energy of $U = e^2/2C_T$ is needed to add or remove one electron. An energy gap comes into the picture which suppresses random charge fluctuations. Consider a case when $Q_0 = -(n+1/2)e$ with the state $Q = -ne$ and the state $Q = -(n+1)e$ exist, the two states are now degenerate and the charge can fluctuate between the two values. So its seen that even at $T = 0$ for all values of Q_0 except when $Q_0 = -(n+1/2)e$ there exists an energy gap. At the condition the energy gap disappears, conduction peaks appear. Now we can predict that the peaks in conductance occur when the average charge on the artificial atom is $-(n+1/2)e$ and the peaks are periodic.

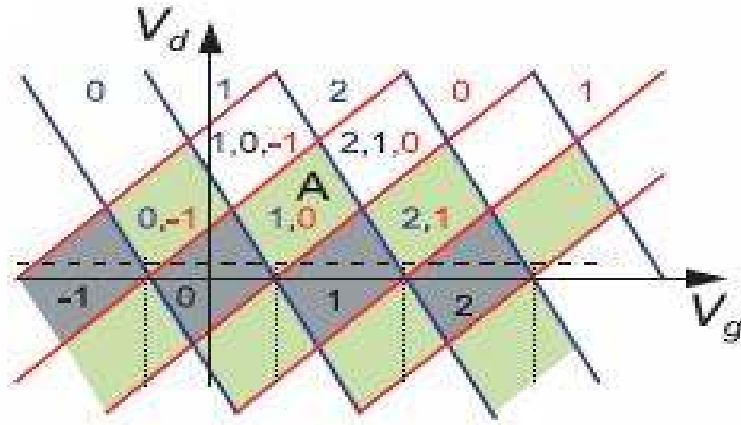


Fig 2.2 The differential conductance of an SET as a function of the source-drain voltage and gate voltage. The gray areas indicates the Coulomb blockade region. [5]

Localization of the electrons which leads to quantization of their charge in this case are related to the island size firstly which I shall explain later and the transmission coefficient of the tunnel barriers. When an electron needs to tunnel across the barriers the RC time constant must be large enough for the energy uncertainty to be less than the charging energy. From this we can deduce that $RC > h/U$ so $R > h/e^2$ approximately. This term is known as the quantum unit of resistance and its value is 25813Ω . This is very important in the field of single electronics since it proves that a tunneling barrier with low transparency could suppress the uncertainty of an electron's location.

Temperature is a major factor that could disrupt this confinement since it could easily supply the necessary energy which until now was being supplied by the charging energy so another condition exists i.e.

$$E_c > k_B T$$

where k_B is the Boltzmann's constant and T is the absolute temperature.

Energy localization is an important factor to be considered when the electrons are restricted to small volumes. If the island is small enough then there will be a few thousand or maybe hundred electrons on it. This might cause the formation of energy levels within the island. The levels might not be sharp and have a typical width Γ . This could be attributed to lifetime broadening since an electron in a level on the island could tunnel to the leads. The eigenstates of the entire system are a combination of the localized states on the island and extended states in the lead. A typical level spacing of $\Delta\varepsilon$ is needed to excite the island with an electron. The condition for energy quantization to exist is $\Delta\varepsilon > \Gamma$.

According to Thouless [6] the current through the device for one quantum level is the charge of the electron against the time t for an electron in a single quantum state to travel across the island staying within that level. Considering the density of states of the island to be $(dn/d\varepsilon)$ the number of current carrying channels between the Fermi energy in the source and drain is $(dn/d\varepsilon)eV_{ds}$. Then the current is given by

$$I = (e/t) (dn/d\varepsilon) eV_{ds}$$

Now $(dn/d\varepsilon) = 1/\Delta\varepsilon$ and $t = h/\Gamma$ so the condition for energy quantization is reduced to $V_{ds}/I > h/e^2$ but $V_{ds}/I = R$ so $R > h/e^2$. We observe that the conditions for energy and charge quantization are the same. I will explain later which phenomenon is more prevalent and what factors does it depend on.

If the SET is adjusted with a V_g so that $Q_0 = -ne$ and when V_{ds} is increased the Fermi level of the source will be at a higher level gets raised proportionally with V_{ds} as compared to the levels on the island and the drain. This condition would encourage an

electron from the source to tunnel to the island and maybe then from the island to the source basically a current will flow. If V_{ds} is increased further more channels are created for the current path since the Fermi level of the source is even higher relative to the island and drain so more electrons are encouraged to tunnel onto the island.. Measuring the tunneling current for a varying V_{ds} and a fixed V_g gives us an idea of the energy level spectrum. The energies can be obtained by measuring the voltage at which the current increases.

Quantum dots are nowadays referred to as artificial atoms since their electronic properties tend to resemble those of an atom. In one such experiment [7] where an impurity-free quantum dot was fabricated, the excitation spectra were clearly observed.

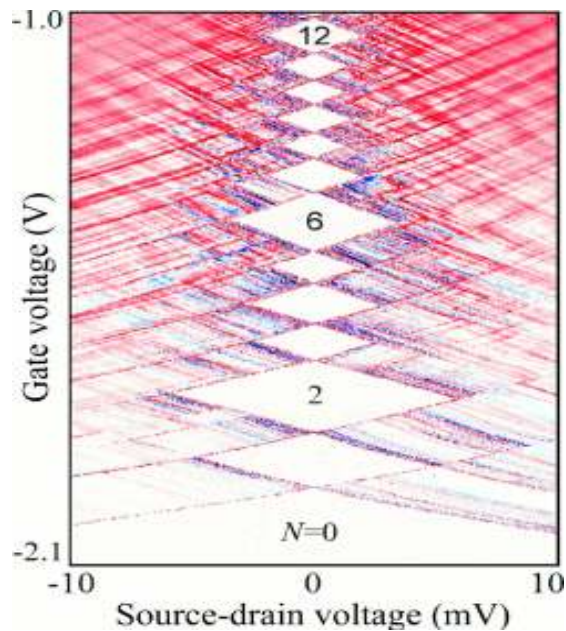


Fig 2.3 Differential conductance plotted in the color scale as a function of V_{ds} and V_g [7]

The white regions inside the diamonds are those when the differential conductance $\partial I/\partial V_{ds}$ is approximately zero due to the Coulomb blockade. The peak spacings along

$V_{ds} = 0$ are not equal here as the energy $\Delta\epsilon$ dominates and the shell structure of the quantum dot is observed. On the $V_{ds} = 0$ axis when adjacent diamonds touch, n changes to $n+1$. The diamond areas for $n = 2, 6$ and 12 are large since they correspond to filled shells. The dot in this case was semiconducting; if it were a metallic particle the size of the diamonds would have been the same. The lines running parallel to the diamond sides are identified to be the excited states. From this we could conclude that to overcome the electron addition energy we can vary V_{ds} or V_g , or a combination of both. Hence U , $\Delta\epsilon$ and Γ are three different energies that are important to understand the working of the SET.

2.1.1. Electron addition energy

The charging energy and the electron quantization energy need to be considered when the size of the island approaches a very small dimension; comparable to the de Broglie wavelength of electrons confined to the island. The combination of the two energies; termed the electron addition energy (E_a), helps us provide a more accurate picture.

$$E_a = E_c + E_k$$

where E_k is the quantum kinetic energy of the electron added. The figure below clearly indicates which energy dominates for different island diameters.

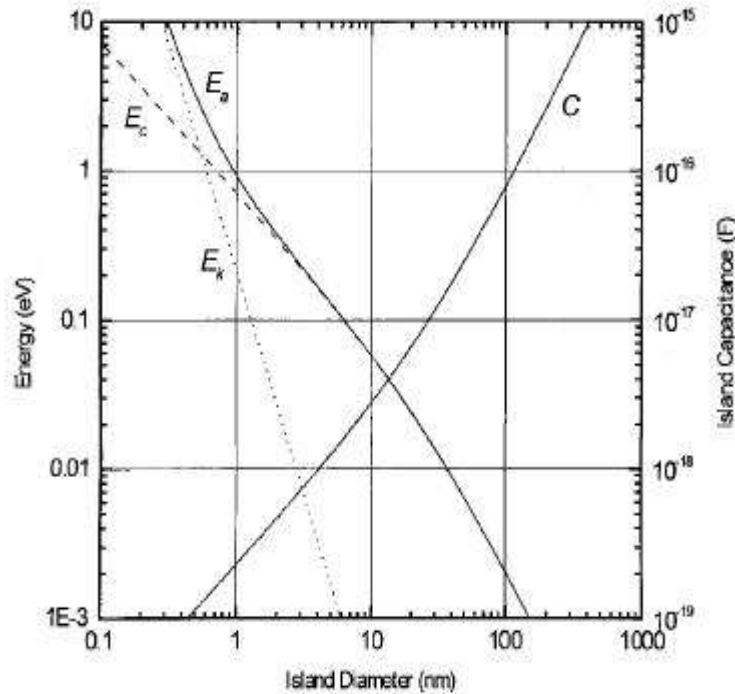


Fig 2.4 Electron addition energy calculated for a small conducting spherical island using a simple model [2]

The simple model mentioned above uses a spherical conducting island with a free degenerate electron gas with electron density $n = 10^{22} \text{ cm}^{-3}$ which is then embedded into a dielectric matrix with a dielectric constant of $\epsilon = 4$ and 10% of the spheres surface area occupied by tunnel barriers with 2 nm barrier thickness. From this model results obtained were as follows; for larger islands E_a is dominated by E_c for a 100 nm island the E_a is in the range of 1 meV and substituting that value for the condition $E_a > k_B T$ we get an operating temperature of about 10 K. If we needed room temperature operation for the device where $T = 300 \text{ K}$ then E_a needed would be approximately 0.025eV which translates to an island size of approximately 10 nm. However considering today's high

standards devices need for digital circuits we must design in a safety factor of about 100 included to prevent any thermal fluctuation problems, hence

$$E_a > 100 k_B T$$

translating the island size to dimensions beyond 1 nm. At this size E_a would be dominated by E_k and the islands become quantum dots or artificial atoms.

While the conditions for charge and energy quantization for $T = 0$ are the same we see that charge quantization survives at higher temperatures. Another argument for this is that the condition needed to observe charge quantization is $U > k_B T$ and for energy quantization we need $\Delta\epsilon > k_B T$. Most SET structures in the early 1990's had larger sized islands and hence $U > \Delta\epsilon$ so energy quantization was impossible to observe.

2.2. Limitations of the SET

The fabrication techniques needed to fabricate the miniscule island sizes for the SET to operate at room temperature or even higher temperatures are very complicated and expensive. The output will be slow and the island sizes might vary. Small variations the size of very small islands (when $E_k > E_c$) will lead to large changes in the energy level spectrum and we might observe unpredictable behavior.

The effect of background charges on the operation of the SET is another shortfall of the transistor. If there were to be a charged impurity trapped in the vicinity of the island it will polarize the island and hence an image charge is created on the surface of the island. This will affect the influence of the external charge which decides the Coulomb blockade threshold.

The intrinsic high output impedance of an SET combined with its capability to carry a small source-drain voltage means that even though the power consumption of the transistor is low the voltage gain of the device is less than desirable.

CHAPTER 3

FABRICATION OF THE SET

Charge quantization was first observed in tunnel junctions containing Sn particles by Zeller and Giaver [8]. Likharev [9] was responsible for discovering that under the influence of an external electrode the Coulomb blockade could be overcome. Fulton and Dolan [10] were the first to report the working of a practical SET and observed blockade oscillations in their device. Their SET device was entirely metallic. Since then, numerous approaches have been employed to fabricate the SET device. Even in narrow silicon FETs where interface charges provide the tunnel barriers SET like behavior has been reported [11]. As the island sizes have reduced energy quantization has been observed even in the limit where the level width could be predicted.

The semiconductor industry currently has such heavy investments in the technology used for manufacturing CMOS circuits that it would be reluctant to invest in a device that needed different machinery for its fabrication. In my opinion using a silicon based approach and incorporating as many conventional CMOS processes as I could was the only alternative. This could have translated to a serious compromise in the island size too. Restricted by considerations made for the industry processes and the availability of facilities in our NanoFab Labs, I devised a plan of action. The most important consideration without a shadow of doubt had to be the device must be fabricated using a silicon wafer. Silicon as we all know is a norm in the semiconductor

world and the evidence of that is very noticeable if you have ever toyed around with a chip board of any electronic gadget.

3.1 Wafer specifications

During the first stages of fabrication I started off with a basic 2 inch silicon wafer with *p*-type doping. The thickness of the wafer was 250-330 microns. The silicon wafer was generally used in the testing phase as the cost of SOI wafers is too high.

After concluding testing with the basic silicon wafer I moved to a silicon-on-insulator (SOI) wafer which basically constitutes of a very thin single crystal silicon layer grown on a thicker insulating silicon dioxide layer which is on top of a very thick poly-crystalline silicon layer. The oxide layer is known as a buried oxide or BOX layer. This BOX layer provides isolation from the substrate. Most SOI wafers are fabricated using the SIMOX (Separation by Implanted Oxygen) process.

The piece of wafer that my supervisor passed onto me was 4 inches in diameter. I would make 1cm x 1 cm pieces using a sharp scribing tool. The reason for this being that the stubs in the SEM and e-beam writer could only hold such small samples. The thickness of the single crystal silicon was 55 nm, the SiO₂ layer was 140 nm followed by a 2 micron thick poly-silicon layer. The entire wafer was undoped and the silicon could be considered intrinsic. There are various advantages of using an SOI wafer. Firstly this technology is already in use for CMOS devices. The thin layer of single crystal silicon is highly pure. After etching by growing a thin layer of oxide on top of the silicon a percentage of the silicon is consumed hence there is shrinkage of the needed silicon island which is beneficial. This would also isolate the island in all

directions by insulating layers of SiO₂. The very thick layer of silicon which is on the backside of the wafer could also be used to pattern on and then used as a back gate. The gate would be capacitively coupled since there is a thick SiO₂ layer separating the two silicon layers providing sufficient isolation.

3.2 E-beam lithography and e-beam resists

Optical lithography for defining the small islands needed was out of the question even though according to a recent report from IBM they have fabricated 29.9 nm lines. The wavelength of light used for this was 193 nm. The use of immersion technology is also an avenue researchers are looking into to extend the limits of optical lithography. The reason the industry is sticking with optical lithography is because exposure is a parallel process hence it takes a very short time. Alternative technologies like e-beam lithography, X-ray lithography and Imprint technology are simply not adopted since they are more expensive and much slower. In the Nanofab labs we do not have the facilities for immersion photolithography but there is an electron beam lithography machine with which the desired island could be patterned and hence my choice was to adopt this technology.

3.2.1. Electron beam lithography

The diffraction limit of light is the limiting factor in the case of optical lithography and as the name suggests since an electron beam is used to pattern in electron beam lithography the diffraction limit, is not an issue. The drawback lies in the speed as the beam scan is a serial process and large patterns can take hours. The electronics industry considers e-beam lithography complimentary to photolithography

since it is used to pattern masks later used for photolithography. The idea for using an electron beam is basically derived from the scanning electron microscope (SEM). Some materials seemed to respond to the electron beam during observation in the SEM. After a few necessary alterations of their properties that evolved into the modern e-beam resists that we know of. If the beam could be controlled exposing only desired areas either by turning the beam on and off or by employing a controlled blanker we could perform lithography.

3.2.2. Secondary electron microscope

The SEM is one the most popular high magnification imagining techniques and used widely as a research tool. The beam of electrons is either generated by thermionic emission from a tungsten cathode or recently by field emission techniques. Condenser coils are responsible for focusing the beam into a very fine size mostly in the range of a few nanometers. Vertical and horizontal scanning coils are then used to manipulate the beam to scan the desired areas in a specific raster pattern. The beam goes through a final lens just before it hits the sample.

When the penetrating beam hits the sample surface the electrons lose their energy through scattering and absorption. The depth of penetration of the electrons for the sample depends on the accelerating voltage of the beam and other properties of the sample. The region of penetration usually has a tear drop like shape. The size and shape of this region determines the maximum resolution.

The interaction between the beam and the sample are divided into two categories i.e. elastic collisions and inelastic collisions. When an electron from a beam

collides with an atom of the sample it loses its energy to the atom effectively ionizing the atom, a secondary electron is emitted to maintain the balance. Secondary electrons have low energies and any electron with energy less than 50 eV is assumed to be a secondary electron. This assumption is not perfect but moderately accurate. For most samples, secondary electrons are emitted from areas very close to the sample surface thus providing a good idea of the topology of the sample. The secondary electron detector detects secondary electrons emitted amplifies the signal and converts it to an image.

There are also backscattered electrons which arise when high-energy electrons from the beam are incident on the sample and undergo elastic and inelastic collisions well beyond the interaction volume on the specimen and they emerge back out from the surface. An electron that escapes with energy greater than 50 eV is termed as a backscattered electron. The number of backscattered electrons increases with an increase in the atomic number of the sample. From information gathered from backscattered electron detectors we can obtain knowledge of the chemical composition of the sample.

Most SEMs are also capable of performing Energy-dispersive X-ray spectroscopy (EDX or EDX). When the incident electron beam manages to knock off an electron from the inner shell of an atom of the specimen being scanned, another electron from a higher energy shell will want to fill the gap. The difference in energies of the shells will result in the emission of an X-ray which can be detected. The

spectrum of energy detected is unique to every element and this becomes a good chemical characterization tool.

The SEM available at our facilities is the ZEISS Supra 55 VP system. It is a field emission microscope and is capable of a variable pressure mode which makes it easier to examine non-conducting samples. Its magnification limits extend from 12 x to 900 kx. The minimum resolution depends on the accelerating voltage but it is capable of a 1 nm resolution at 15 kV. The accelerating voltage ranges from 0.1 to 30 kV. The detectors I used for most purposes were the SE2 and InLens. The scope is also equipped with a EDAX Genesis 4000 system.

3.2.3. Nanometer Pattern Generation System

Joe Nabity started his company called JC Nabity Litography Systems in 1988. He was the person responsible for the development of Nanometer Pattern Generation System (NPGS). NPGS is a SEM based lithography system the best selling point for it is its low cost and performance as compared to most other systems. The system basically modifies a SEM to perform lithography, the compromise being the speed of operation when compared to a dedicated beam writer. The pattern generation process can be broken down into three functional steps.

Pattern design is done using a DesignCAD which is a modified CAD program. The basic DesignCAD program has been modified and enhanced for ease of use to design regular patterns. Patterns can be either imported from other CAD formats or designed from the start using DesignCAD. Parameters such as exposure dose, exposure point spacing, beam current and microscope magnification can be varied for different

elements of a single pattern by using multiple layers and colors schemes. I used different layers whenever a variation in aperture sizes was required. Aperture size can not be varied for different elements of a layer. The smart choice hence is to separate larger elements and smaller elements by designating them to a different layers. I varied colors when I wanted to expose the different elements of a single layer to varied doses.

The **Run File Creation** stage is where the user can alter the exposure conditions for the designed pattern. The run file has a lot of features too numerous to even list.

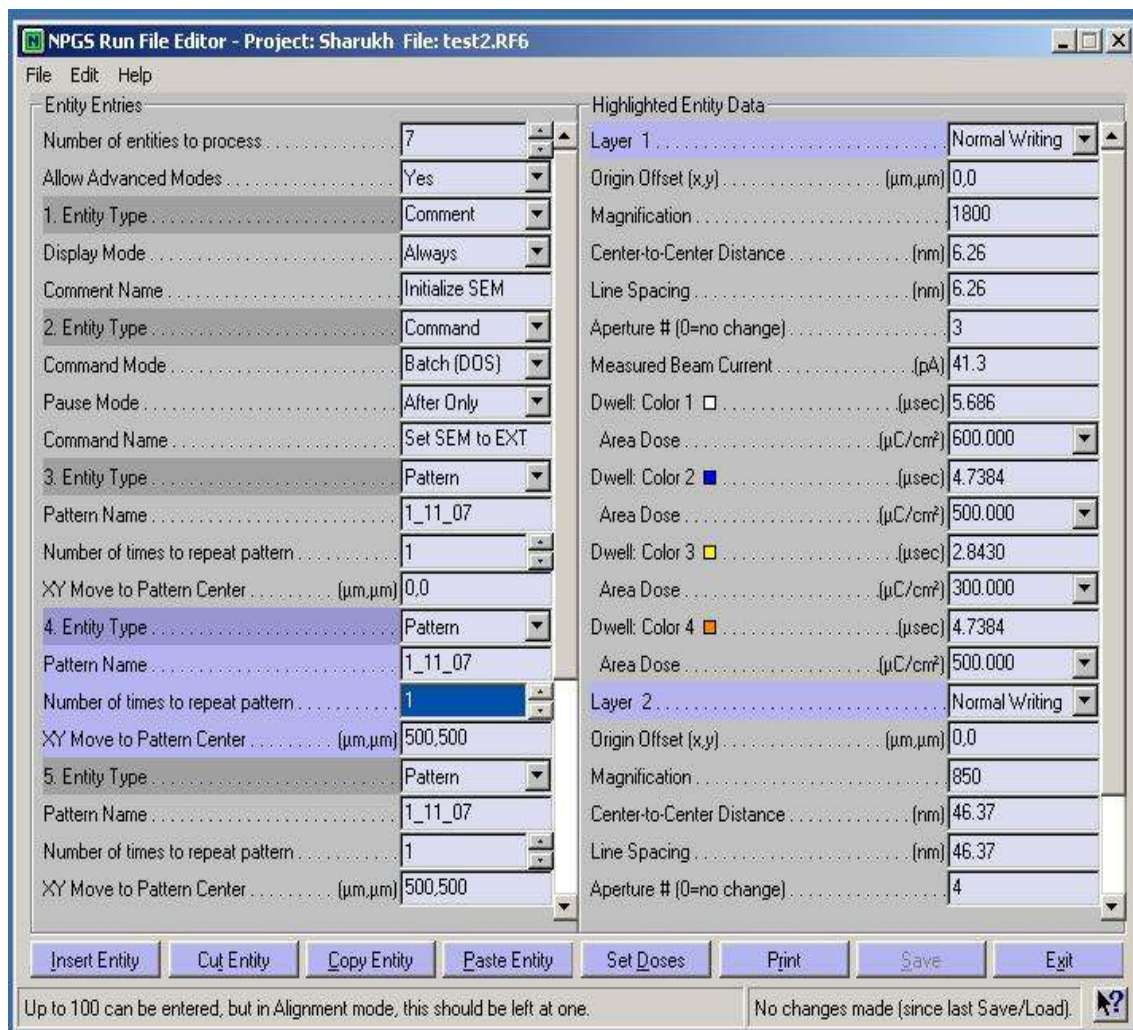


Fig 3.1 A typical Run file

I will try and explain some of the entities of the run file editor.

Allow Advanced Modes

This must be set to Yes to list advanced modes as seen on the right side

Entity Type

It is used to describe the function of that entity. The Comment option displays user defined messages on the screen. The Pattern option is used when actually writing. Command is used to make the NPGS actually run a few calibration tests.

The first two entities in the run file above are entities that I have incorporated into every run file I have created. The first one is a Comment entity where once I instruct the NPGS to start writing it changes modes and then displays a message on the screen reminding me to turn on the Raith blanker and toggle the switch of the blue box from the FIB to SEM mode making sure the machine is in the SEM mode. The second Command entity is used to calibrate the DAC.

Entity three and onwards are the pattern entities let me explain the parameters of that

Pattern Name

The design file name that needs to be patterned

Number of times to repeat pattern

The number of times the same pattern of that entity will be repeated

XY Move to Pattern Center

This instructs the stage to first move the number of units entered and then align with the center of the design.

When a pattern entity is selected you will see the right hand side quite similar to the one seen in the figure. On the right hand side we see layer wise organization.

Normal writing

This is what I typically use for writing patterns since we have a good blanker installed.

Magnification

It sets the magnification the microscope should use to write the pattern. The limits are chosen by the editor itself it is recommended to use a value slightly lesser than the upper limit.

Center-to-center spacing

It is the distance between adjacent exposure points for a line to be patterned. The chosen magnification decides the limits for it. A small value is recommended.

Line spacing

The distance between adjacent lines when an area is to be patterned since the beam performs multiple sweeps across an area when it is patterned. The magnification decides the limits. A small value is recommended.

Aperture #

We can choose the number of the microscope aperture we need that layer to be patterned with.

Measured beam Current

The measured beam current found using by focusing the beam with the aperture entered above on a Faraday cup. It will be used to calculate the doses and dwell times.

Now the organization is color-wise. I can assign different doses to each element designed with the respective color

Dose

Doses can be either area-type, line-type or point-type. To find the needed doses we use the formulae

$$\text{Area dose} = (\text{Beam current}) \times (\text{Exposure Time}) / ((\text{Center-to-center distance}) \times (\text{Line spacing}))$$

$$\text{Line dose} = (\text{Beam current}) \times (\text{Exposure Time}) / (\text{Center-to-center distance})$$

$$\text{Point dose} = (\text{Beam current}) \times (\text{Exposure Time})$$

I decided doses based on inspection of a pattern after development.

Dwell

This is amount of time the beam will expose each point. It is set automatically when the dose is selected.

Pattern alignment and writing is the final stage when all the parameters fall into place. If alignment marks need to be aligned before writing it must be done at this stage. The writing of the pattern can be made fully automated or manual according to the options set in the run file.

3.2.4. Electron beam lithography equipment

UTA has a converted SEM to perform lithography. The SEM itself is a ZEISS 1540 XB Crossbeam. It is also equipped with the capabilities of performing Focused Ion Beam operations. The FIB is a micro-machining tool. The best resolution capable in SEM mode is 1.1nm at 20kV. Magnification is possible from 20 x to 900 kx. The

acceleration voltage can be varied from 0.1 kV to 30 kV. The NPGS v9 version was used. For NPGS v9 a single PCI516 DAC board is used. The PCI516 is a high speed (up to 6MHz) 16 bit DAC board that connects the NPGS computer to the SEM control station.

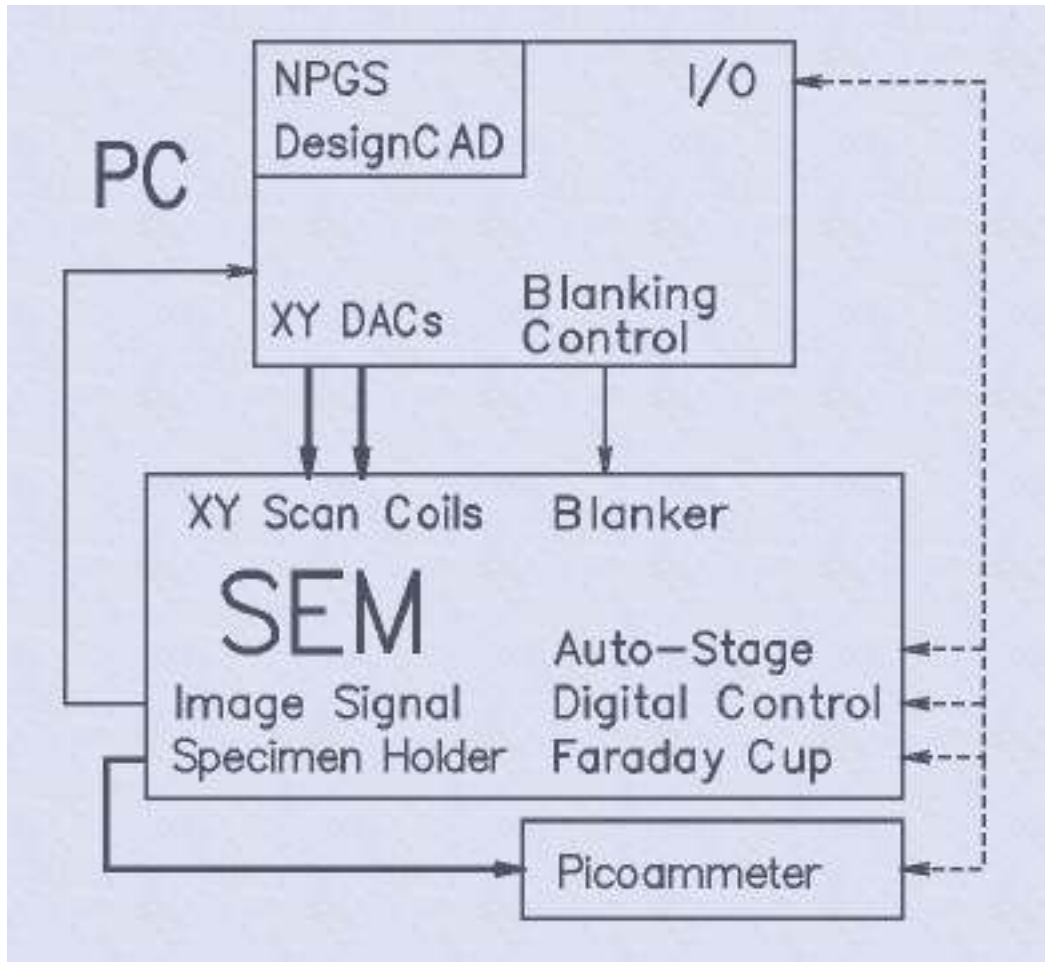


Fig 3.2 Connection diagram for the NPGS and the SEM system [12]

3.2.5. Electron beam resists

There are many e-beam resists available commercially. The resists are either negative or positive type of resists which means that the areas exposed to the electron beam will either be left behind or taken off respectively after development. The resists I

used throughout was dictated by whichever resist we could get a hold off through Dr. Kirks colleagues.

3.2.4.1. UVN30

UVN30 is a negative-tone electron beam resist. It is versatile and can be used as Deep UV and X-ray resist too. Structures of 150 nm have been resolved using UVN30. Some of the unique features of the resist are its greater than one hour post-exposure bake stability, nine months shelf life and metal etch resistance. The resist can be spun on silicon, organic and inorganic anti-reflective substrates. The surfaces need to be coated before the resist is spun on with hexadimethyldisilazane (HMDS); an adhesion promoter. UVN needs to be stored away from heat and sunlight in a sealed container at 30⁰-50⁰F. [13]

3.2.4.2 Polymethyl methacrylate (PMMA)

PMMA can behave as a negative or positive-tone resist. The dosage decides the way the resist acts during development. It can be used for a Deep UV and X-ray resist too but is predominantly used as a positive e-beam resist. The resists acts as a positive resist at lower doses when polymer chain scissions dominate. At higher doses polymerization dominates where the polymer chains link up and become insoluble in the developer. Using the negative PMMA process it has been possible to achieve isolated lines of approximately 12 nm width with the distance between adjacent lines being 25 nm [14]. An issue with negative PMMA is its stability after development with structures too close to each other sticking to each other. PMMA also has poor dry etch

resistance which means an accurate pattern transfer after development is very hard to achieve.

3.2.4.3 Hydrogen silsesquioxane (HSQ)

HSQ has been used commonly as a spin on glass and a low dielectric constant material to fill vias. In March 1997, Namatsu, Yamaguchi, Nagase, Yamazaki and Kurihara reported that it could be used as a negative type e-beam resist [15]. They documented in their work the effects of the granular structures on various resists when exposed to low e-beam doses, the aim being to investigate the effect of the granules on the linewidth fluctuations for the resist. HSQ showed minimum linewidth fluctuation which they attributed to a closed three dimensional framework which had a rigid polymer that did not easily spread and was not easily entangled.

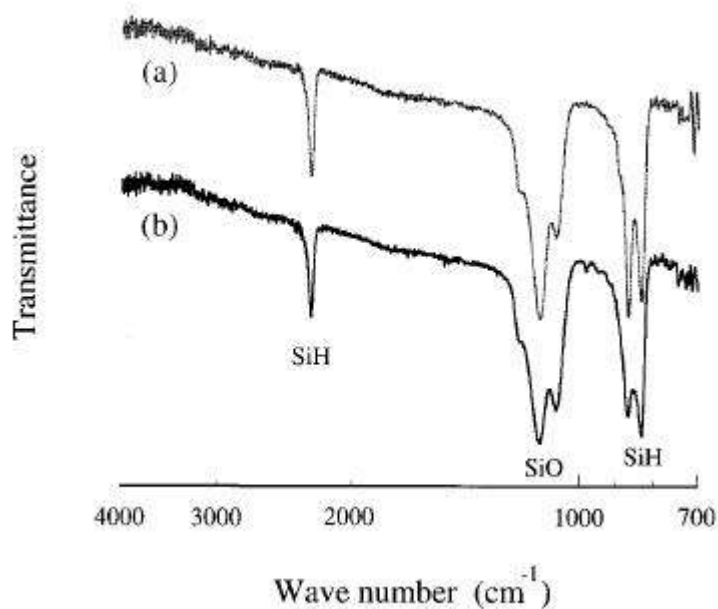
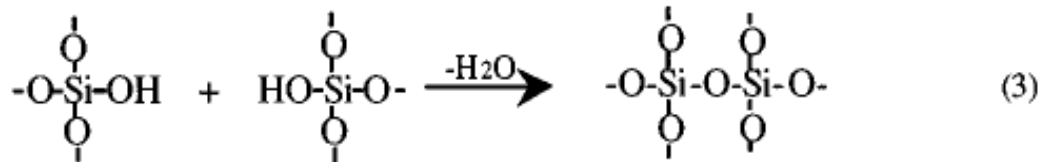
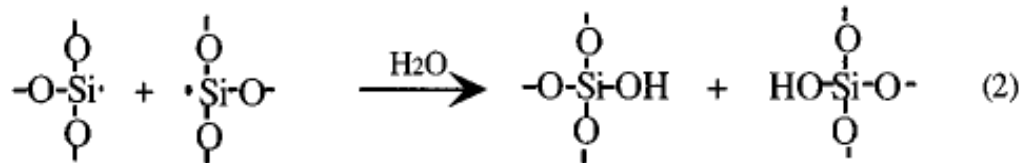
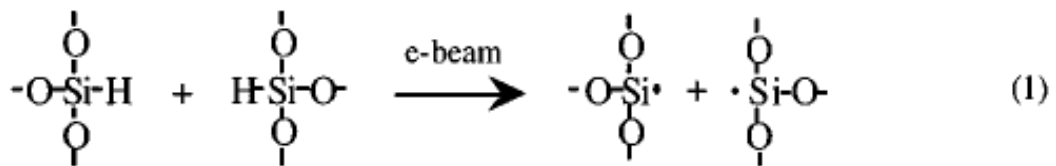


Fig 3.3 IR spectra of HSQ (a) before (b) after e-beam exposure [16]

In the IR spectra peaks are observed at 2260, 1130-1080 and 860-830 cm^{-1} . The double peaks located close to each other indicate a crosslinked cage like structure. On exposure to an electron beam the IR spectrum indicates that the transmittance of SiH peaks and SiO peak at 1030 cm^{-1} decreased while that of the SiO peak at 1080 cm^{-1} increased; indicating that the SiH bond scission was responsible for crosslinking. The following chemical equations were obtained from [16].



During development the dissolution of the e-beam exposed parts of HSQ is decreased as the bonds are more stable due to the crosslinking. The small difference in the degree of crosslinking due to e-beam exposure creates a significant change in the developing rate. HSQ is one of the new e-beam resists and is capable of very high resolutions. Lines of 7nm width have been demonstrated [17].

HSQ is an inorganic resist and its etching durability during a poly-Si etch using a chlorine plasma generated by electron cyclotron resistance (ECR) is poor. The solution to this issue is by applying an oxygen plasma treatment.

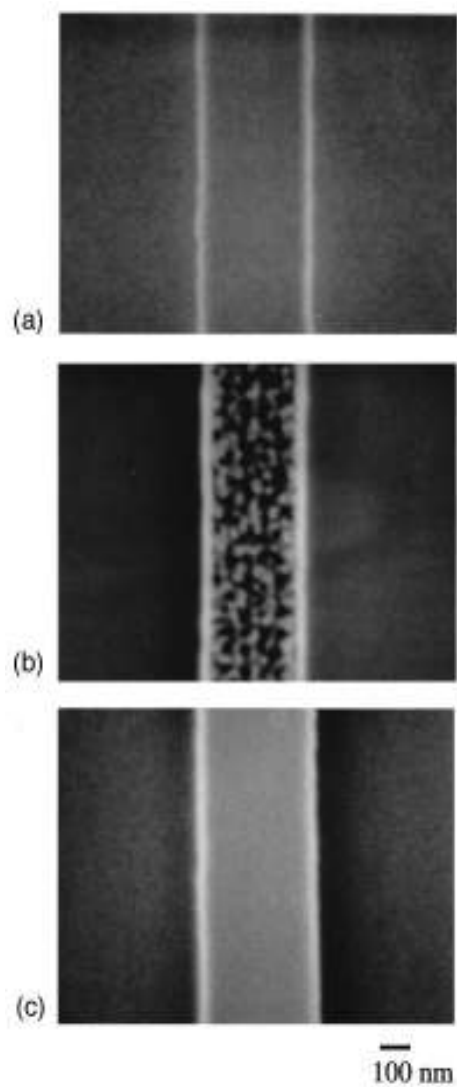


Fig 3.4 SEM images of a HSQ line (a) after development (b) after a chlorine plasma ECR etch without oxygen plasma treatment (c) after being treated with oxygen plasma and a chlorine plasma ECR etch [16]

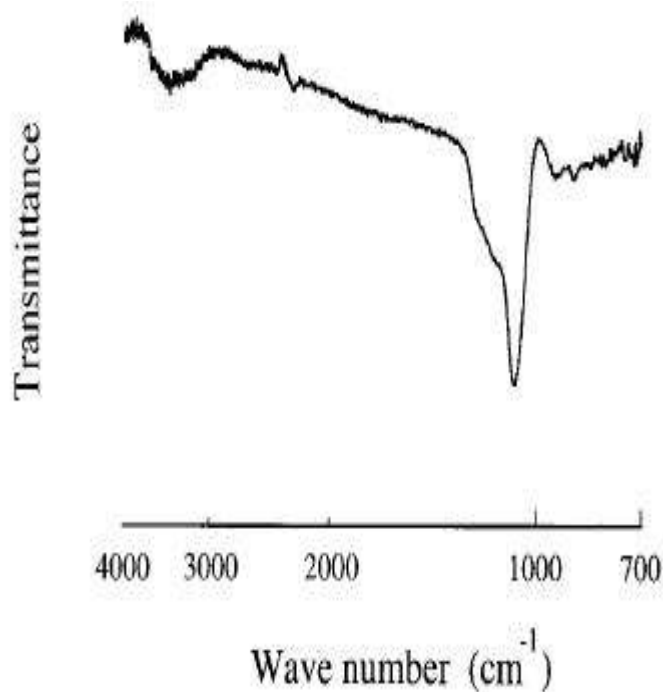


Fig 3.5 IR spectrum of HSQ after oxygen plasma treatment [16]

The IR spectrum above indicates that the SiH peaks and the SiO peak at 1130 cm^{-1} are not observed whereas a strong peak for SiO at 1080 cm^{-1} is present. This indicates complete crosslinking and thus an improvement in etching durability when a chlorine based ECR etch is employed. The etch rate of the oxygen treated HSQ is faster in CF_4 based RIE than untreated HSQ since CF_4 etches SiO_2 at a high rate. Thermal curing is proposed to improve the etch resistance of HSQ; if HSQ is baked for a long period above 300°C [18]. Another novel approach to increase the etch resistance of HSQ in CF_4 based RIE is by exposing the HSQ to the electron beam then developing HSQ and then exposing the sample to another run in the e-beam machine with very high doses [19].

Another drawback associated with HSQ systems is that any time delay between processing steps and aging play an important role in the results obtained after development. Adverse results are observed if there is a large delay between the pre exposure bake and the exposure, with the sensitivity decreasing and the contrast increasing. The effect of a delay between the exposure and development is not as significant though [20]. The resist is said to have a shelf life of six months.

HSQ is sold by the Dow Corning Corporation under the name of XR-1541 and comes with different percentages of the HSQ solid mixed in a MIBK solvent. We have used an XR-1541 which has 4% HSQ solids in the MIBK solvent. The spin speed curve was obtained from a company representative.

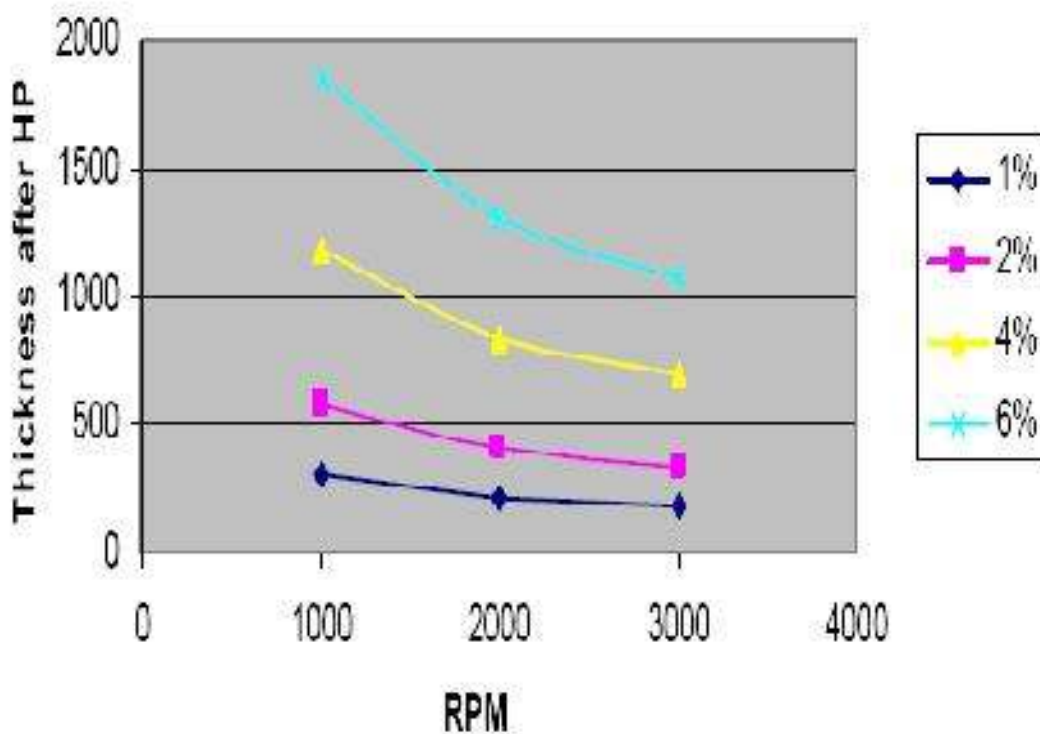


Fig 3.6 Spin speed versus thickness graph for XR-1541. Thickness is in Angstroms

3.3 Reactive Ion Etching

The basic principle behind all reactive ion etching (RIE) methods is that a chemically active plasma attacks the surface of the wafer that needs to be etched. The formation of plasma due to applied RF potential causes a breakdown of the gas molecules into free radicals or fragments. These might then get ionized in the plasma and travel with significant speeds within the confined etching chamber. Some of those ions will be incident on the sample surface where they might react with the surface atoms forming molecules or compounds. These by-products are desorbed from the surface if their vapor pressure is reasonable and diffuse into the bulk of the gas.

The UTA Nanofab Lab is currently equipped with a Technics MicroRIE800 machine and one Trion Technology DRIE machine. The Technics is a low frequency (30KHz) reactive ion etcher. It is a parallel plate etcher equipped with two gasses: CF_4 and O_2 . The etcher was designed for etching substrates, photoresist ashing and surface cleaning.

The Trion Technology DRIE (deep reactive ion etcher) is capable of etching very high aspect ratio vertical trenches and through-the-wafer etches in silicon. It is also capable of fast selective etching of patterned oxide and nitride wafers. Though the two machines operate using the same principle, the Trion is a high-end system equipped with all the bells and whistles. It is equipped with gasses like SF_6 , CF_4 , O_2 , He and Ar. There is a turbo pump operating at 19800rpm enabling the pressure in the etch chamber to be pumped down very quickly. There is a provision for an electrostatic chuck which holds down the wafer during etching while a small flow of Helium cools the backside of

the wafer. An Inductively Coupled Plasma (ICP) electrode which provides a high power output providing the necessary power to a downstream high density plasma when required.

CHAPTER 4

RESULTS AND DISCUSSION

In this chapter I shall try and present most of the significant work that has been done on this project in chronological order as far as possible. I have tried to provide explanations of observed results and the reason behind why alterations were made to the processes if the results were unsatisfactory.

Initially Dr. Vans Ley was responsible for all the e-beam exposures and SEM images as he was the only trained E-beam or SEM machines operator. The first resist system we chose to work with was UVN30. Knowing very well successfully patterning of the design using UVN30 was an uphill task considering the resolution limit of UVN30 was approximately 150nm and the design consisted of features of 75 nm, we decided to investigate writing using PMMA simultaneously.

4.1 The first generation of DesignCAD patterns

We chose to include a few standard NPGS patterns alongside our structures. This is recommended for users to familiarize themselves with the system and new resist systems and assess the results obtained. We did have a few redesigns initially but settled on a design with the components and dimensions described below.

The first entity was a 50 micron square and is set as a filed polygon which meant that the beam will sweep inside the square effectively delivering the prescribed area dose.

The next pattern was a standard NPGS pattern named SAMPLE0.dc2. It is a wheel with spokes.

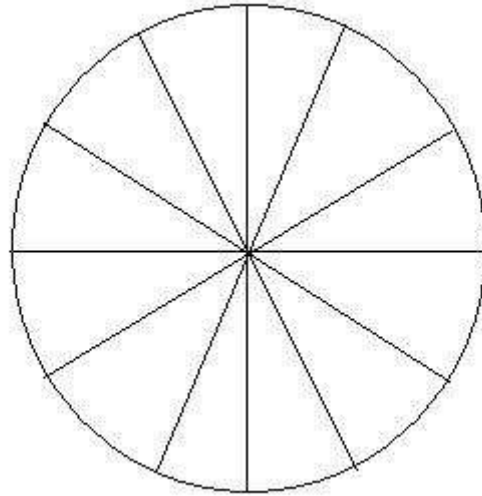


Fig 4.1 The wheel pattern

The diameter of the wheel is 10 microns. This design file had nine wheels of different colors which were written in 3 x 3 matrix form. This meant that each wheel could be given a different dose. The wheel pattern was designed with solid lines which meant that the e-beam would only pass over the lines delivering the prescribed line dose. This is a great test for checking the operator skills and checking for astigmatism.

The SET structure was designed using two layers.

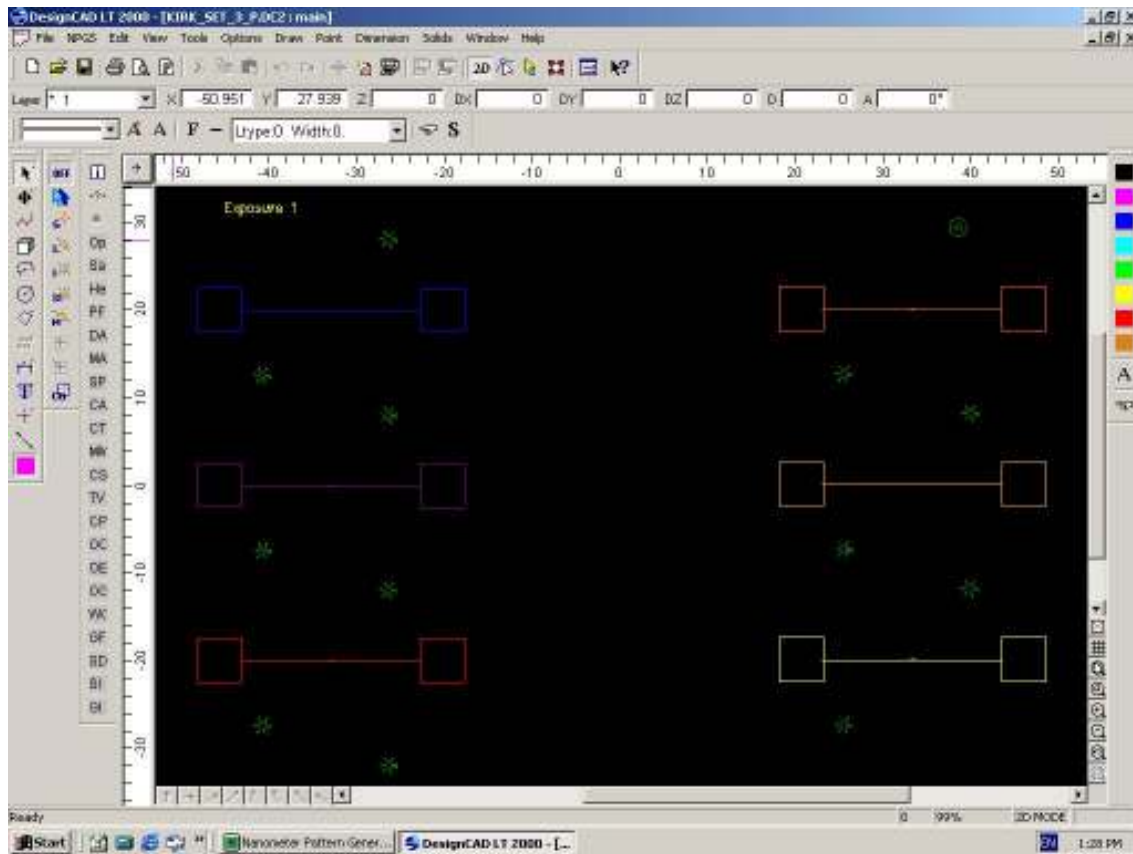


Fig 4.2 The DesignCAD pattern file

The figure above does not reveal all the details of the pattern hence I have diagrammatically redrawn the pattern. Six SET structures of different colors were inputted so that they can be given varying doses if desired. The asterisk marks are dump points which are used when the beam blanker is not in use. Their principal function is to direct the beam to follow them from the end point of one structure to the start point of the next structure to be written. Along the dump point path the beam has time to stabilize.

The large boxes (pads) are 5 microns squares. They will form the source and drain electrodes for our structure. They were designated to Layer 2. They are also set

as a filled polygon which means that the e-beam will sweep inside the polygon effectively delivering the prescribed area dose. The long rectangles (fingers) are 10 microns by 150 nm. The circles (islands) are 75 nm in diameter. The fingers and islands are set to be given line doses which means the e-beam will just travel around the perimeter of the structures delivering the prescribed doses. The fingers are detached from the nearest islands by 10nm and the separation between consecutive islands is 85 nm. This was done knowing that 10 nm was too small a distance to be resolved after lithography and the finger and the island next to it would merge and hence the effective structure would taper down and its width would be very similar to the central islands width. The islands and fingers were designated to Layer 1. Different layers were designated to allow for the pads to be written with a larger microscope aperture since their accuracy was not significant and writing them with a smaller aperture would be time consuming.

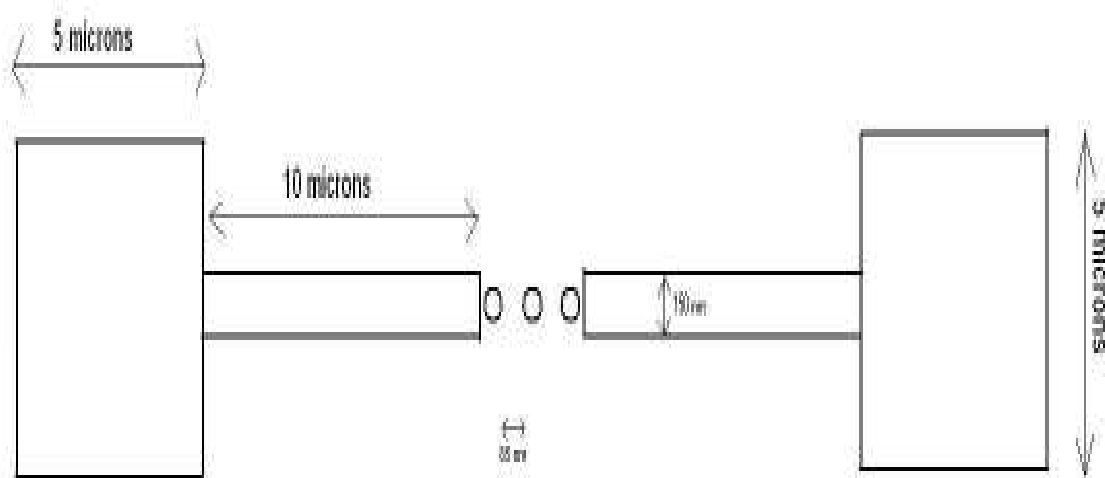


Fig 4.3 A diagrammatic representation of the designed SET structure

4.2. The first test

The first pattern was written using the UVN30 resist system. The design file was quite different from that aforementioned. The wafer specifications, e-beam parameters and the recipe for development are mentioned under first UVN30 wafer in Appendix A.

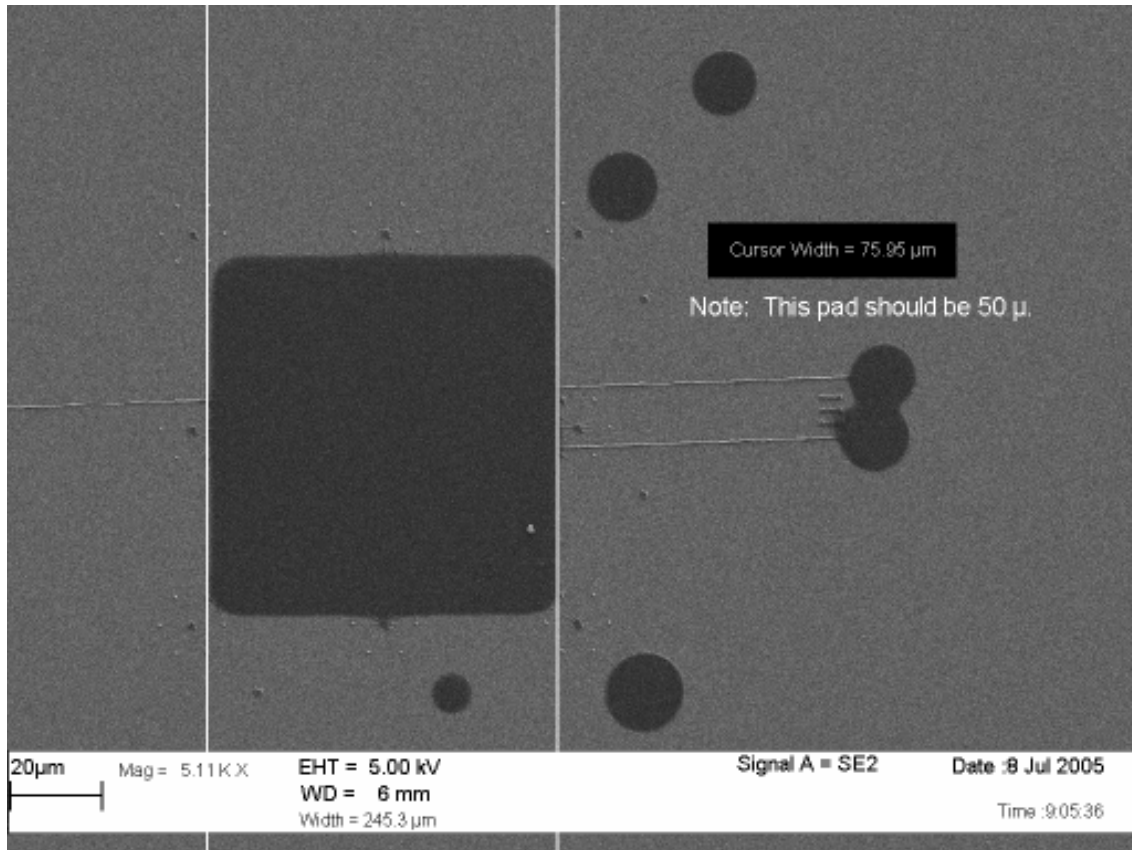


Fig 4.4 The 50 micron pad after development using UVN30 as the resist

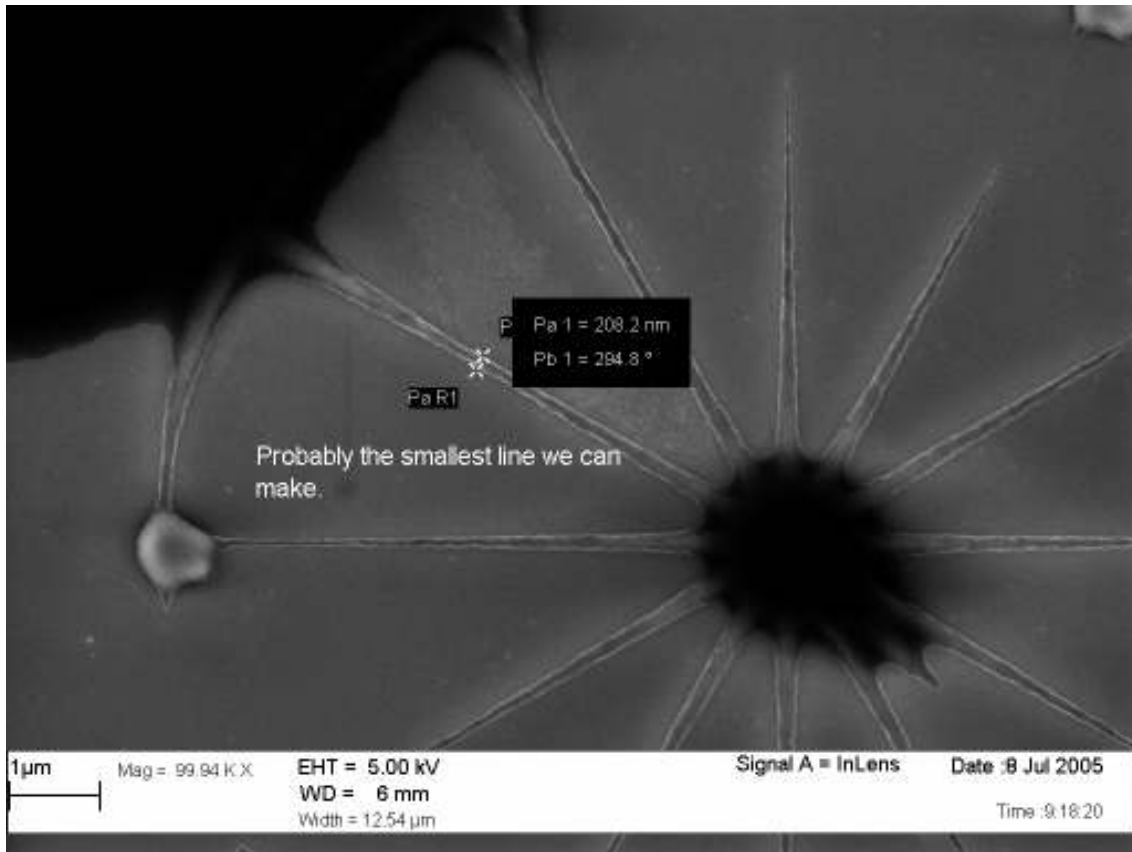


Fig 4.5 The wheel pattern after development using UVN30 as the resist

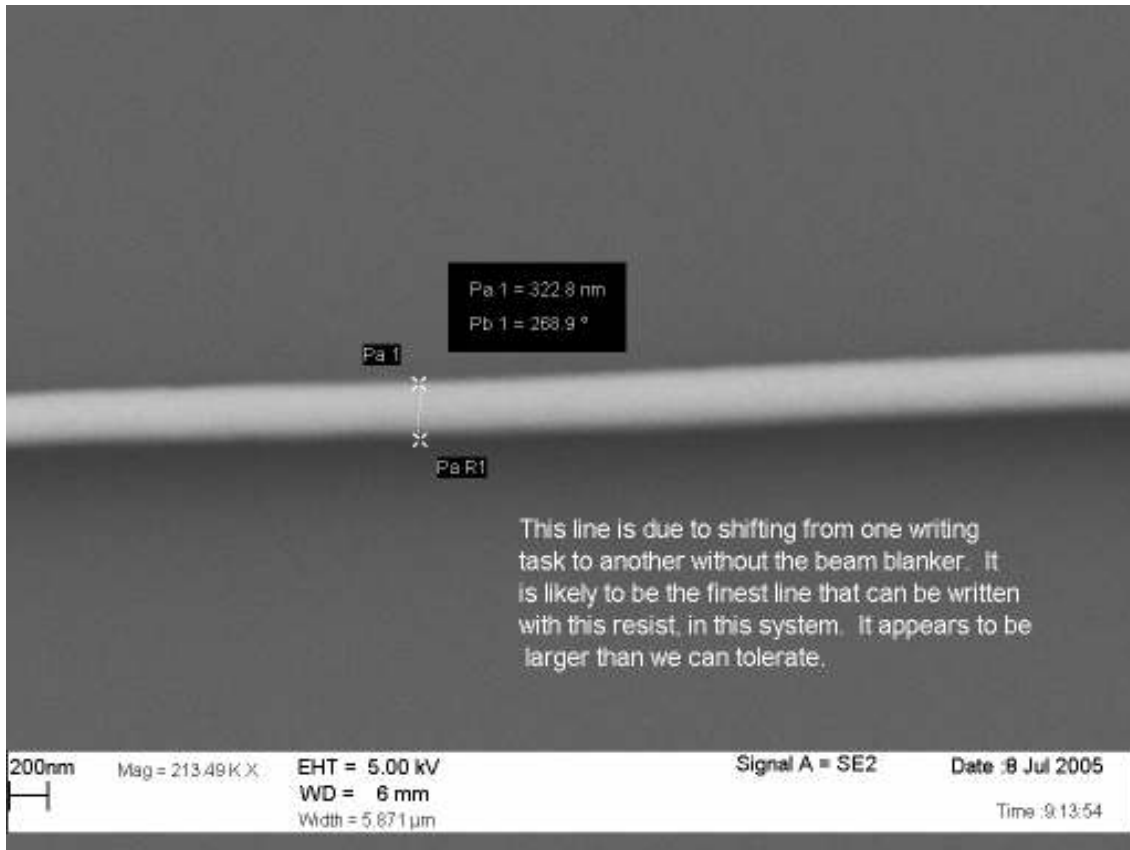


Fig 4.6 A line of the wheel pattern after development using UVN30 as the resist

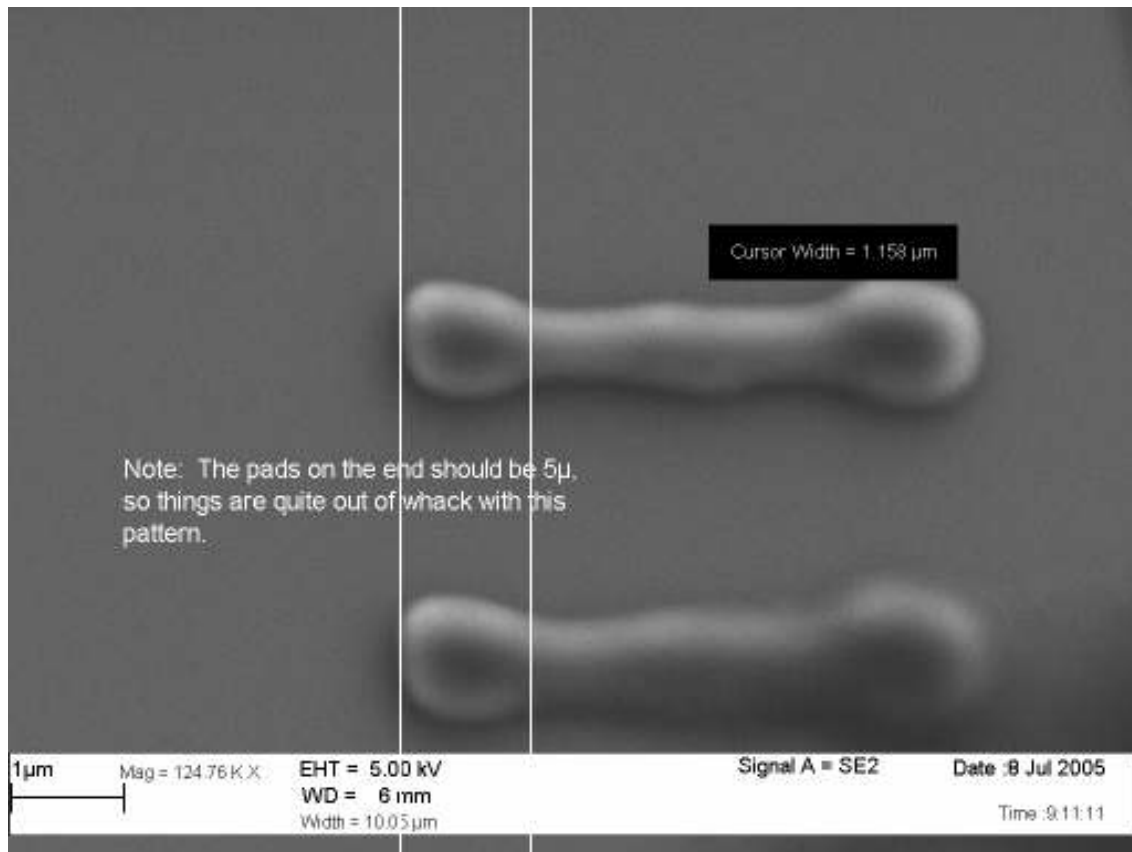


Fig 4.7 The SET pattern after development using UVN30 as the resist

This test proved that either our doses were off by very large values or UVN30 just was not suited for the resolution we needed. We tried another run with this resist following this failure.

4.3 UVN30 and PMMA tests

The design file was modified with the pads for the structures increased in size considerably to get a better measure of the sensitivity of the resist. The doses were reduced too. The wafer specifications, e-beam parameters and the recipe for development are mentioned under second UVN30 wafer in Appendix A.

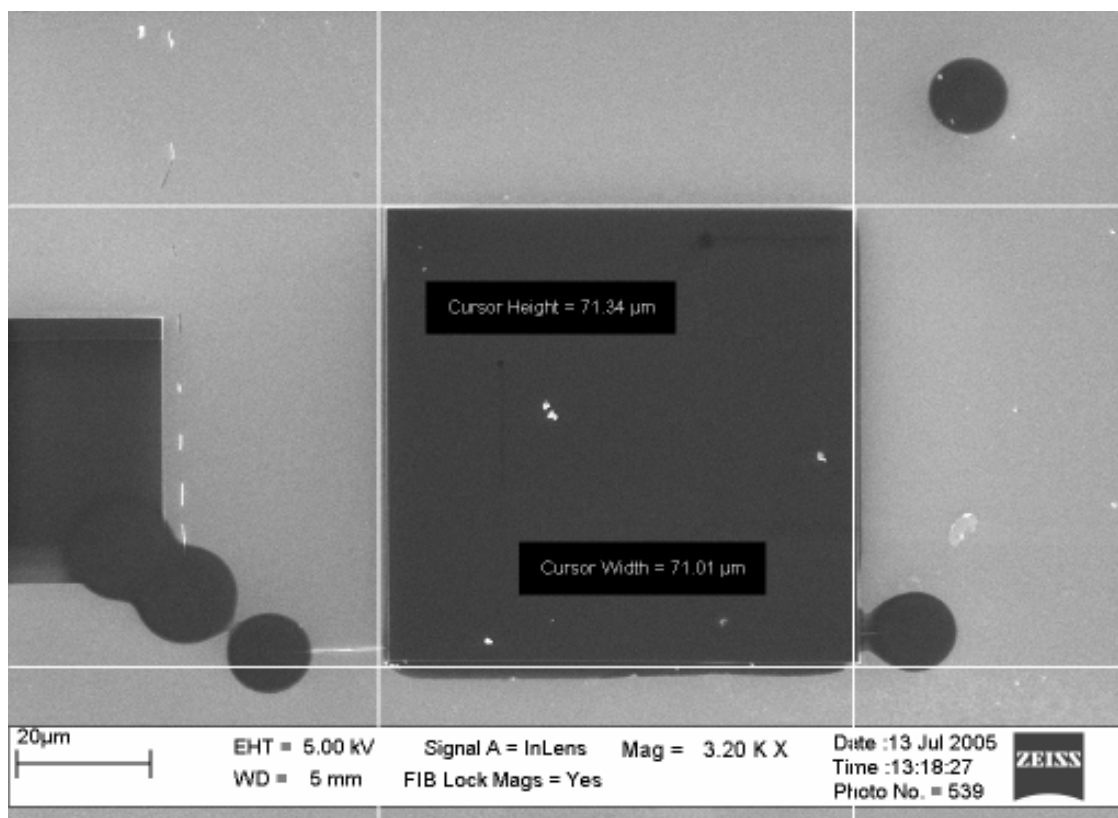


Fig 4.8 The 50 micron pad after development using UVN30 as the resist

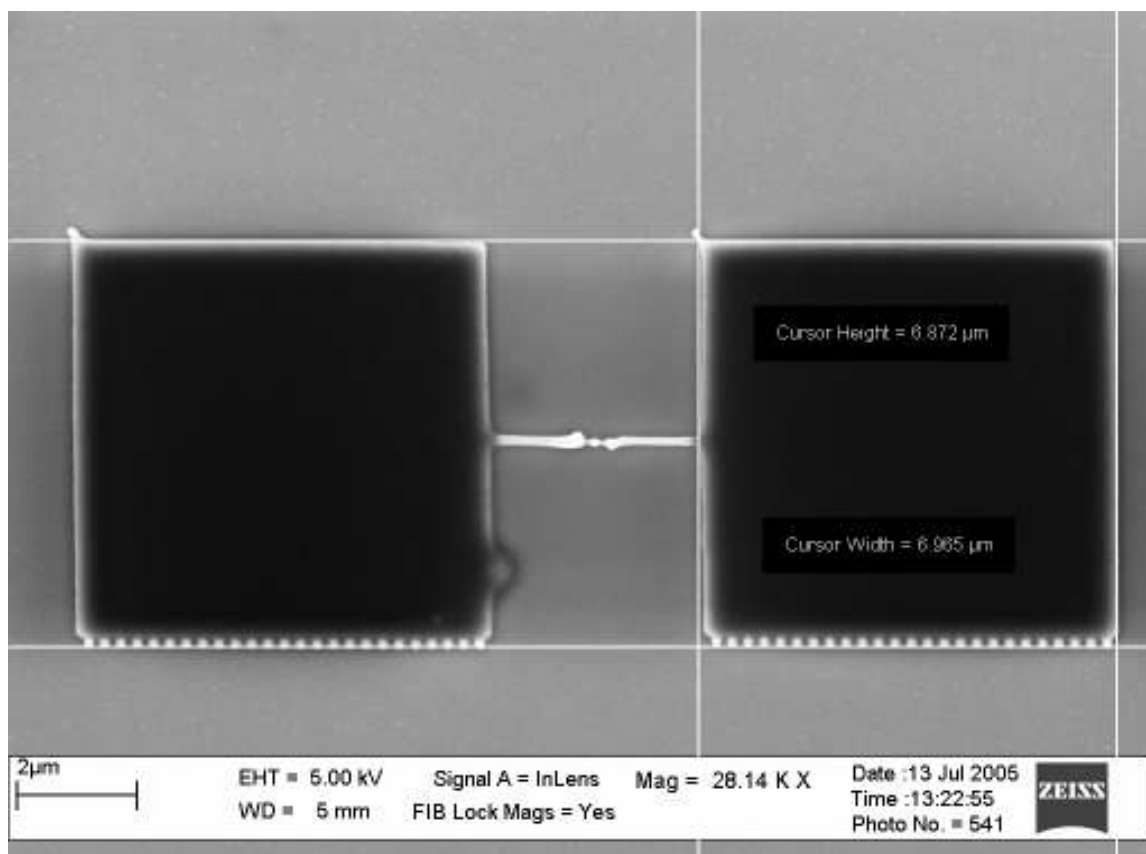


Fig 4.9 The SET pattern after development using UVN30 as the resist

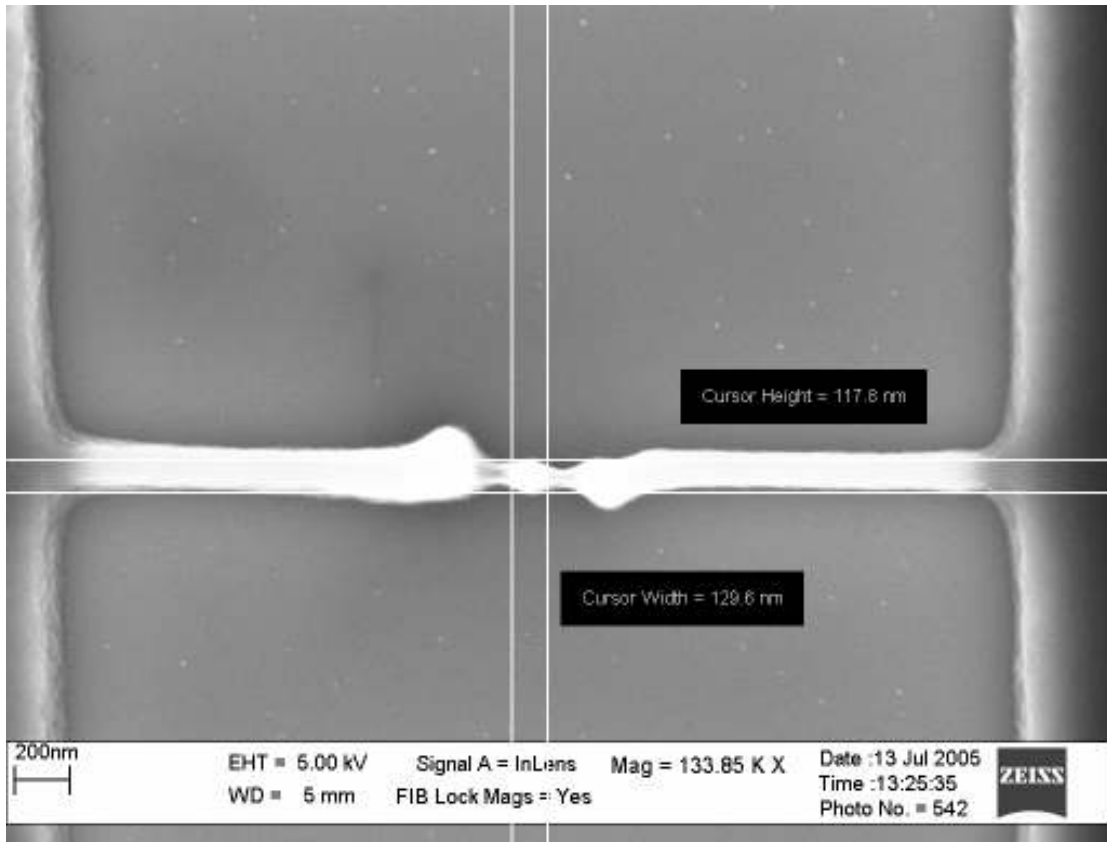


Fig 4.10 The SET structure after development exposed at the lowest dose using UVN30 as a resist

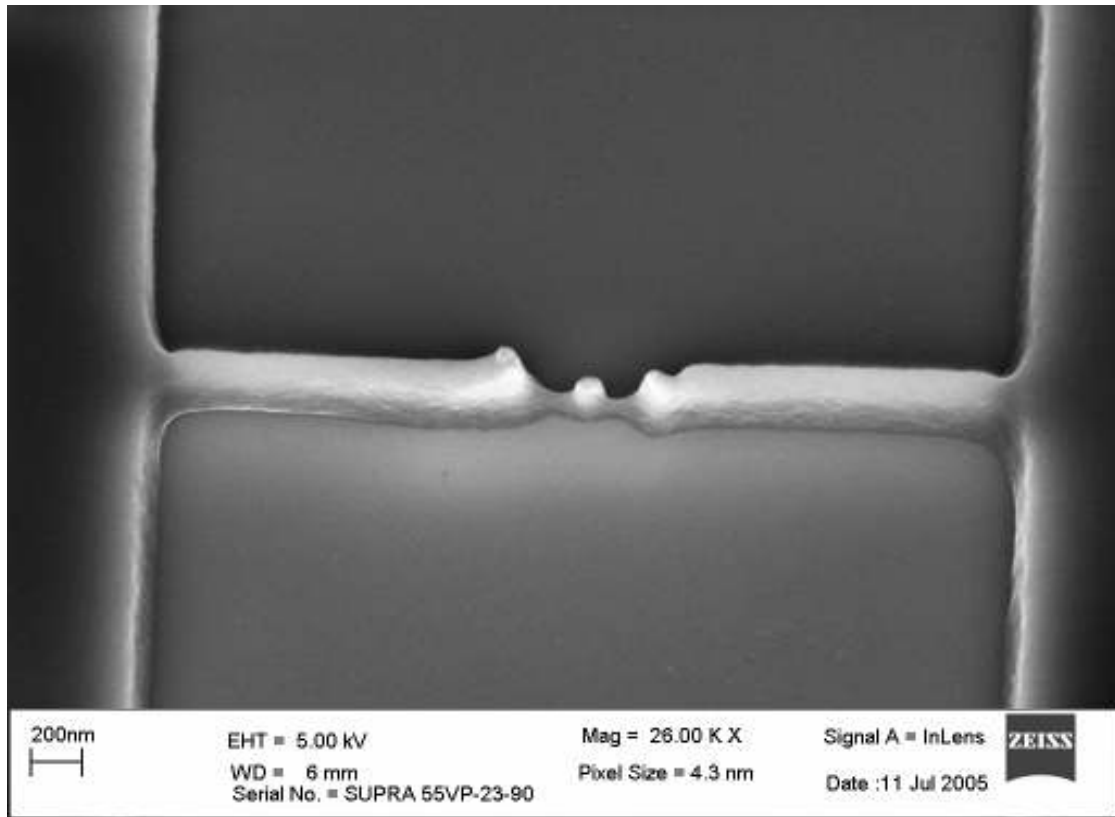


Fig 4.11 The SET structure after development imaged at a 60° tilt using UVN30 as a resist

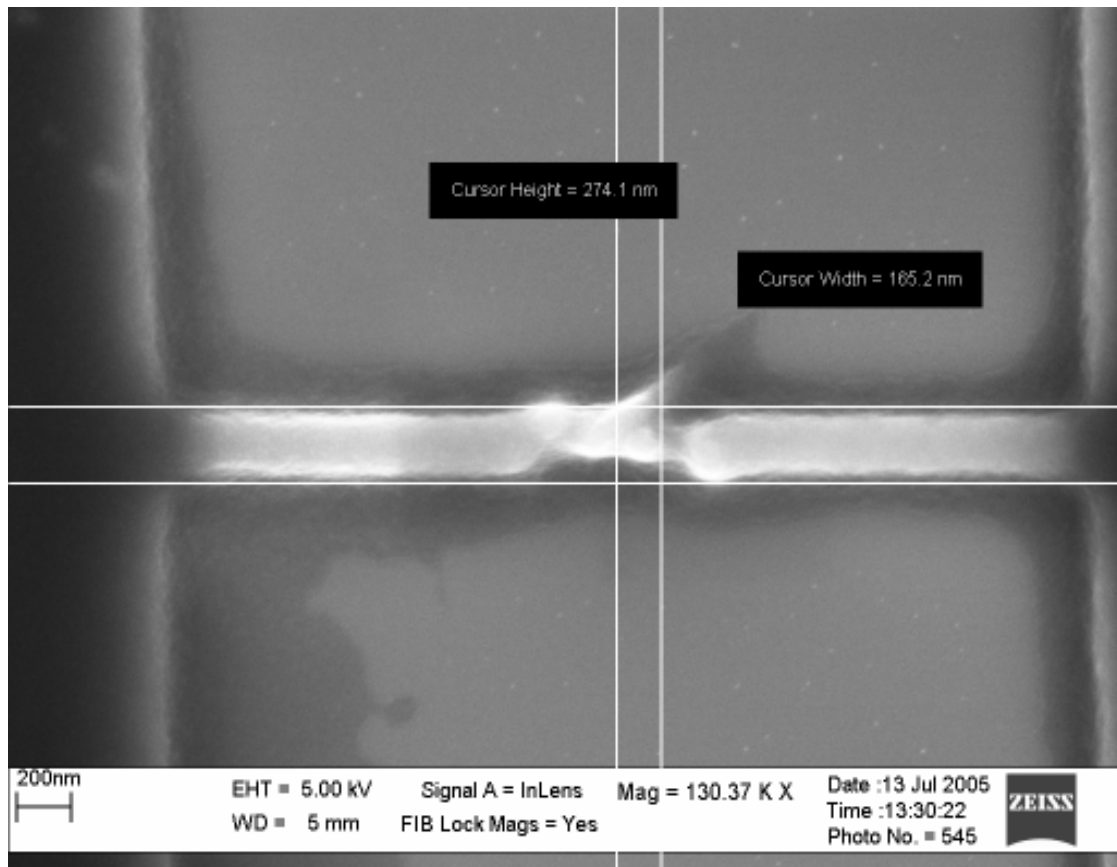


Fig 4.12 The SET structure after development exposed at the highest dose using UVN30 as a resist

It is evident that after altering most of the doses the 50 micron pad and the source and drain pads are overexposed. The dimensions of the 50 micron pad did decrease slightly with the slim reduction in dosage, thus indicating the prescribed dosage being the issue here. The fingers and islands were twisted and looked very haphazard even at the lowest dosage. We had exceeded the resolution limits of the resist system and this was probably the reason behind such aberrant behavior.

For the next sample PMMA was used. It was first diluted to make a 2% PMMA mixture. It is known that if PMMA is exposed with a very high electron dose almost a hundred times more than that needed to make it behave like a positive resist then a

polymerization process dominates causing PMMA molecules to crosslink and form networks making them insoluble in the developer and effectively PMMA acts in negative resist fashion. We desired this behavior of PMMA and the sample was exposed to heavy doses to make PMMA behave as a negative resist. The wafer specifications, e-beam parameters and the recipe for development are mentioned under first PMMA wafer in Appendix B.

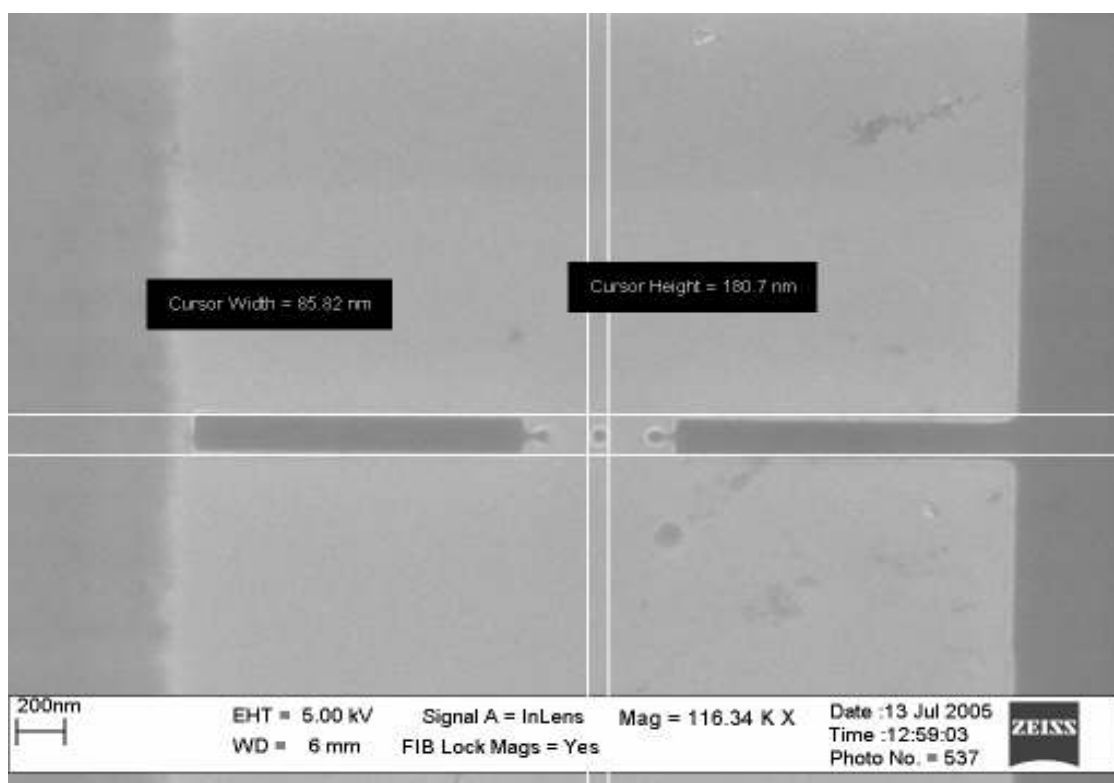


Fig 4.13 A SET pattern after development exposed at the lowest dose using PMMA as the resist

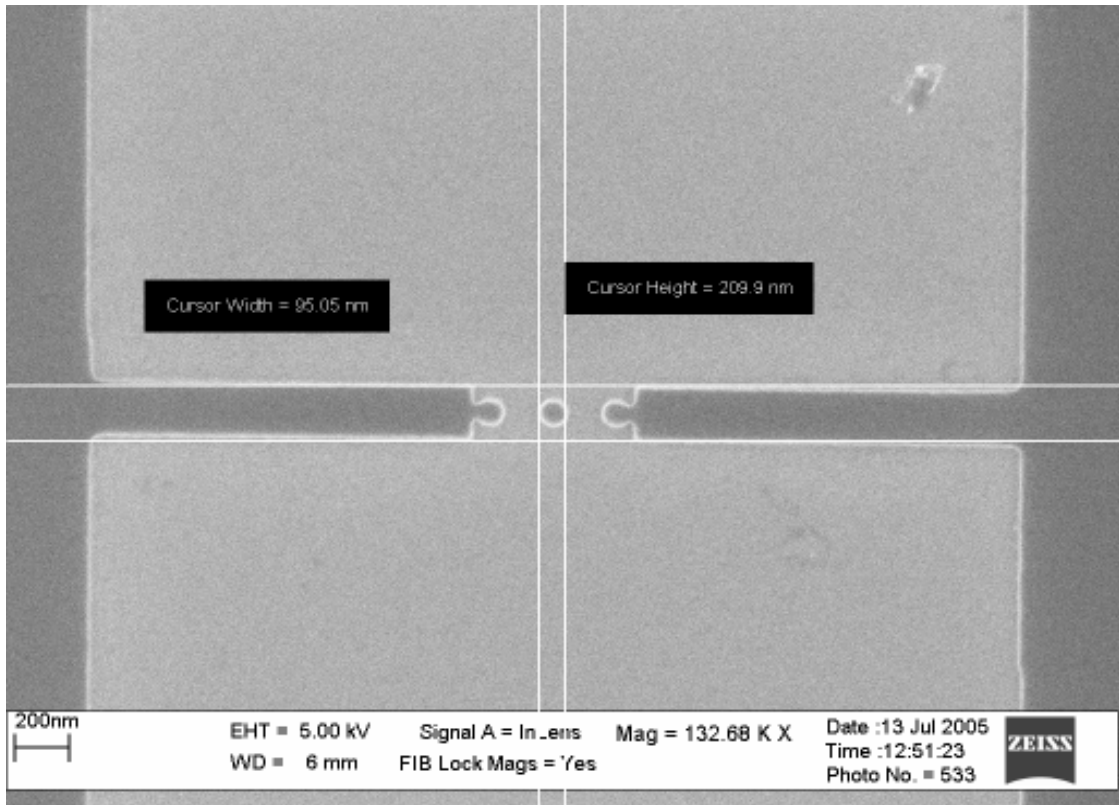


Fig 4.14 A SET pattern after development exposed at a moderate dose using PMMA as a resist

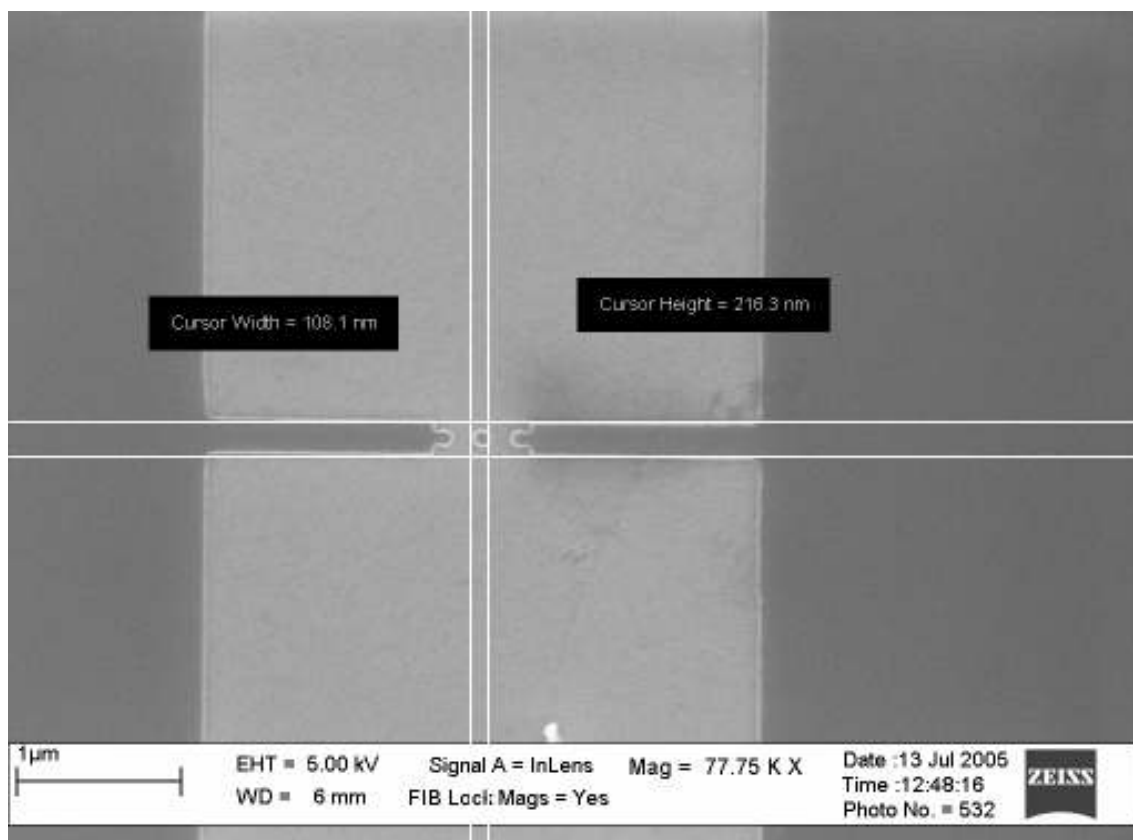


Fig 4.15 A SET pattern after development exposed at the highest dose using PMMA as a resist

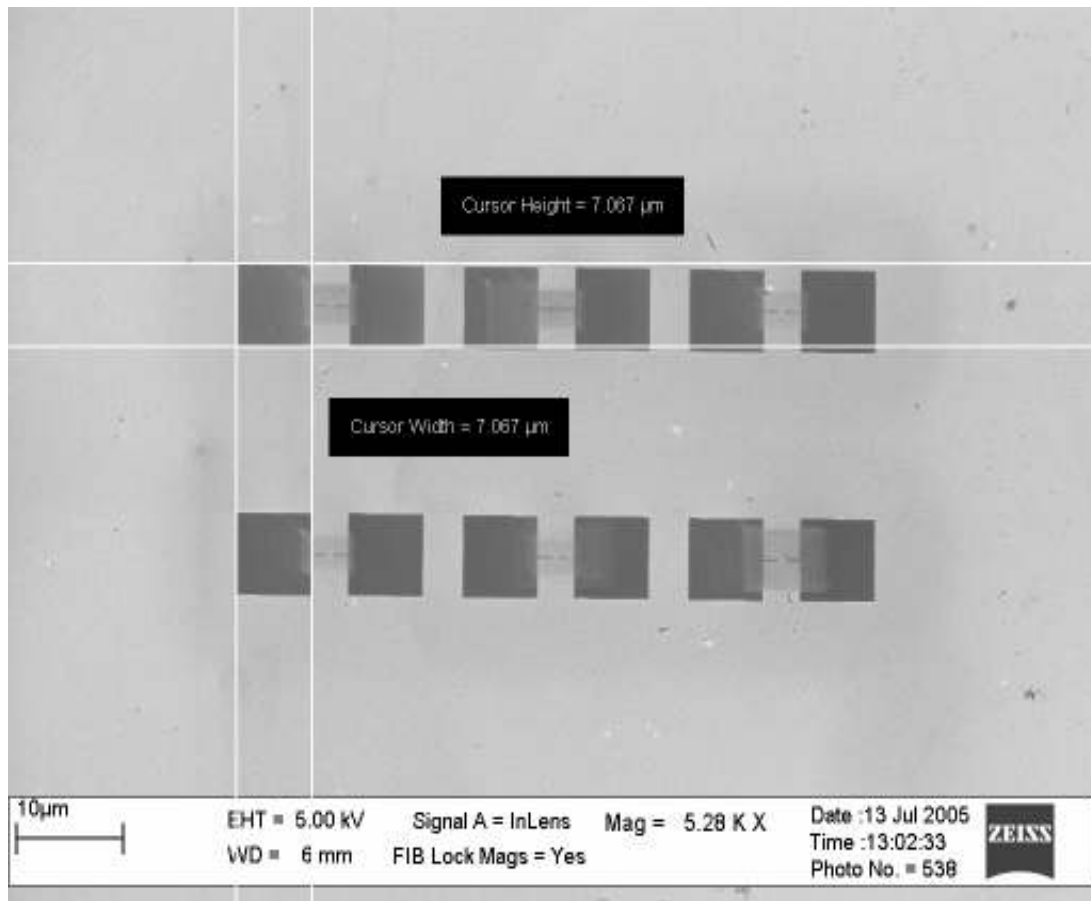


Fig 4.16 The array of SET structures after development using PMMA as a resist

Since PMMA had been used extensively used as e-beam resist there was a lot of documentation regarding it. The doses were approximated for the structures by calculating and comparing results from various other publications for structures with similar feature sizes. The dose for all pads was the same and it is evident that they were overdosed. On inspection of the fingers and islands for the lowest dose structures the island was slightly overdosed as it was 85 nm instead of 75 nm. The finger was also larger in width than designed. As the doses kept increasing the structures seemed to enlarge in their dimensions. Overall this test was a success.

Another design file was created before exposing another UVN30 sample. The source and drain pad design was changed again. The wafer specifications, e-beam parameters and the recipe for development are mentioned under third UVN30 wafer in Appendix A

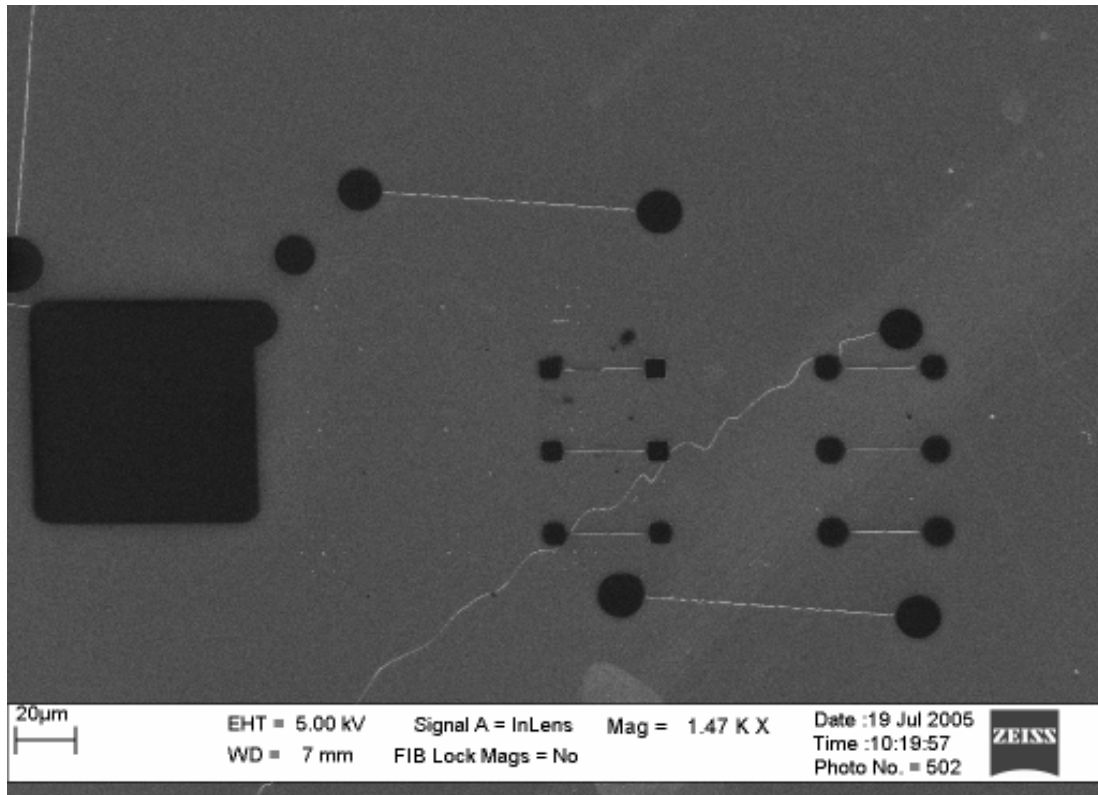


Fig 4.17 The SET array and the 50 micron pad after development using UVN30 as the resist

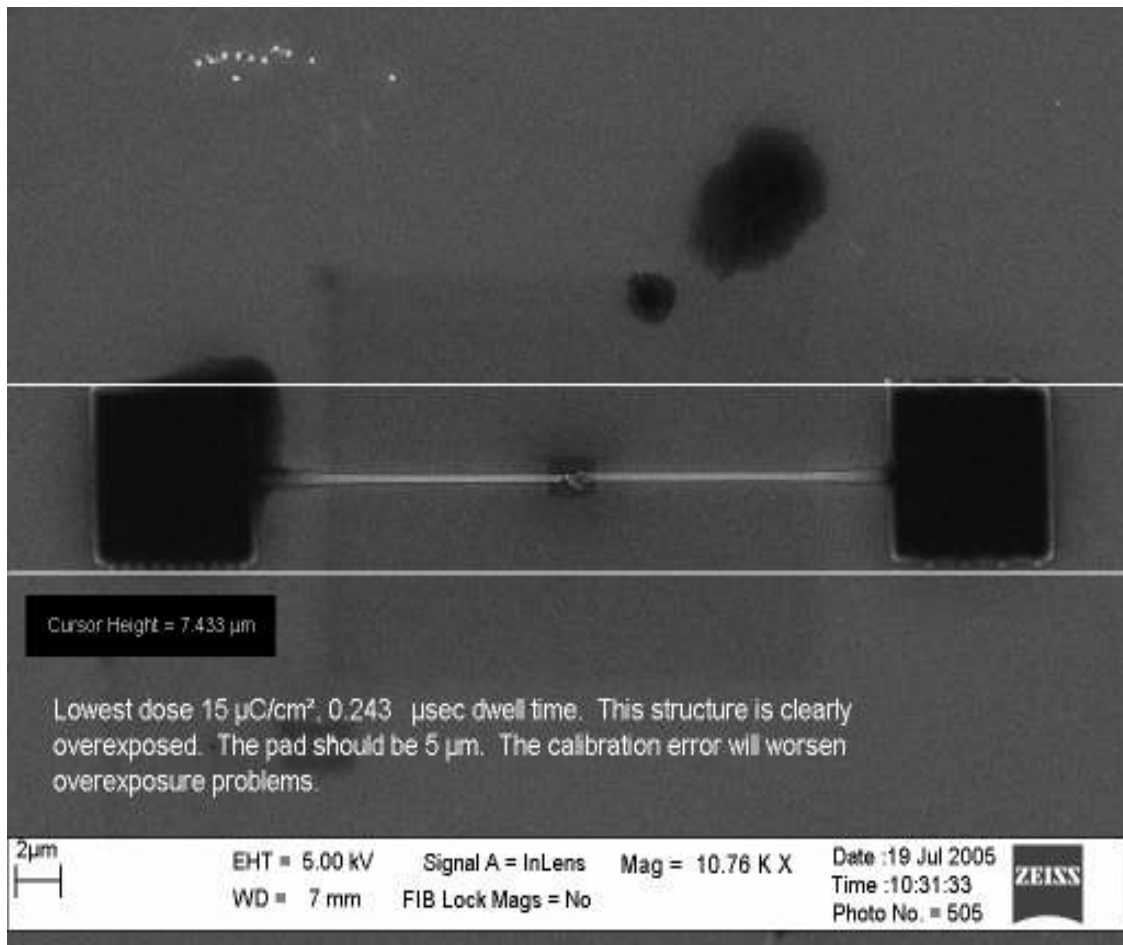


Fig 4.18 A SET structure exposed after development exposed at the lowest dose using UVN30 as the resist

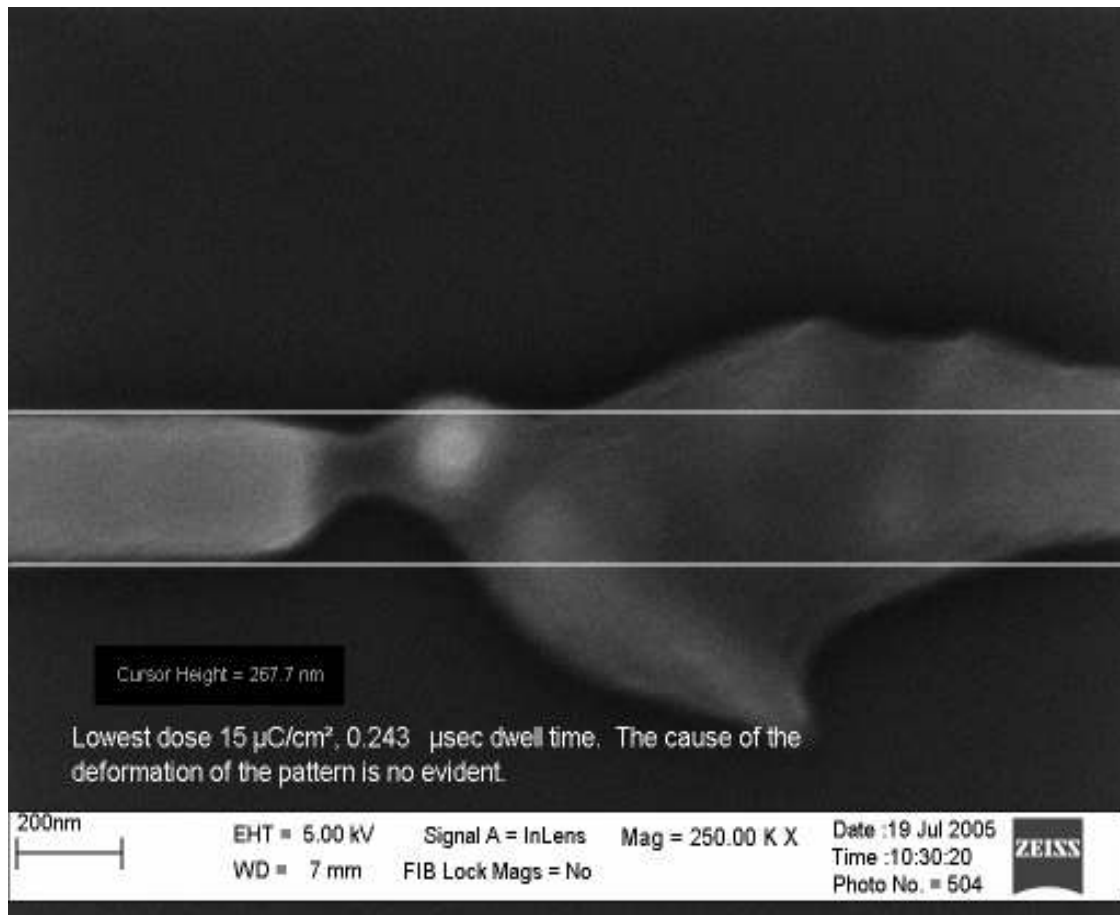


Fig 4.19 The central part of a SET structure exposed after development exposed at the lowest dose using UVN30 as the resist

Clearly even at the lowest dose the structure seemed deformed and overexposed. The strategy for the next wafer was to see if the post bake and HMDS (the adhesion promoter) layer thickness had any effect on the quality of writing. The HMDS was spun on at the same speed but the spin time reduced to a third of its original value. The post bake was also carried out a lower temperature. The wafer specifications, e-beam parameters and the recipe for development are mentioned under fourth UVN30 wafer in Appendix A.

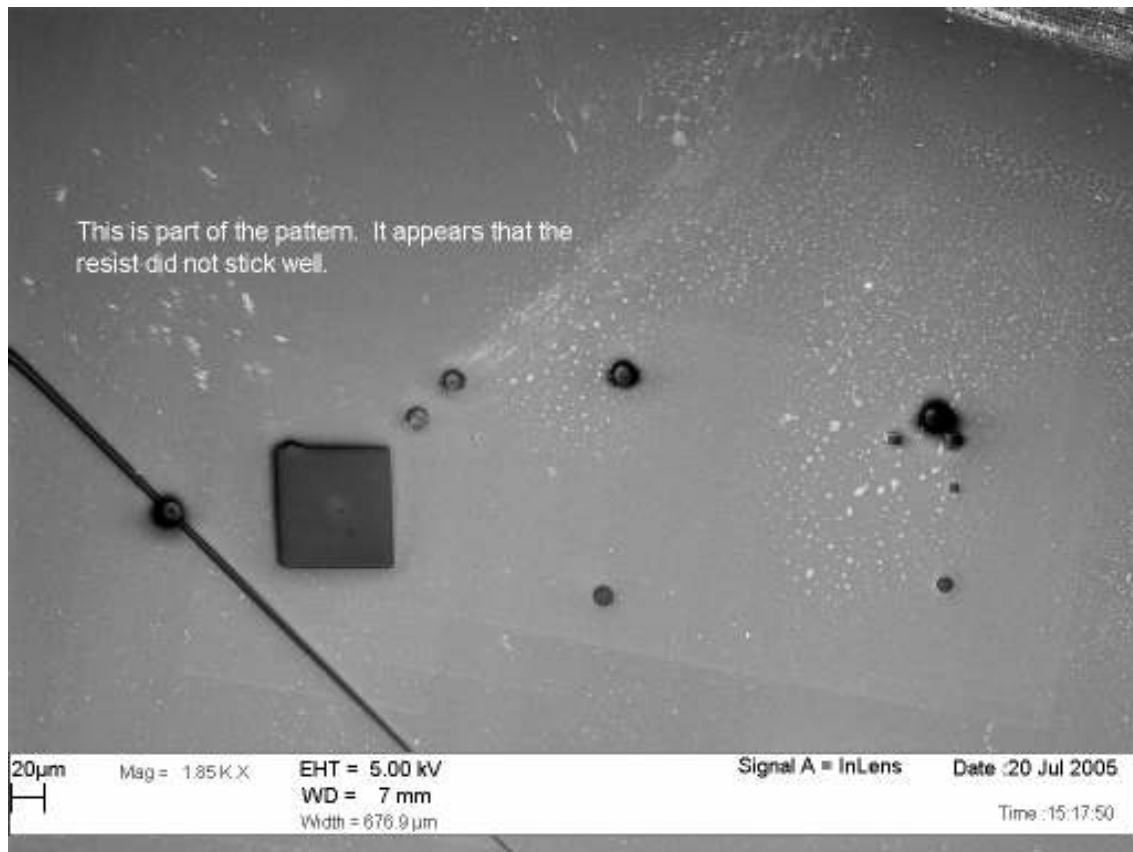


Fig 4.20 The 50 micron pad after development using UVN30 as a resist

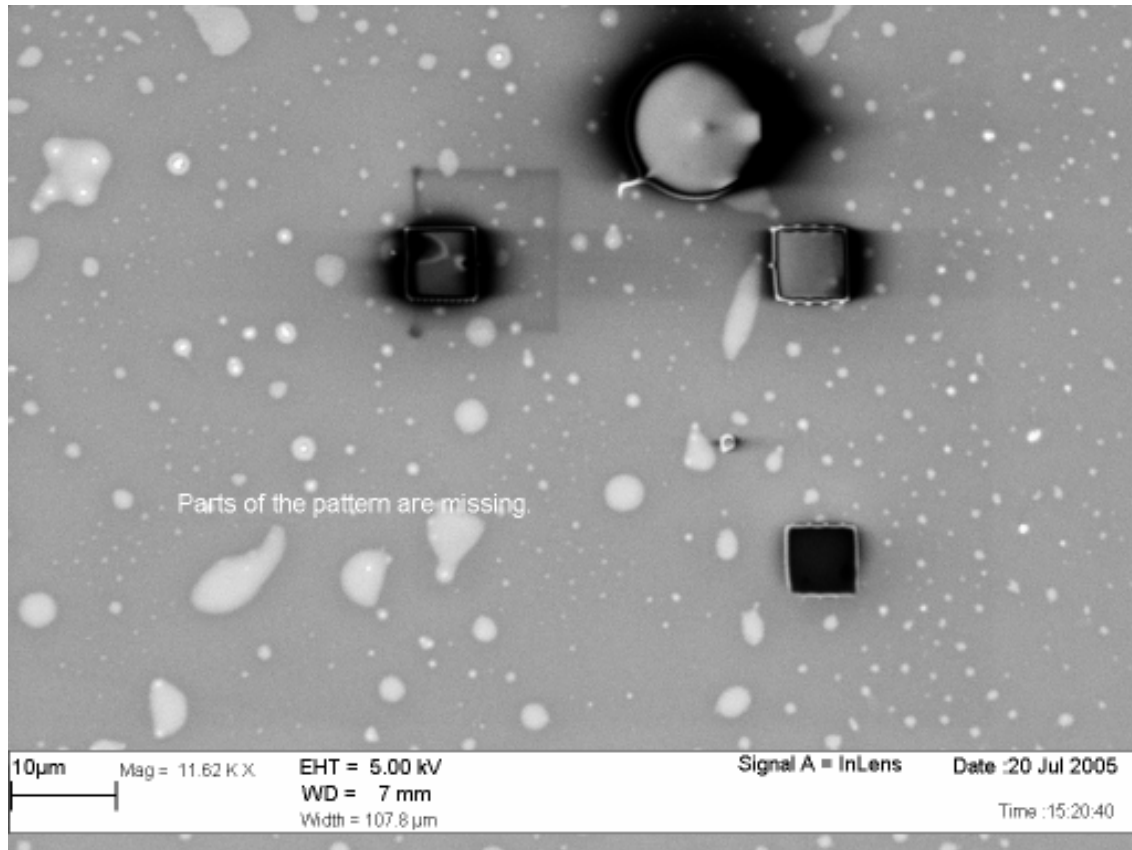


Fig 4.21 The SET structures after development using UVN30 as a resist

The test was a horrible failure as there was a large time gap between the exposure and post exposure bake. The effect of the HMDS layer thickness or the post-exposure bake was overshadowed by the time-delay effect.

We continued to test with UVN30 hoping to observe better results. Henceforth we decided to use line doses to expose the wheel pattern instead of area doses. This would give us a better idea of the resolution capability of the resist system. The wafer specifications, e-beam parameters and the recipe for development are mentioned under fifth UVN30 wafer in Appendix A.

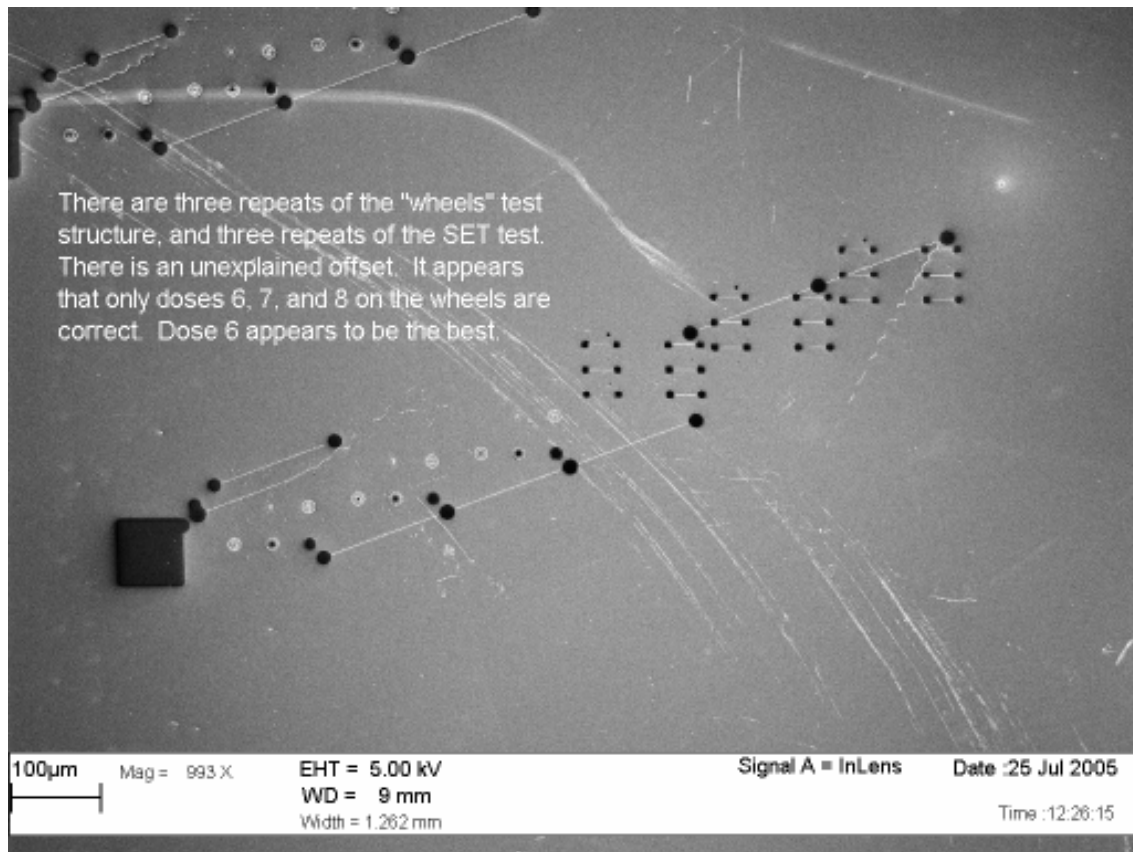


Fig 4.22 The whole pattern of the run file after development using UVN30 as a resist

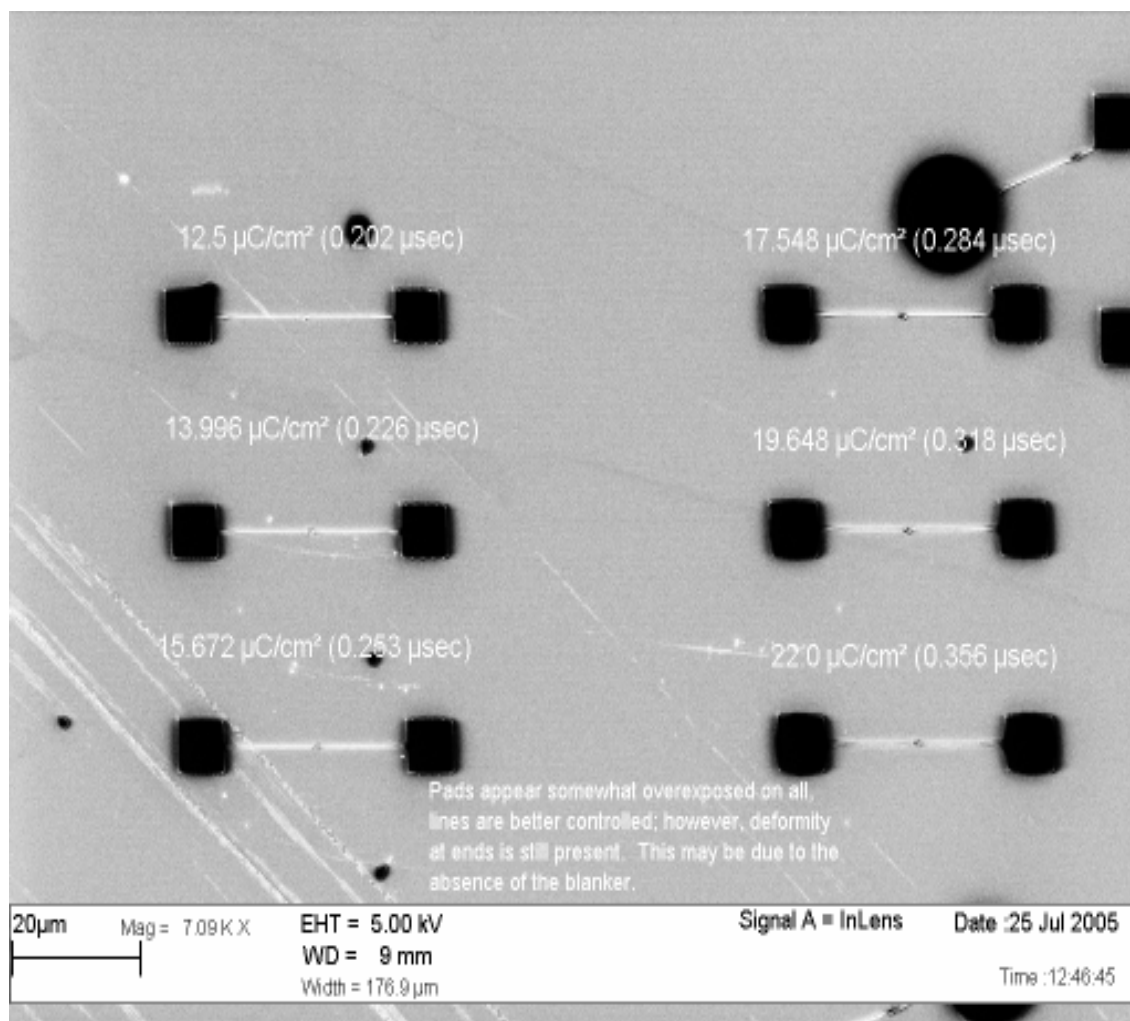


Fig 4.23 The array of SET structures in UVN30

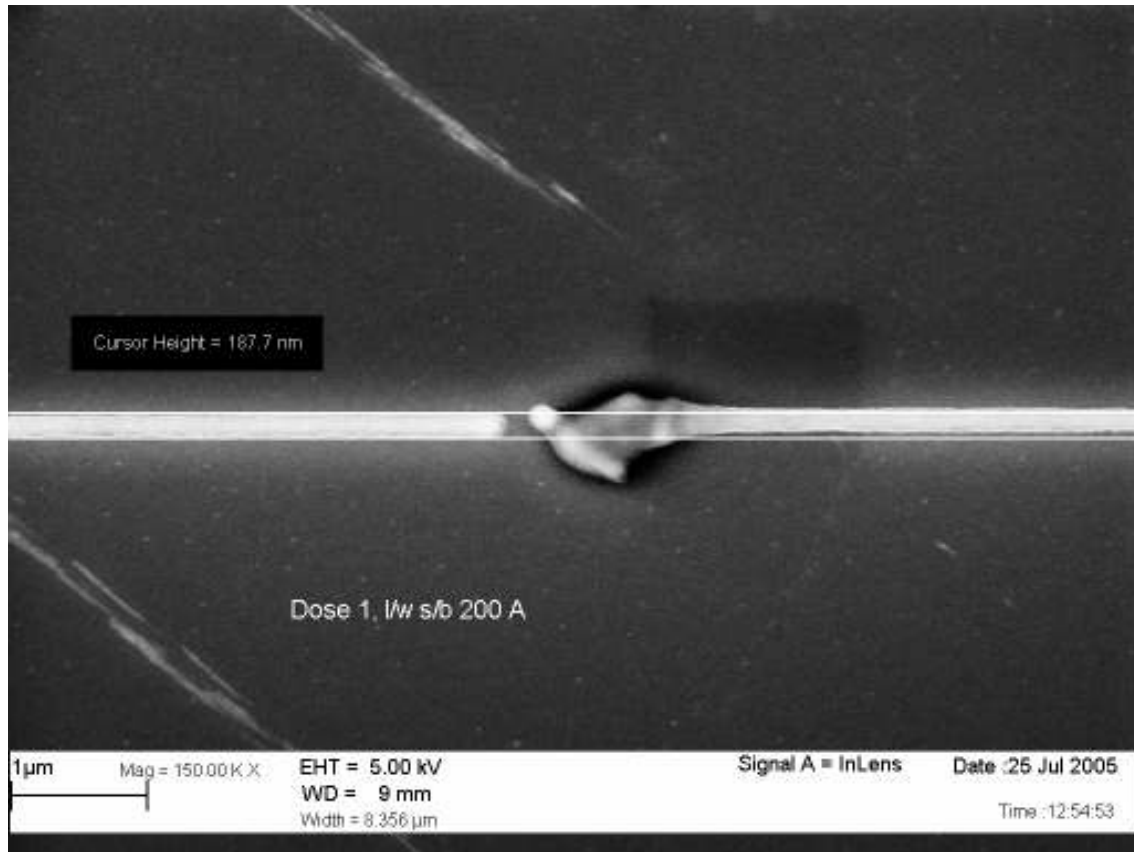


Fig 4.24 The SET structure after development exposed at the lowest dose using UVN30 as a resist

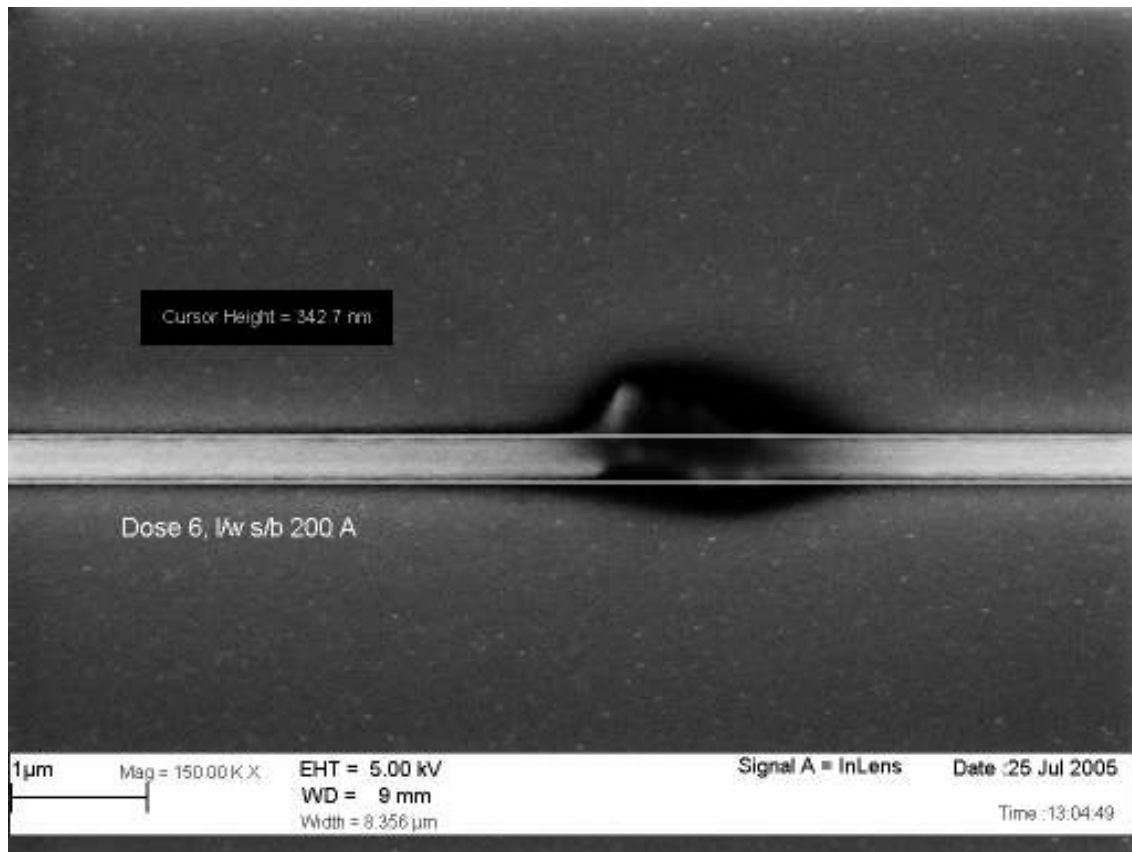


Fig 4.25 The SET structure after development exposed at the highest dose using UVN30 as a resist

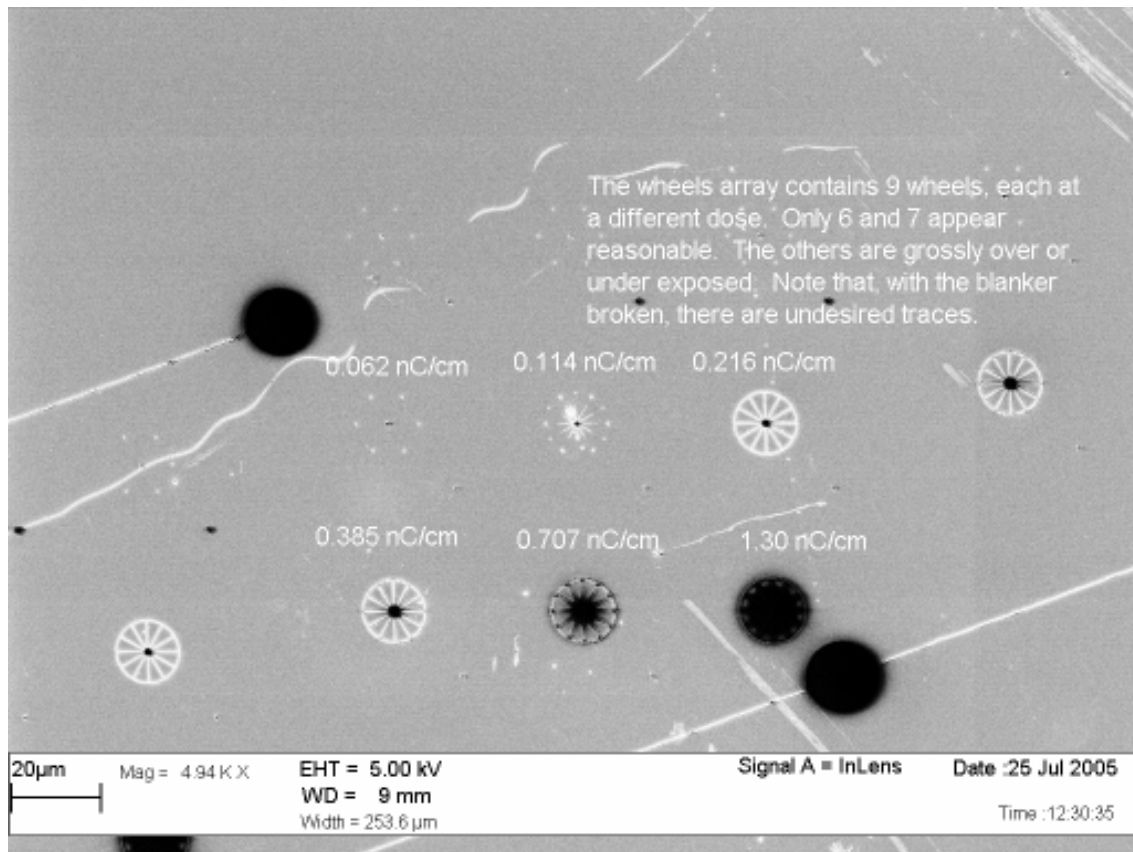


Fig 4.26 The array of wheels after development using UVN30 as a resist

Even at the lowest dose the fingers and island structures were not like those desired. The islands in the middle seemed impossible to pattern exactly as needed, at the time the installed beam blanker was not operational and this definitely could be a factor.

We waited for the beam blanker to be repaired and then conducted the last test with UVN30. The doses were further reduced from the previous test. The wafer specifications, e-beam parameters and the recipe for development are mentioned under sixth UVN30 wafer in Appendix A.

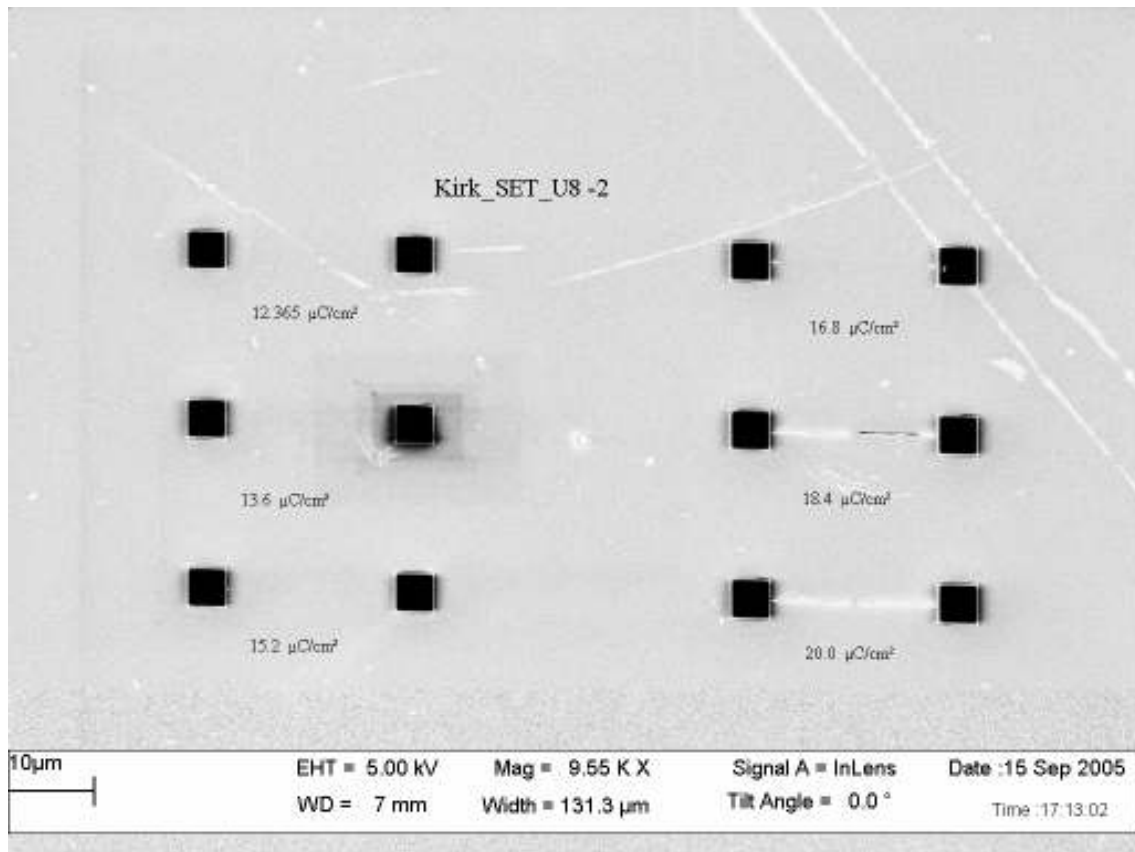


Fig 4.27 The SET array after development using UVN30 as a resist

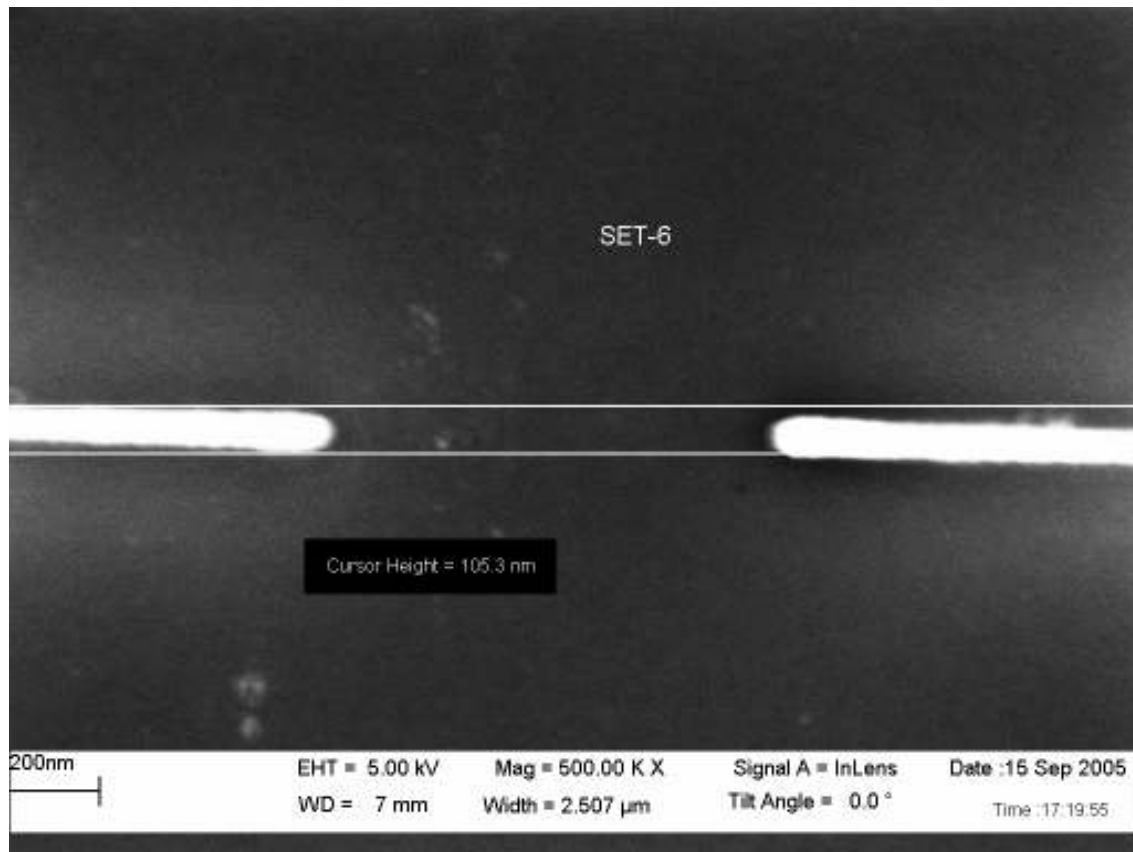


Fig 4.28 The SET structure after development exposed at the highest dose using UVN30 as a resist

The results of this test indicated that even the highest dose was not enough to even define the islands accurately. The width of the fingers at the highest dose were about 105nm, the startling thing about this was that we had gone well below the resolution of UVN30. At the time it seemed like a remarkable discovery but the fingers were so distorted that it was nothing to be enthusiastic about. UVN30 was discontinued because of poor resolution and an irregular resist profile and the results obtained using PMMA were significantly better.

While we tried all the tests with UVN30 we were concurrently working with a lot of samples using PMMA as a resist. The design file for PMMA exposure was

changed. The difference from the most recent UVN30 design file being that the structure was designed over two layers. The fingers and islands were designated to Layer 1 and received area doses. The source and drain pads were designated to Layer 2 and received line doses. The first test involving PMMA was for a totally different pattern involving different dosage techniques and not much could be borrowed from there. The wafer specifications, e-beam parameters and the recipe for development are mentioned under second PMMA wafer in Appendix B.

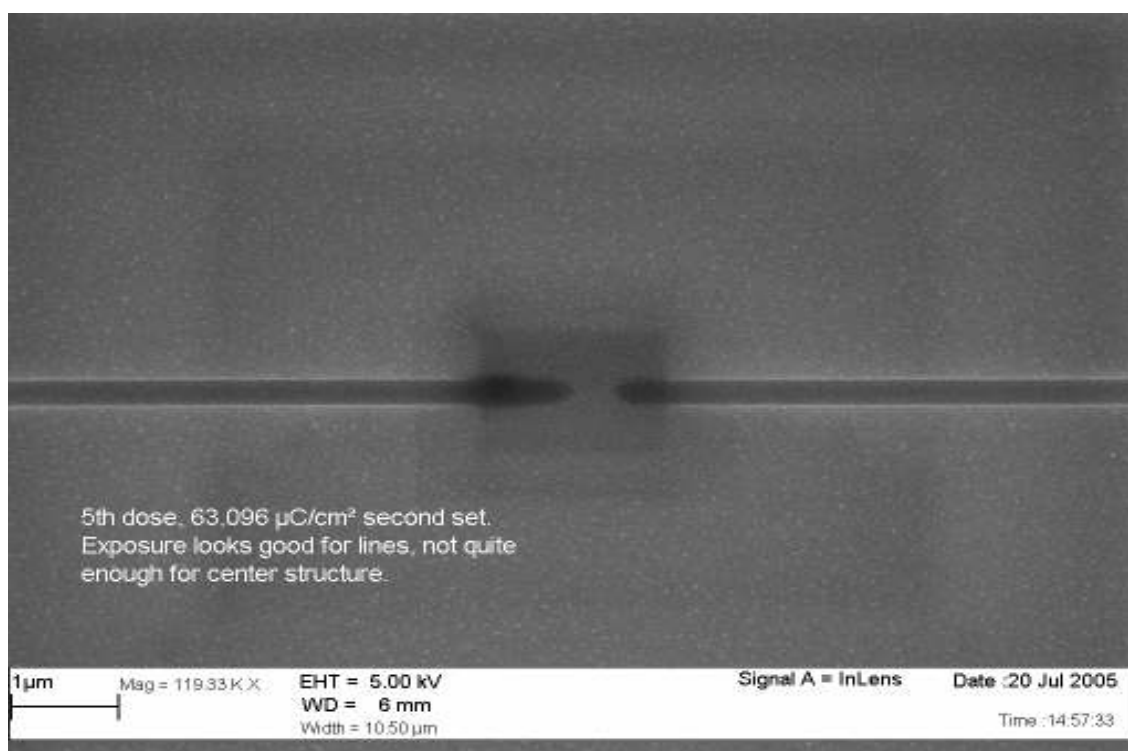


Fig 4.29 The fingers of a SET structure after development using PMMA as a resist indicate that the dose was enough for defining the fingers but not the islands

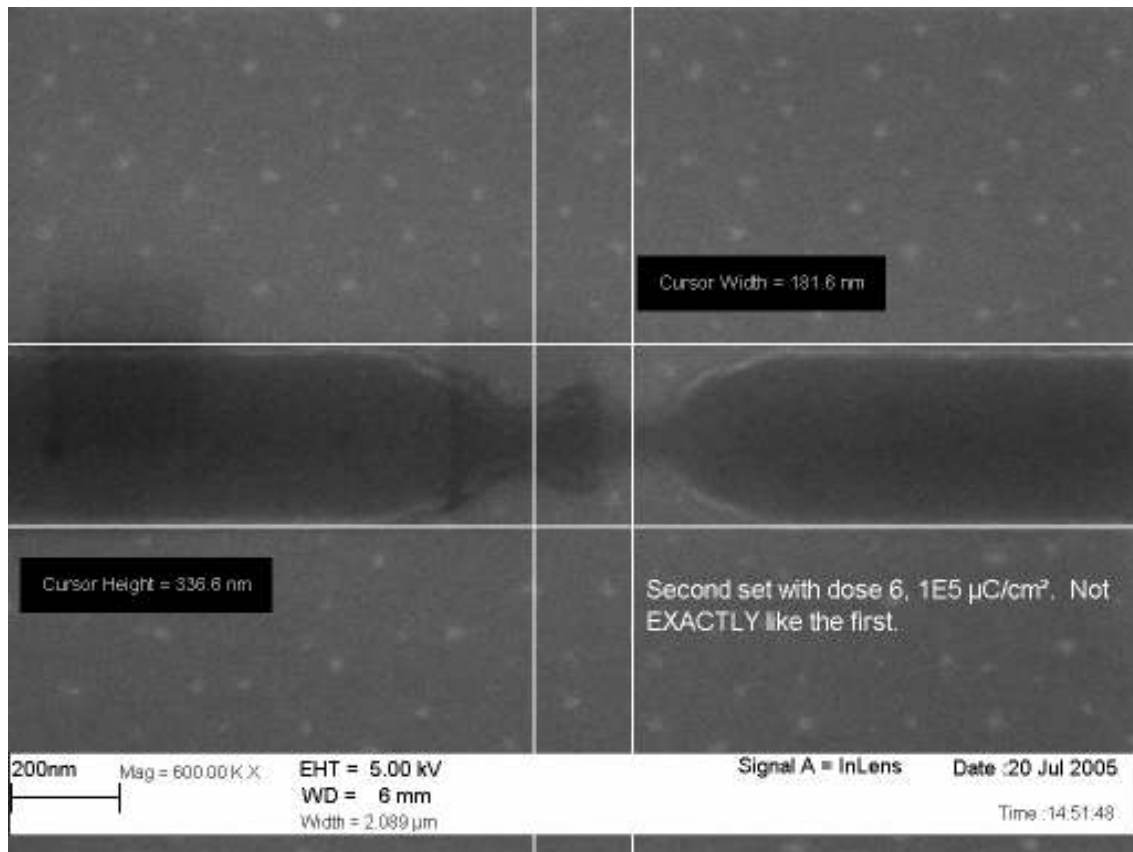


Fig 4.30 The fingers of a SET structure after development using PMMA as a resist exposed with a slightly higher dose than the one above

The aim of the experiment was finding the exact dosage needed for the pattern to be realized exactly as designed, after development. There was a huge error made in the run file though we should have given line doses to the islands and fingers while giving the large 5 micron pads an area dose. This mistake was rectified and the run file altered. For the next test sample we decided to change the PMMA layer thickness by spinning it at a slightly slower speed. The doses were altered too and development time increased. The wafer specifications, e-beam parameters and the recipe for development are mentioned under third PMMA wafer in Appendix B.

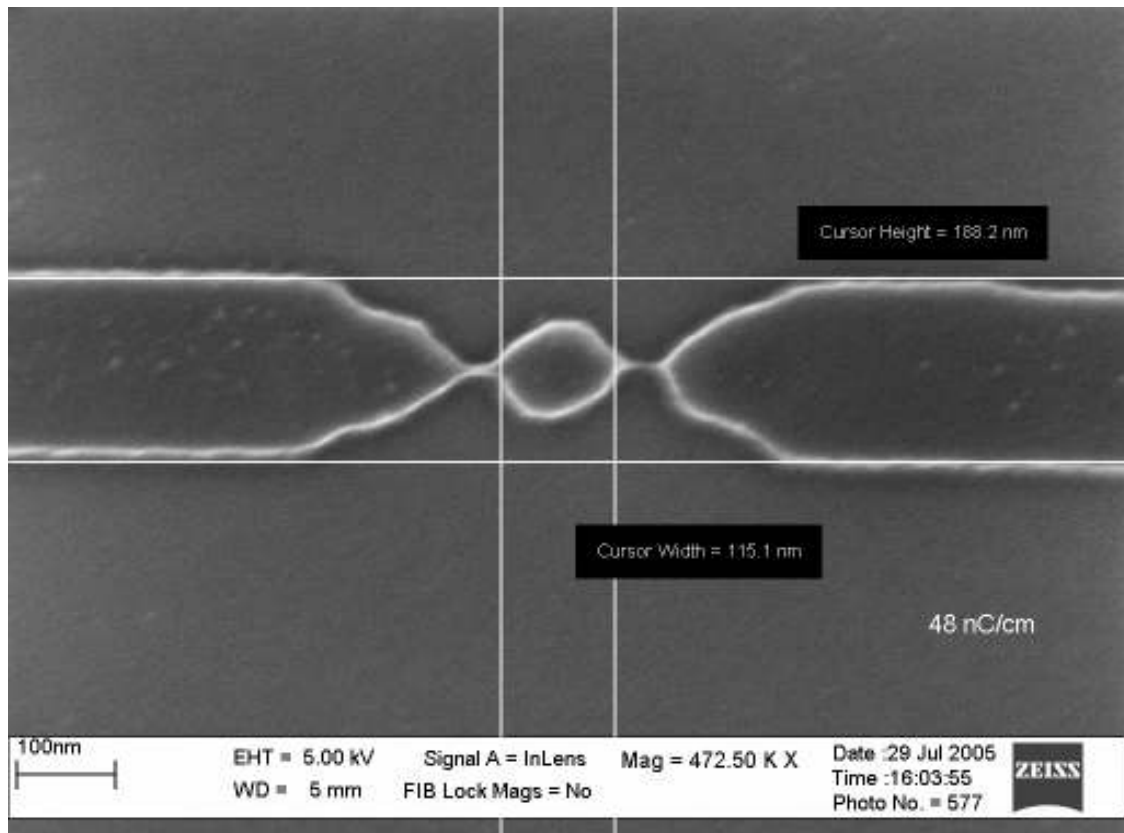


Fig 4.31 The central part of a SET structure after development exposed at the second lowest dose using PMMA as a resist

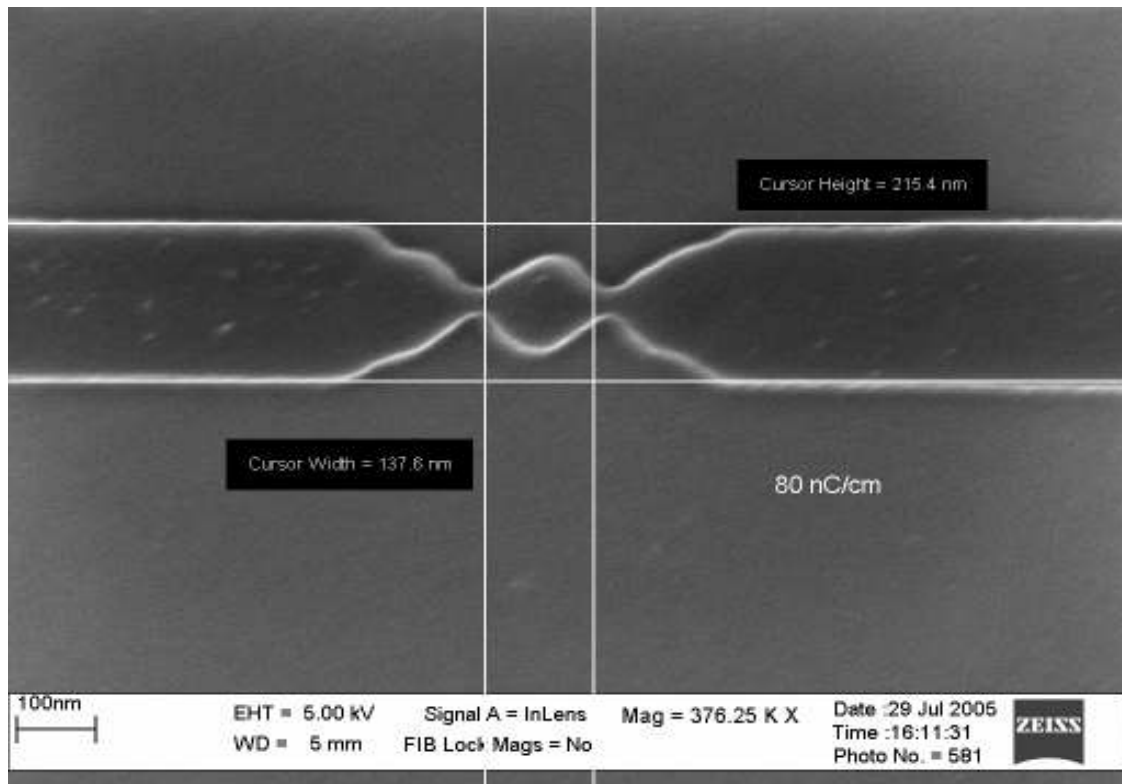


Fig 4.32 The central part of a SET structure after development exposed at the highest dose using PMMA as a resist

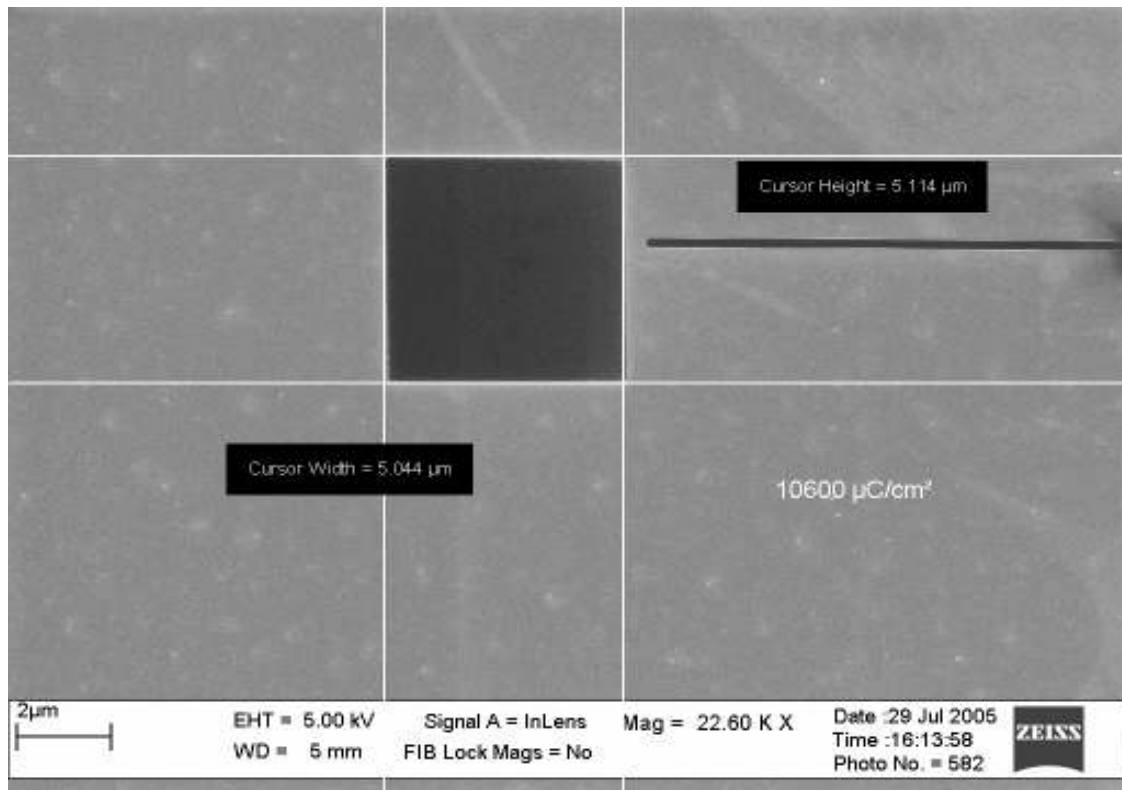


Fig 4.33 The pad of a SET structure after development using PMMA as a resist

The results were moderately satisfactory, the pattern was not exact like the design but we were much closer to gauging the required doses now.

For the next two wafers processed we kept all factors identical to the previous wafer. The only alterations were the spinning speed used to spin coat PMMA on the two wafers. The first wafer was spun at a speed of 4000 rpm for 1 minute and the second at 2500 rpm for 1 minute. The purpose being to study the effect of spin speed (thickness of resist layer) on the ideal doses needed for patterning. The wafer specifications, e-beam parameters and the recipe for development for both wafers is collectively mentioned under fourth PMMA wafer in Appendix B.

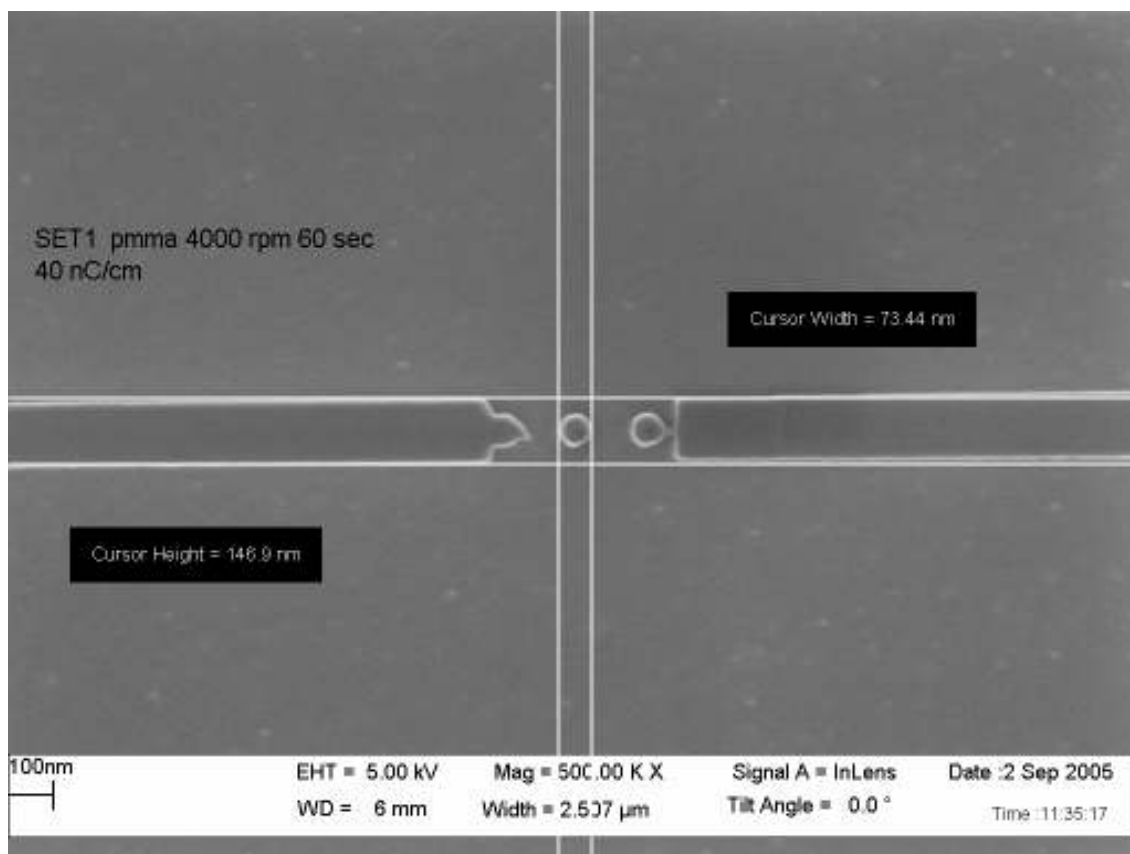


Fig 4.34 The central part of a SET structure after development exposed at 40nC/cm using PMMA as a resist

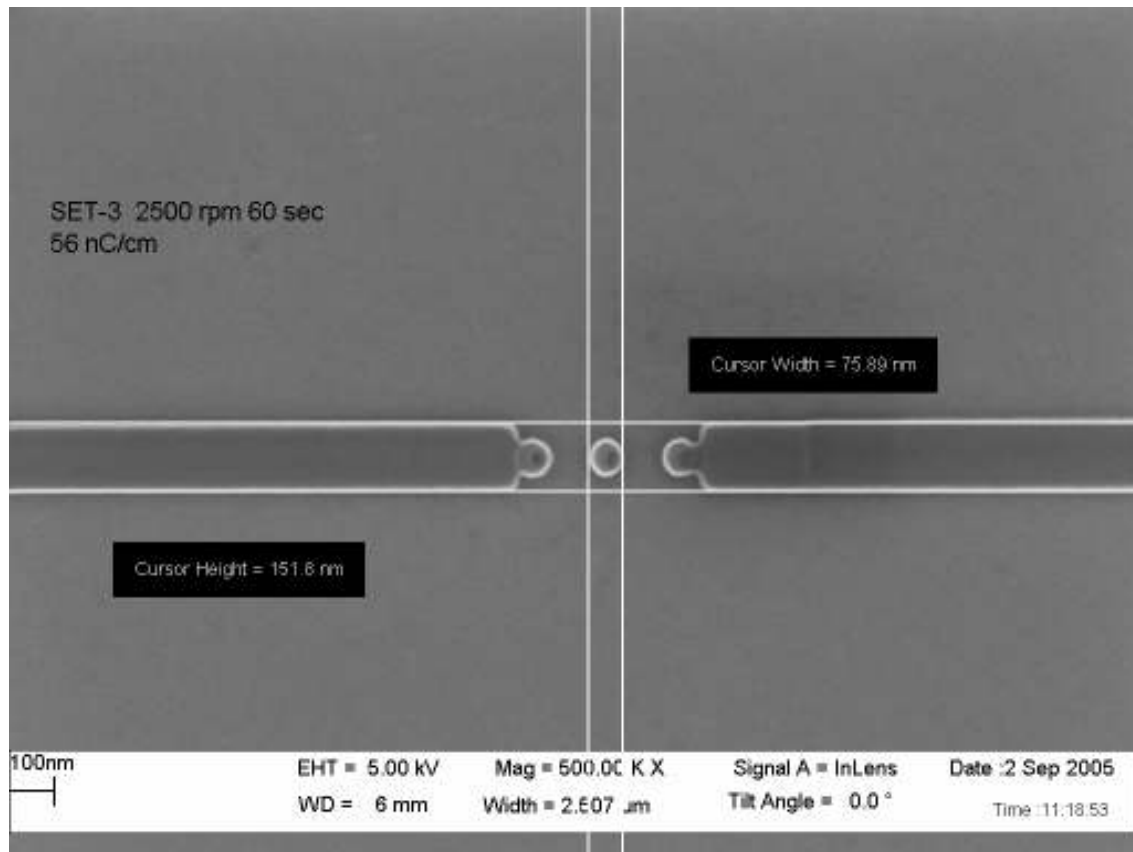


Fig 4.35 The central part of a SET structure after development using PMMA as a resist. The test indicated that ideal doses needed to pattern wafers with different resist layer thicknesses varied considerably. For the wafer with a thin layer (4000 rpm) the ideal structure was obtained at an exposure dosage of 40nC/cm whereas in the case of the much thicker layer (2500 rpm) a higher dose of 56nC/cm was needed for ideal patterning. This could be attributed to the fact that for a thicker resist layer a heavier dose is needed to perform to same extent of penetration that a lower dose does in a thinner layer. For the same set of wafers we also observed the best resolution for PMMA in one of the lines of a wheel structure.

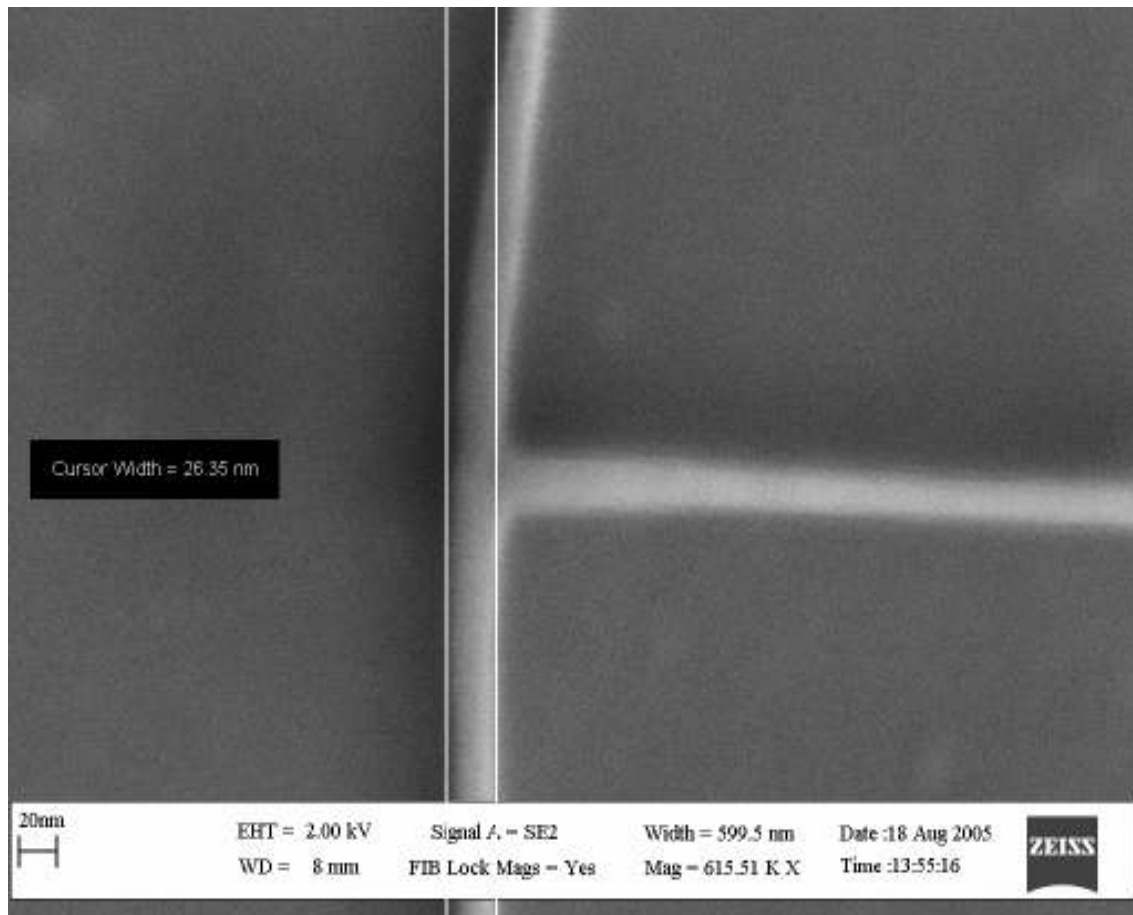


Fig 4.36 The edge of a wheel after development using PMMA as a resist. It indicates the best resolution possible with PMMA

The problems with PMMA started when we tried to etch silicon in the Technics Micro-RIE using CF_4 and O_2 using the patterned PMMA as an etch mask. The conditions for the test are mentioned under first PMMA test in Appendix D. The first test was conducted for 30 minutes where no PMMA was left on the wafer at the end. For the next few tests all the conditions were kept constant except the etch time which was reduced drastically down to 5 minutes but still the PMMA did not last through the etching. I decided to stop using O_2 hoping that it would prove successful but even with just CF_4 , PMMA was not to be found on top of the wafer.

A test was conducted to see the effect of the e-beam dose on the etching durability. The large 50 micron pads were given a very high dose of $50000\text{nC}/\text{cm}^2$ instead of the usual $15000\text{nC}/\text{cm}^2$. The pad was then etched in just CF_4 plasma at half the usual power for just 30 seconds. The test conditions are mentioned under second PMMA in Appendix D. The PMMA was found still on top of the wafer and a small amount of the silicon was etched too. Another similar pad was etched in the same fashion but with O_2 at a very low gas flow rate this time the PMMA was gone though. The test conditions are mentioned under third PMMA test in Appendix D.

It is known that pure CF_4 yields a low etch rate for Si. The trick is to add small amounts of O_2 . The etch rate for Si continues to increase until about 12% of O_2 is present in volume. A slight addition of O_2 was having a horrible effect on PMMA though. We had to devise another way to transfer the pattern to the silicon layer.

We decided to try to coat the wafer with wafer with 62.8 nm of Aluminum before spinning on PMMA. The details for the experiment are mentioned under PMMA and Al test in Appendix D. A 50 micron pad was exposed with a very high dose and then development followed. Then an aluminum wet etch was conducted this was done to remove Al from areas which was not covered by the developed PMMA. The underlying Si now had to be etched so we placed it in the Technics Mirco-RIE using just CF_4 and not O_2 since with oxygen in the mixture would oxidize aluminum. The etch was monitored carefully to observe if there was any removal of Al during the etch. After a total etch time of 12 minutes I decided it was enough.

The remaining Al was now removed using a wet etch again. The SEM was used to examine the sample.

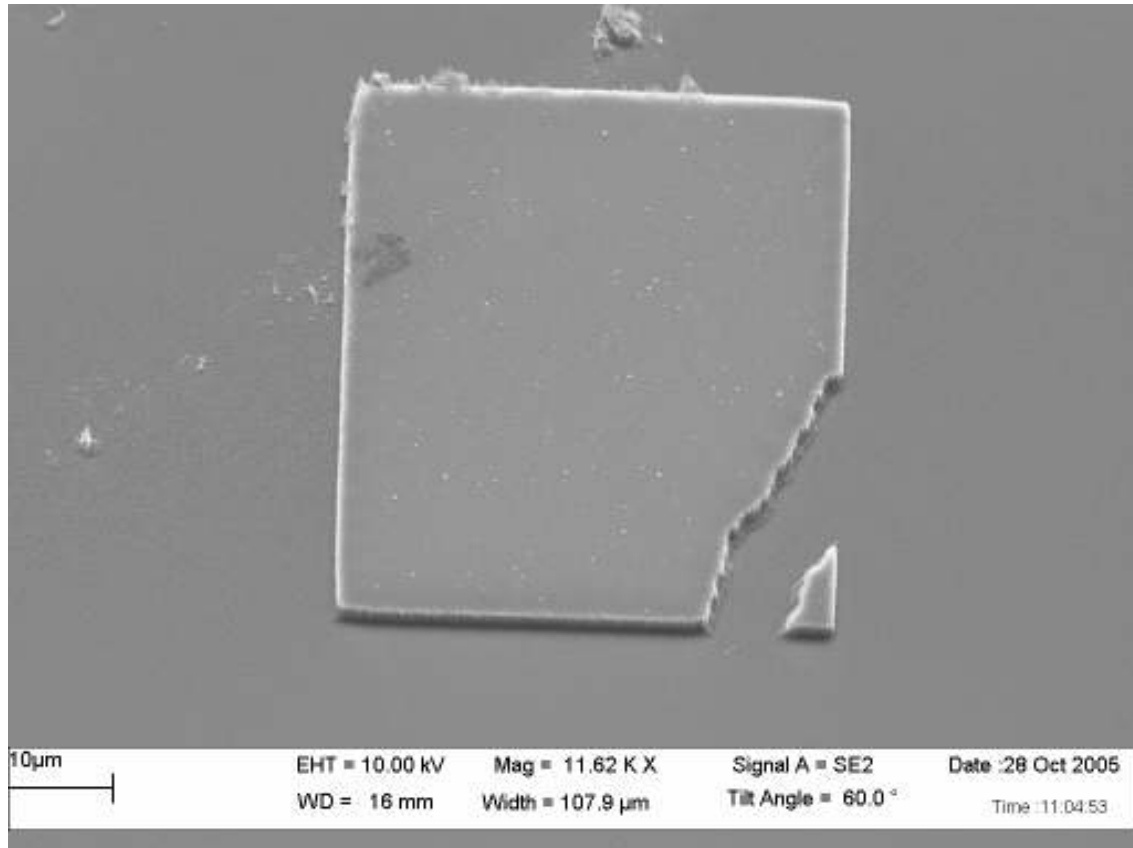


Fig 4.37 The 50 micron silicon pad left after aluminum removal

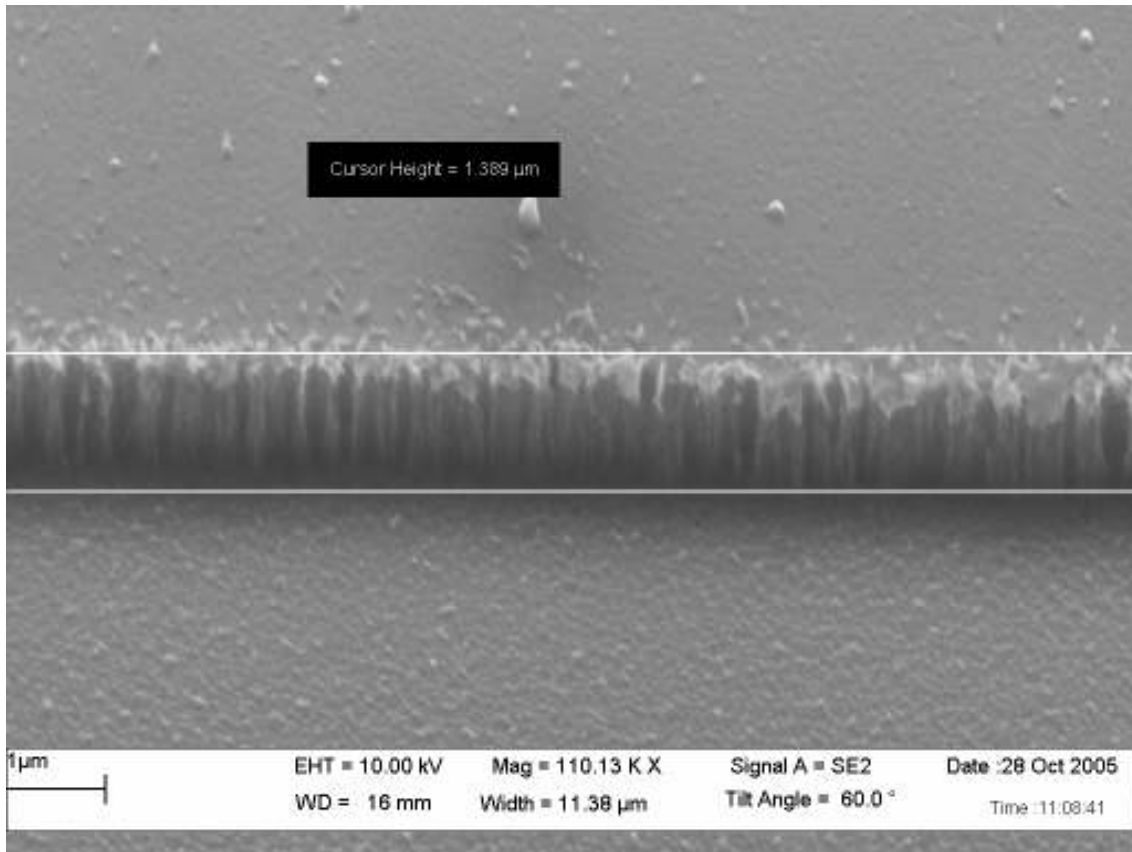


Fig 4.38 The sidewall of the 50 micron pad after aluminum removal.

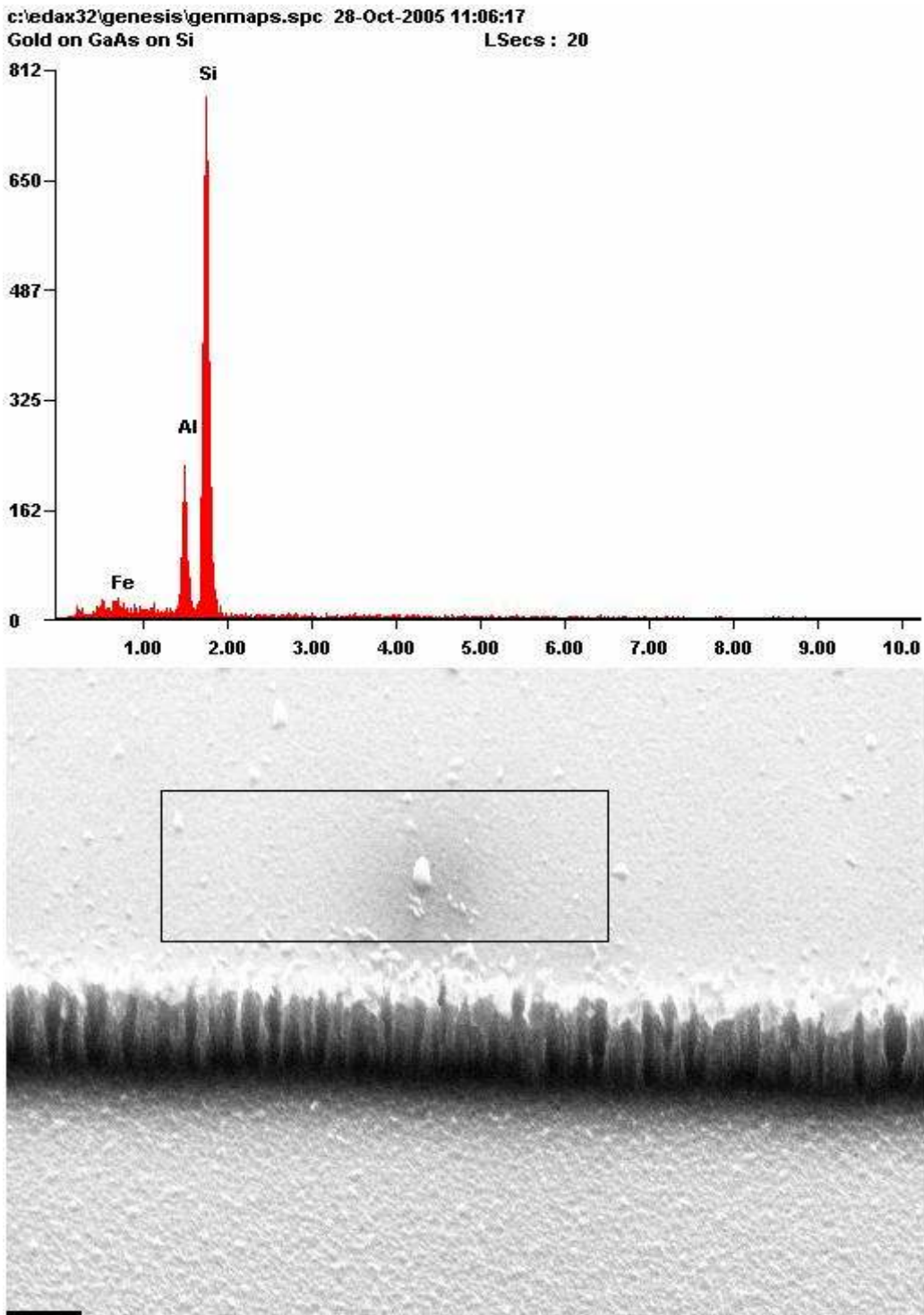


Fig 4.39 EDX of the top of the pad after RIE and aluminum etch

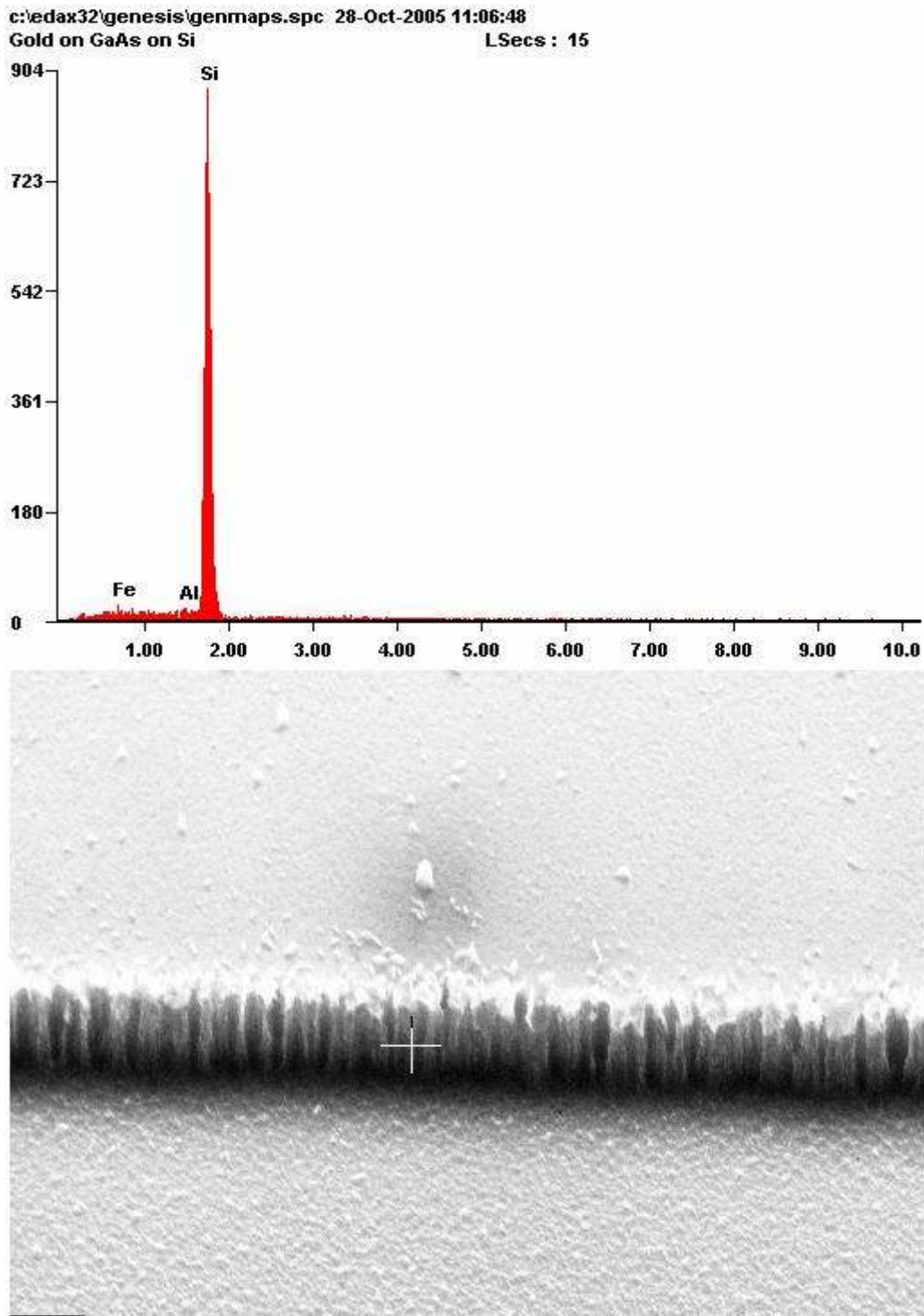


Fig 4.40 EDX of sidewall after RIE and aluminum etch

The EDX spectra indicate that after the second wet etch all the aluminum was removed and we had successfully managed to etch silicon. During the real fabrication all we would need was to etch 55nm of silicon. The issues with this approach was that resolution decreased when it came to finer structures and there was serious undercut after performing wet etching. This approach was hence abandoned.

A test was conducted to also inspect the etch resistance of UVN30 with O₂ and CF₄ plasma for about three minutes and the UVN30 seemed to withstand the etch and allowing the unwanted silicon too be etched away. The resolution of the resist was the only issue.

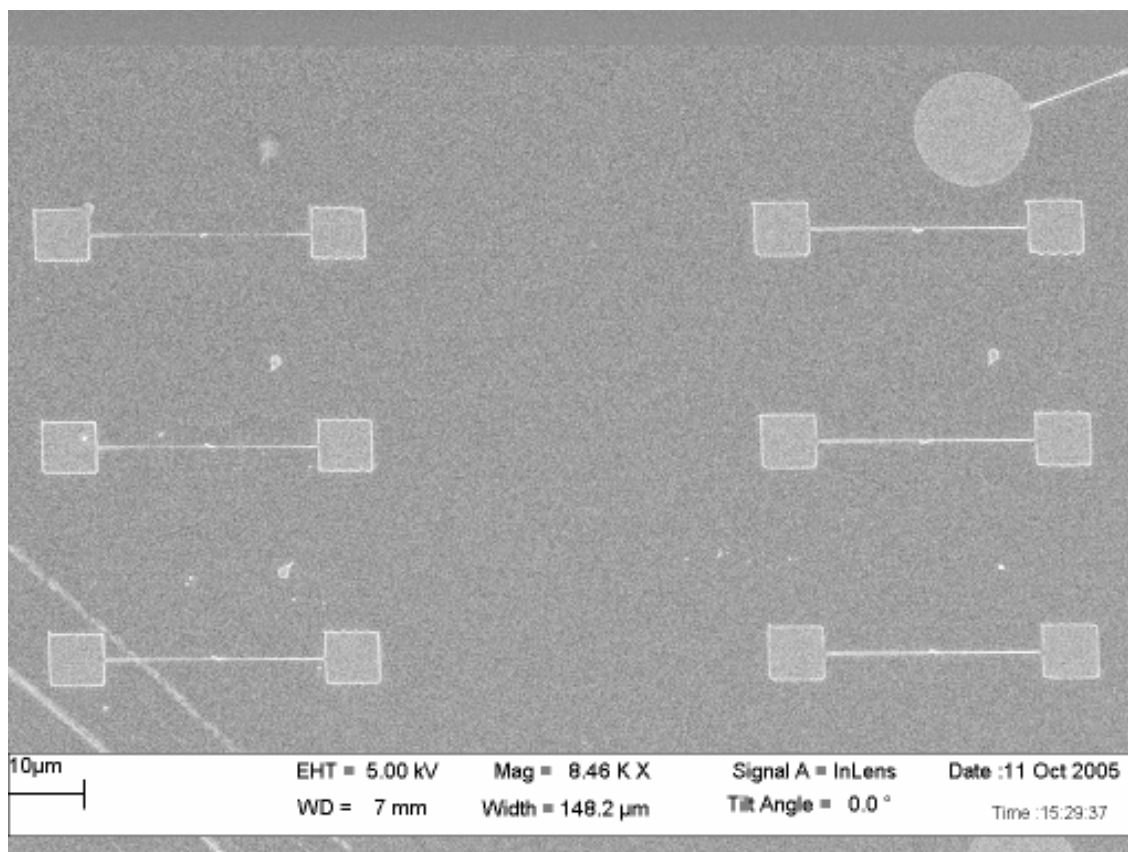


Fig 4.41 The SET array after RIE with UVN30 acting as an etch mask

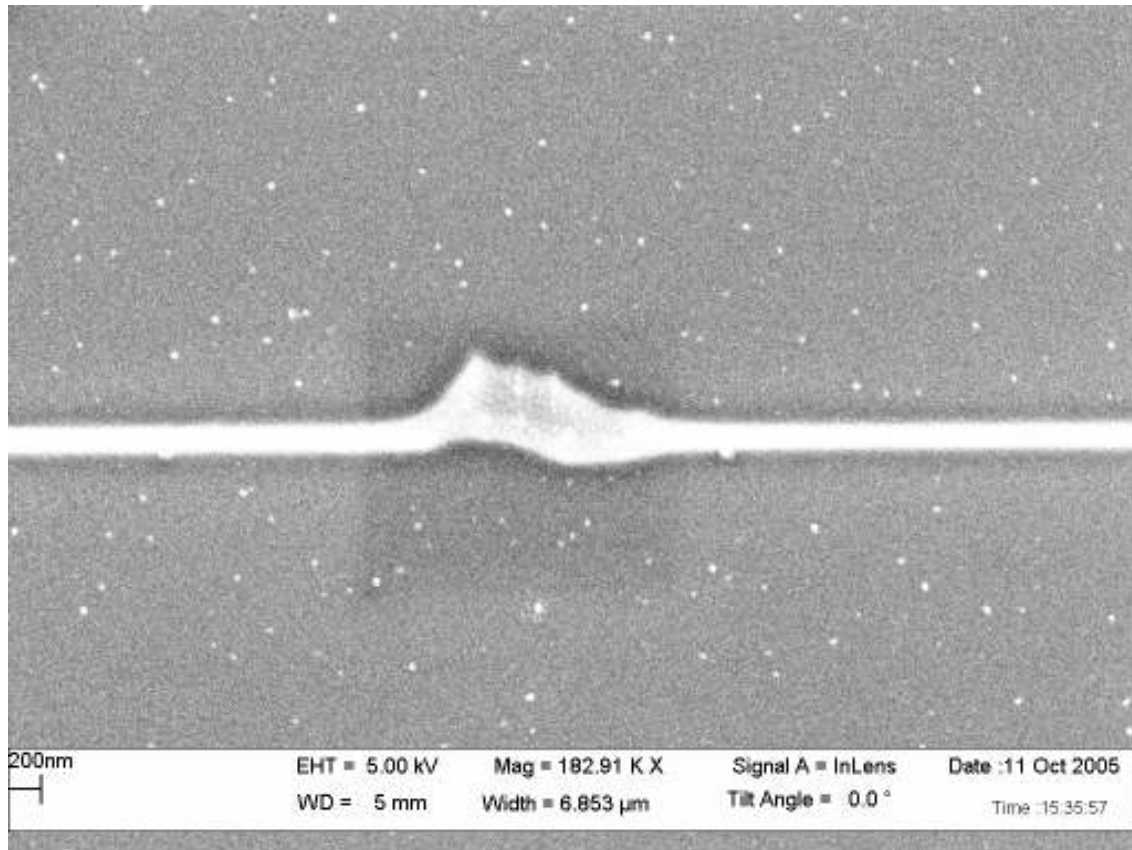


Fig 4.42 The central part of a SET structure after RIE using UVN30 as an etch mask

4.4 HSQ tests

As we looked for more resists that we could opt for we obtained a few milliliters of HSQ (XR-1541) from Mr. Preston Young and thought about giving it a shot. Not a whole lot of documentation on the resist existed since it was fairly new. The resist though held a lot of promise and very small features had been fabricated by a few researchers around the globe.

For the first tests with HSQ the design file and the run file was borrowed from the last PMMA exposures. For the first test the doses were slightly altered from that used for PMMA exposures. To our amazement we obtained good results. The wafer

specifications, e-beam parameters and the recipe for development are mentioned under first HSQ wafer in Appendix C.

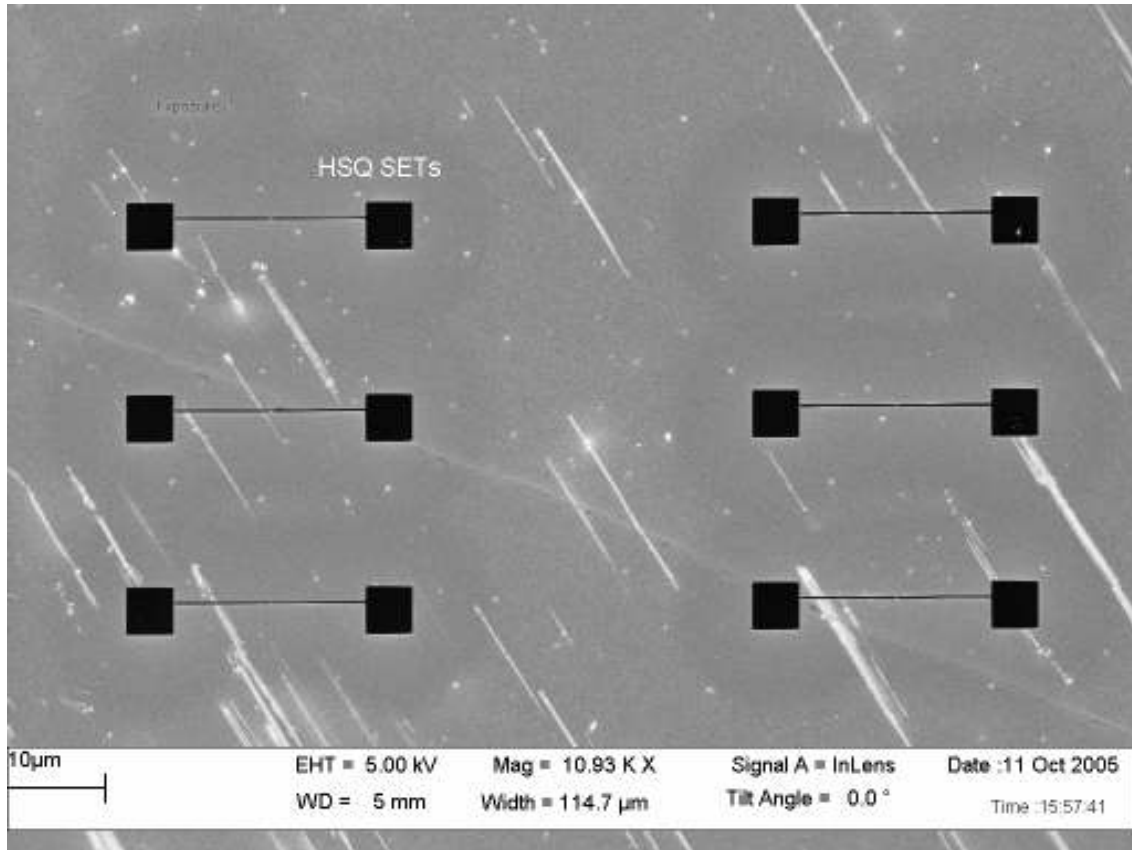


Fig 4.43 The SET array after development using HSQ as a resist

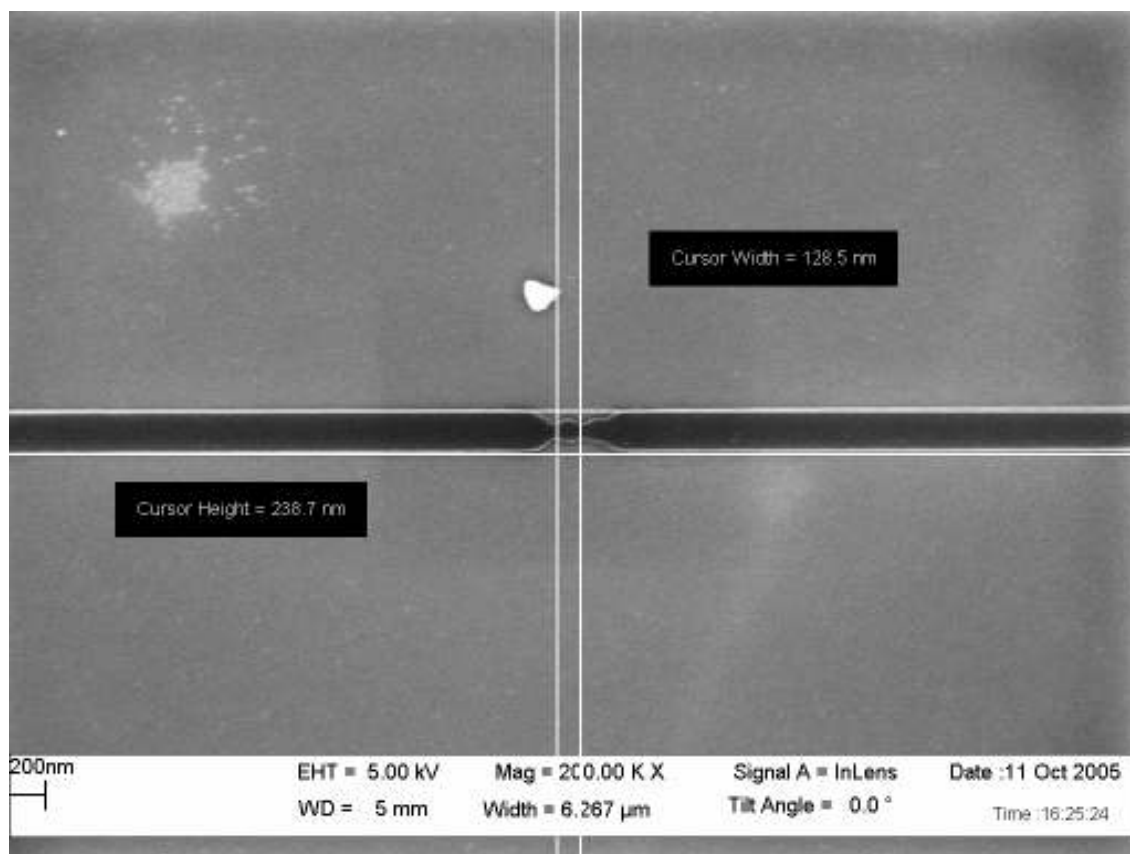


Fig 4.44 The SET structure after development exposed at the lowest dose using HSQ as a resist

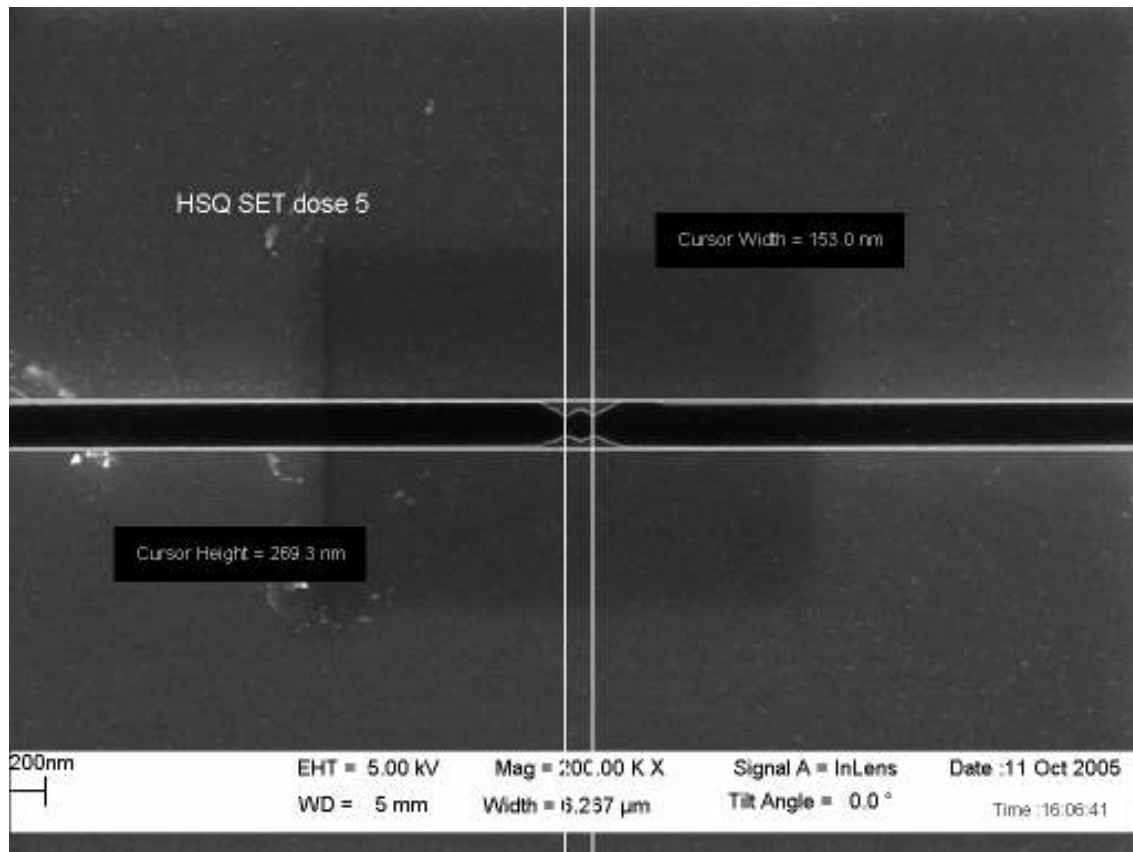


Fig 4.45 The SET structure after development exposed at the highest dose using HSQ as a resist

Another test was conducted soon after the above one with the exact e-beam parameters to try and repeat results. The spin speed, pre exposure bake conditions, post exposure bake conditions and development strategies were changed. I borrowed them from an unpublished paper claiming that those conditions were ideal for HSQ based lithography. This time the wafer was not examined after development rather it was etched in the Technics Micro-RIE using a CF_4 at a low gas flow rate and then examined under the SEM. The observations were different this time though. The wafer specifications, e-beam parameters and the recipe for development and etching

parameters are mentioned under second HSQ wafer in Appendix C. The etching conditions are listed under first HSQ test in Appendix D.

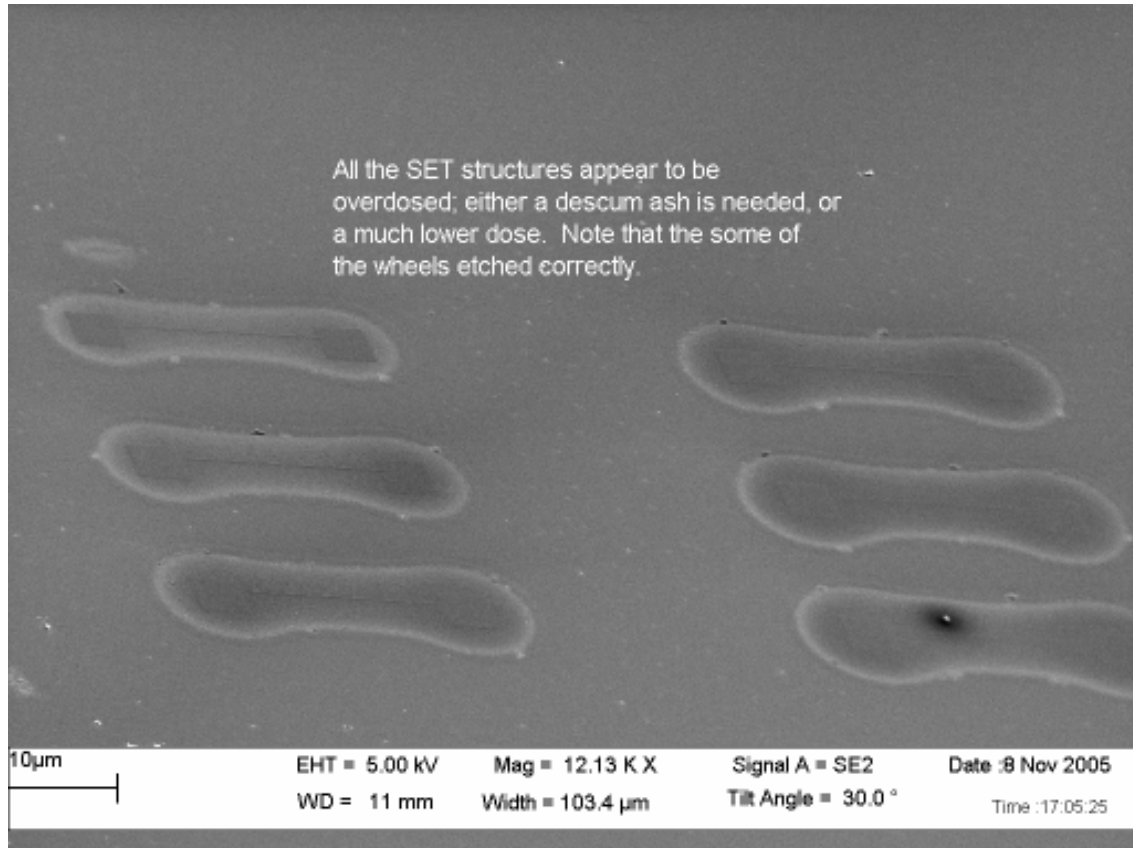


Fig 4.46 The SET array at a 60° tilt after RIE using HSQ as etch mask

The structures seemed to be overdosed. It would have better if we did check for this after development but we went back to the other wafer and when the brightness and contrast was altered on that wafer, we did notice a halo like effect around the structures there too. Our initial excitement was subdued to a silent lull now.

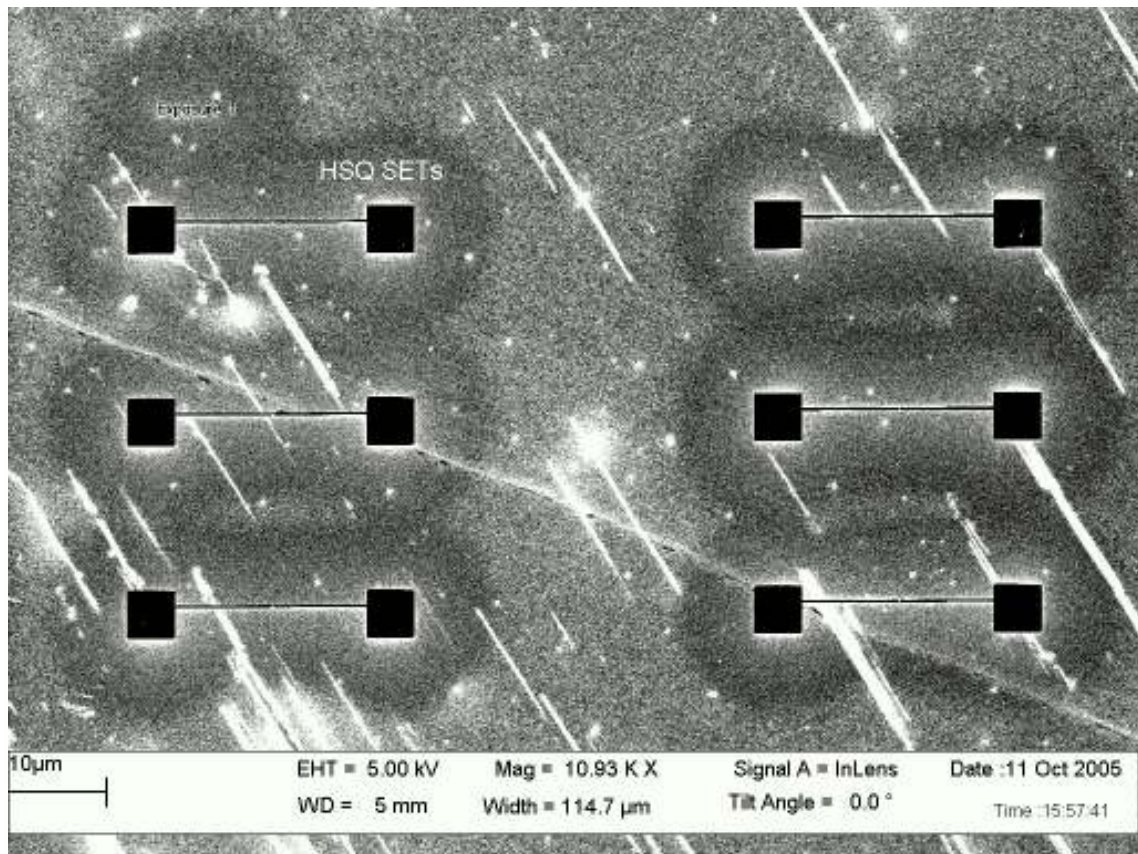


Fig 4.47 The SET array from the first HSQ wafer with the brightness and contrast adjusted

This was something we had not observed with the other resists. Alongside with this wafer we had also processed a wafer which had aluminum evaporated on its surface prior to HSQ being spun on. Then exposed and unwanted Al not covered by HSQ was removed with an aluminum etchant. All other parameters were maintained. It was then etched exactly like the above wafer. The wafer specifications, e-beam parameters and the recipe for development are mentioned under first HSQ and Al wafer in Appendix C. The etching conditions are listed under first HSQ and Al test in Appendix D.

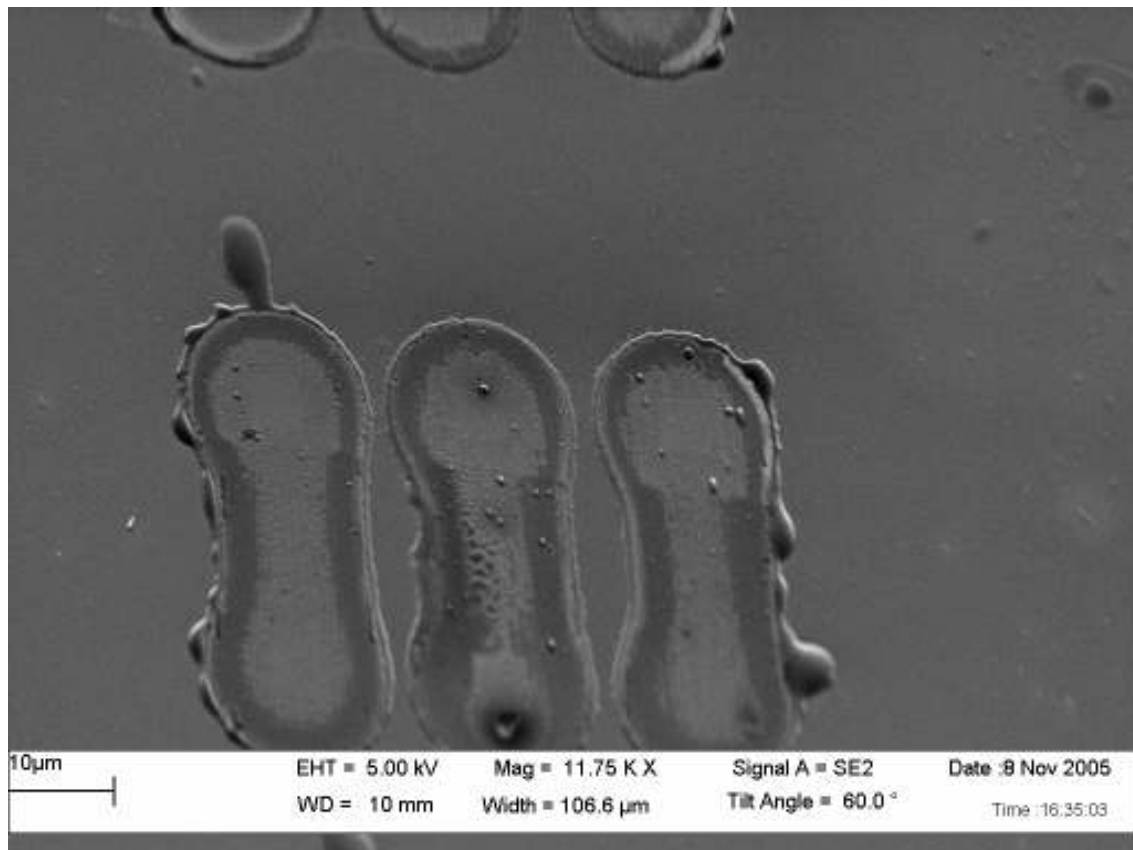


Fig 4.48 The SET structures at a 60° tilt after RIE using Al and HSQ as etch masks. The results here were even worse. This strategy was scrapped i.e. using an Al layer, as more tests provided very disappointing results. We did not tackle the halo effect problem rather concentrated our efforts on testing the etching resistance of HSQ.

I attempted numerous strategies by modifying most of the RIE parameters. Gas flow rate, power settings and etch durations were varied for samples with developed HSQ acting as an etch mask after e-beam exposure. The main problem lie in the fact that after e-beam exposure the chemical structure of HSQ became similar to that of an oxide of silicon and the etch had to be to very selective. Silicon had to be etched without etching HSQ. The best results were found when only 7sccm of CF₄ was used,

the power turned down to 75 Watts and a etch time of 60 seconds. The wafer specifications, e-beam parameters and the recipe for development are mentioned under third HSQ wafer in Appendix C. The etching conditions are listed under second HSQ test in Appendix D.

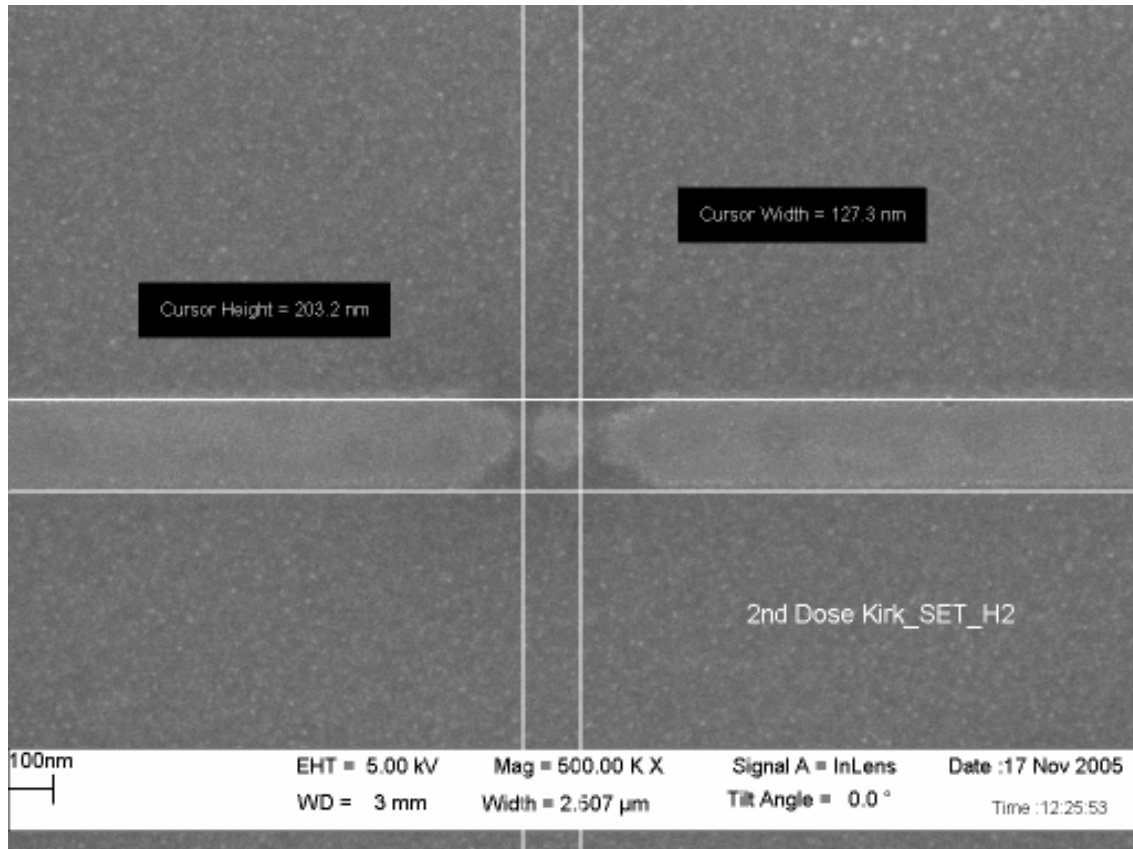


Fig 4.49 The SET structure after RIE using HSQ as an etch mask

For samples that were etched for durations above 60 seconds no structures could be observed using the SEM. It was evident that HSQ was being removed (ashed) without any significant amount of silicon being etched. Utilizing low CF_4 flow rates and reduced power for such short periods in the RIE etching even a few nanometers of silicon seemed impossible. During this period a slew of research papers had been

published; most of them employing a chlorine based electron cyclotron resonance (ECR) etching strategy in their experiments. The use of HBr in the RIE was also being suggested to be selective in removing silicon without attacking SiO₂ significantly. None of these strategies could be used utilized since we did not have the facilities for the processes. Using chlorine or HBr cylinders and connecting them to the existing Technics Micro-RIE was not an option as they are known to be toxic and corrosive gasses.

At this juncture Dr. Ley decided to pursue a career elsewhere quitting his job at Nanofab, Dr. Basit was now responsible for the e-beam lithography and SEM imaging. I had a word with him about the presence of the so called halo effect to which he suggested that the doses being administered were too high. The run file was modified and the doses were reduced significantly. On this occasion it was decided that we would inspect the wafers under the SEM after development without subjecting the wafer to etching. The wafer specifications, e-beam parameters and the recipe for development are mentioned under fourth HSQ wafer in Appendix C.

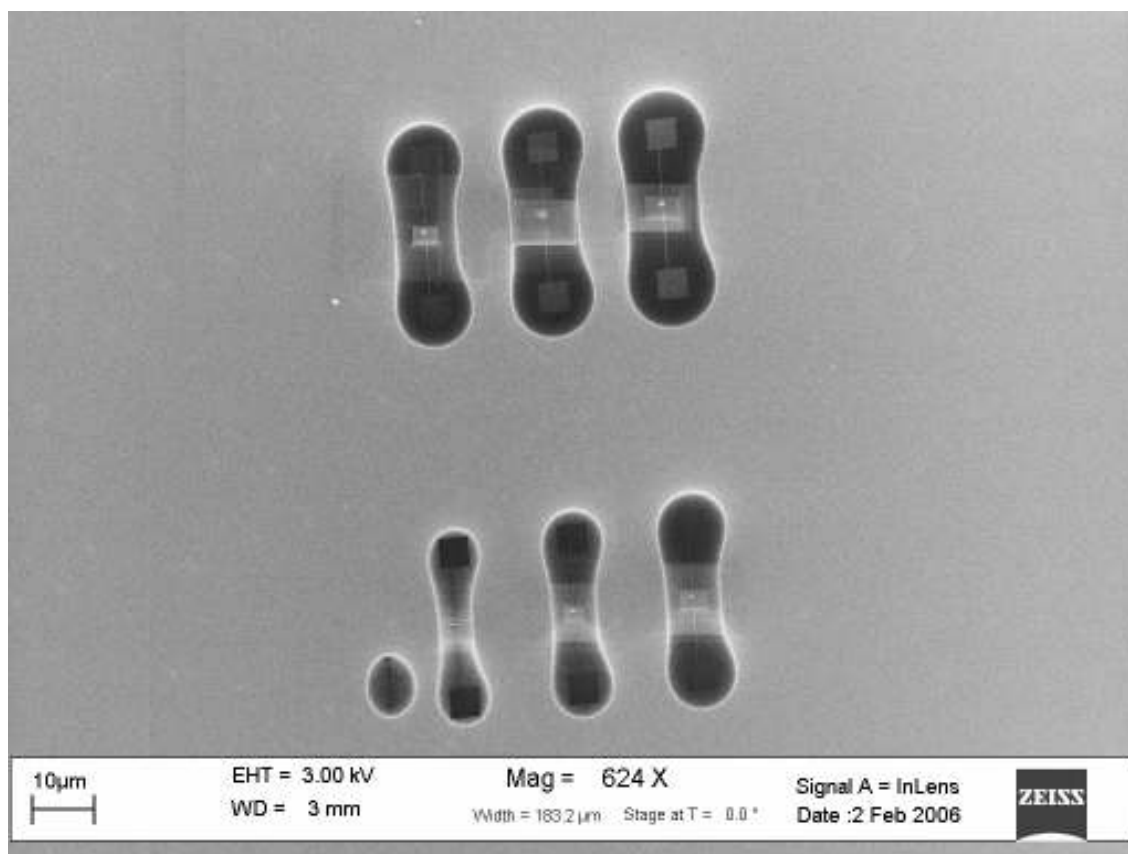


Fig 4.50 The SET array after development using HSQ as a resist

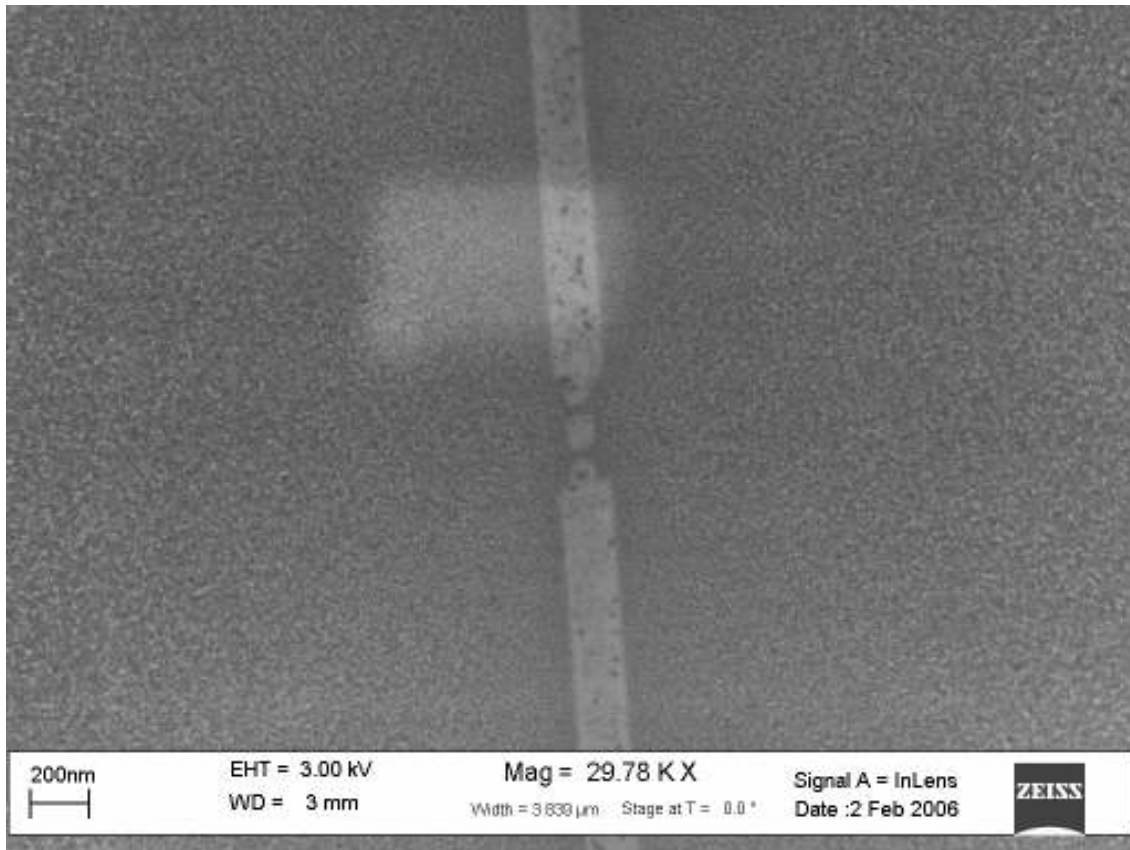


Fig 4.51 The SET structure after development exposed at the lowest dose using HSQ as a resist

Clearly we were able to see from the array image that for structures exposed with low doses the halo effect was less pronounced. The halo effect still existed in the lowest dose structures too. On closer inspection of the structures the images seemed grainy around the structures. It was concluded that either the doses were too high or the development procedure was inadequate. Samples with varied development times were tested but the results were not very encouraging.

W.-C. Liu et al. [21] contained details about the effect of a temperature curing process on the molecular structure of HSQ. The transformation of the molecular structure after a long high temperature exposure was similar to a short exposure under

an electron beam. The effect of a high temperature cure on the hardness of HSQ was studied by Liou and Pretzer [22]. The paper suggested that a high temperature bake conducted for a long duration increased the hardness of HSQ manifold. I thought about incorporating a high temperature bake after development to examine any improvement in the etching durability of HSQ. I thought about incorporating this into my procedure and for the first few tests the results were not that encouraging. The etching durability was enhanced but not significantly. There was some documentation on how an O₂ plasma treatment for HSQ prior to etching would enhance its etching durability I planned to introduce a low flow of O₂ gas into the chamber along with CF₄. The strategy being that this small amount of oxygen would firstly help etch silicon faster and also prevent the HSQ removal whose structure, is similar to that of silicon dioxide, after e-beam exposure. The combination of the bake and introduction of O₂ was moderately successful but gave me hope that HSQ would be a suitable resistance to continue experimentation with.

I planned to start working with pieces of the SOI wafer henceforth. This would be slightly different from the poly-Si wafer since the top layer of the SOI wafer was single crystal silicon. The most substantial difference being the deviance in etch rates. For the first tests the same procedure for spinning, exposure, development were carried out then the wafer was baked in a inert atmosphere at 400°C for 30 minutes. The wafer specifications, e-beam parameters and the recipe for development are mentioned under fifth HSQ wafer in Appendix C.

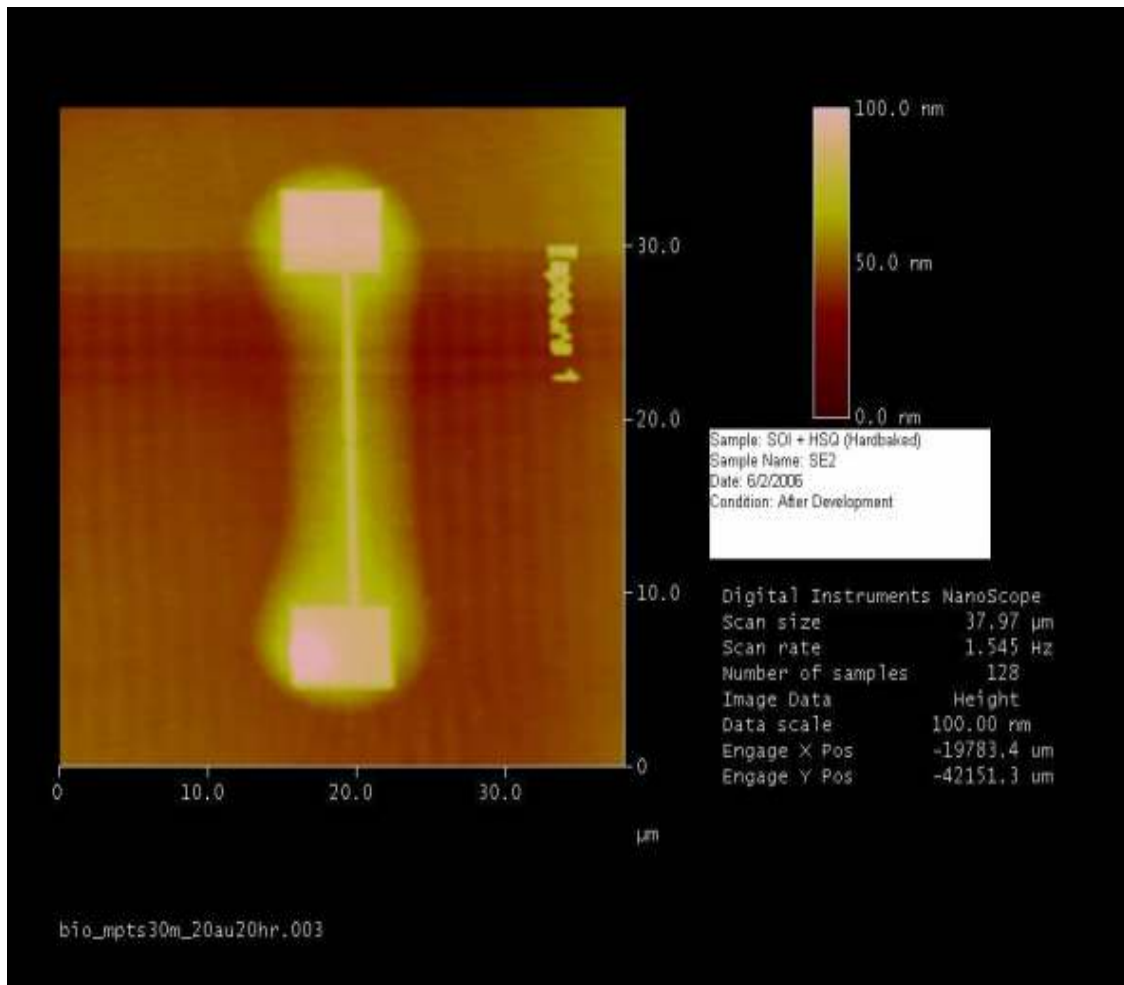


Fig 4.52 AFM image of the SET structure after thermal curing using HSQ as a resist

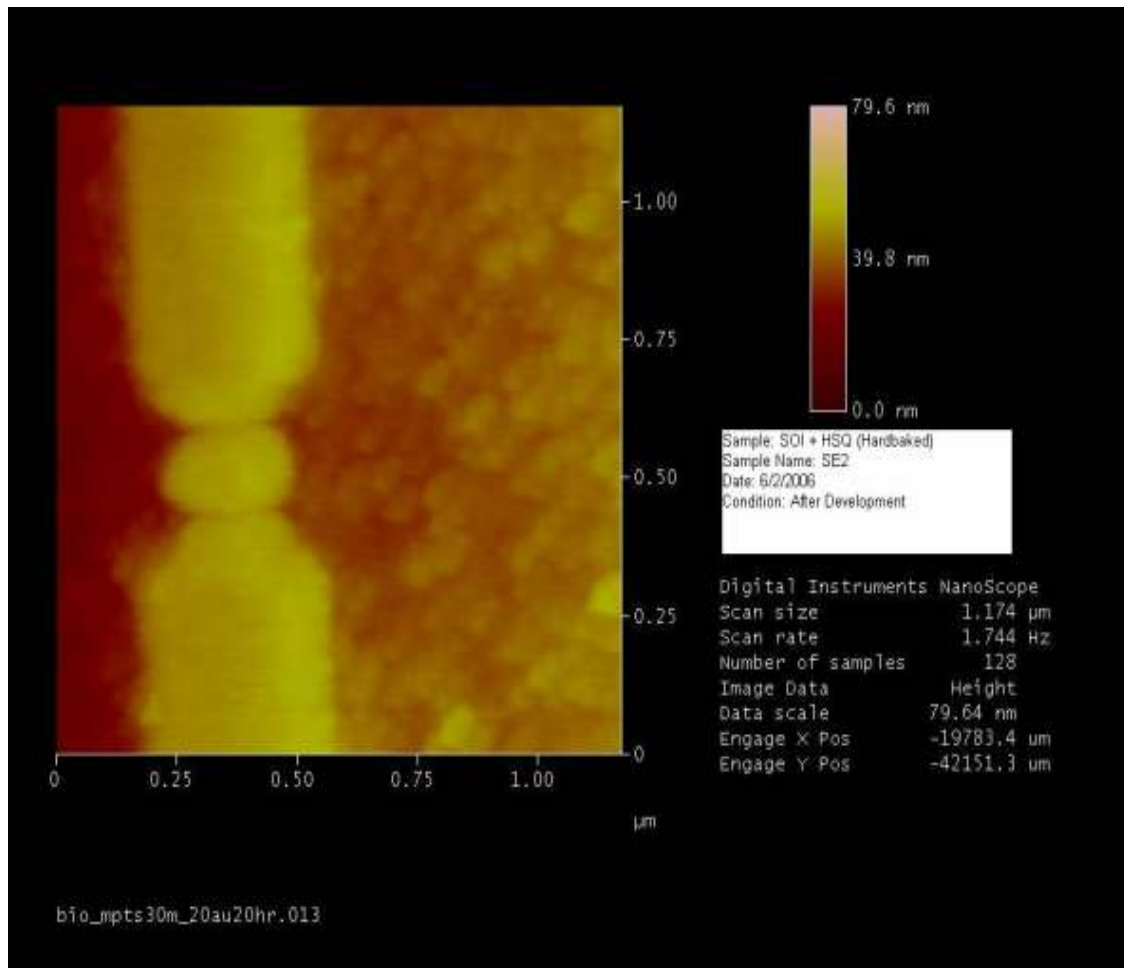


Fig 4.53 The central part of an SET structure after thermal curing using HSQ as a resist

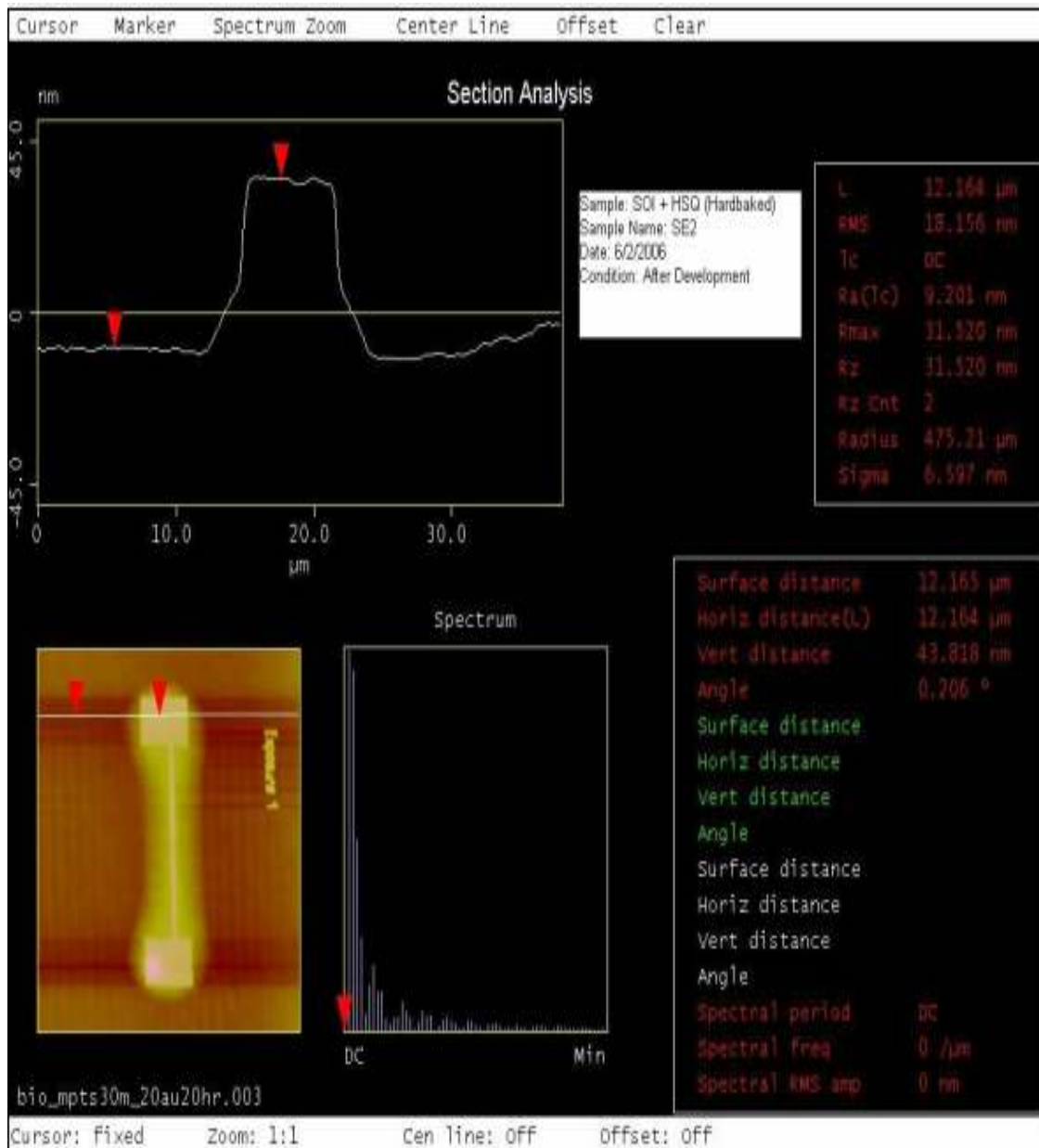


Fig 4.54 Height measurement for a pad after thermal curing

I used the Atomic Force Microscope (AFM) extensively to study the height of the structures after development or an etching step so that I would know when to stop etching. The Digital Instruments Dimension 5000 AFM was used for this purpose. The images clearly indicated that the halo effect was observed on the SOI wafer too.

The parameters which are of prime importance for a good e-beam operation are optimizing the focus and preventing astigmatism of the beam. The operator needs to be skilled to optimize the microscope prior to writing. In the case of XR-1541 there was a deficiency of reading matter especially when it came to comparing doses or accelerating voltages for exposure. The problem was compounded by the fact that XR-1541 was sold in many concentration combinations. I tried to discuss this issue with people well versed in e-beam lithography and my results intrigued them too. Ruling out focus and astigmatism issues; in my opinion I could narrow down the effect to certain other factors like a very thin resist, a very high temperature pre-exposure bake, very high doses and development time miscalculations. The first three factors have almost similar effects. If you were to spin a very thin layer of resist in our case HSQ was being spun at 4000 revolutions per minute for 60 sixty seconds which gave us a 39-54 nm thick resist layer and then bake it at 225°C for 120 seconds yielding a very thin and hard layer for the beam to penetrate and if a high dose was given then during exposure this would lead to scattering. Scattering could be of two kinds, forward scattering and backscattering.

In forward scattering the incident electron coming from the beam collides with an atom of the resist or the substrate. After transferring some of the energy to the atom the incident electron changes direction. An electron in the atom could be excited to change energy levels or ionized creating a secondary electron. This is termed as inelastic scattering as the incident electron loses its energy in the process. Inelastic scattering angles are usually low.

The backward scattering mechanism is as follows. If an electron from the beam collides with a nucleus in the resist or substrate an elastic collision follows. The electron does not lose a lot of energy but the scattering angle is usually large. The electron then proceeds to travel and starts losing energy by inelastic collisions. As the angle is large the exposure due to backscatter electrons can be very far from the point of penetration. If two structures were placed very close to each other then the dose from one could affect the other due to scattering. This is the much discussed 'proximity effect'.

It is difficult to predict which one of the two effects dominates but for thin resist layers backscatter seems more probable. The electrons from the beam could also be penetrating through the resist and then bouncing back from the substrate surface and traveling back upwards through the resist exposing more areas of the resist than desired. Most researchers had used 70-100kV operating voltages for testing with HSQ but our scope was limited to a maximum of 30kV. For obtaining a very precise narrow beam it is recommended to use the highest accelerating voltages using the smallest aperture.

For my next experiment HSQ was spun on the wafer at 2000 rpm for 60 seconds to provide for a thicker HSQ layer. The pre-exposure bake, the doses and the post exposure bake procedures were not altered. The development time was increased slightly. The wafer specifications, e-beam parameters and the recipe for development are mentioned under sixth HSQ wafer in Appendix C.

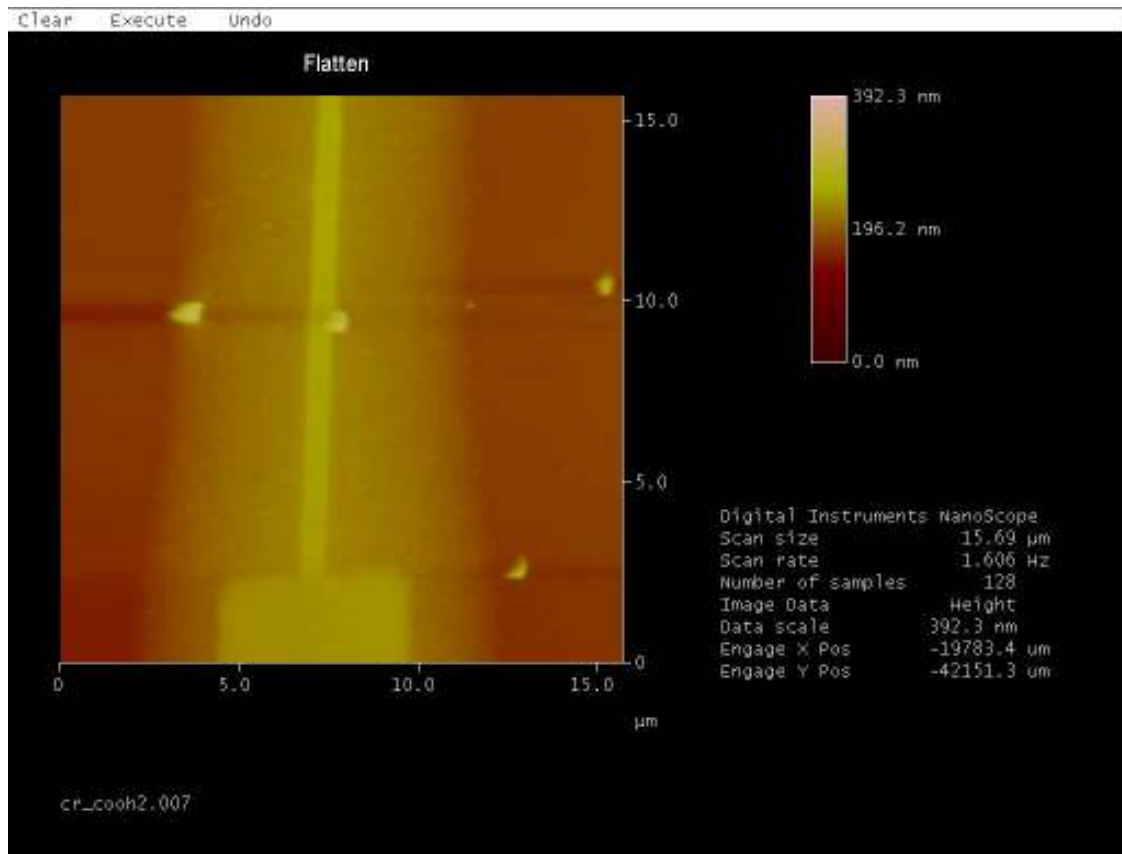


Fig 4.55 The SET structure after development and curing using HSQ as a resist

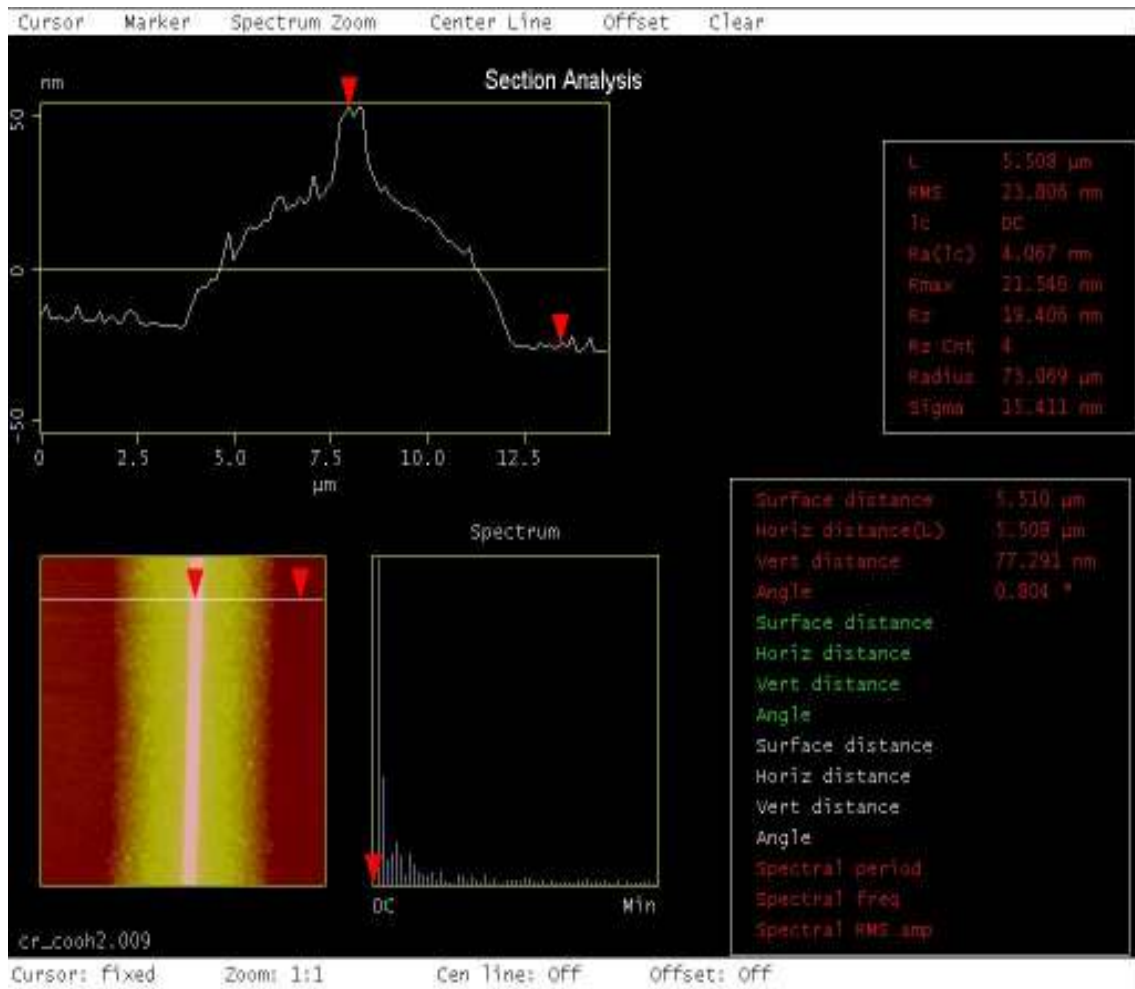


Fig 4.56 Height measurement for the SET structure shown above



Fig 4.57 An SEM image of the wheel pattern after development and curing, employing HSQ as a resist

After development and the curing it was seen that the slower spin speed resulted in a thicker resist layer as expected. The thickness was approximately 80nm. The halo effect was still observed though.

The wafer was then etched in the Technics Micro-RIE for 60 seconds. Only CF_4 was used as a process gas. The etching conditions are mentioned under third HSQ test in Appendix D.

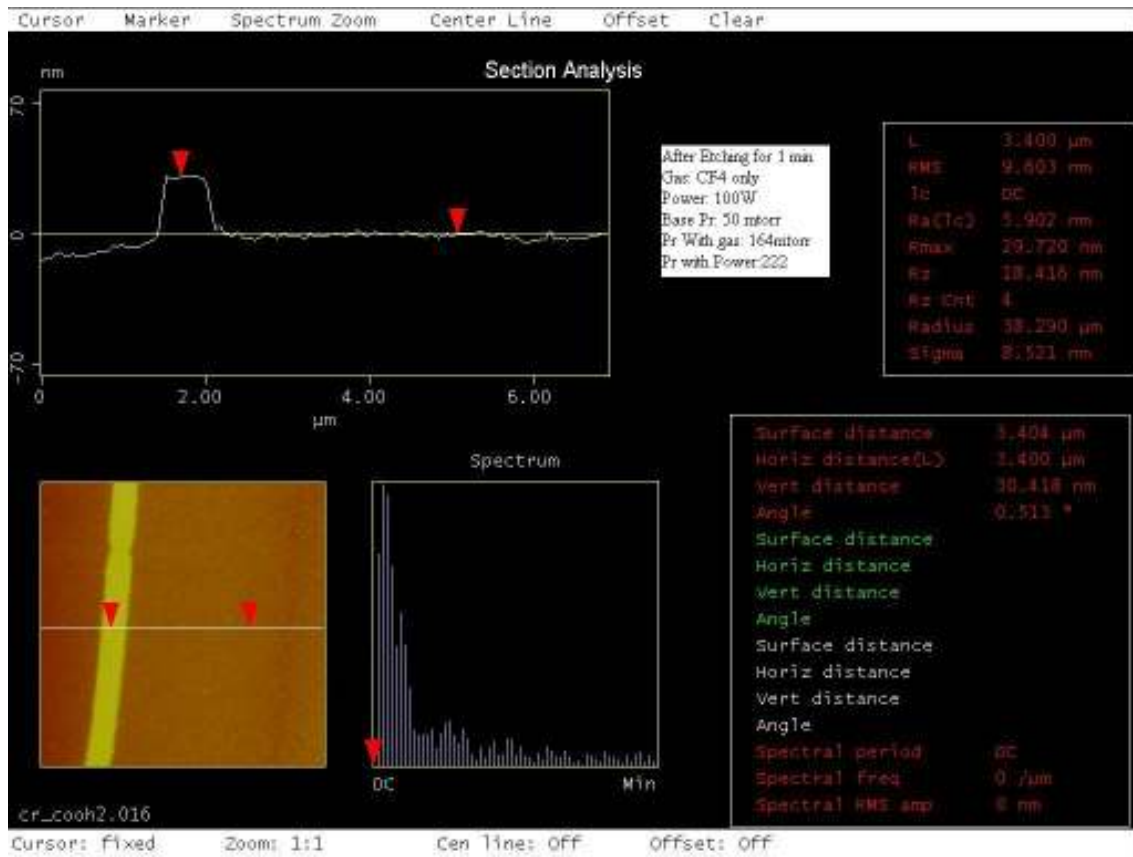


Fig 4.58 Height measurement of the SET structure after the etch

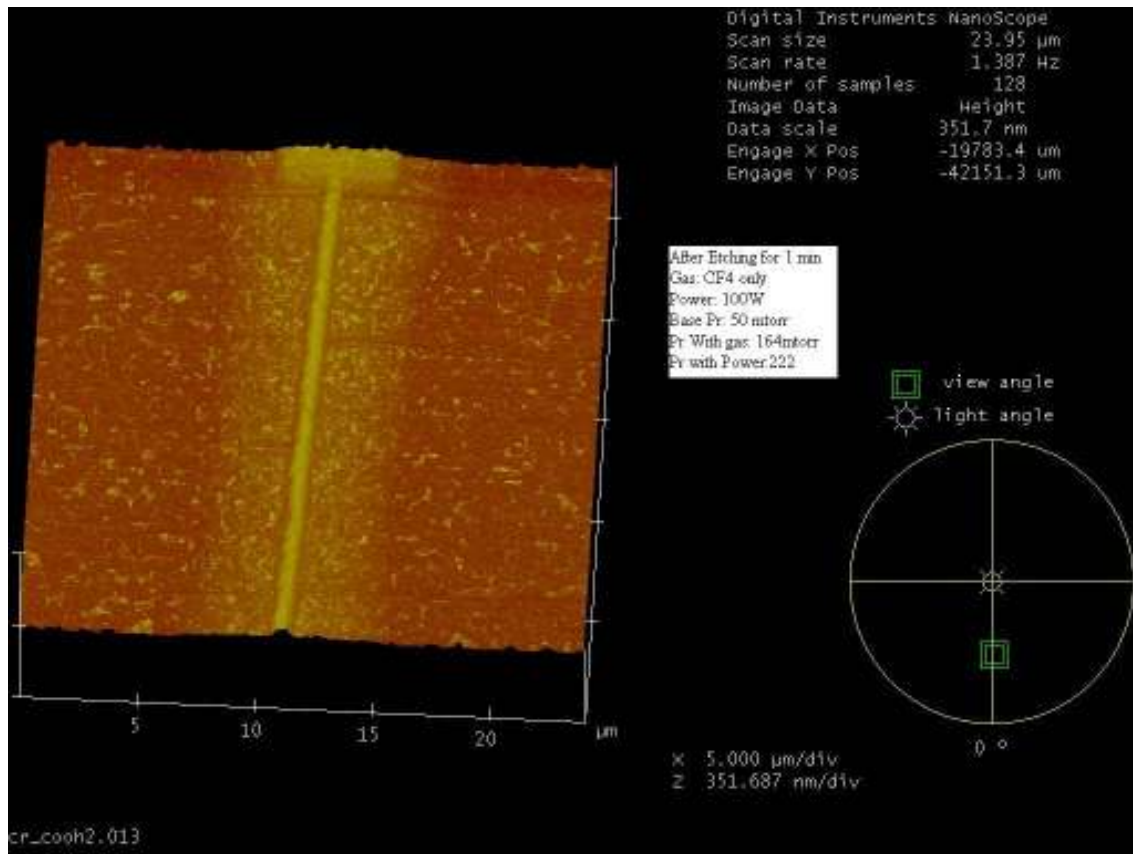


Fig 4.59 A 3D view of the SET structure and its surrounding area

The images above indicate that wafer is now littered with particles on it this could be contaminants from the RIE chamber. There are many researchers using the RIE and large gamuts of materials are etched in the chamber. The contamination could have been a result of residues left behind after the last etch operation by another user. Also the structure height which was 77 nm initially should have increased to a larger value but instead dropped down to 30nm. This meant that a lot of HSQ was removed during the etch too. To test this I put the wafer in a buffered oxide etch solution for 15 seconds which is very selective in etching SiO_2 without affecting Si.

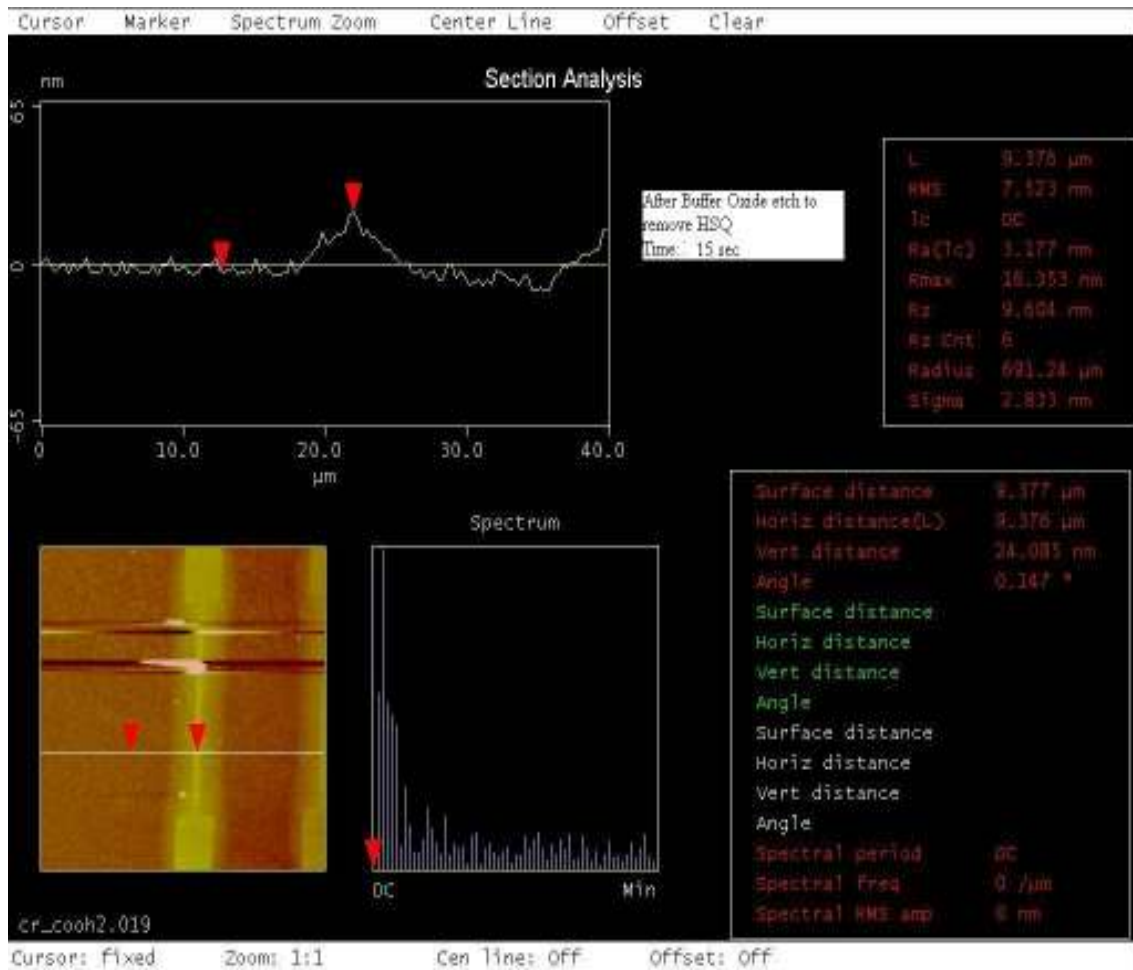


Fig 4.60 Height measurement of the SET structure after a 15 second Buffered oxide etch

The height went down from 30nm to 24nm which meant that only 6nm of HSQ was left after the RIE. The 24nm structure that was left standing on the wafer surface was Si but we needed the silicon to be about 55 nm high. The reason why is as follows. The SOI wafer has a 55nm thick single crystal silicon layer on it. After the RIE procedure, I desire to reach the SiO₂ layer of the wafer and after the Buffered oxide etch I could remove the slivers of HSQ left and expose the Si under it. Now the only Si that is left on the top surface would be for the structures. This means that when a voltage would

be applied to it, the current would not leak in the lateral direction or downwards. It would be restricted in the downwards direction by the insulating SiO₂ and it would have no where to go in the lateral direction. The structure is hence confined. To confirm that all the HSQ was removed and the SiO₂ layer was not reached the wafer was exposed to the buffered oxide etch for another 15 second etch. The height of the structure remained unchanged. If the height had increased it would indicate that the buffered oxide etchant was removing exposed SiO₂ i.e. SiO₂ layer had been reached.

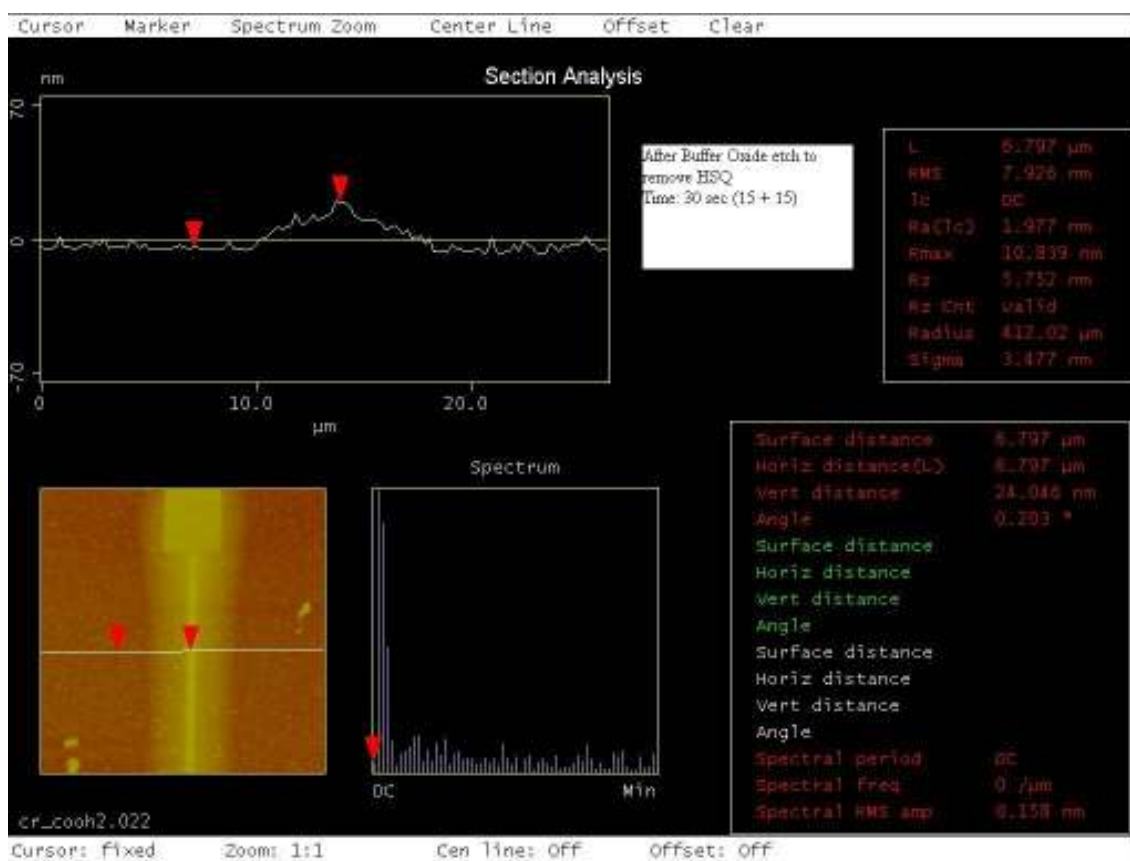


Fig 4.61 Height measurement of the SET structure after an additional 15 second buffered oxide etch

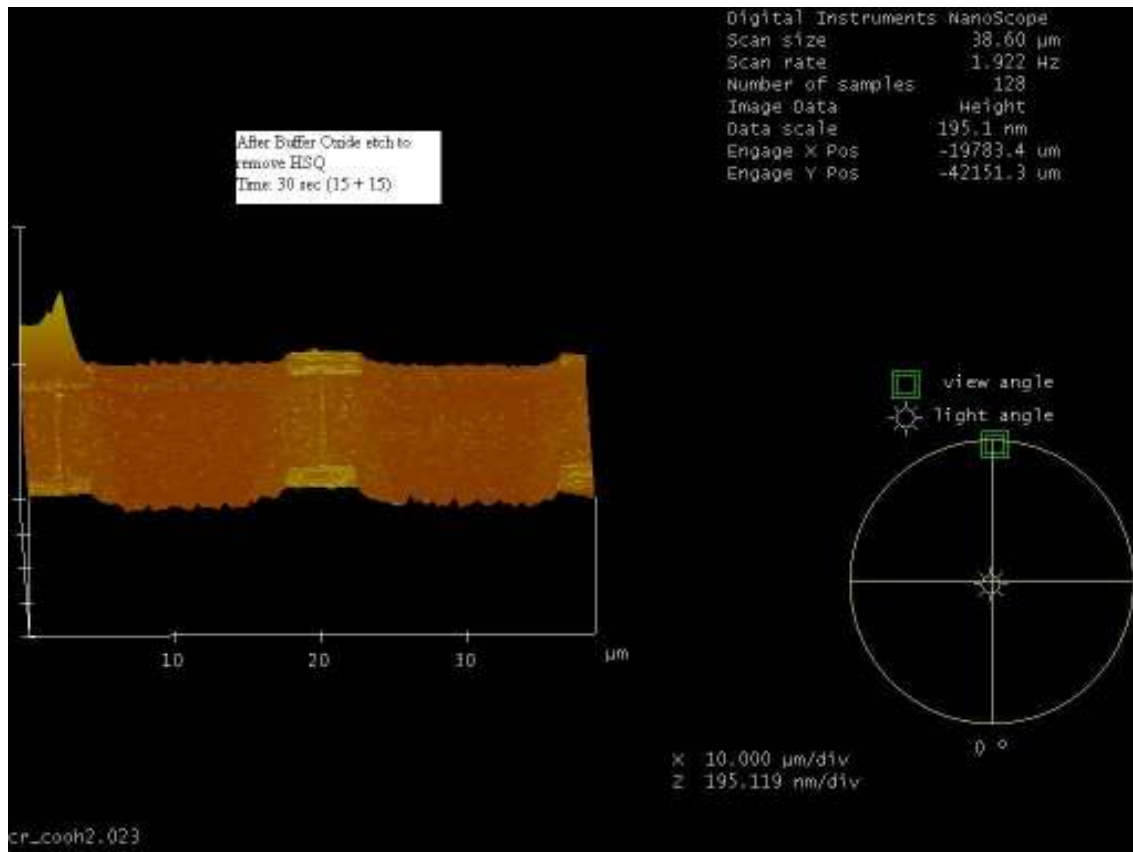


Fig 4.62 Side view of the SET array after the additional 15 second buffered oxide etch

I decided to investigate into using a bilayer resist approach. This could reduce backscatter as the other resist could absorb most of the electrons as it would be softer than the Al or the substrate and it also it would help us use the current RIE technique without needing the HSQ to act as an etch mask that role would be served by the other layer.

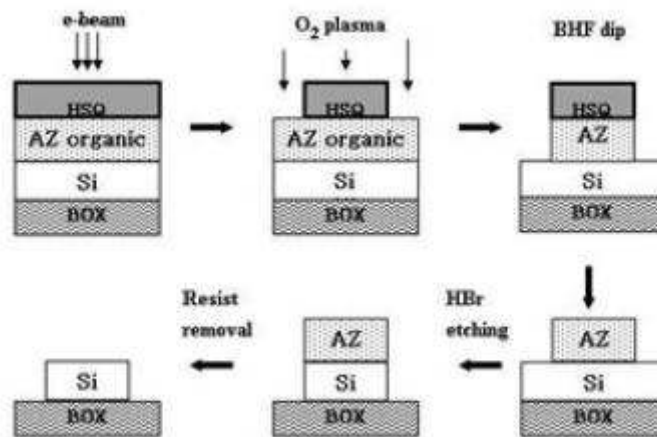


Fig 4.63 Schematic of the steps for the bilayer resist approach [23]

The only difference from the schematic would be that instead of HBr etching we would use CF_4 to remove unwanted Si. The experiment also needed the AZ organic layer to be quite thin to avoid undercut and distortion errors post-etching. The first few experiments conducted using AZ2020 indicated that the 1.8 micron thick AZ2020 layer was far more than needed. The halo effect though was still prominent. The undercut after etching was significant in the first few experiments. Using a prescribed thinner we could manage to make the AZ2020 to be about 110nm but the company did not recommend such a highly diluted mixture of the resist and cautioned me that the etching durability of the AZ2020 resist could be seriously reduced. The SEM images for the bilayer resist wafer with 110nm of AZ2020 and HSQ were not favorable either. The approach was finally scrapped.

The good news was that a new etching machine had been bought. The Trion DRIE system was purchased. We could now use SF_6 which had been proven in being more selective to etching Si over SiO_2 . To test this theory a wafer was prepared. The

wafer specifications, e-beam parameters and the recipe for development are mentioned under seventh HSQ wafer in Appendix C. Height measurement post-development gave us a result of 20-25nm. This indicated the height of HSQ. The wafer was then etched in the Trion DRIE using SF₆. The wafer went through a number of etch steps until a height of 80 nm was indicated. The number was important as 25 nm of HSQ added to 55 nm silicon gives us 80nm, a number at which I was sure that I had reached the underlying SiO₂ layer. The post etching images are shown below.

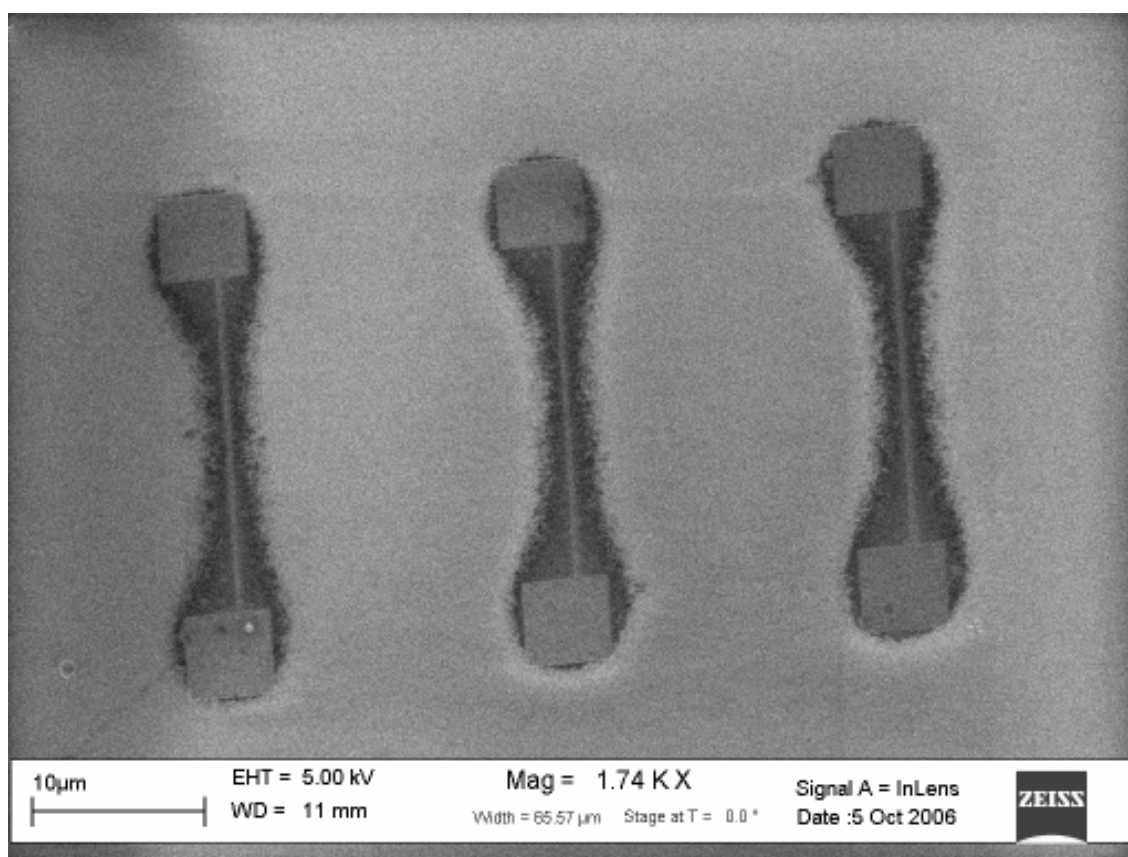


Fig 4.64 The SET array after the SF₆ etch employing HSQ as an etch mask

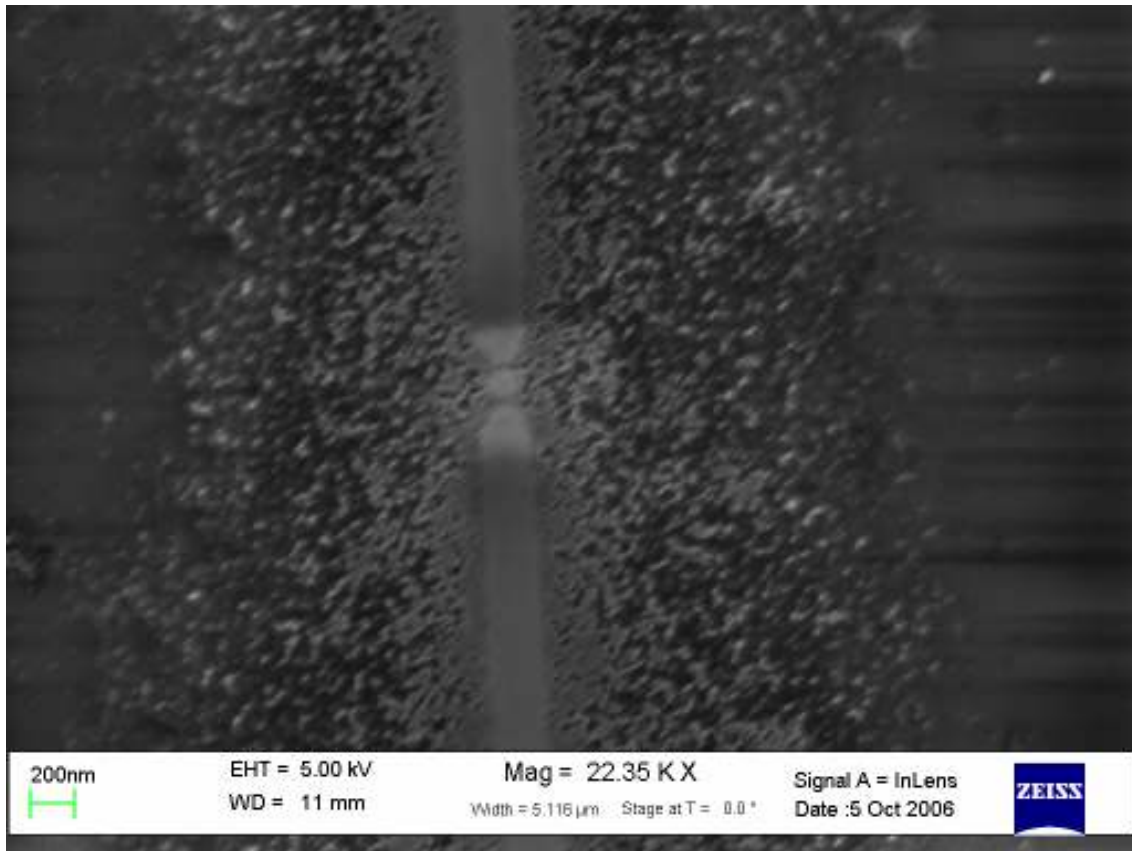


Fig 4.65 The SET structure after the SF₆ etch employing HSQ as an etch mask

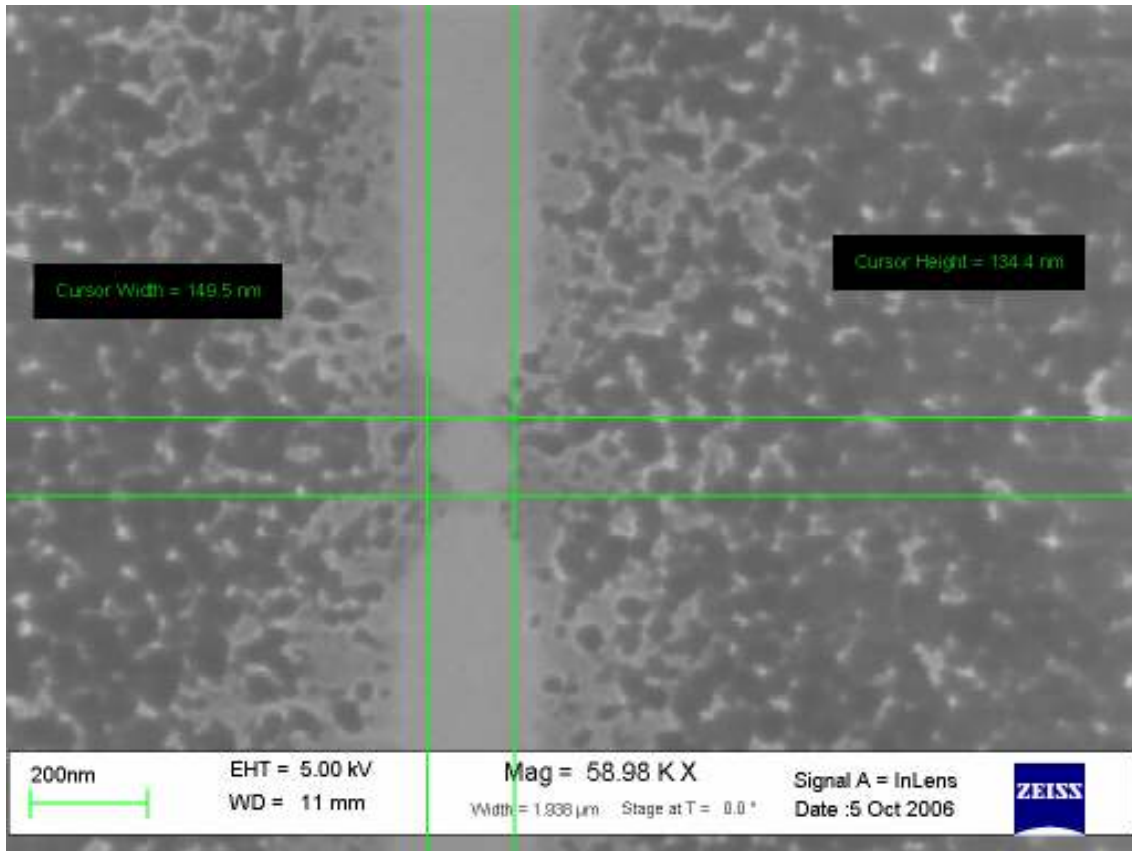


Fig 4.66 Another SET structure after the SF₆ etch employing HSQ as an etch mask

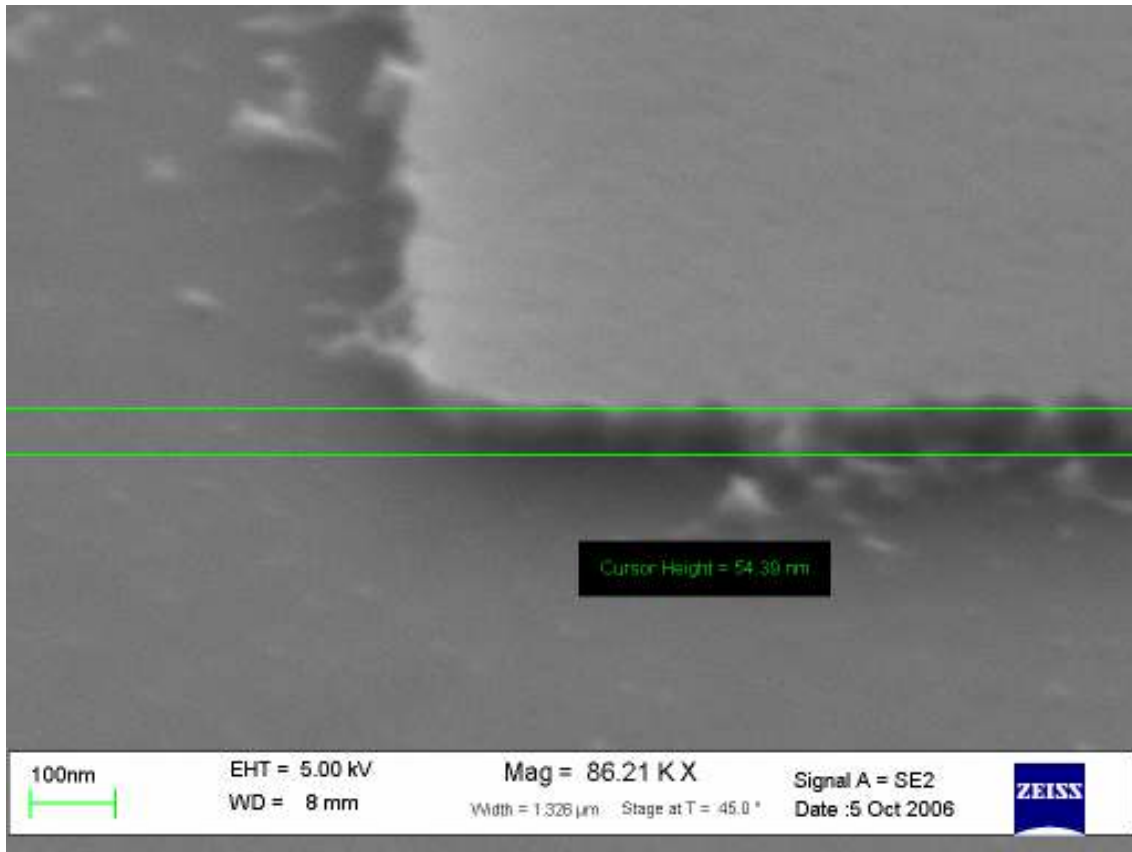


Fig 4.67 The 50 micron pad imaged at a 45° tilt after the SF₆ etch

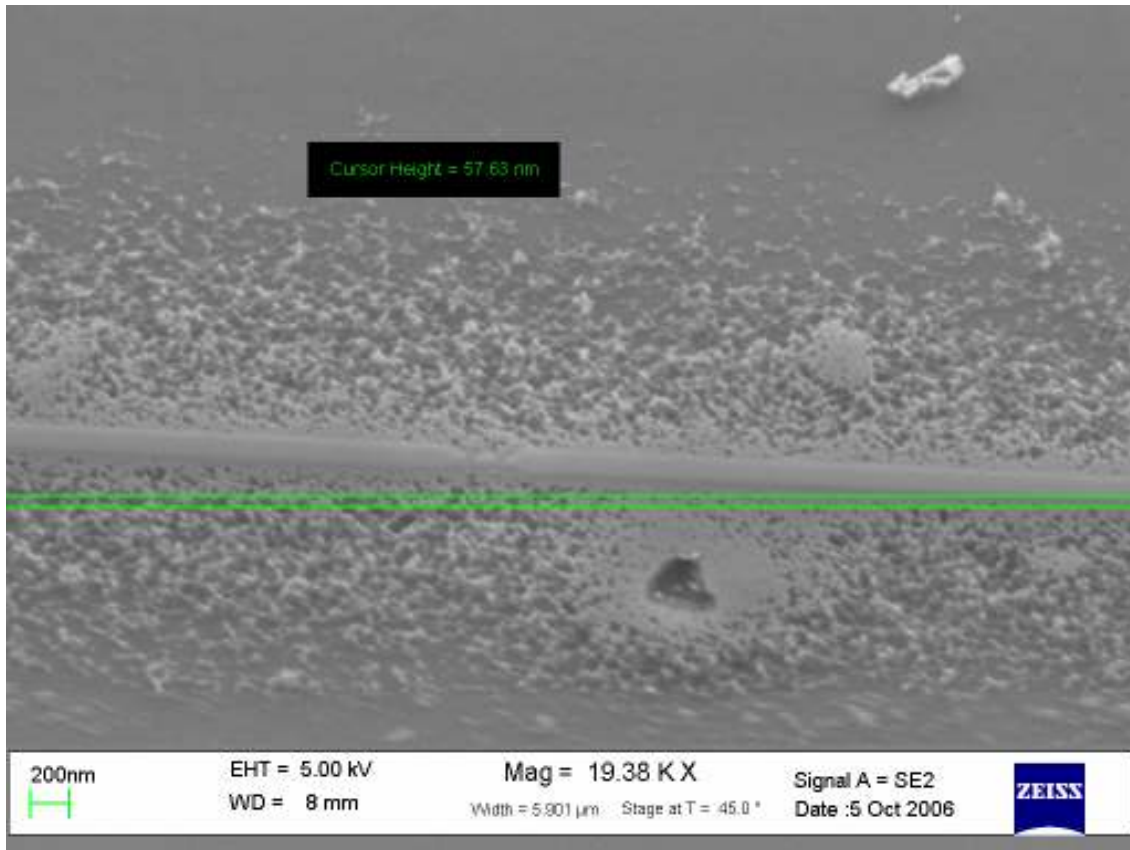


Fig 4.68 The SET structure imaged at a 45° tilt after the SF₆ etch

The height of the structures from the SEM images was $57.63 / \cos 45 = 81.501\text{nm}$ exactly matching those measured by the AFM.

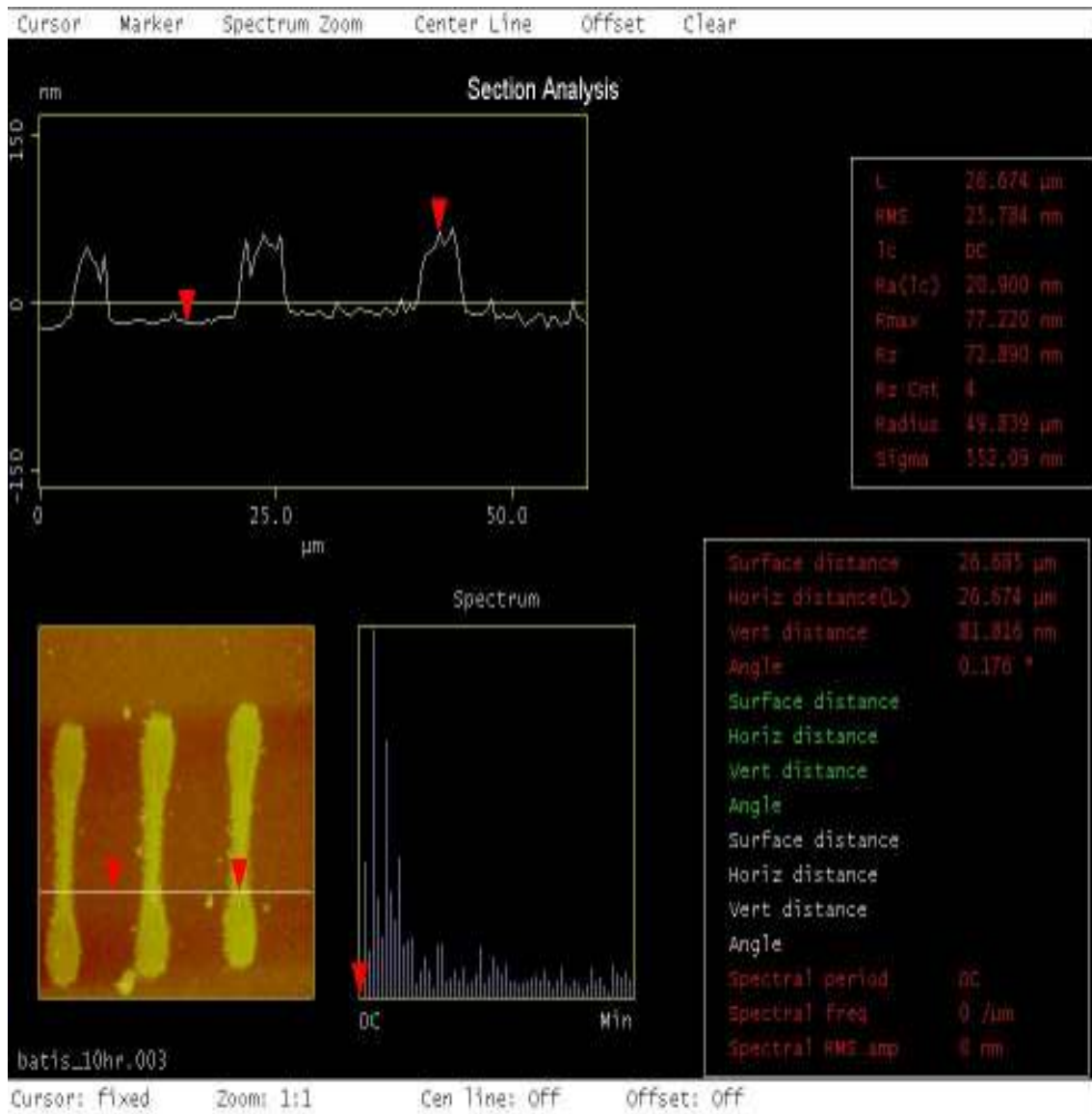


Fig 4.69 AFM image of the SET array after the SF₆ etch

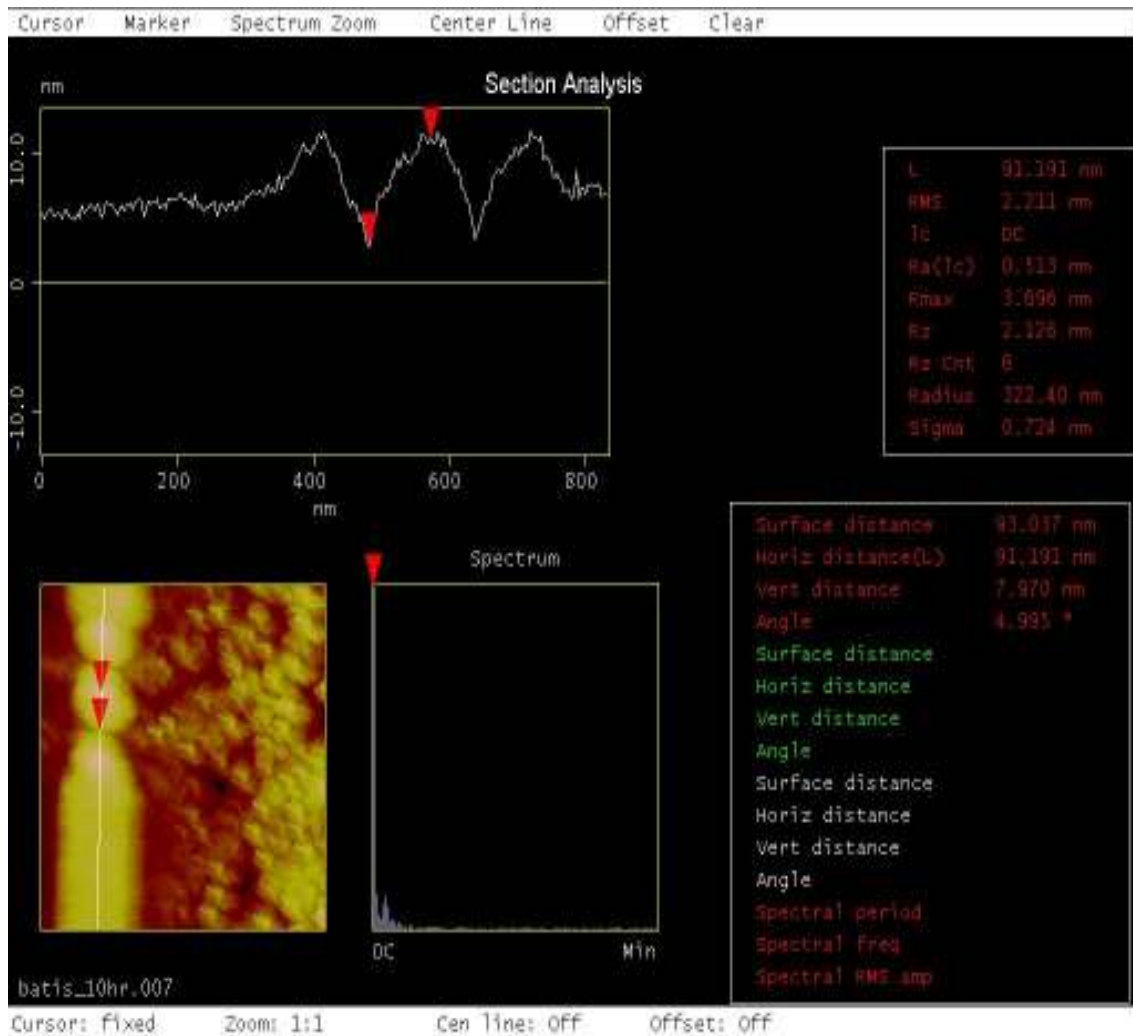


Fig 4.70 The height profile for the finger and island part of a SET structure in HSQ after the SF₆ etch

I now had a grip on the etching procedure. I could surely say that the SiO₂ layer was exposed; all that was left to do was to remove the HSQ from the top of the structures. This could be another predicament in itself. I if used the buffered oxide etch it would attack the HSQ and the SiO₂ layer. The etch had to be conducted for a very short period. The etch being a wet etch technique could lead to undercut and if the wafer was kept long enough in the etchant could remove the SiO₂ which is directly underneath the

standing silicon structures and the silicon structures could topple or be removed completely. To prevent this from happening I chose to etch the wafer for 60 seconds in the Technics Micro-RIE using only CF_4 only. This way the undercut would not be significant; RIE being an anisotropic etching technique.

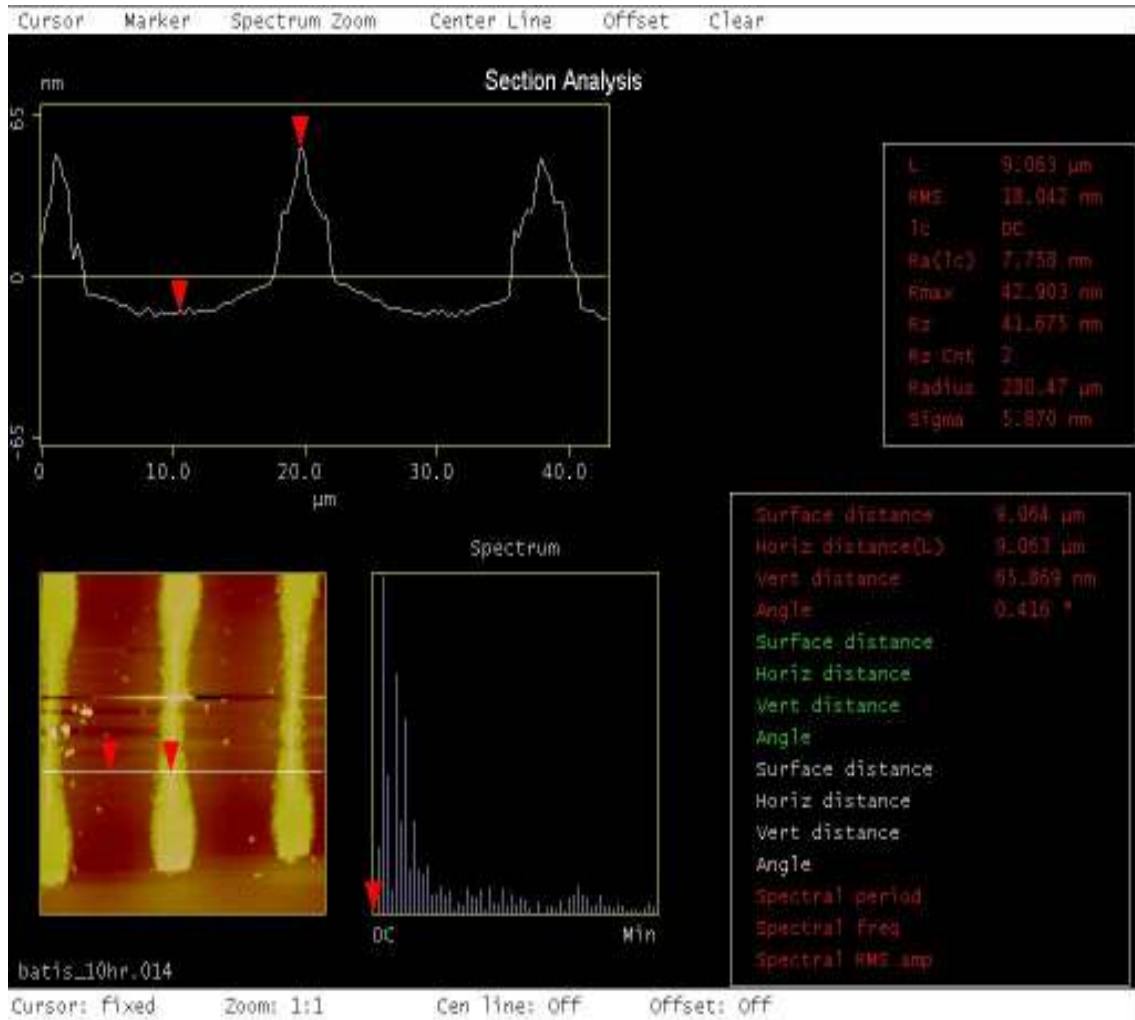


Fig 4.71 The SET array after the CF_4 etch

The height reduced from 80nm to 65 nm indicating removal of at least 15 nm of HSQ. This also indicated that approximately 10nm of HSQ was lost during the SF_6 etch. As a surety test I used the buffered oxide etch process this time only for five seconds.

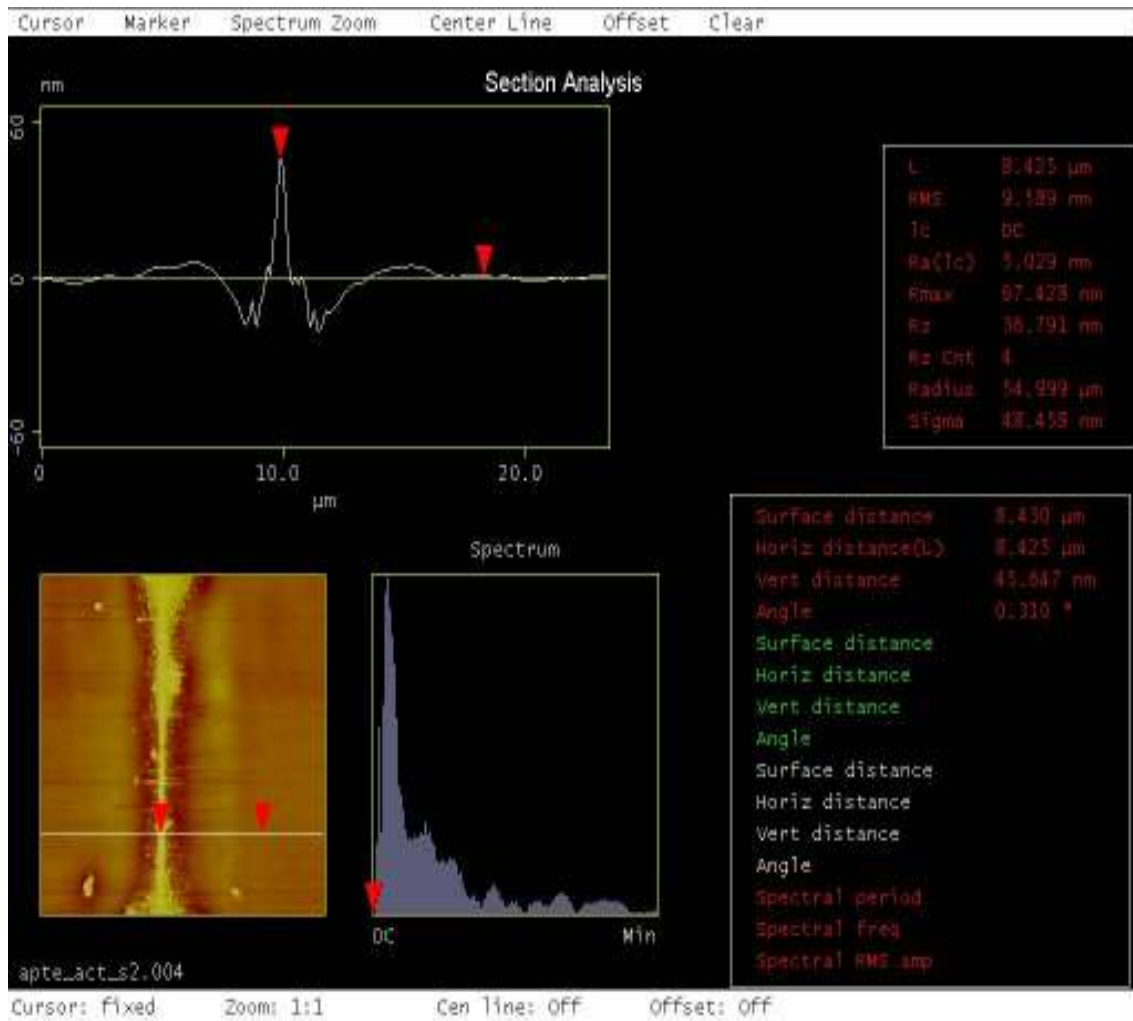


Fig 4.72 Height measurement of the SET structure after the buffered oxide etch. The height reduced to 45nm since the SiO₂ layer was also attacked severely during this dip

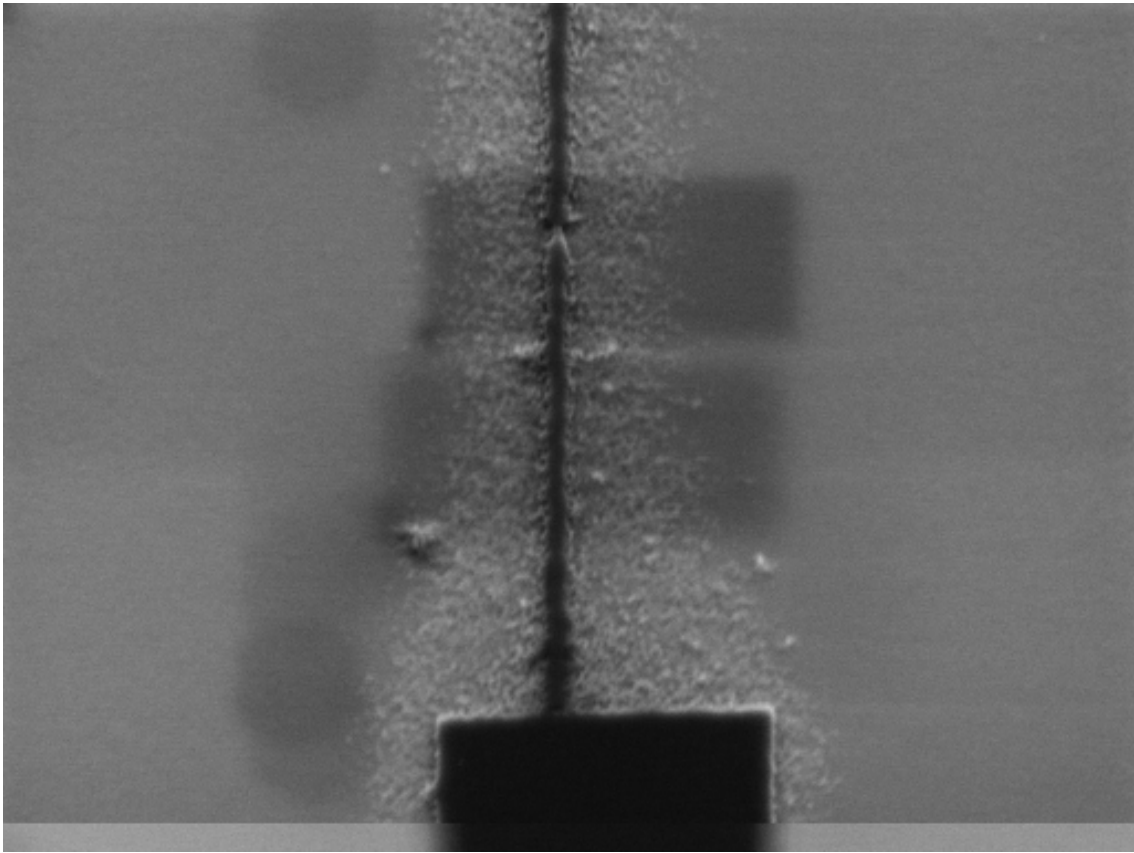


Fig 4.73 The SET structure after the buffered oxide etch

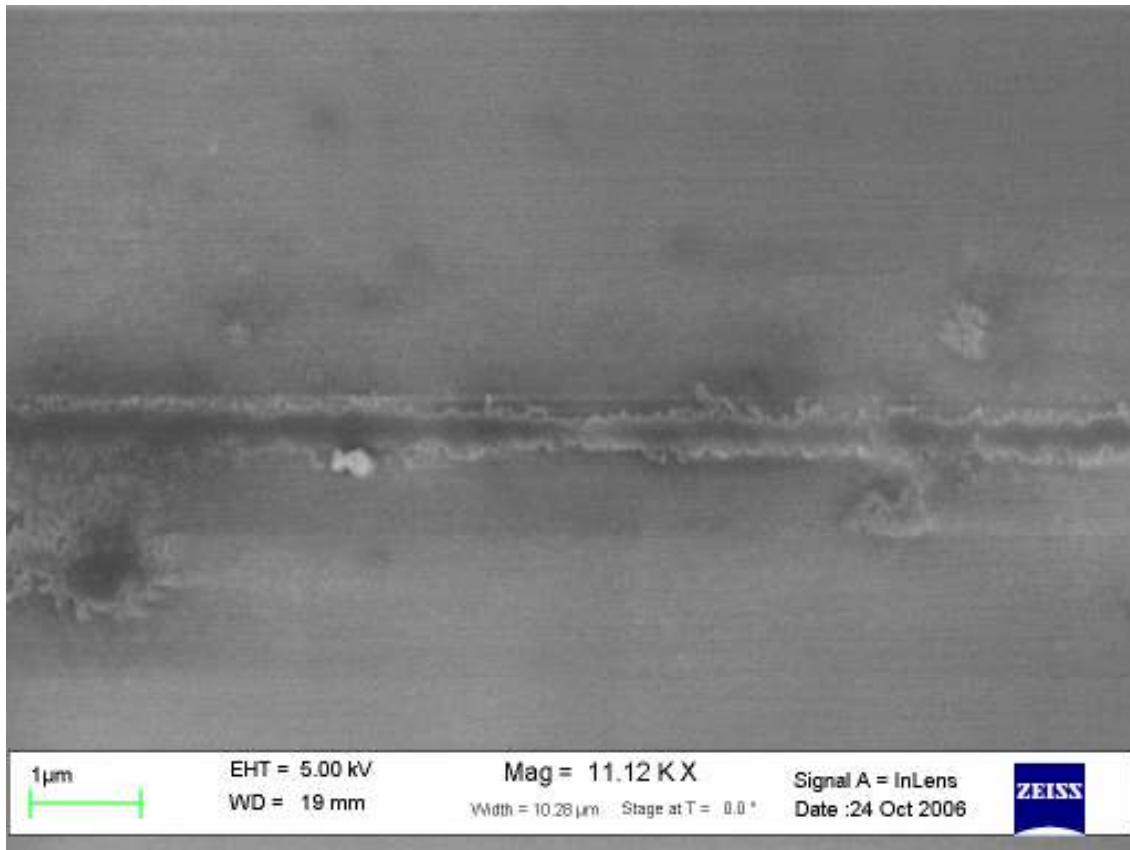


Fig 4.74 The SET structure after the buffered oxide etch imaged with the InLens detector

The SEM images indicated that though the etching was successful the end product was still not as desired. The roughness of the structure and that of its surroundings were too significant an issue to disregard. I felt this was a direct consequence of the halo effect and if the effect could be avoided, the roughness could be rather minimal.

Another issue was that since the pads of the structure which would function as the source and drain electrodes for the SET were just 5 by 5 microns. At the measurement stage it would be impossible to use the probe station in our laboratory. The minimum feature size for probing was 100 by 100 microns. With all these issues

taken into consideration our designed seemed plagued, a redesign for the pattern was imminent.

4.5 The new pattern

A new pattern was chosen mostly inspired from a publication by Hu, Hwang, Fang, Pan, and Chou [24]. A few modifications were made to the pattern from the paper.

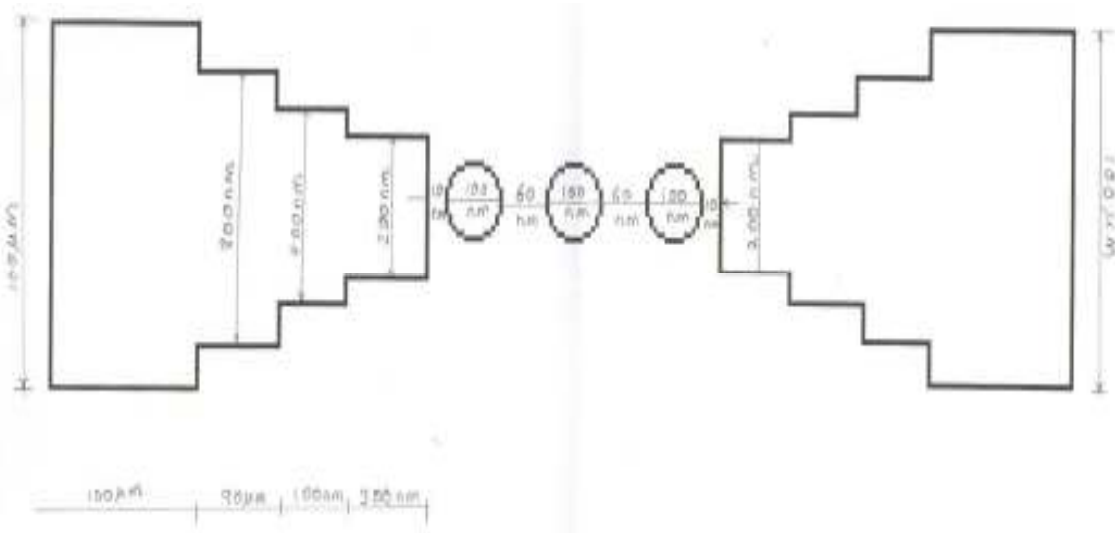


Fig 4.75 A diagrammatic representation of the new SET design

The biggest change made from the previous design was the inclusion of the 100 by 100 micron pads so that probes could be placed on them at a latter stage. The structure then tapered down towards the dimensions of the island diameter (100nm), which were increased from 75nanometers. The spacing between islands was slightly decreased though. The finger as a whole consisted of three structures. It was much longer than before to provide enough isolation thus preventing any capacitance between the two 100

micron pads. By decreasing the total capacitance of the structure we can make the charging energy larger thus increasing the operating temperature of the device.

The design file was then made using DesignCAD and this time all the structures including the fingers and islands were inputted to be filed polygons which meant the beam would sweep inside them until the prescribed dose was delivered. This would be a tougher task but a more accurate way to know exactly what doses are needed to define the various polygons.

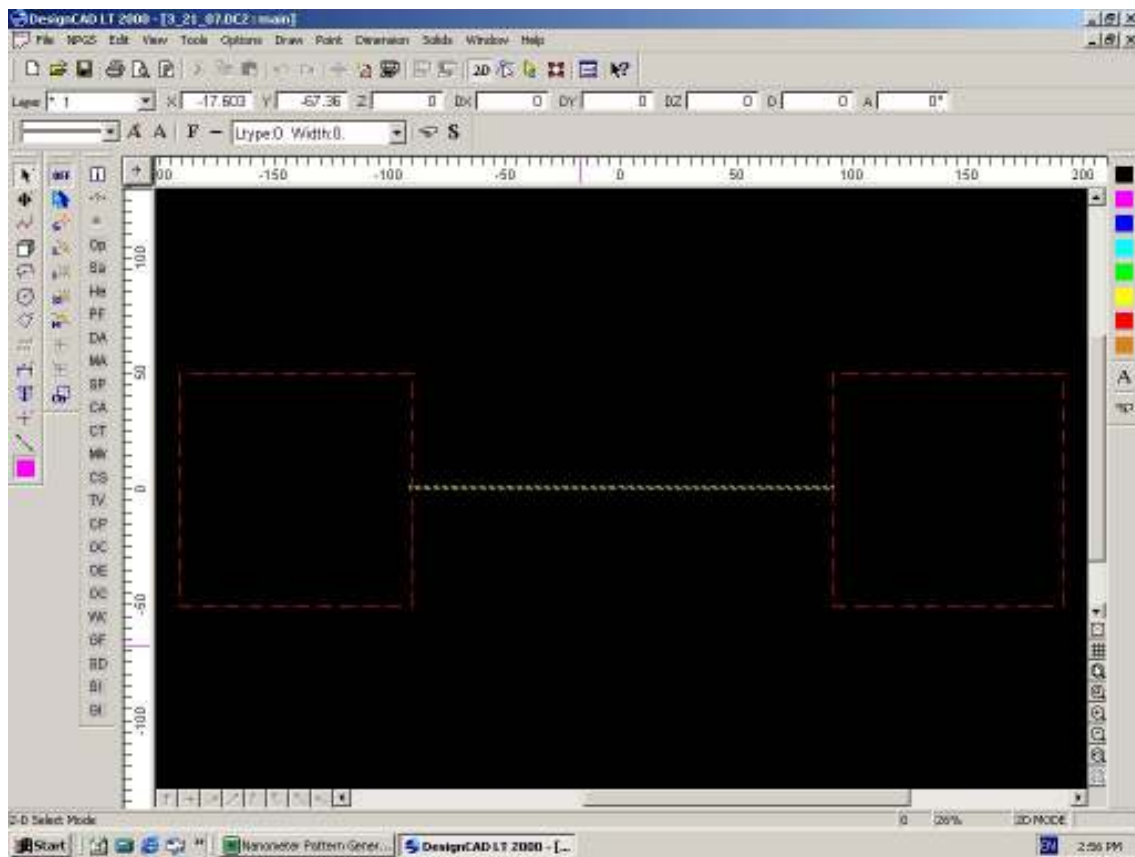


Fig 4.76 The design file of the new pattern

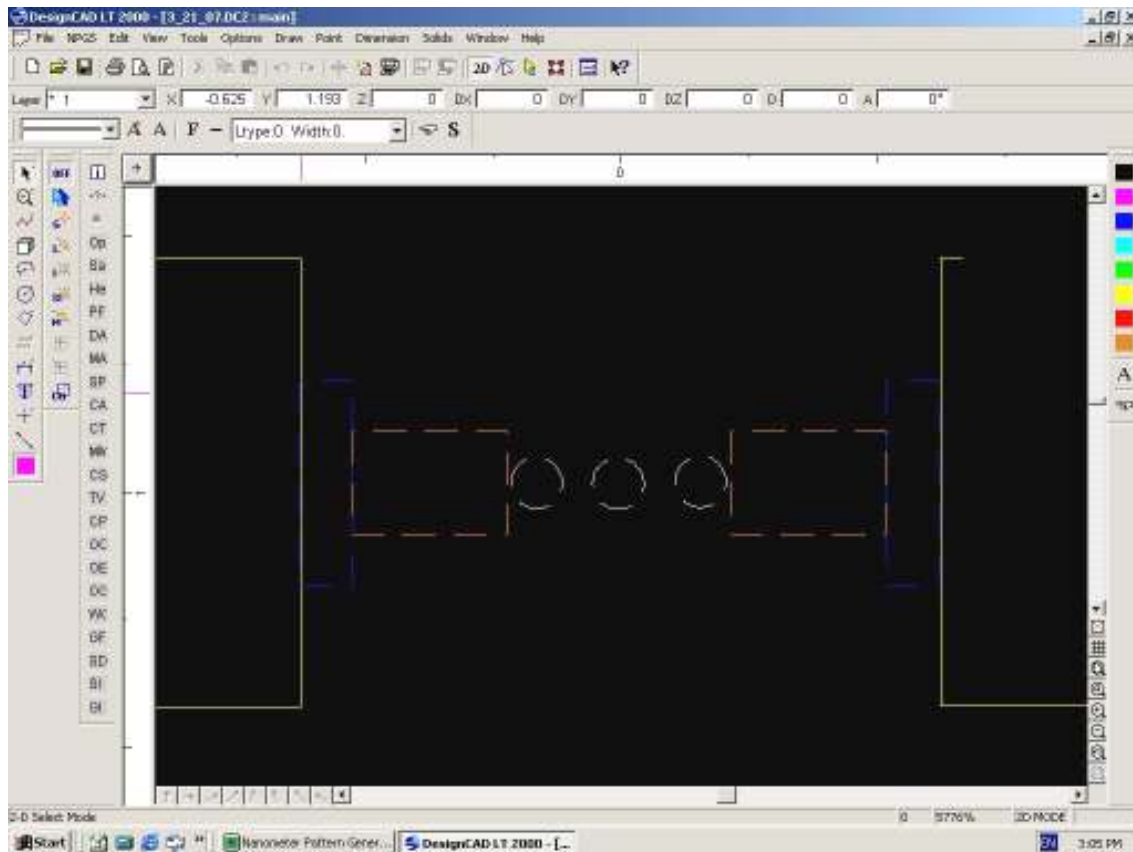


Fig 4.77 A zoomed in view of the design file displaying the islands

The 100 by 100 micron pads were assigned to layer 2 while the others were on layer 1 this was done so that the pads could be written using a larger aperture size since writing them with a smaller aperture size would be time consuming and accuracy in writing the pads was not that critical. Every separate polygon of the entire structure was designated a color enabling me to administer a different dose to each one.

For the first few tests my main aim lie in perfecting myself in optimizing the SEM before writing any samples followed by avoiding the halo effect by altering all the variables. The final aim was to obtain a sample with a pattern look exactly like it was designed in the DesignCAD file. For the first test the spin speeds and development

techniques were kept quite similar to those that I had used for the last run with the old pattern. The wafer specifications, e-beam parameters and the recipe for development are mentioned under eight HSQ wafer in Appendix D.

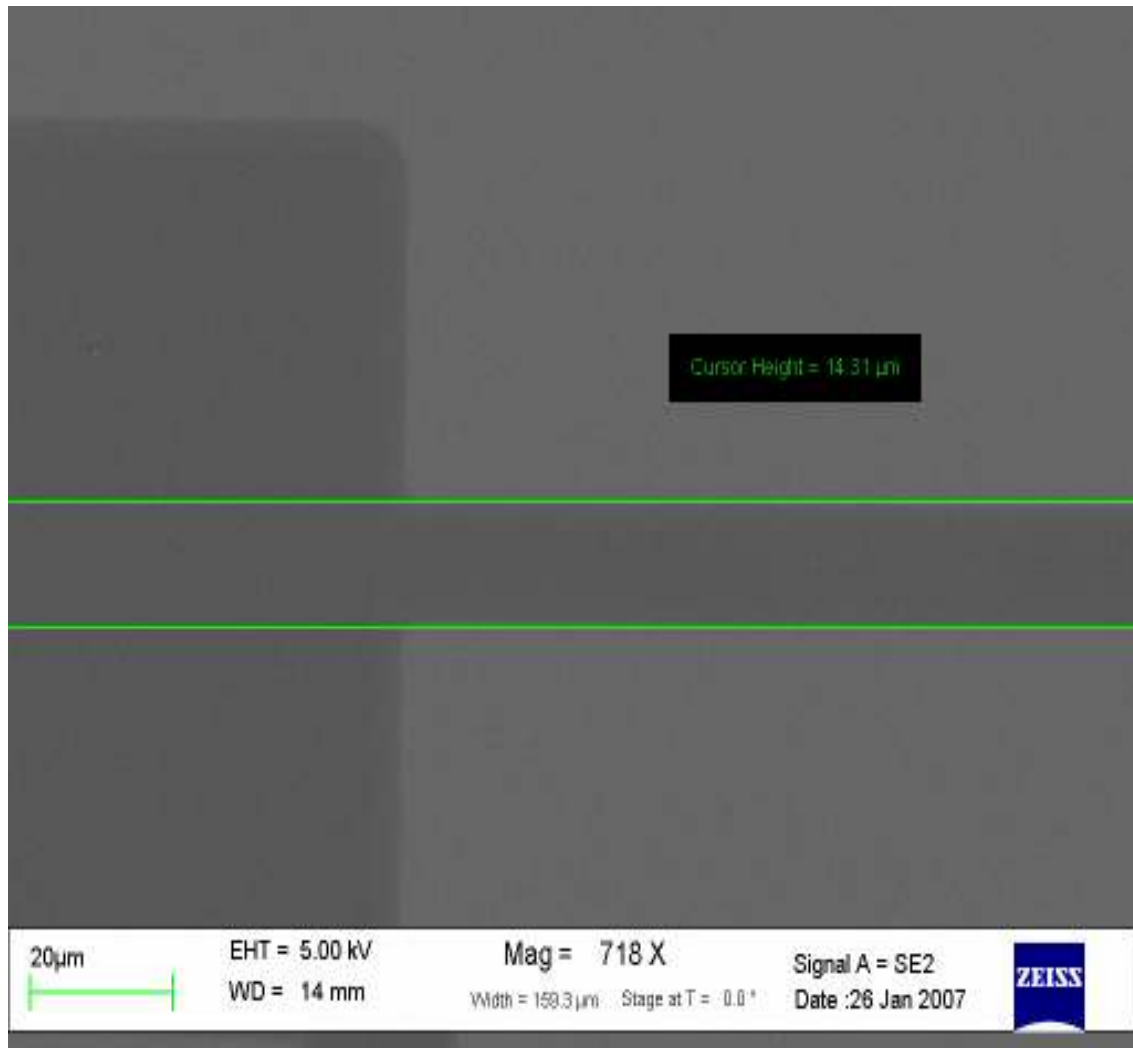


Fig 4.78 The SET structure after development using HSQ as a resist

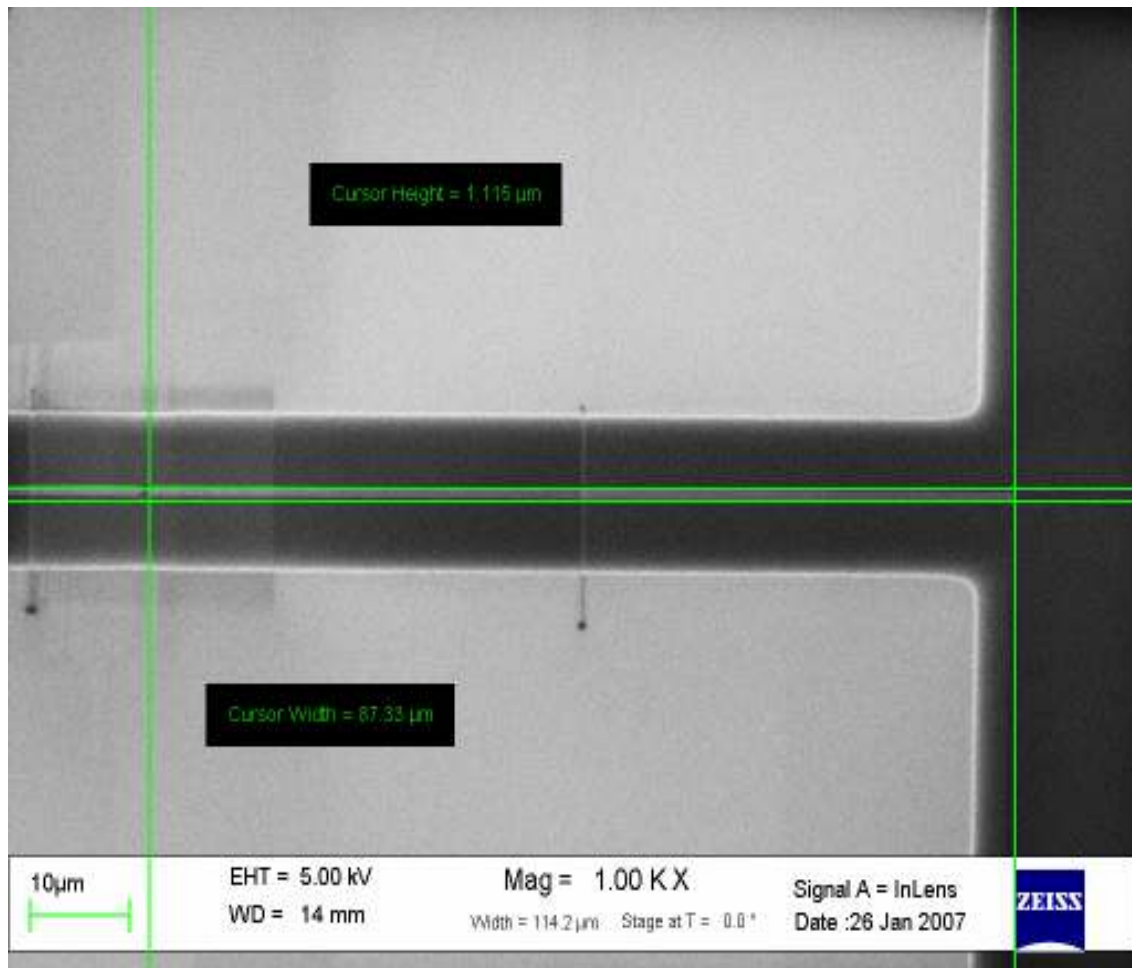


Fig 4.79 The SET structure after development using HSQ as a resist

The images clearly indicate that the halo effect still existed. The first part of the finger which was designed to be 800nm wide and 90 micron long appeared to be 1.1 micron wide and 90 micron long. Including the halo in the calculation though gave us a width of 14.3 microns. This was grossly off the mark. For the next few wafers the development strategy was changed slightly and also the spin speeds used to spin on HSQ spinning were reduced, but the changes in the halo size were not significant.

The next strategy was to reduce the doses. I decided to cut the doses down by almost 90% of their original value. A reduction in doses did lead to a smaller halo size but at times the doses were not enough to define the central structures and the islands. The idea dose for defining the 100 micron pads i.e. $300\mu\text{C}/\text{cm}^2$ was obtained by observing images from the previous attempts. A wafer was processed in which all the pads were given a dose of $300\mu\text{C}/\text{cm}^2$ and the rest of the structure the doses were varied from $50\mu\text{C}/\text{cm}^2$ to $2000\mu\text{C}/\text{cm}^2$. The wafer specifications, e-beam parameters and the recipe for development are mentioned under ninth HSQ wafer in Appendix C.

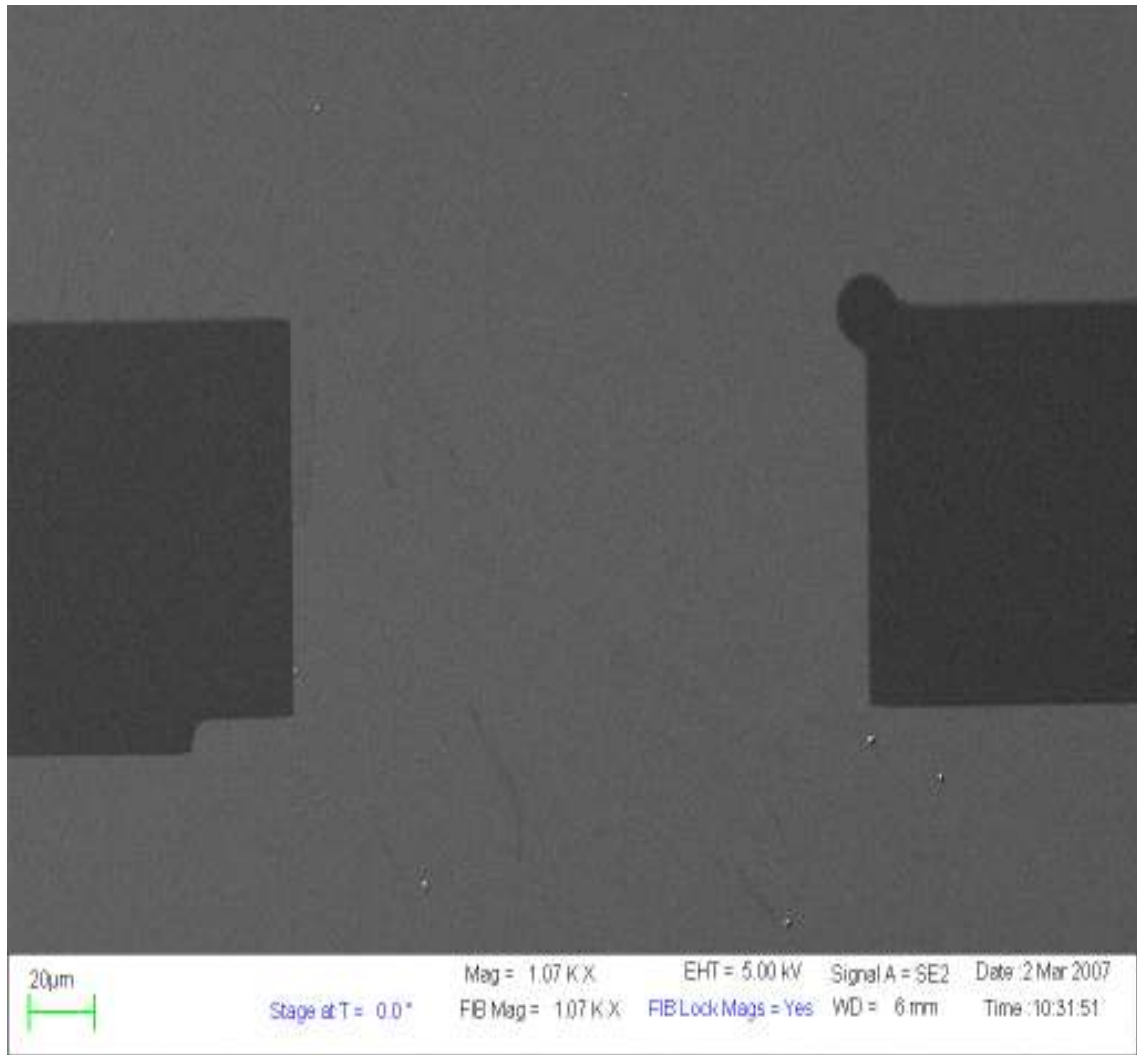


Fig 4.80 The SET structure after development in which the fingers and islands were exposed to an electron dose of $50\mu\text{C}/\text{cm}^2$

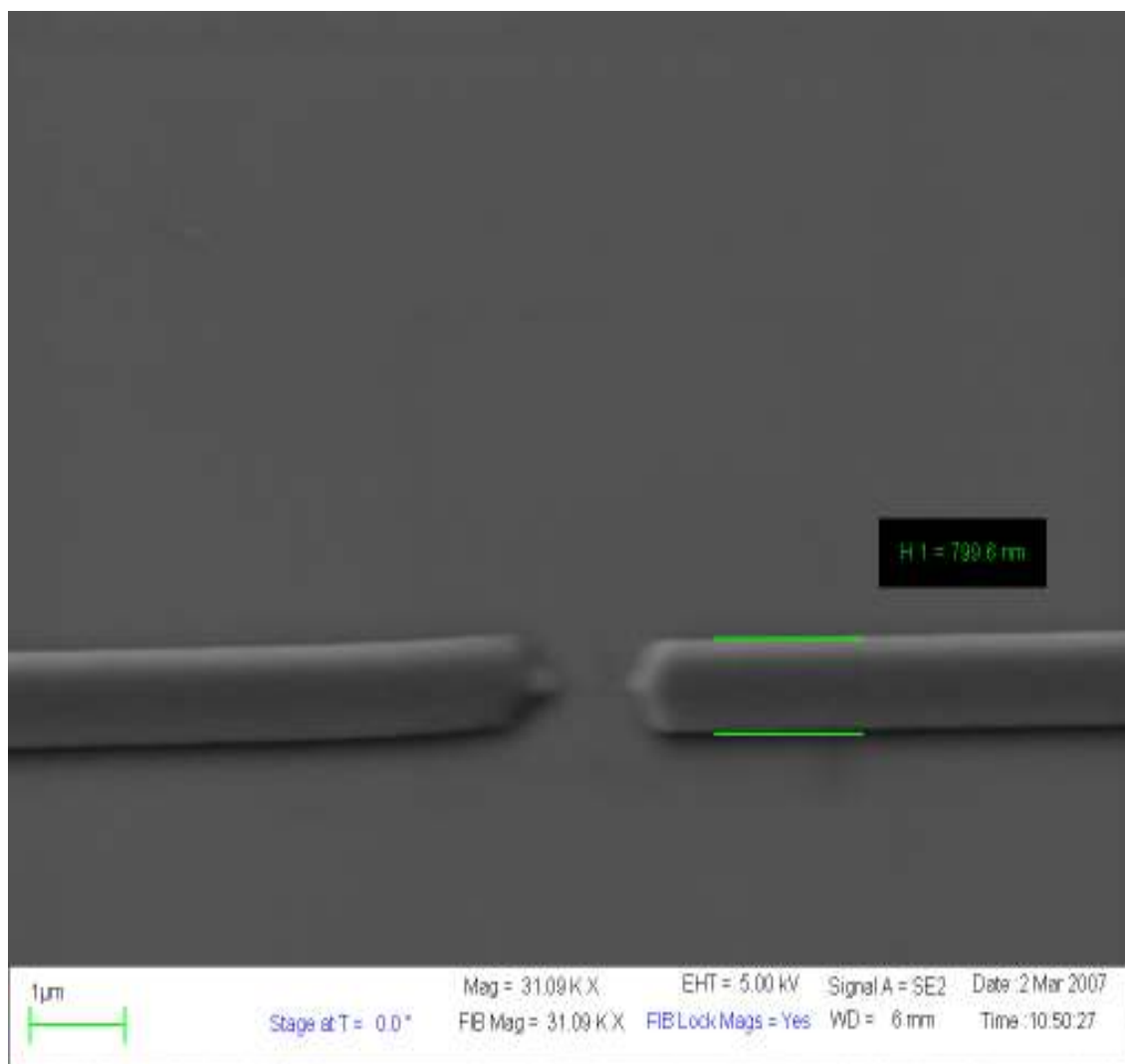


Fig 4.81 The SET structure after development which was given a dose of $200\mu\text{C}/\text{cm}^2$

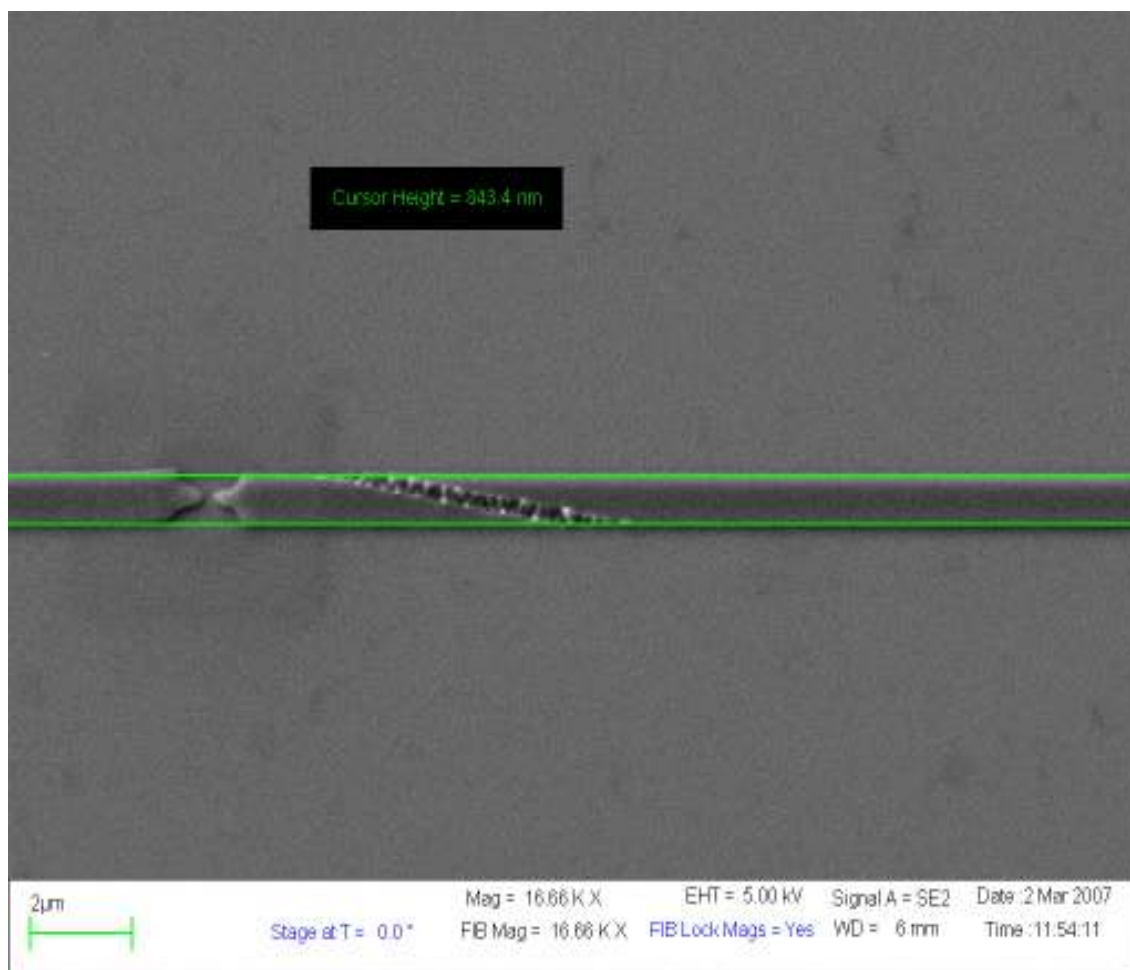


Fig 4.82 The SET structure after development which was given a dose of $600\mu\text{C}/\text{cm}^2$

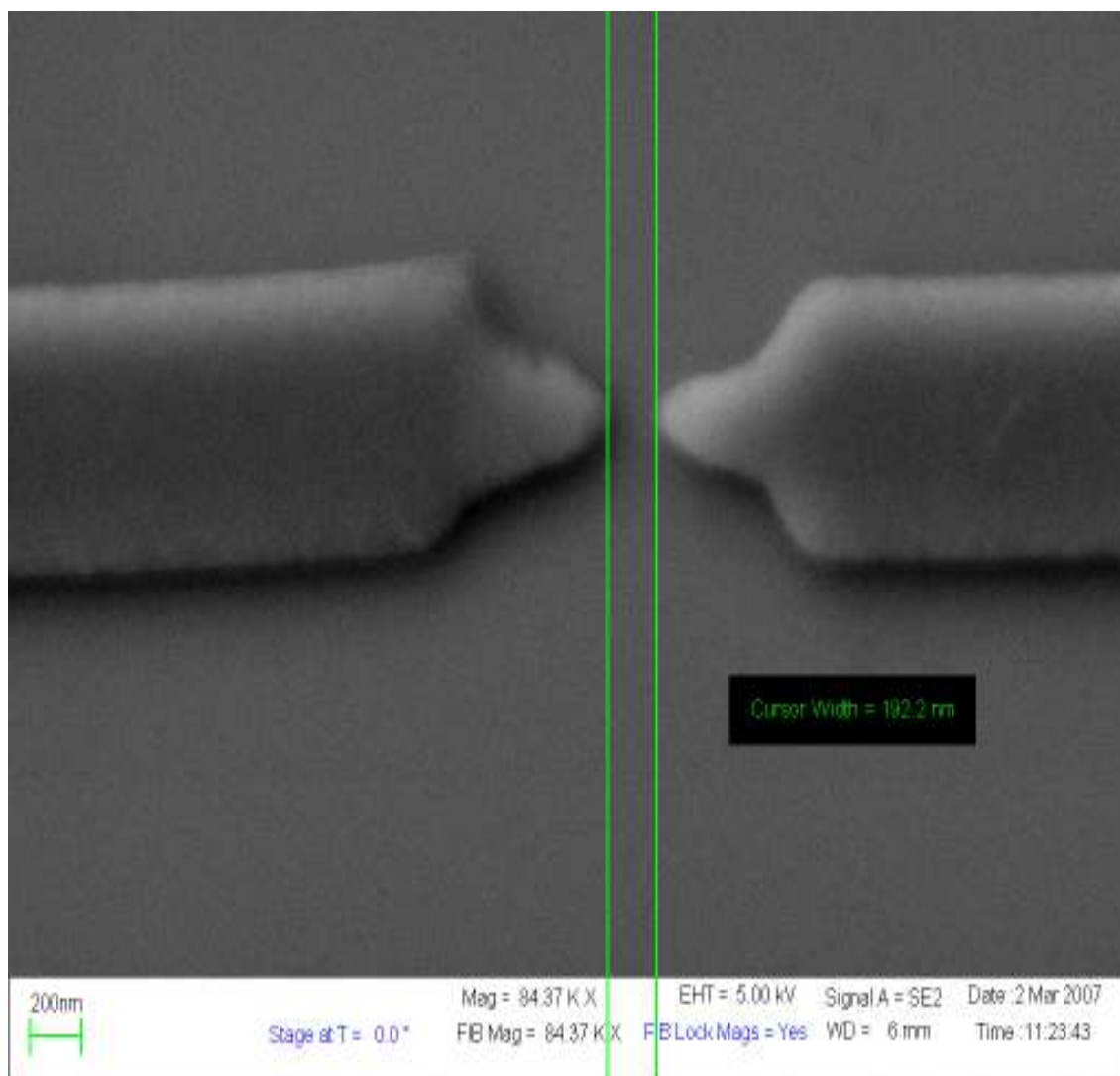


Fig 4.83 The central part of an SET structure after development which was exposed with a dose of $600\mu\text{C}/\text{cm}^2$

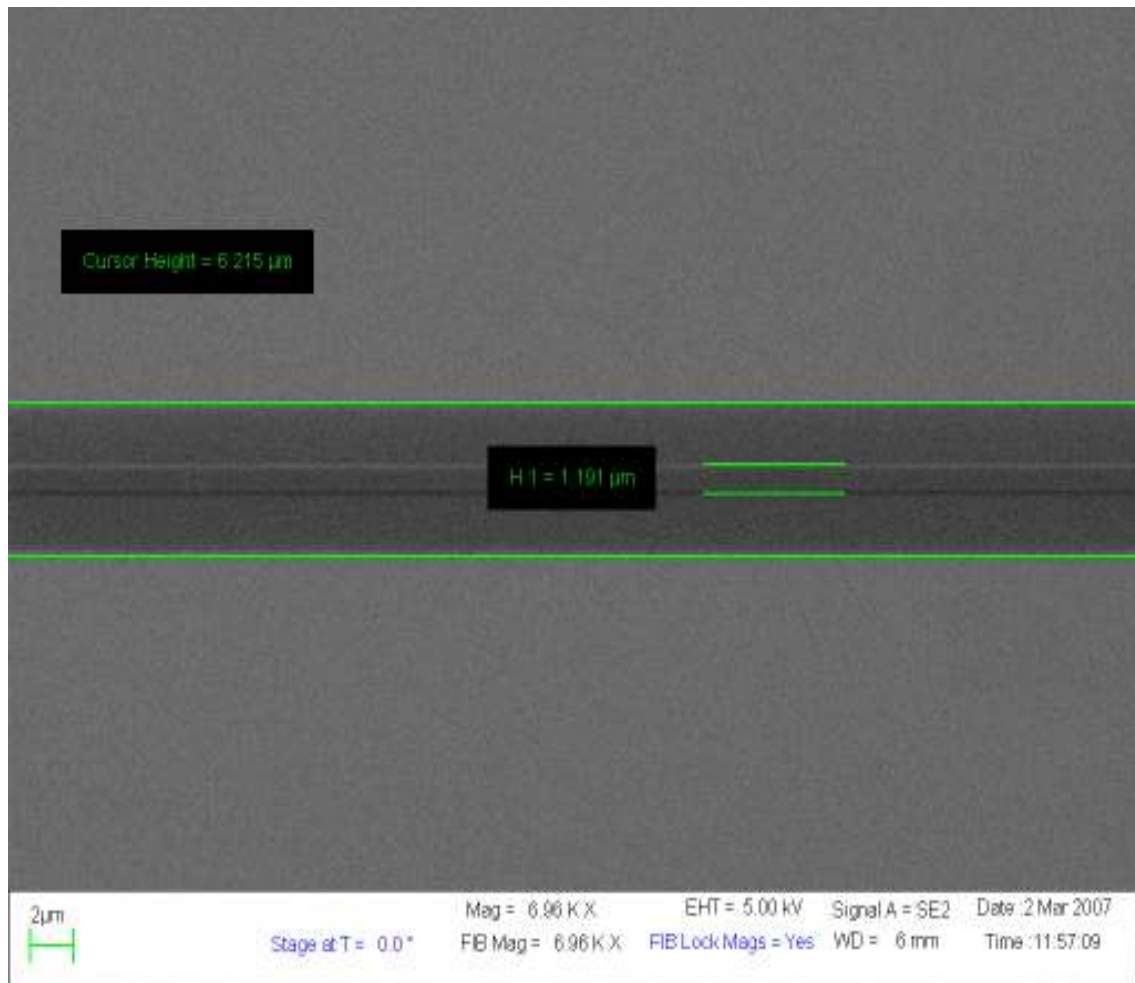


Fig 4.84 The SET structure after development which was exposed with a dose of $2000\mu\text{C}/\text{cm}^2$

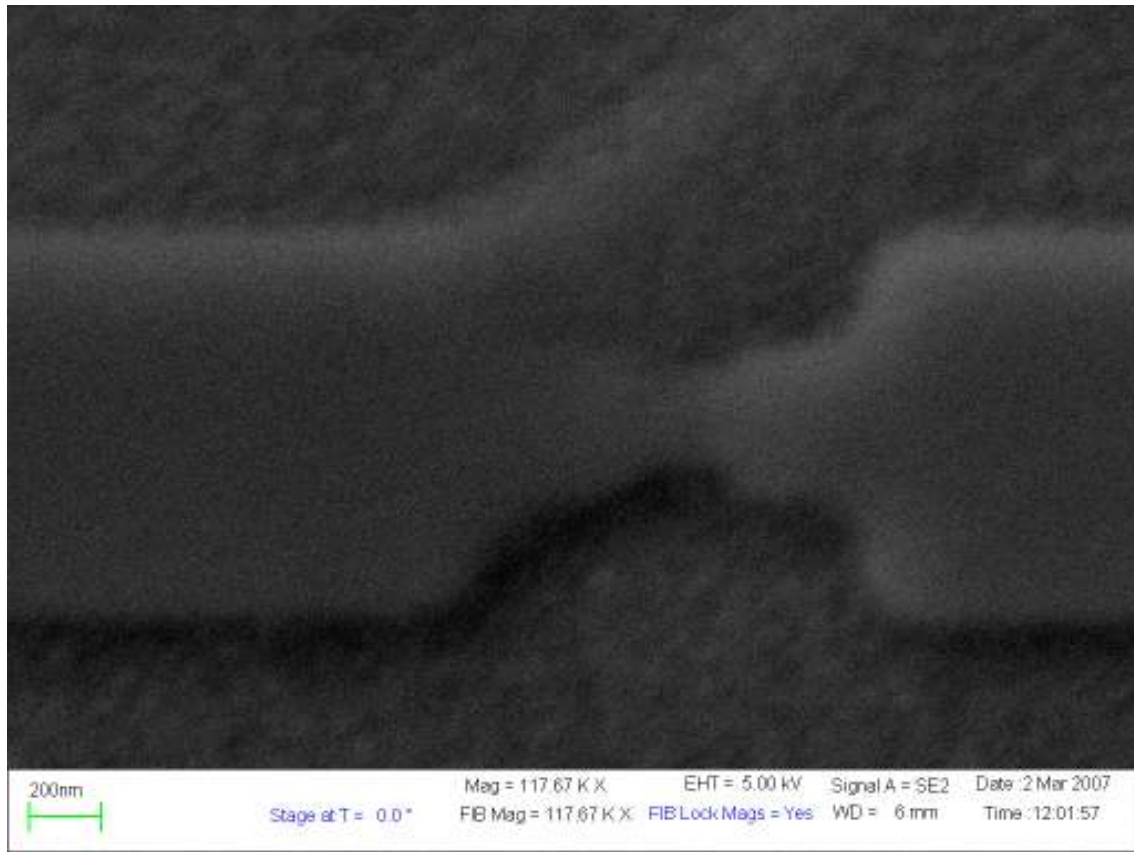


Fig 4.85 The central part of the SET structure after development which was exposed with a dose of $2000\mu\text{C}/\text{cm}^2$

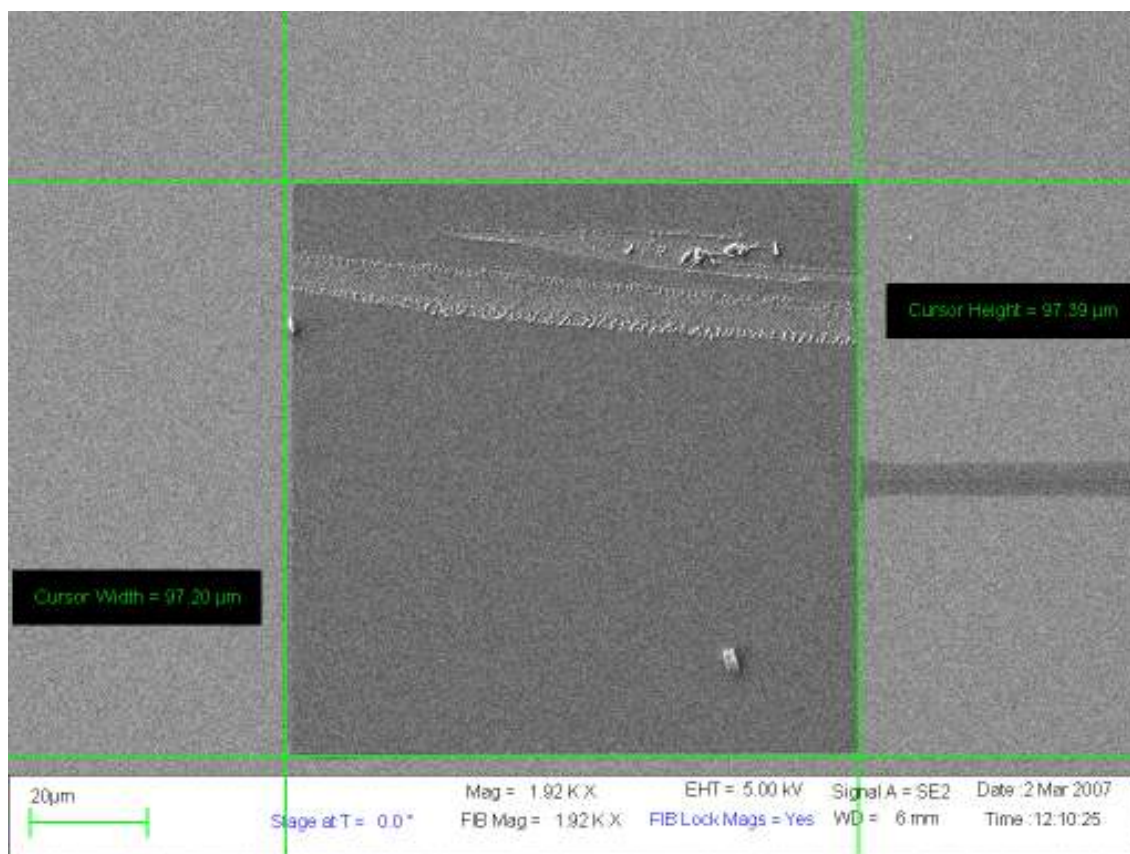


Fig 4.86 The pads of a SET structure after development which were exposed with a dose of $300\mu\text{C}/\text{cm}^2$

The images indicated that for a dose of $50\mu\text{C}/\text{cm}^2$ the fingers and islands were not defined. The dose of 200 and $600\mu\text{C}/\text{cm}^2$ worked slightly better. The fingers were defined without any halo but the islands were not to be seen. The structure exposed with the high dose of $2000\mu\text{C}/\text{cm}^2$ showed a clear halo effect. The pads were defined as needed and the dosage for them was exact.

In a discussion with Keith Bradshaw over at UT Dallas who had plenty of experience performing e-beam lithography it was suggested by him that I should experiment with the technique of spin-developing. My current technique for development involved dipping the wafer in the developer then dipping it in a diluted

solution of the same developer and then dipping it in DI water followed by drying it with a nitrogen blow gun. During each dip the beaker was shaken slightly to provide a slight agitation. He suggested that the spin technique would help in removing debris from the wafer and dislodge particles of the resist close to the exposed areas. The first test using this technique was carried out. The wafer specifications, e-beam parameters and the recipe for development are mentioned under tenth HSQ wafer in Appendix C.

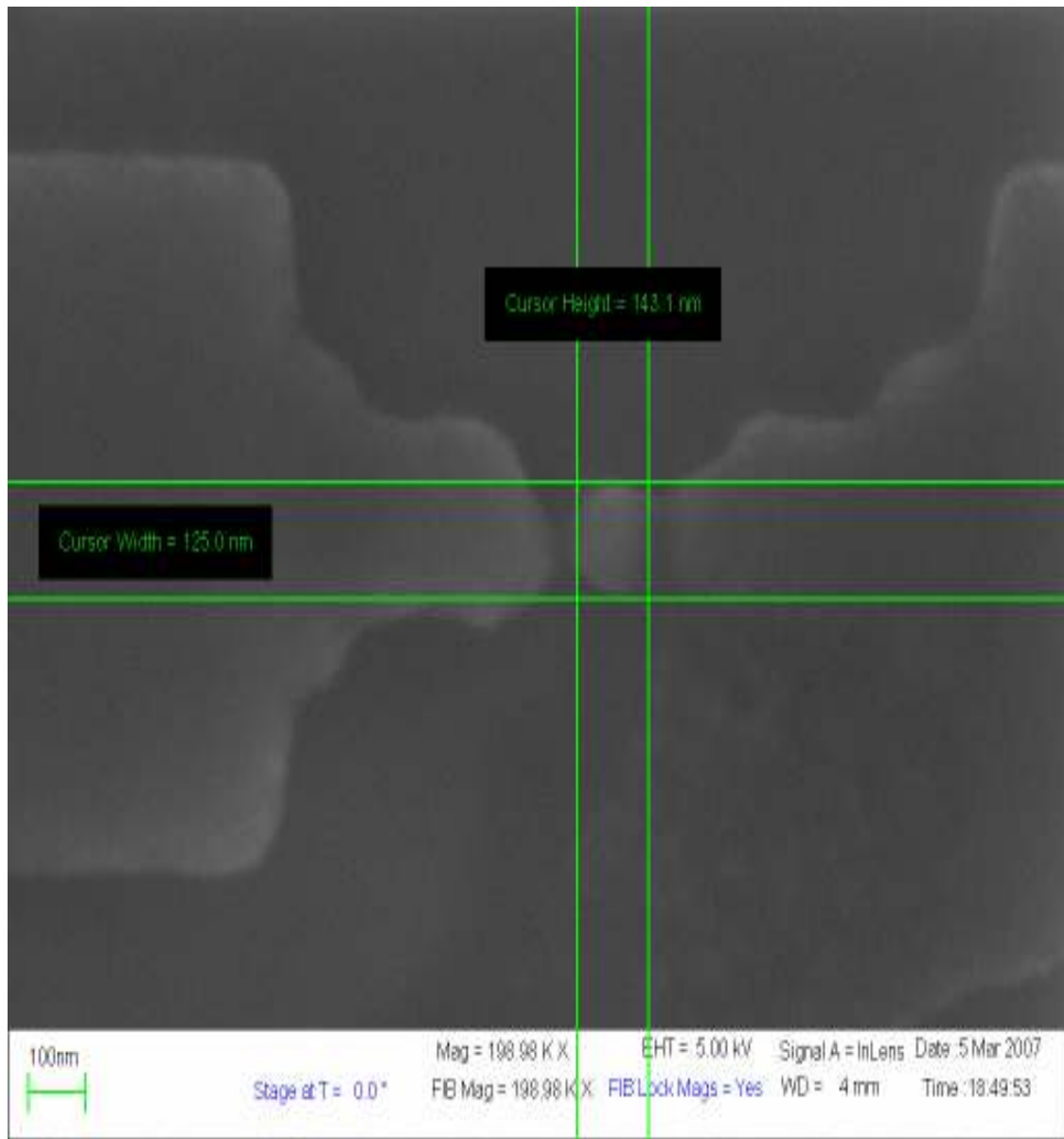


Fig 4.87 The central part of the SET structure after development exposed with a dose of $500\mu\text{C}/\text{cm}^2$

The results were encouraging as the island was defined at a slightly lower dose. I started to experiment with more doses and different development times for the using this new spin technique. I also altered the pre and post exposure bake temperatures and times. After several attempts and a lot of experimentation I also noticed how each

polygon of the finger and the islands needed to be subjected to a different dosage. The best results obtained are shown below. The wafer specifications, e-beam parameters and the recipe for development are mentioned under eleventh HSQ wafer in Appendix C.



Fig 4.88 The central part of a SET structure after development



Fig 4.89 The width of a finger of an SET structure after development

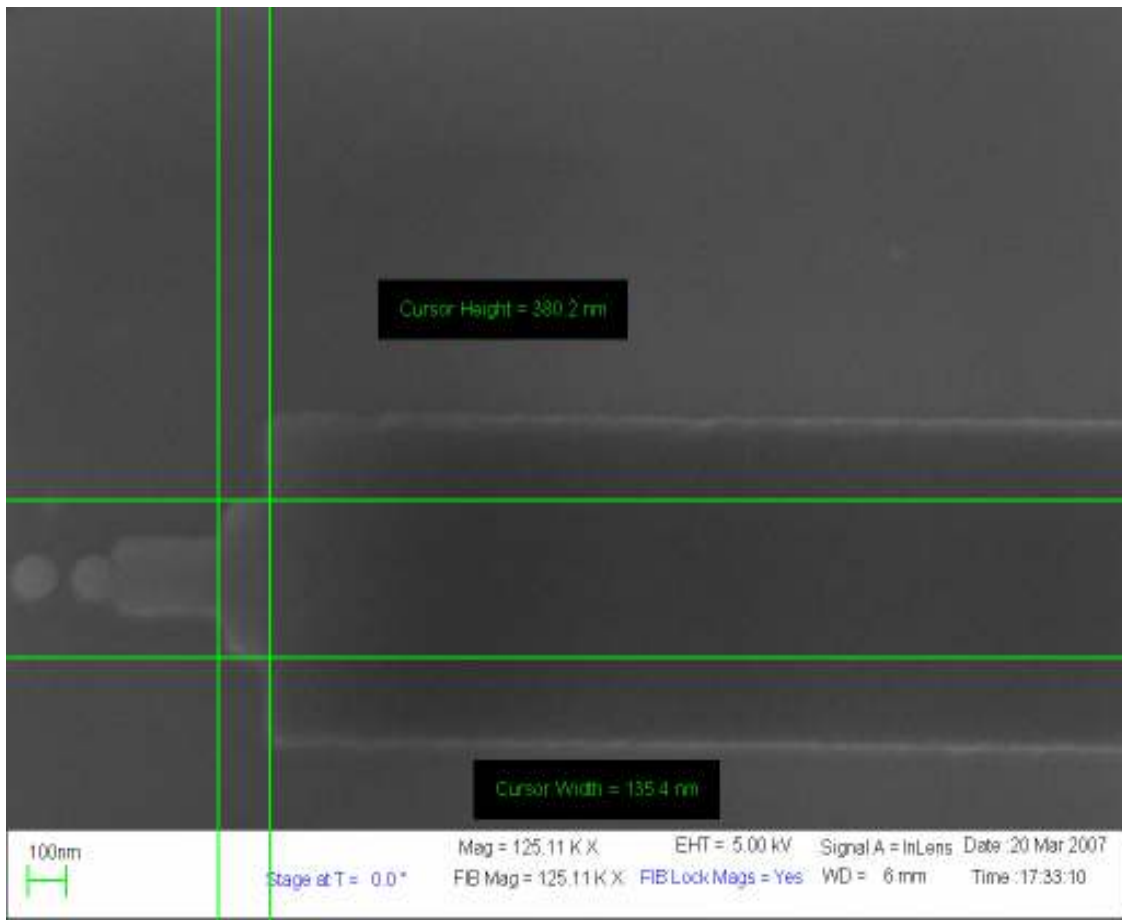


Fig 4.90 Width and length of the first tapered part of the finger after development

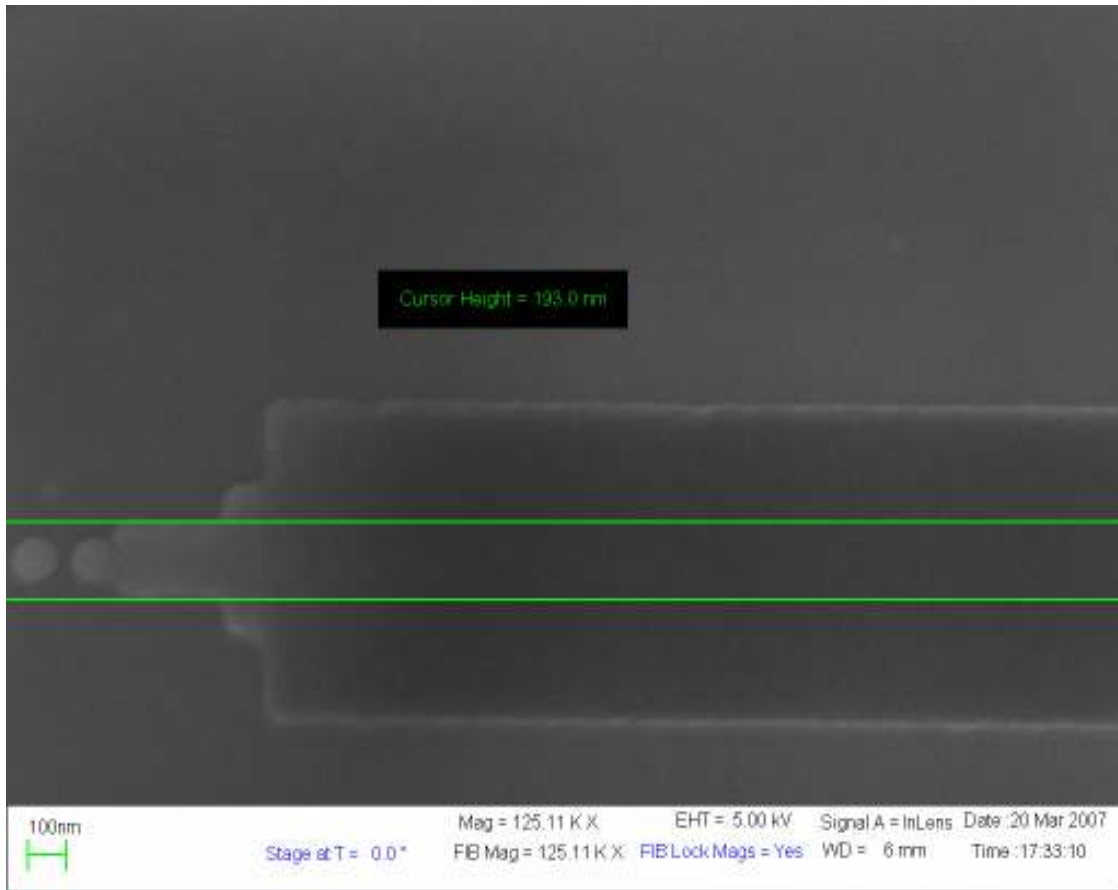


Fig 4.91 Width of the second tapered part of the finger after development

These images indicate that each and every dimension has been exactly reproduced. The only issue was that this wafer was dropped on the floor after the pre-exposure bake and so the wafer was littered with dirt. There was also a beam withdrawal issue since the beam blaster was not quick enough and when the beam exited it left a trail. This issue was discussed with Joe Nabity from J C Nabity Lithography systems and he suggested some strategies to work around this problem. The most significant conclusion that could be drawn from this test; was that now I had nailed the exact doses needed to expose each element of the design. The extraction of the doses was a result of extensive

experimentation followed by a very thorough examination and evaluation of results obtained from the experiments. I had now successfully patterned a structure where the exact individual doses needed to pattern the different elements of the design file had been coalesced.

Now that I knew the exact doses that were needed, I wanted to increase the doses of the islands slightly so that after development there would be a link between them. This would occur due to the proximity effect. If the islands were exposed at with a high dose the surrounding areas would be slightly exposed too and the developer would not be able to remove HSQ from those regions. The function of the link is as follows: if the width of this junction between the islands is small and if there are no impurity atoms in the volume of junction they would act as tunnel barriers. This type of intrinsic region is highly resistive at low temperatures [24]. Since I was dealing with single crystal silicon, which is highly pure would certainly function as a tunnel barrier if the width was small. The wafer specifications, e-beam parameters and the recipe for development are mentioned under twelfth HSQ wafer in Appendix A.

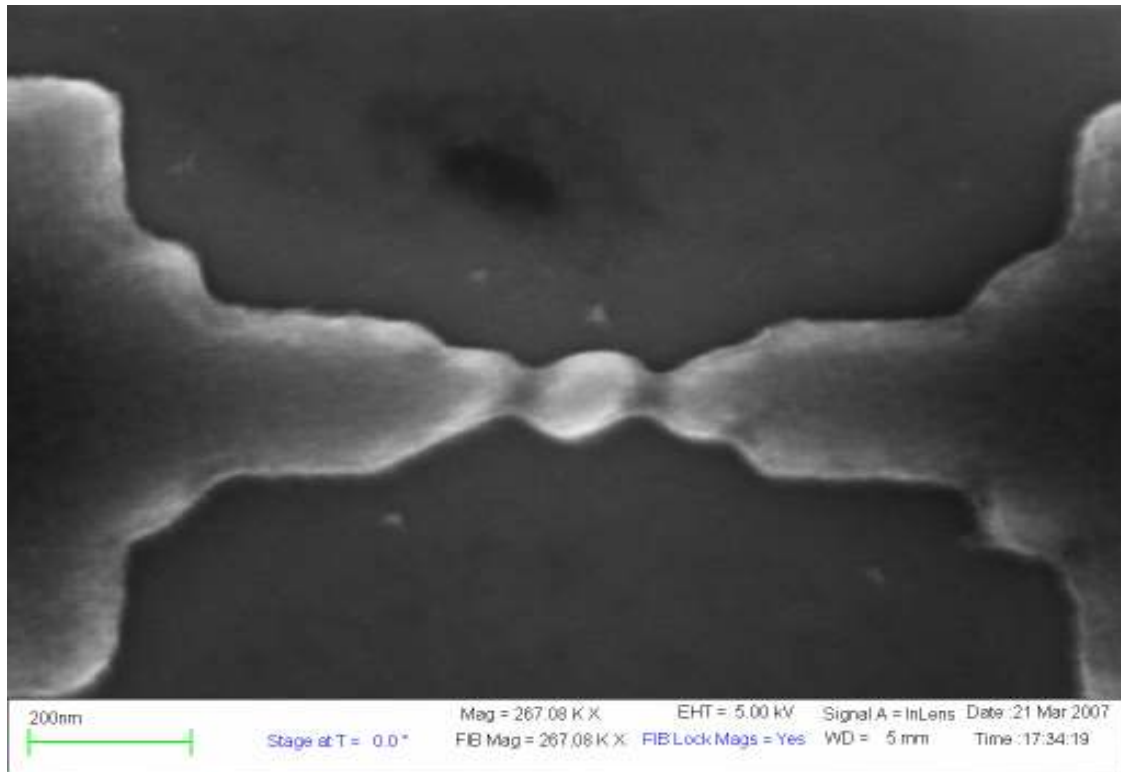


Fig 4.92 The SET structure after development with the dose for the islands altered to form constrictions

Now the etching rates were to be calculated and also the effect of baking to be evaluated. For wafers that were unbaked it was noticed that HSQ would eventually get removed during the etching. Various baking strategies were tested and finally I decided on the one which showed decent results in enhancing the etch durability of HSQ in the DRIE machine. The Trion DRIE is also loaded with a lot of options and an etching strategy needed after devised too.

After various baking and etching strategies were tested on numerous wafers I felt confident enough, finalized them and started work on the same wafer whose image is the one included directly above. The bake was conducted in the Blue M oven which bakes samples in an inert atmosphere. The oven does not have a cooling fan installed

so during a stage when a temperature drop is needed it can not be exactly timed. The baking conditions are also mentioned under twelfth HSQ wafer in Appendix C.

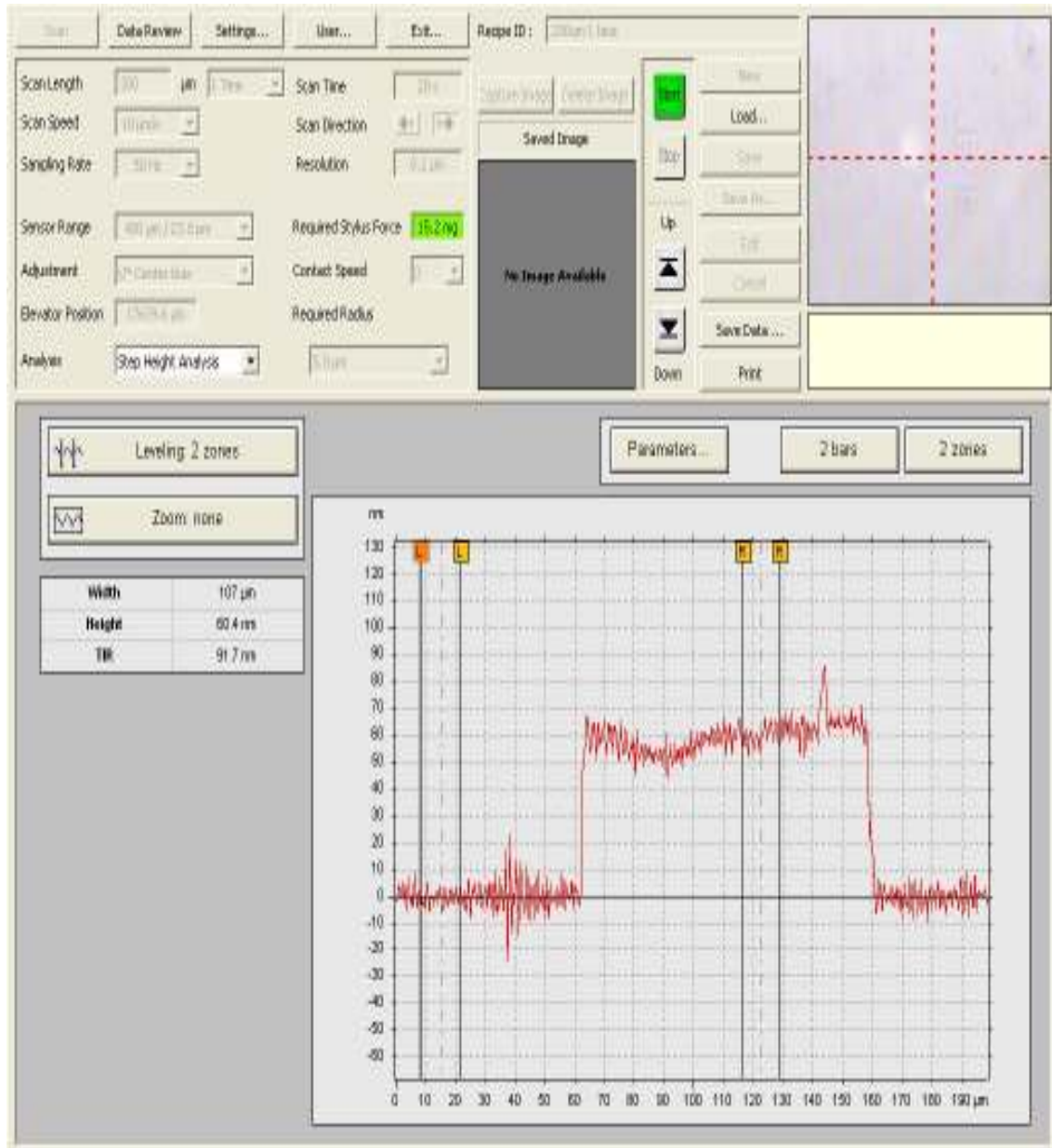


Fig 4.93 Profile for the top pad of the SET structure #1 after development

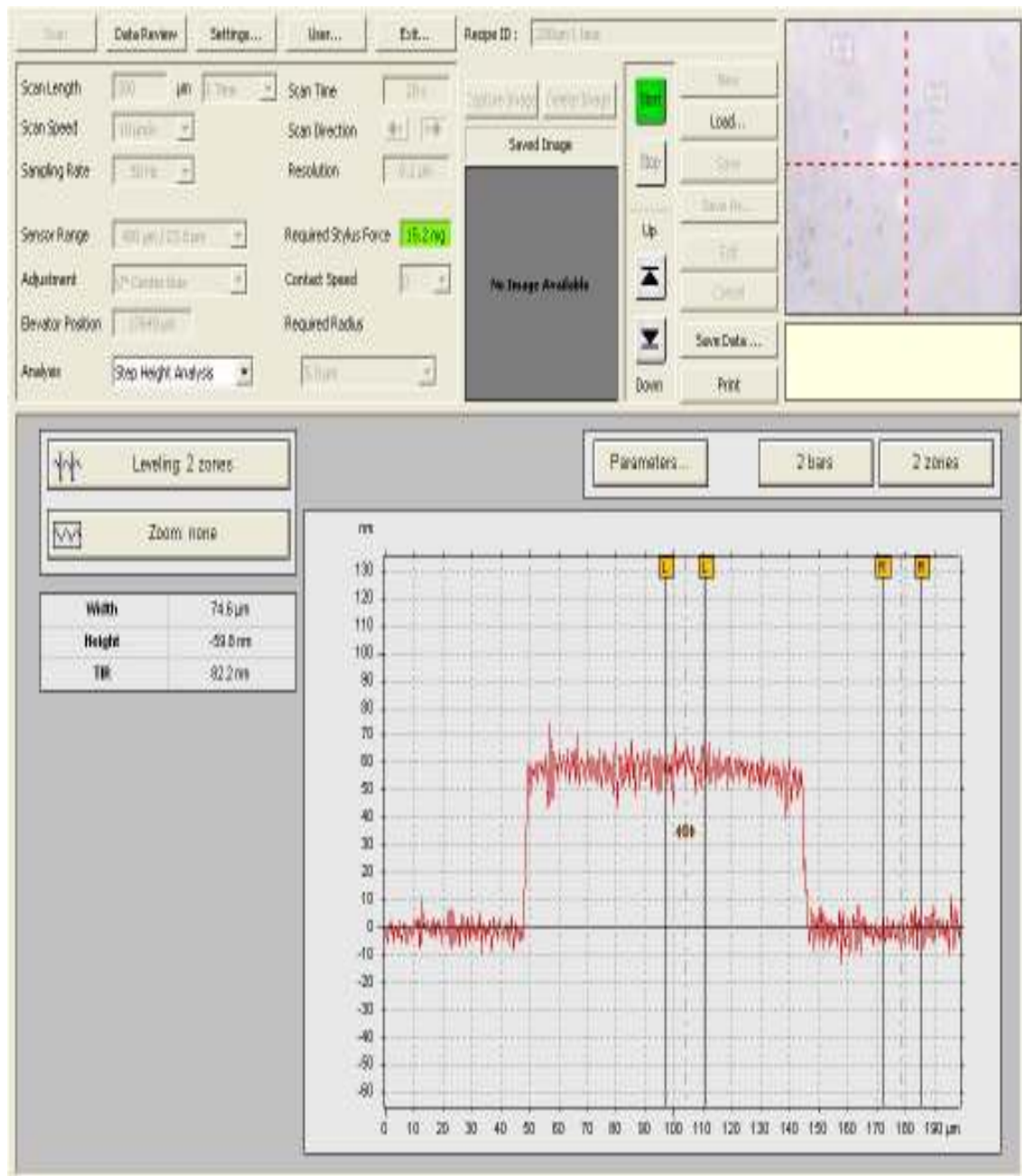


Fig 4.94 Profile of the bottom pad of the SET structure #5 after development

These images indicate that after development the height of structures is approximately 60 nm. This is basically the thickness of the HSQ that is left on top of the structures after development.

The wafer is now baked. It is expected that there will be a slight shrinkage in the lateral and vertical direction. This is because HSQ undergoes further crosslinking at high temperatures as mentioned in sections above.

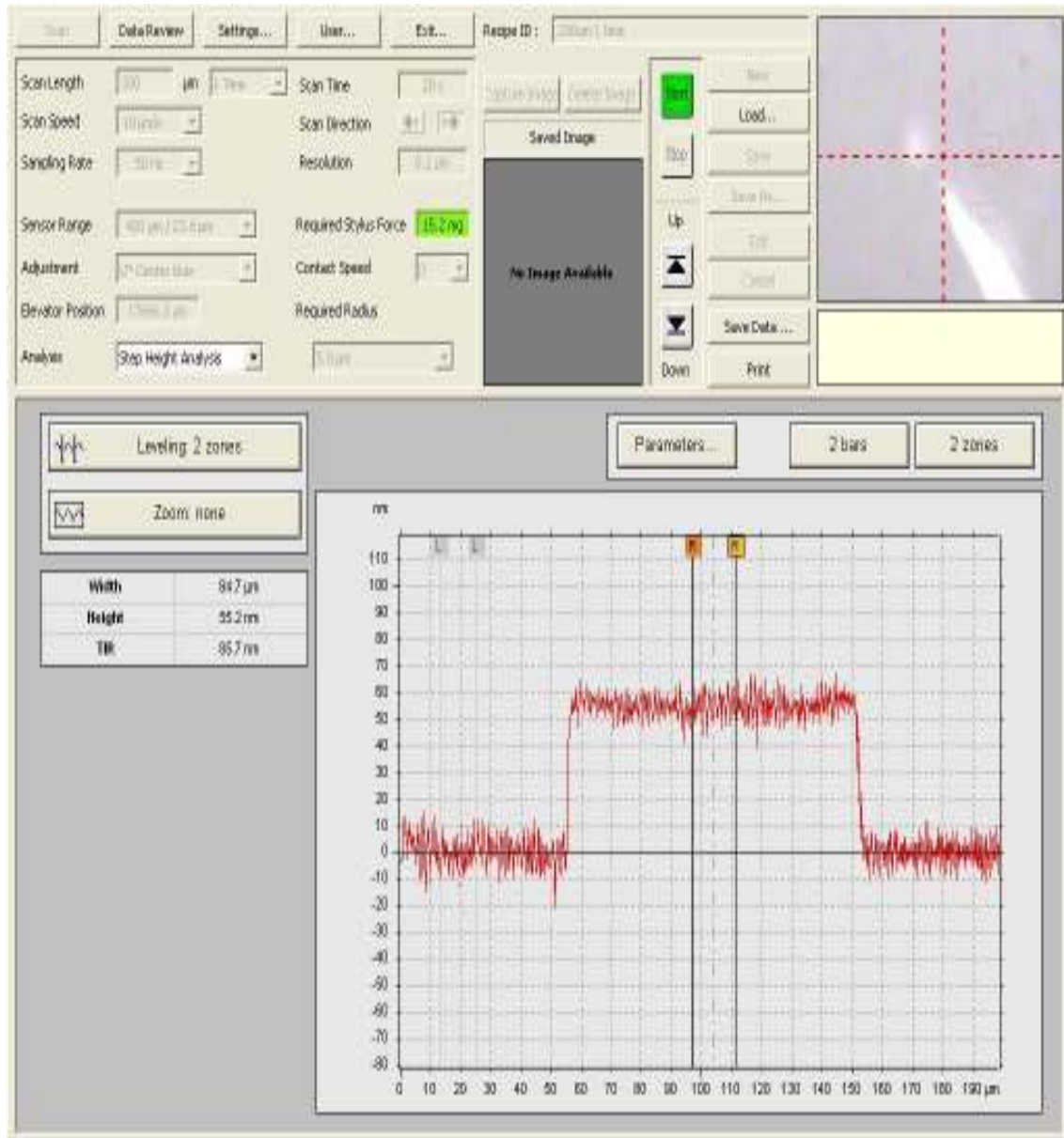


Fig 4.95 Profile for the top pad of the SET structure #1 after baking

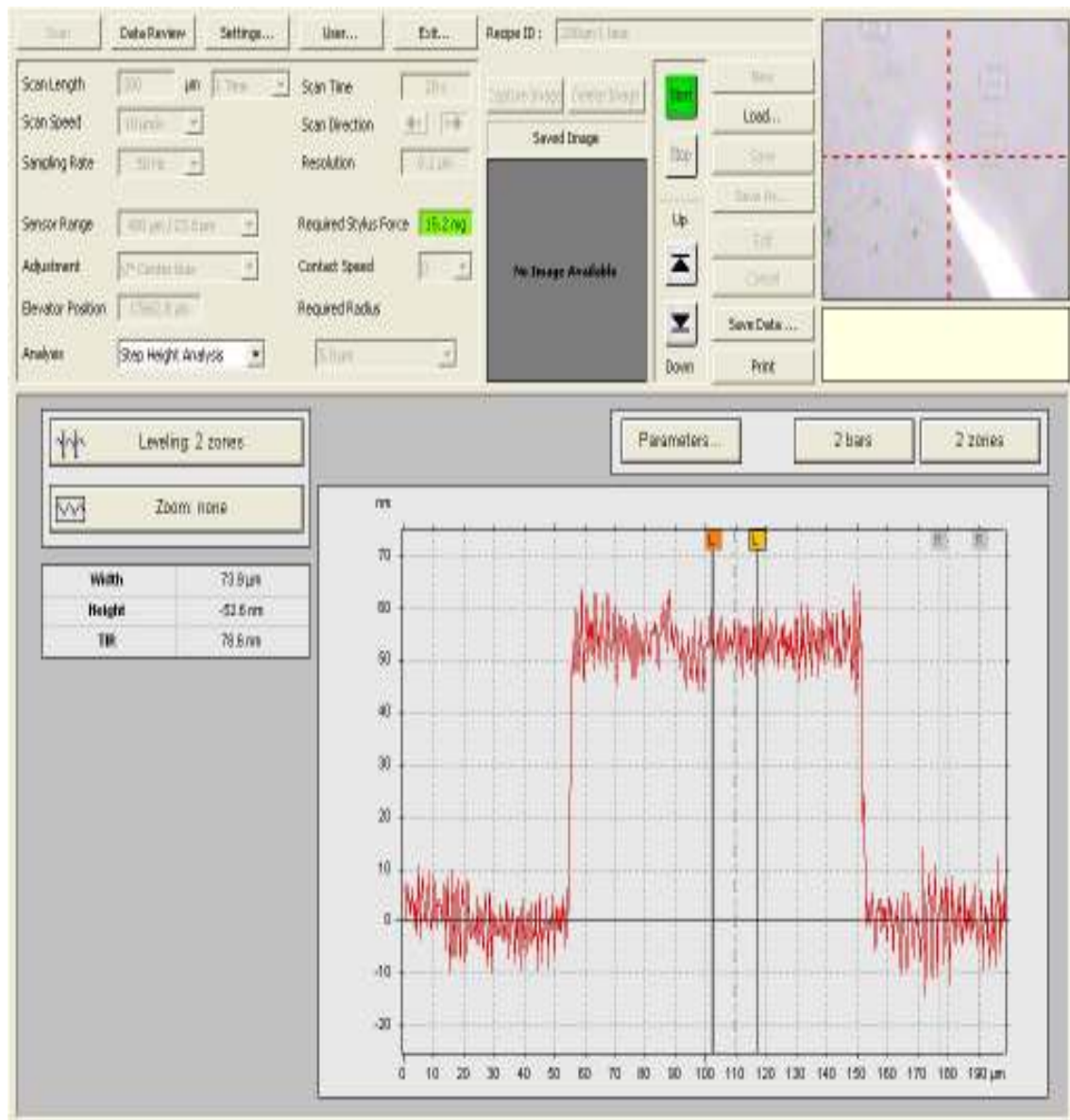


Fig 4.96 Profile for the bottom pad of the SET structure #5 after baking

After the baking we see that the structures did shrink a little in height approximately 6.2 nm. The etching was now conducted in the Trion DRIE using SF₆, O₂, He and Ar. The use of He and Ar is common in the industry for obtaining smooth sidewalls, since the

machine was equipped with these gasses and I decided to use them. The etching conditions are mentioned under fourth HSQ test in Appendix D.

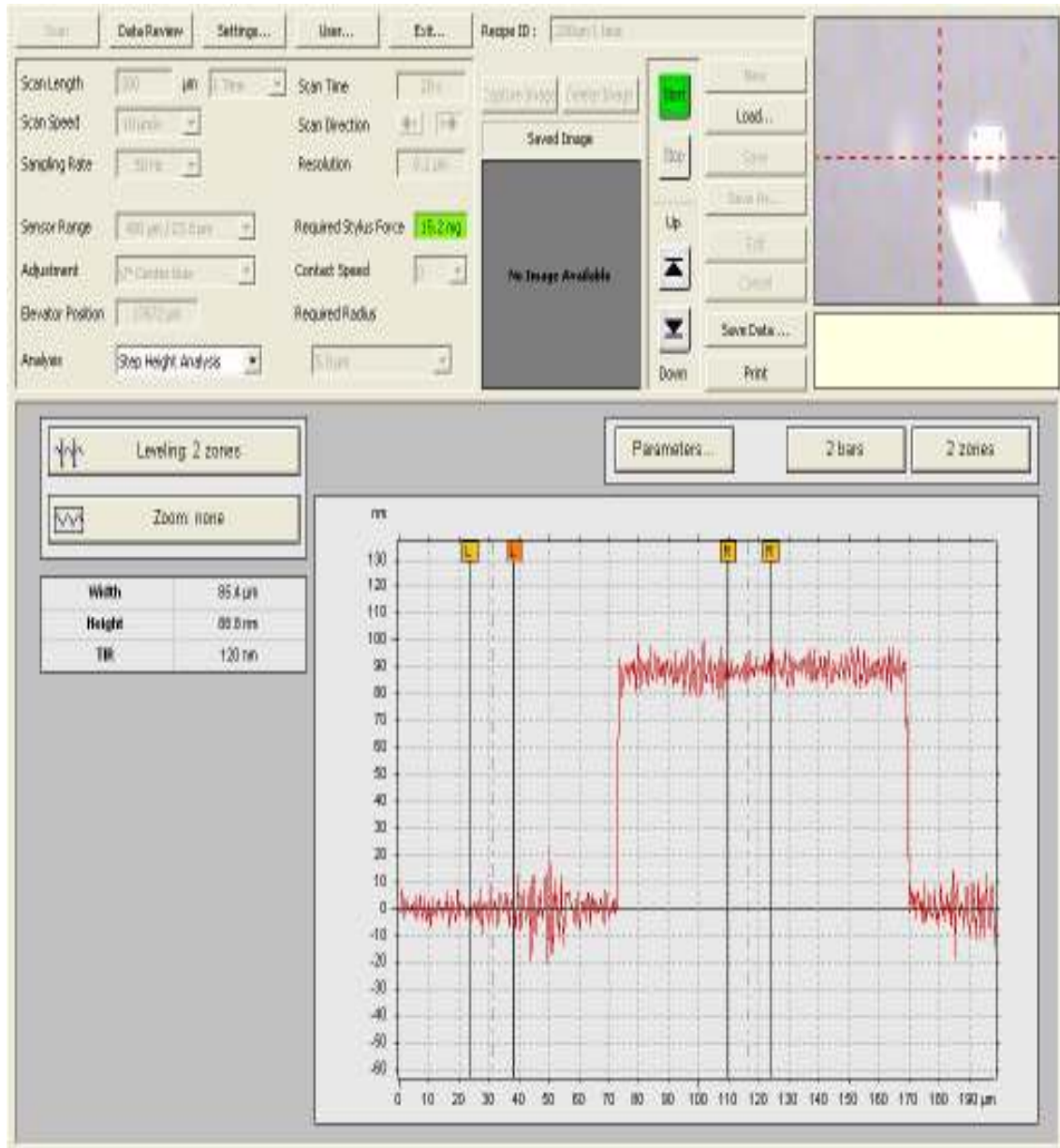


Fig 4.97 Profile for the top pad of the SET structure #1 after the first etch

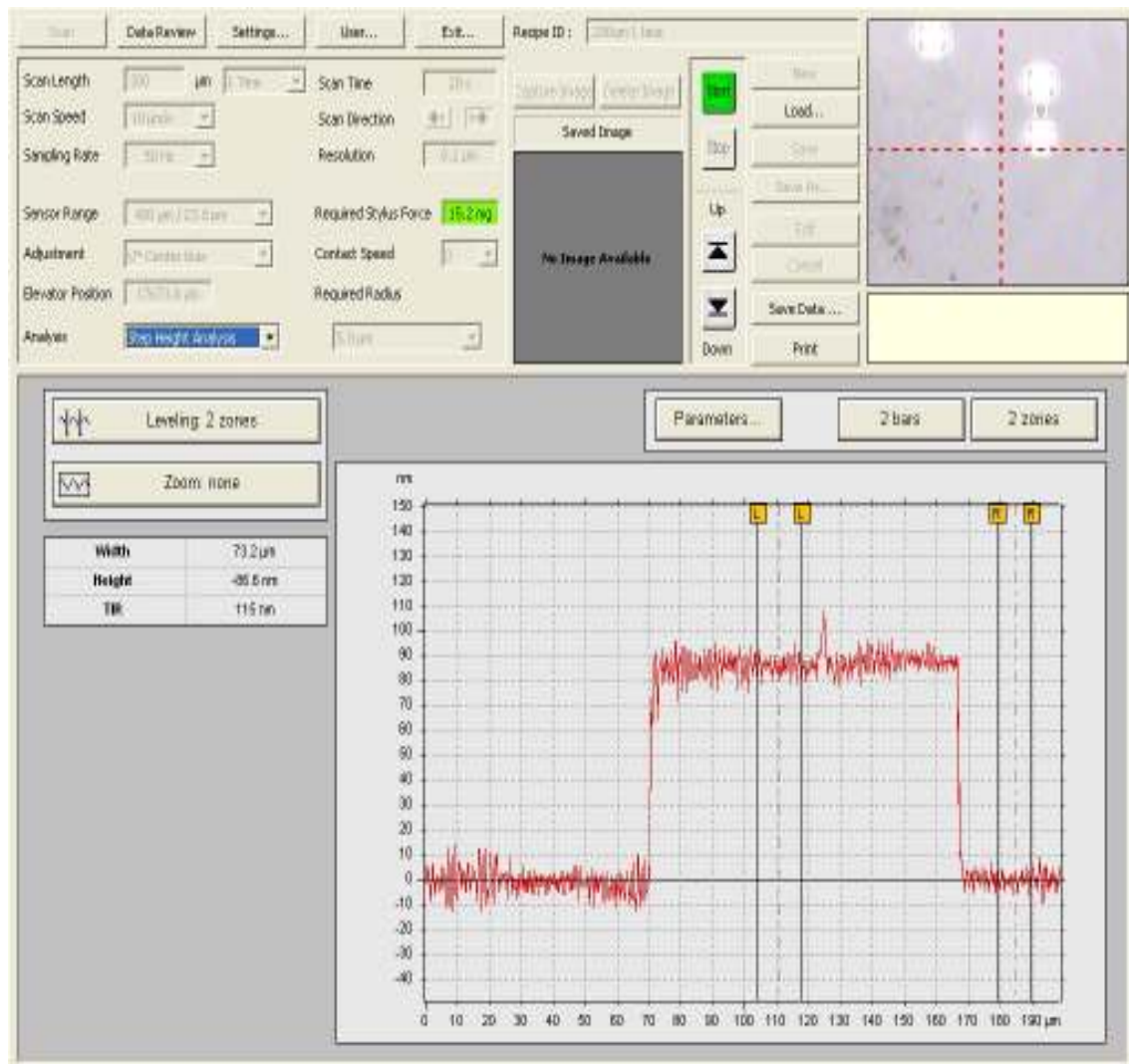


Fig 4.98 Profile for the bottom pad of the SET structure #5 after the first etch

After the first etch the surface of the wafer on top of the structures was still pink which is the color of the wafer after HSQ is developed, but the rest of the wafer was bluish green. This clearly indicated that there was HSQ on top of the structures protecting it and acting like an etch mask. I estimate that some of the thickness of HSQ is lost during etching. The average difference in height is about 34.7 from the bake and the etch so considering no HSQ lost at all during the etch (not a sound assumption), the etch

rate of single crystal could be approximated to be 34.7nm/min. In all reality since some HSQ was removed too more than 34.7 of Si was surely etched. Another additional etch was conducted just to make sure that all the 55nm of Si was etched away.

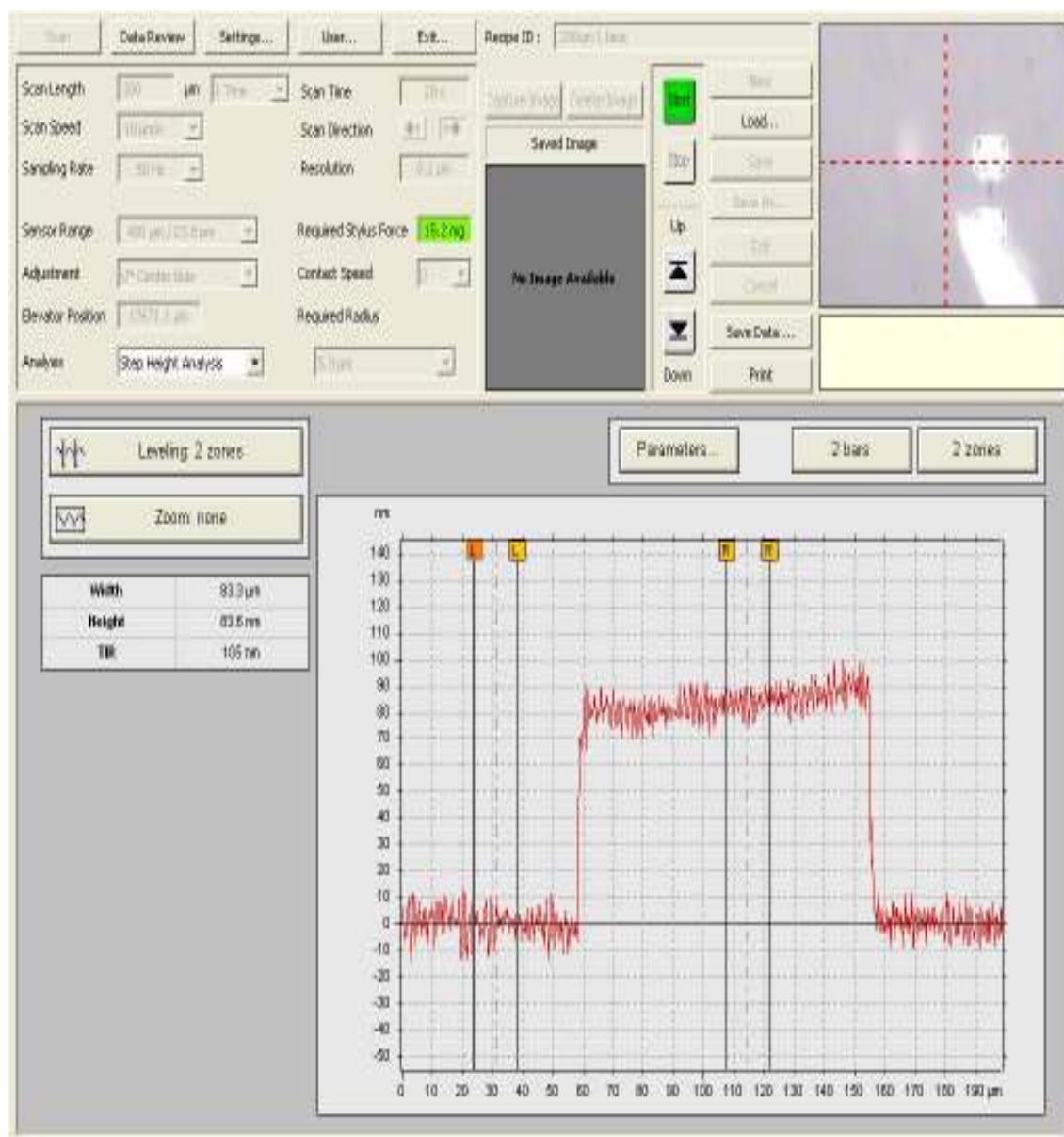


Fig 4.99 Profile for the top pad of the SET structure #5 after the second etch

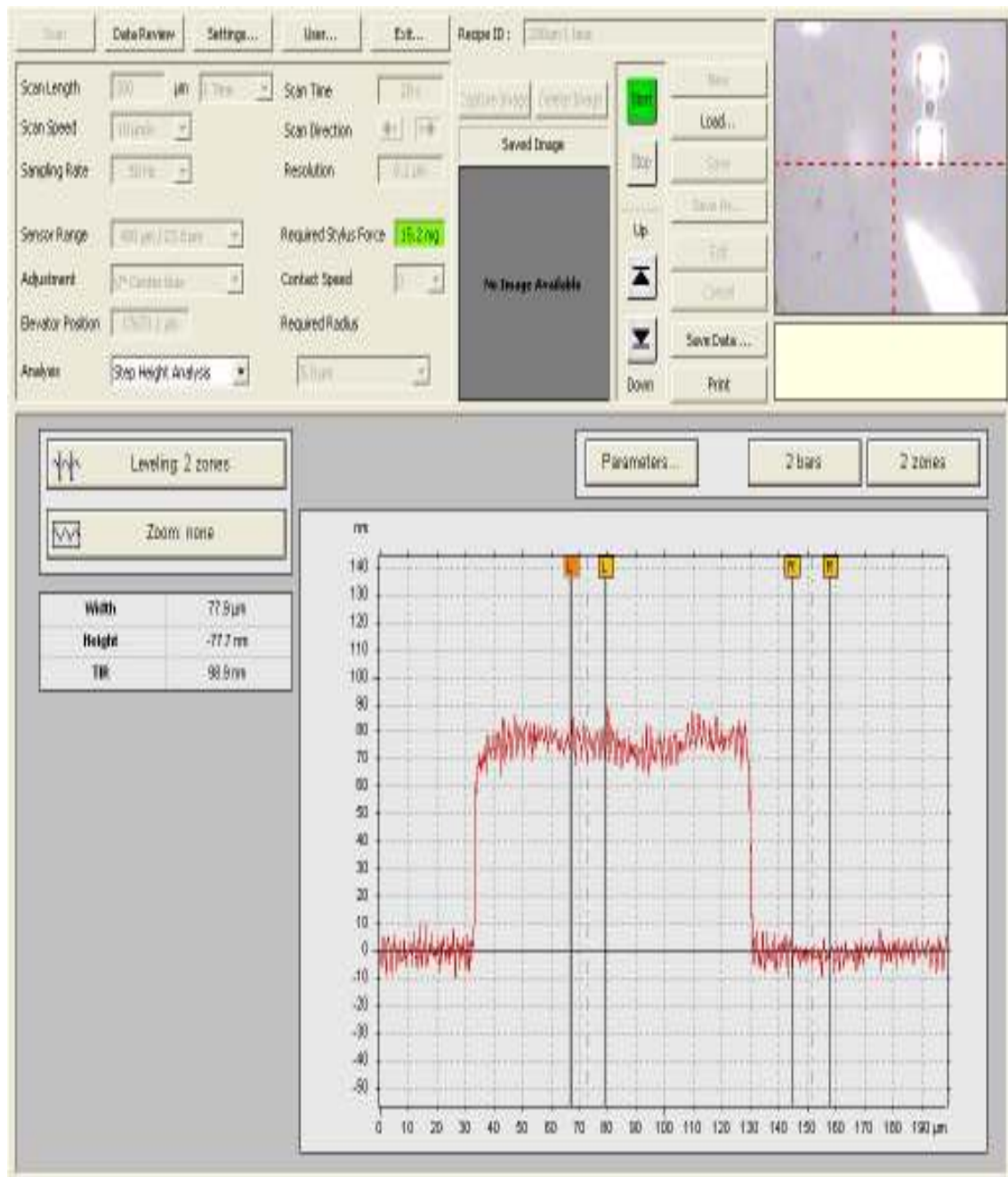


Fig 4.100 Profile for the bottom pad of the SET structure #5 after the second etch

After the second etch the surface on top of the structures seemed metallic or silverish grey and in some places it was slightly pink which was due to slivers of HSQ still left. The grey color indicated silicon. The rest of the wafer was slightly more greenish now.

I can definitely conclude that we had Si left only on the structures and the SiO₂ layer had been reached. To double check this, the wafer was dipped in the buffered oxide etchant and the height of the structure increased like expected indicating that buffered oxide etchant attacked the SiO₂ layer. The slivers of HSQ were also removed now. As the DRIE machine needs a 4 inch wafer and our samples were 1cm pieces we used an *n*-type 4 inch poly crystalline silicon wafer to place our samples on. The sample also acted like an etch mask as the rest of the carrier wafer etched away.

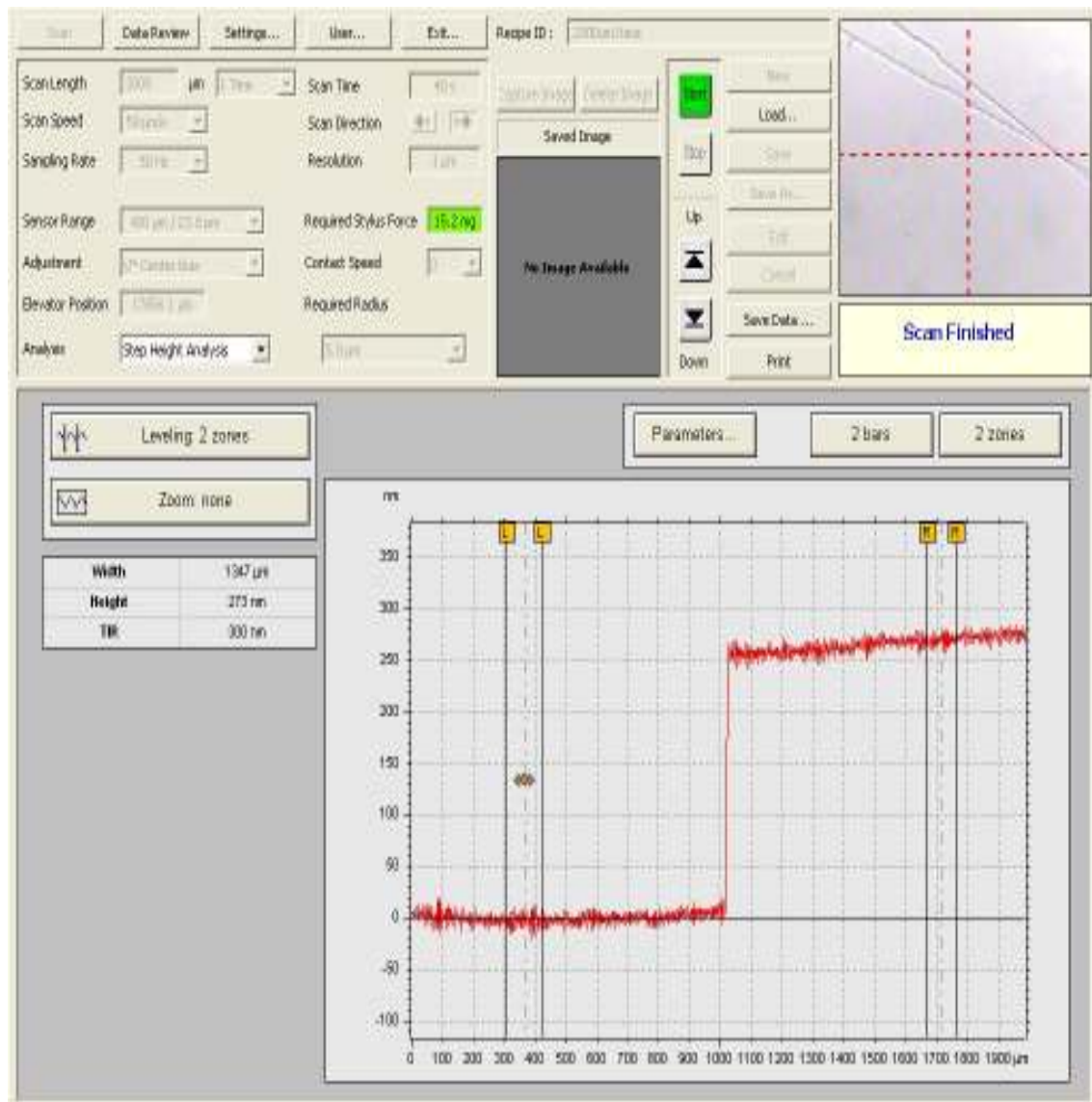


Fig 4.101 Profile of the carrier wafer after a 125 second etch

The etch rate for the carrier wafer is thus determined to be 156 nm/min.

CHAPTER 5

CONCLUSION

5.1 Summary

As the consumer demands increase for better performing and smaller gadgets the semiconductor industry will look for alternatives to the current CMOS technology. At that time the industry will look to adopt a digital technology which shows great performance, promise and one which uses most of the current technologies used for manufacture thus a full restructure of the plants will be avoided and billions of dollars saved.

Single electron devices are currently being used in various areas of research. Single electron devices hold the promise of high scalability and low power consumption. The performance of the single electron transistor will actually improve as the size of the device decreases which means that the technology might be limitless. Right now researchers have fabricated all sorts of devices using single electron devices. Logic circuits [25], highly sensitive charge detectors [2] and memories [26] are some of the circuits that have been fabricated. The use of single electron devices in ultra large scale integrated (ULSI) circuits face many problems. The current technologies used by researchers are not feasible and are ruled out for use in the industry as they are too slow.

With this aim in mind I went on a search for finding simple techniques for fabricating a single electron transistor. There were various complicated techniques out there some involving nanotubes and some with gold particles placed between electrodes. My approach was to incorporate as many current technologies as possible.

Using SOI wafers, an HSQ based e-beam resist system and a SEM converted to perform e-beam lithography I have been able to pattern a SET structure. Even though I had no choice but to use e-beam lithography I am hoping that when the industry does adopt this technology they will have incorporated parallel e-beam writers or they could use immersion lithography techniques.

Along the way I have investigated two other e-beam resist systems, their resolution limits, their sensitivity to different electron beam doses and etching durability in a reactive ion etching system using CF_4 and O_2 . UVN30 a negative e-beam resist though promised great etch resistance was not suitable owing to the fact that its resolution limit was higher than what we needed for defining the islands. PMMA which is mostly used as a positive e-beam resist was instead used a negative e-beam resist. The structures were well defined but could not withstand the gas mixtures used in the RIE to etch silicon.

Table 5.1 Pros and Cons of different resists used

Resist System	Pros	Cons
UVN30	Good dry etch resistance in CF_4 plasma	Resolution limited to 150 nm
PMMA	Good resolution	Poor dry etch resistance
HSQ	Good resolution	Adequate etch resistance

I encountered problems with HSQ exposure and development procedures initially; however but managed to work my way out by conducting numerous profound experiments. After being trained on the e-beam and SEM machines I had better judgment and more control on the exposure doses and microscope parameters. I faced a

few difficulties in designing the new SET pattern using DesignCAD but with Mr. Joe Nability's aid I was able to allay them out. He made valuable suggestions for modifying the design which enabled me to work my way around the limitations imposed due to a slow blanker installed in the e-beam machine. After obtaining the desired SET structure in HSQ post-development the next challenge lie in etching silicon using HSQ as an etch mask. The quandary here was that after e-beam exposure and development HSQ's chemical structure would be similar to that of an oxide of silicon. I was limited by the fact that our laboratory did not have an etcher that had provisions for using gasses like HBr or chlorine. A fluorine based etch was the only option. The purchase of the Trion DRIE machine was a god send since it was capable of handling gasses like SF₆ and Ar. The use of SF₆ instead of CF₄ proved to be more selective in etching Si over HSQ. Though HSQ does get removed during the etch eventually I discovered the conditions that would minimize it enabling me to reach the SiO₂ layer of the wafer thus effectively removing all the Si from the top side of the wafer except that below the patterned HSQ. Removal of HSQ following the etch was done by dipping the wafer in a buffered oxide etchant for a very short duration. The pattern transfer was now complete and a standing silicon structure was fabricated.

5.2 Future work

The SET device cannot be considered complete yet, a couple of processing steps are still needed. It would be much easier to start off with an *n*-type doped silicon layer. The doping should be moderate just enough to make a few electrons available in the source and it would also ease the transport of electrons through the device. Doping the

source and drain regions post etching is possible but is more complicated. First the dopant ions would have to be implanted and then annealed to provide electrical activation.

Dry thermal oxidation of the wafers already fabricated in an ambient oxygen atmosphere at about 1000°C is needed. This has been used by other researchers to shrink the width and height of the tunnel barrier regions and the island [27]. This process is called pattern-dependent oxidation (PADOX). The process from a fabrication point of view could be explained as follows; oxidation occurs at the interface of the Si and buried SiO₂ layer interface also. The oxygen atoms penetrate through the top layer of SiO₂ and the Si layer from the sides of the pattern reaching the Si and buried SiO₂ layer interface. Oxidation occurs not only at the top of the pattern but also at the edges of the pattern whereas the centre of the pattern (the core of the islands and tunneling barriers) oxidation is suppressed due to the stresses accumulated due to oxidation happening all around it. With an oxide layer surrounding the island and barriers now they are confined in every direction thus preventing leakage.

It is also known that silicon is consumed during oxidation roughly 44% of the final oxide thickness. This would enable the island and tunneling barriers to shrink considerably. After oxidation it would be advantageous to view the cross-sectional profile for the island. This would help in calculating the oxidation time needed for a desired island size.

A highly doped *n*-type gate structure on top of the oxide layer is needed to control the island charge. I would recommend a poly-Si structure being deposited to perform that function. As there is a thick oxide layer separating the two silicon layers

of the wafer the backside of the SOI wafer (where there has been no patterning) which is a thick layer of silicon could function as a gate too. To provide contacts for test probes the source and drain pads have to be coated with conducting materials. Evaporating Aluminum of top of the pads only would be the simplest strategy. This would complete the entire fabrication procedure.

Measuring the source-drain conductance with respect to the changes in gate voltage at a very low temperature would be of prime importance after fabrication. If conduction oscillations are observed further characteristics should be measured. The temperature should also be raised until the oscillations are smeared out. If oscillations are not observed then the simplest solution would be increasing the oxidation period to facilitate further shrinkage of the island and barriers. There is a threshold point after which the oxidation rate will reduce considerably or stop.

With the current design and considerable shrinkage after oxidation I expect to observe the conductance oscillations at temperatures around 10 K or lower. Reducing the doses used for patterning could also be used to reduce the island diameter and the width of the tunneling barriers.

APPENDIX A

UVN30 RECEIPES

First UVN30 wafer

Wafer specifications

1cm x 1cm piece from a poly crystalline silicon wafer, p-type doping

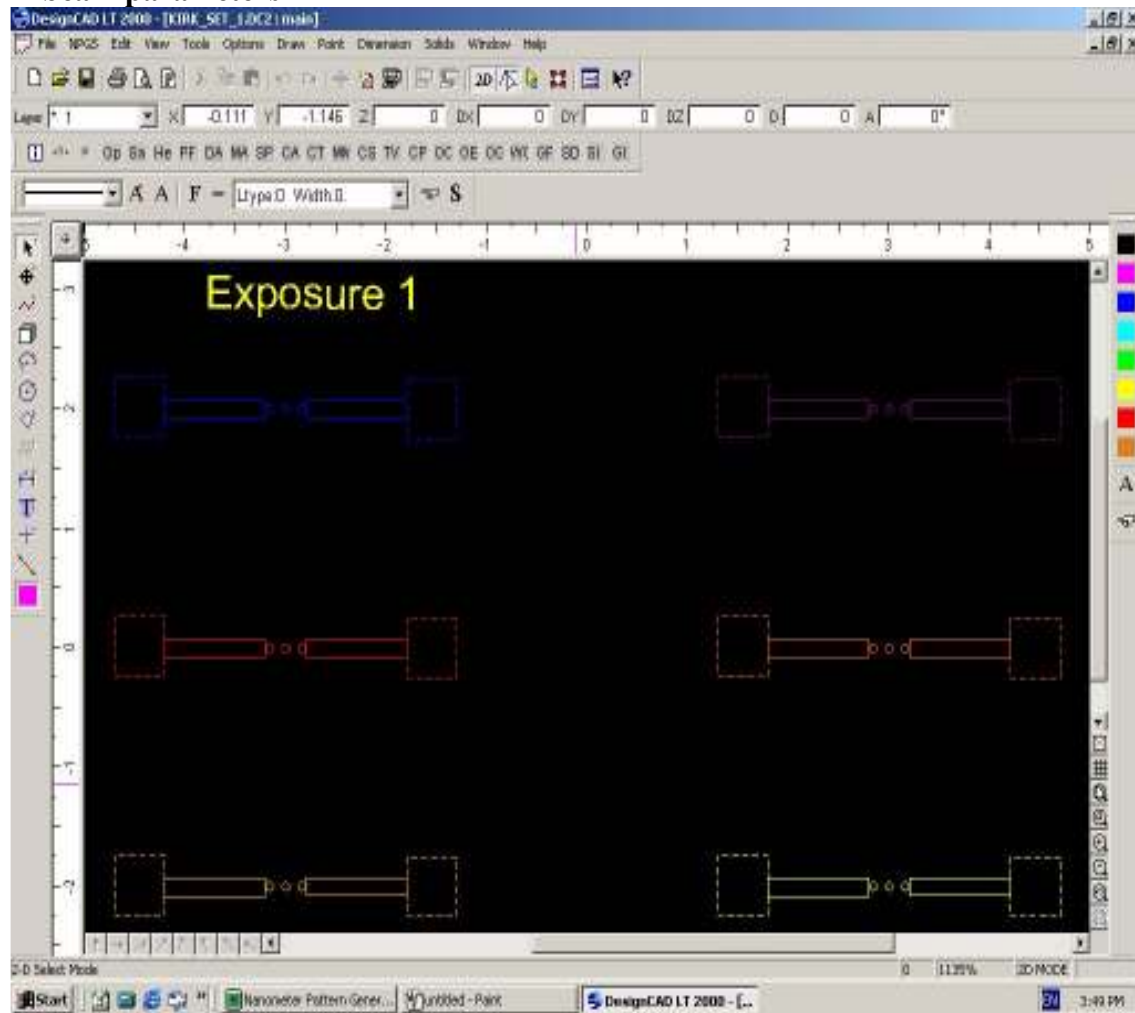
Samples are prebaked at 140°C for 10 minutes on hot plate

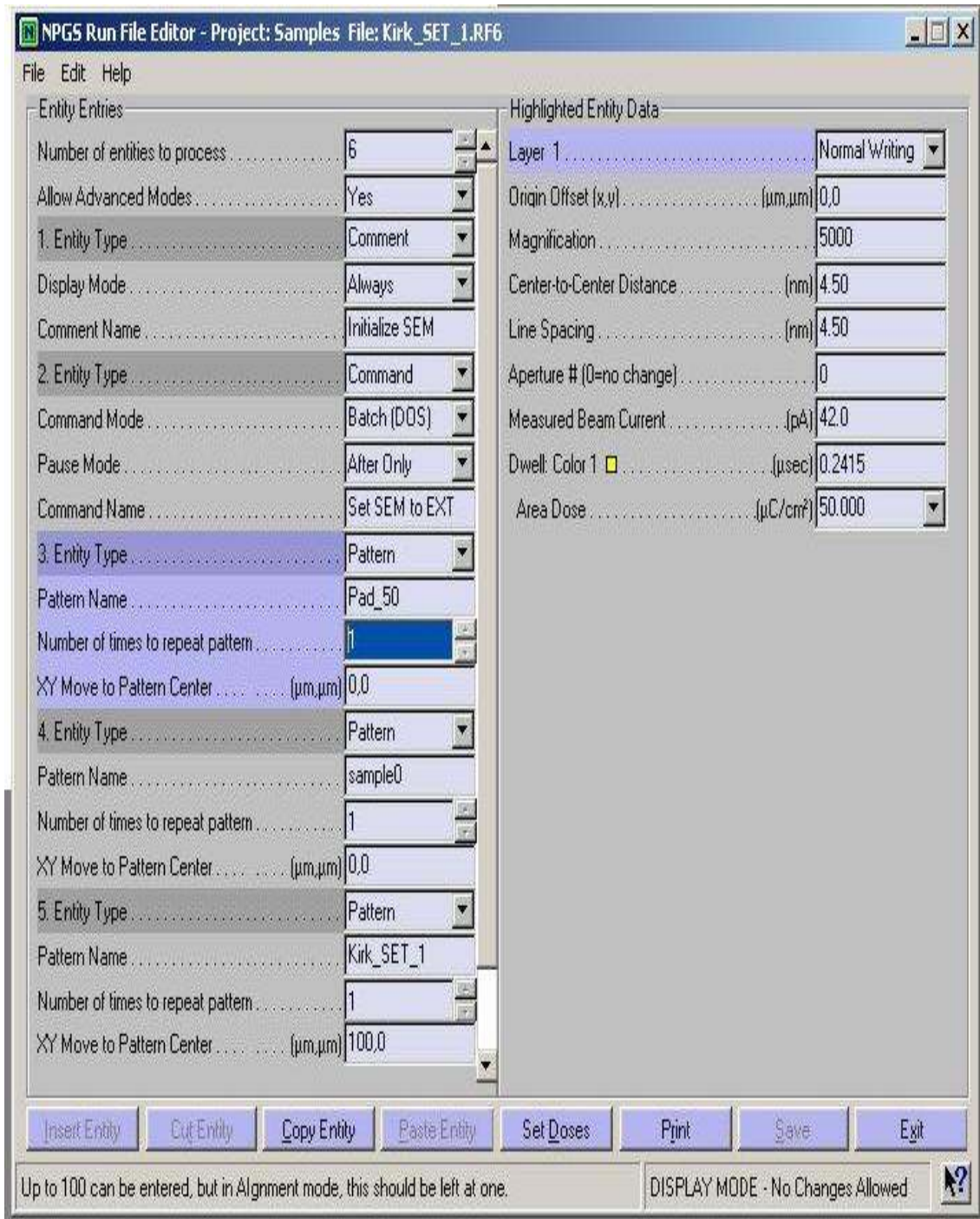
HMDS was spun on at 3000 rpm for 30 seconds

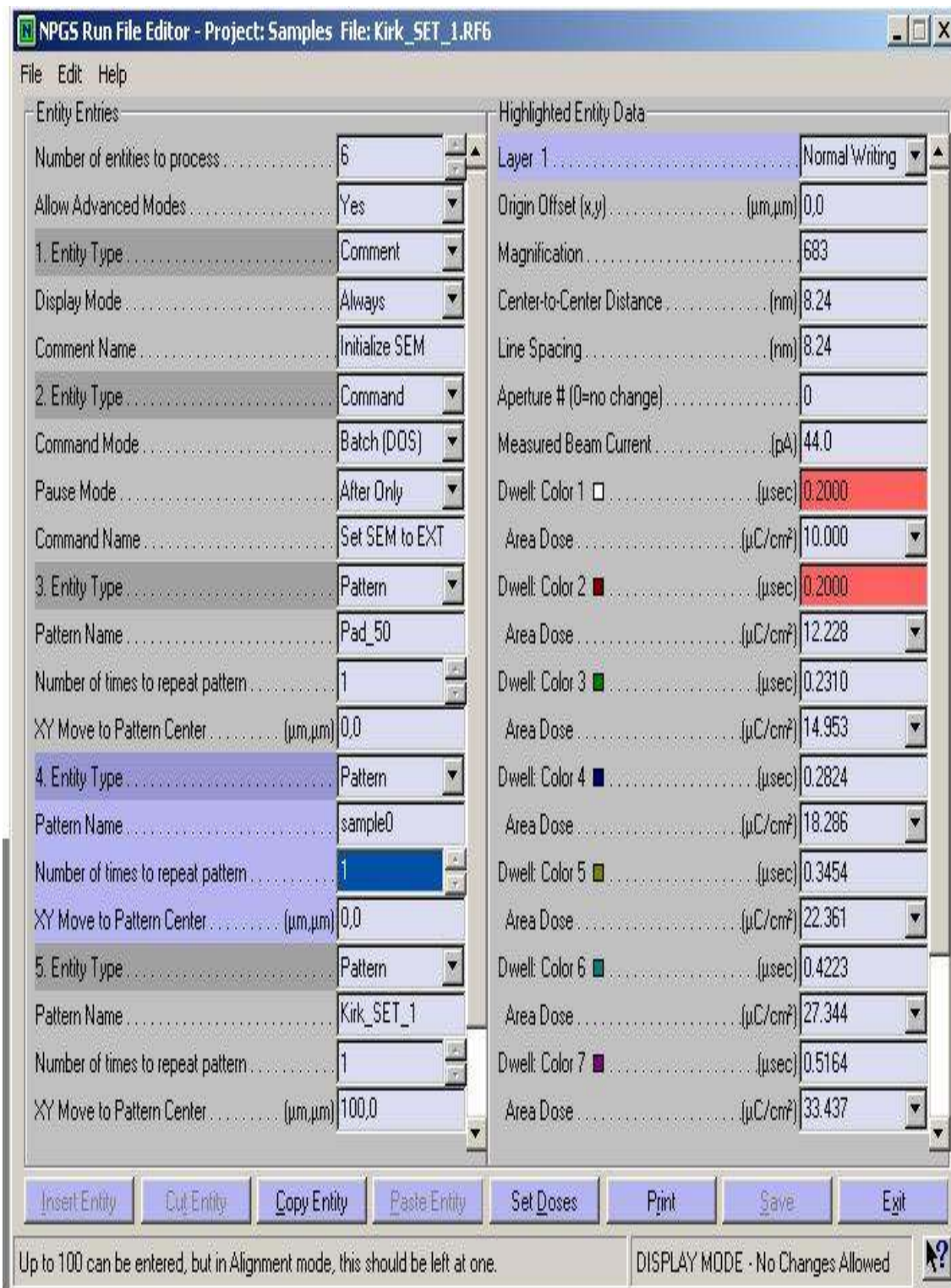
UVN30 was spun on at 5000 rpm for 30 seconds

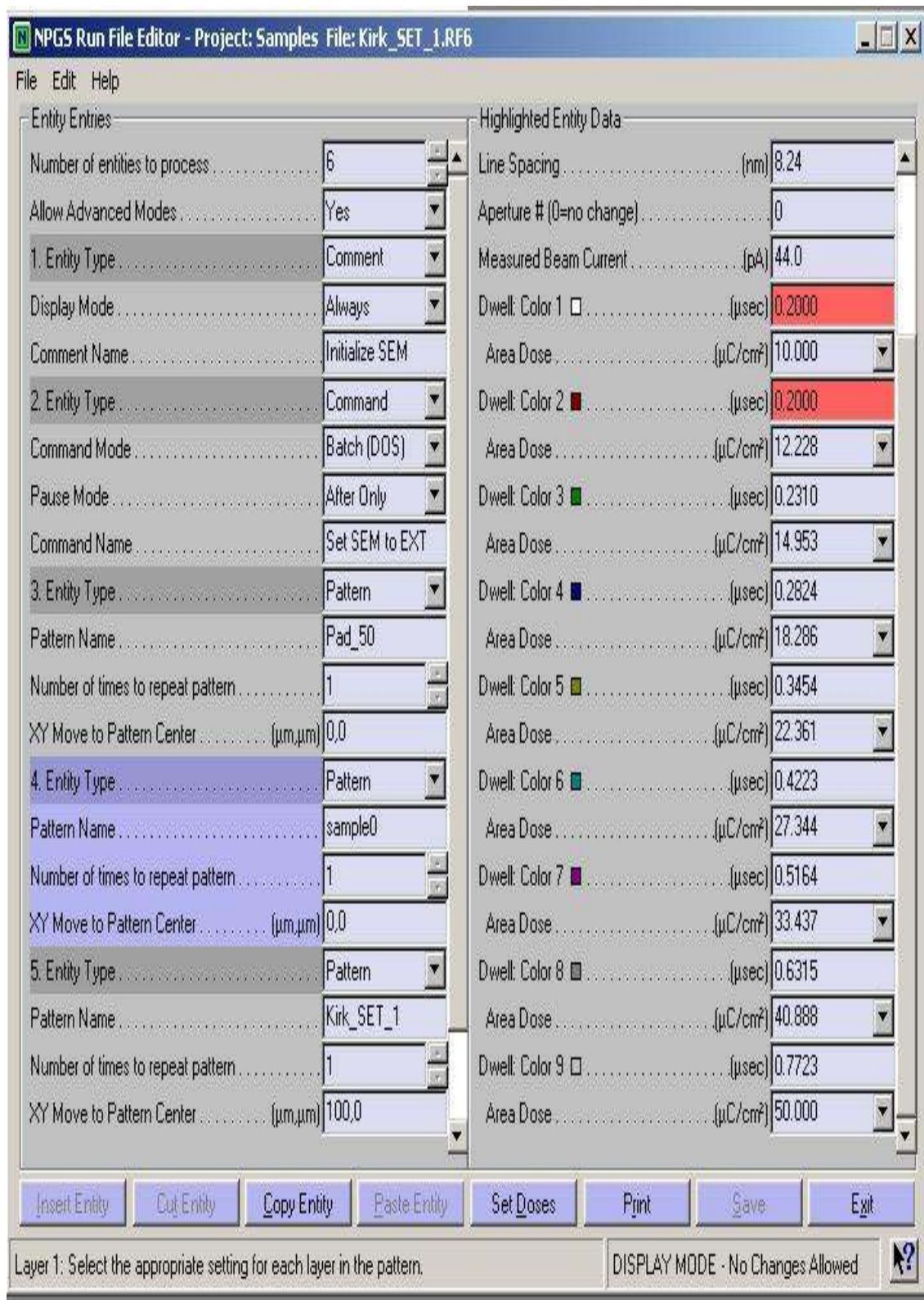
Pre-exposure bake 140°C for 90 seconds

E-beam parameters











Development procedure

Post exposure bake for 130°C for 40seconds.

MF702 dip for 90 seconds

DI water dip

Blow dry with Nitrogen

Second UVN30 wafer**Wafer specifications**

1cm x 1cm piece from a poly crystalline silicon wafer, p-type doping

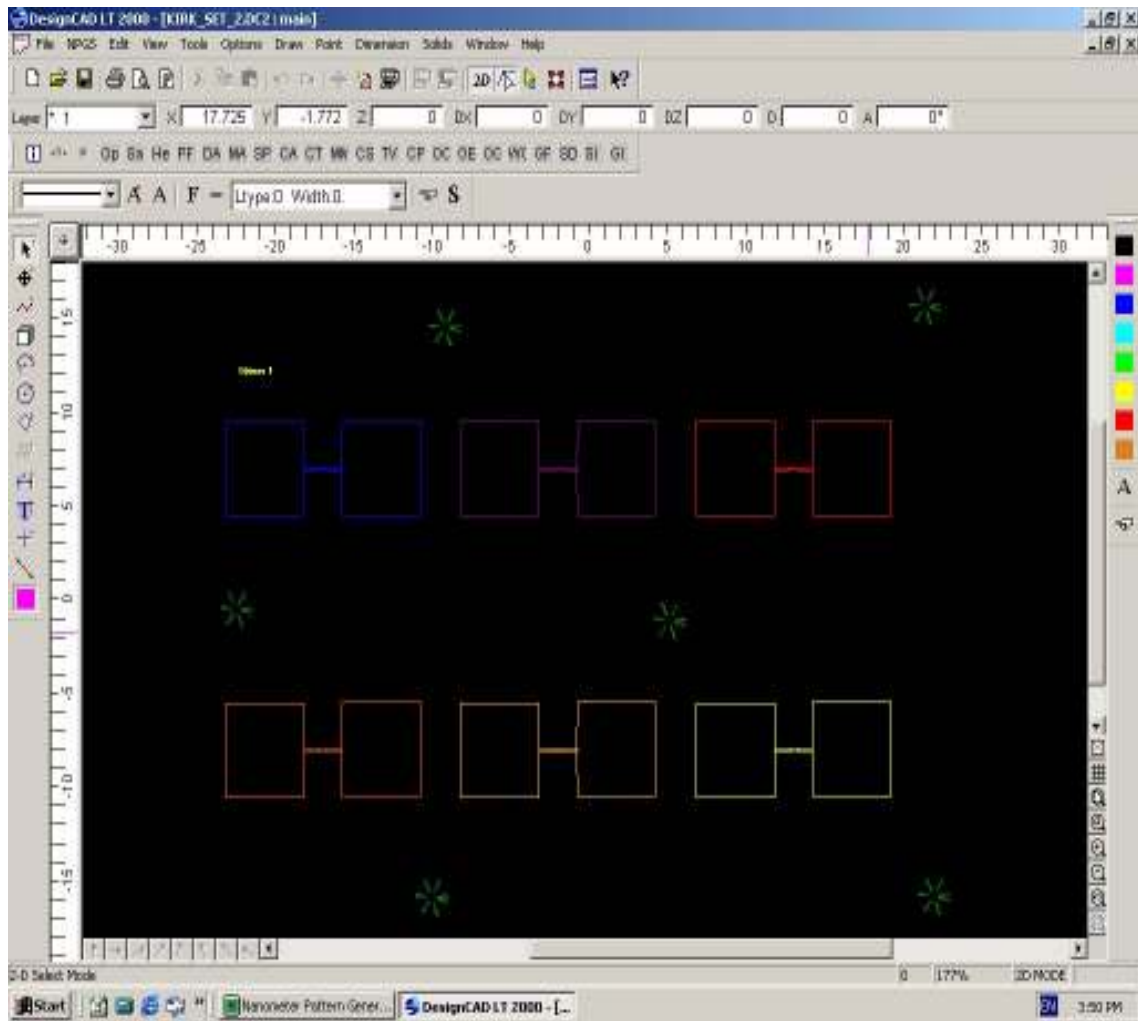
Samples are prebaked at 140°C for 10 minutes on hot plate

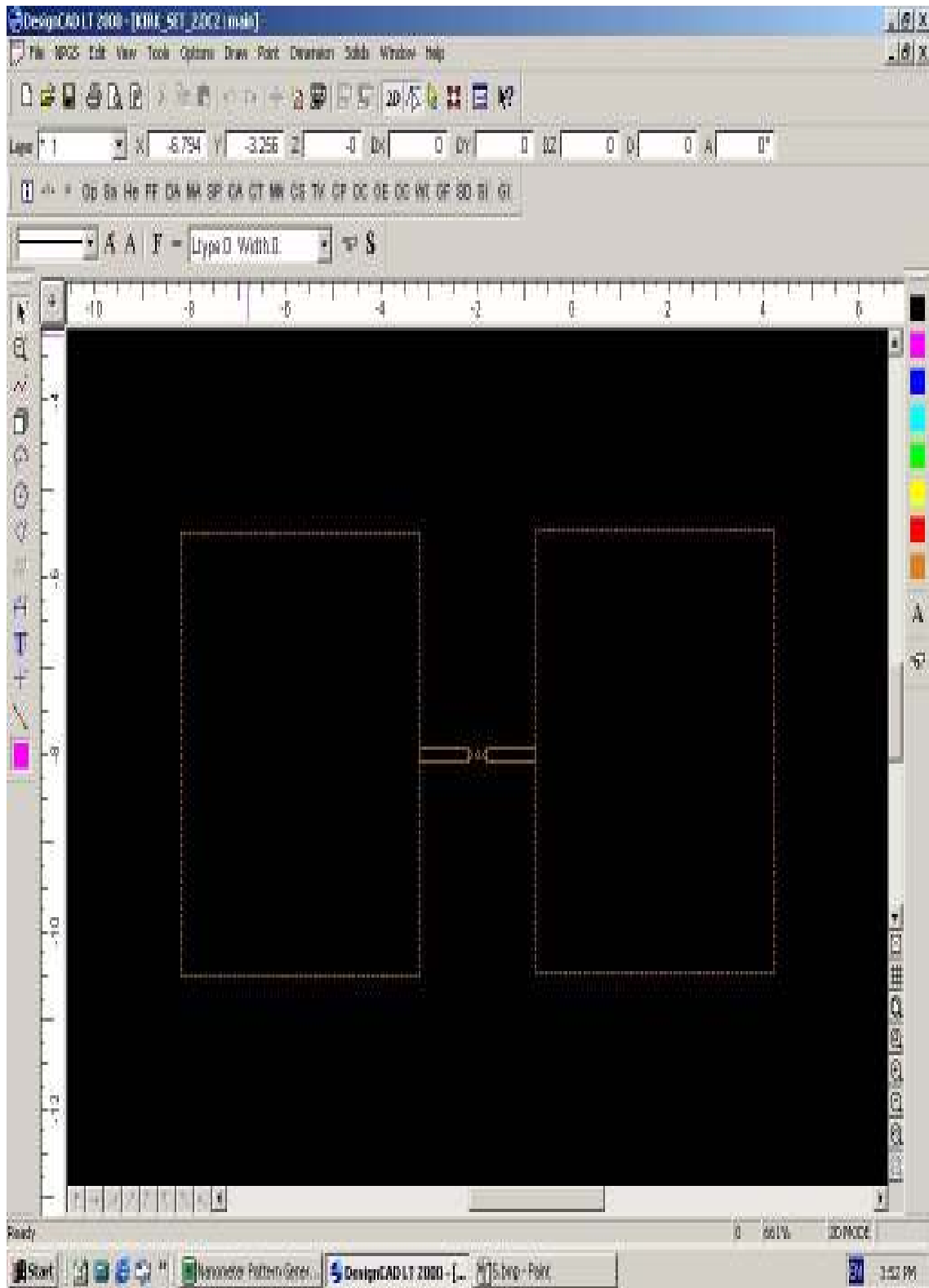
HMDS was spun on at 3000 rpm for 30 seconds

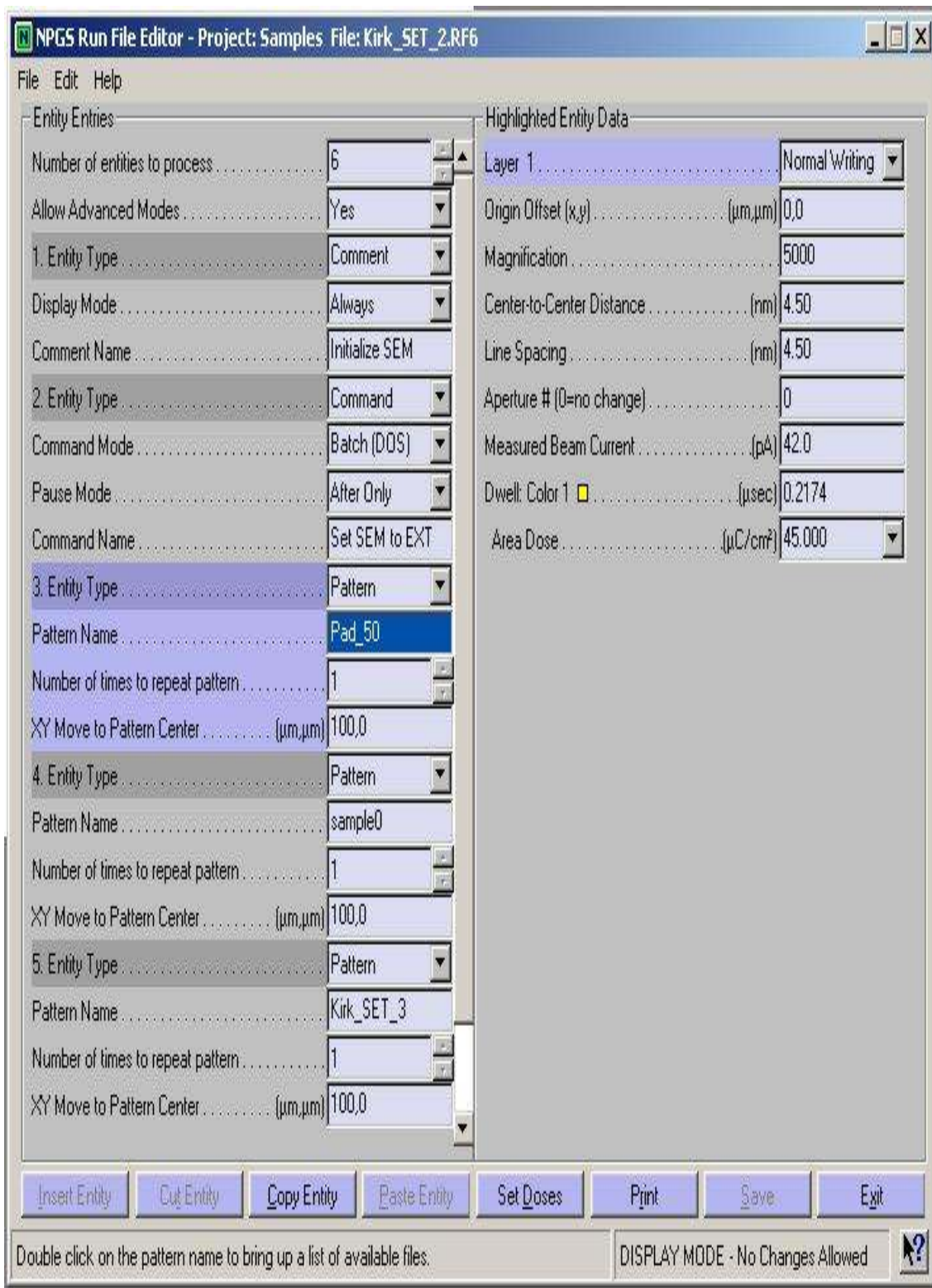
UVN30 was spun on at 5000 rpm for 30 seconds

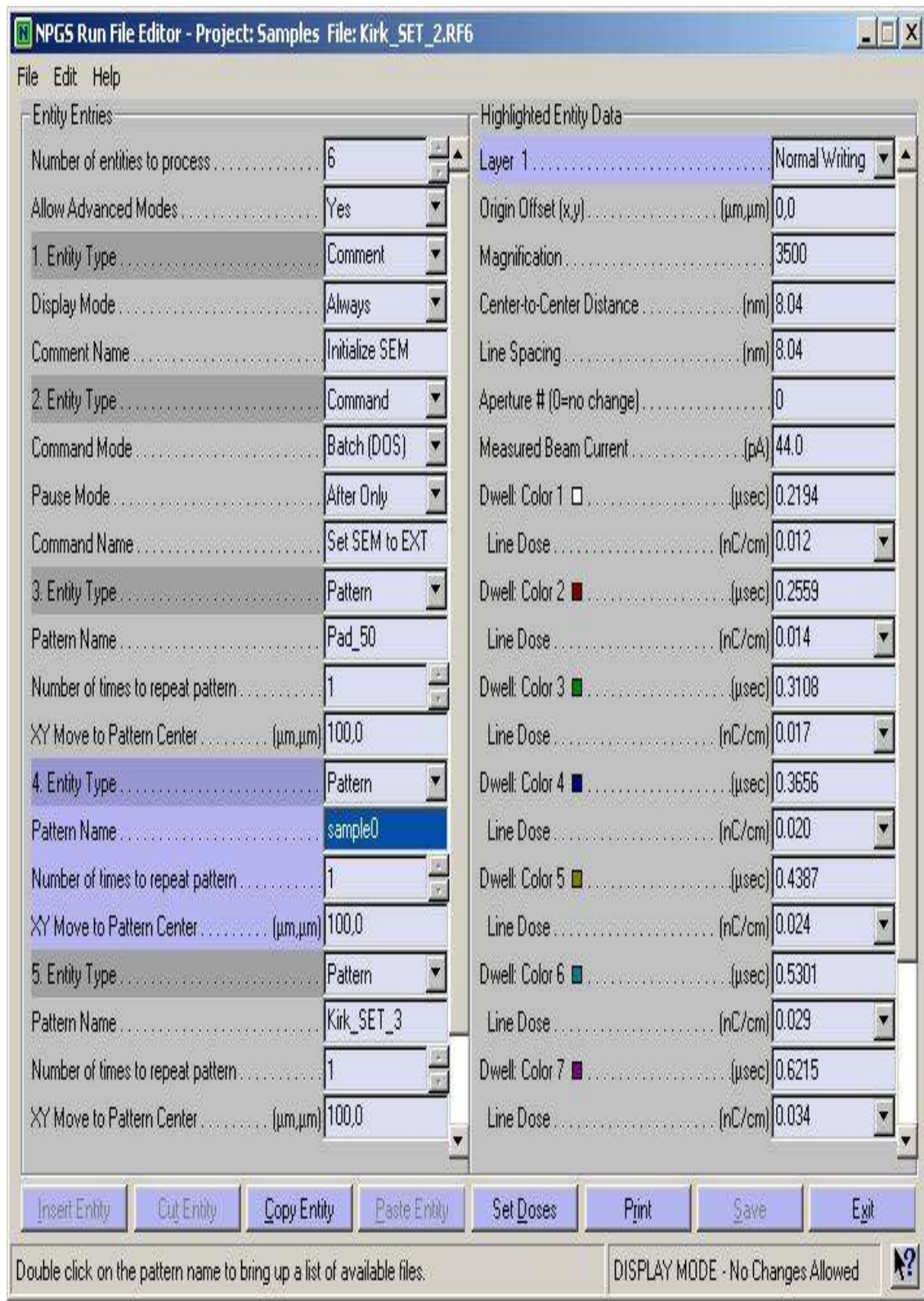
Pre-exposure bake 140°C for 90 seconds

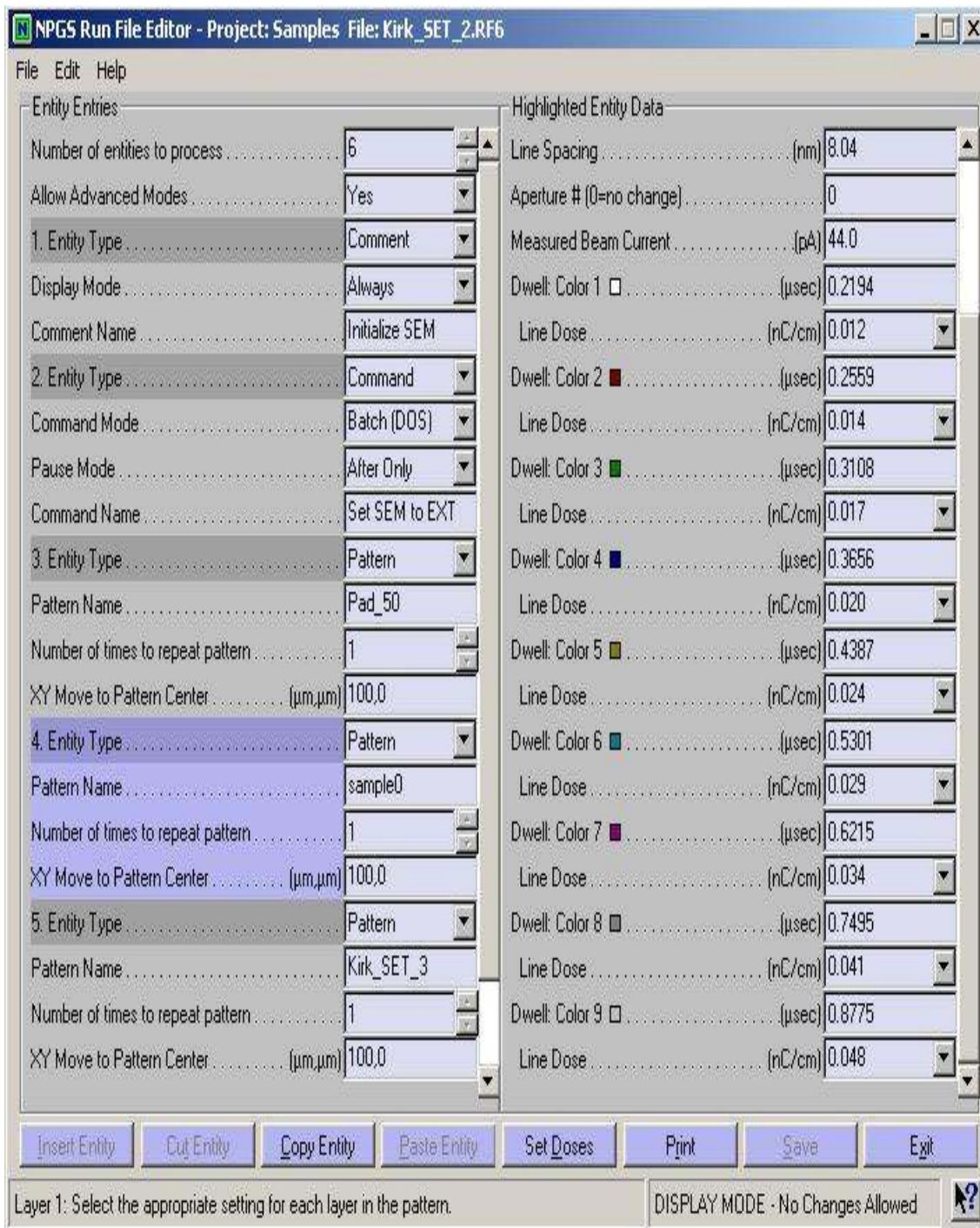
E-beam parameters













Development procedure

Post exposure bake for 130°C for 40seconds.

MF702 dip for 90 seconds

DI water dip

Blow dry with Nitrogen

Third UVN30 wafer**Wafer specifications**

1cm x 1cm piece from a poly crystalline silicon wafer, p-type doping

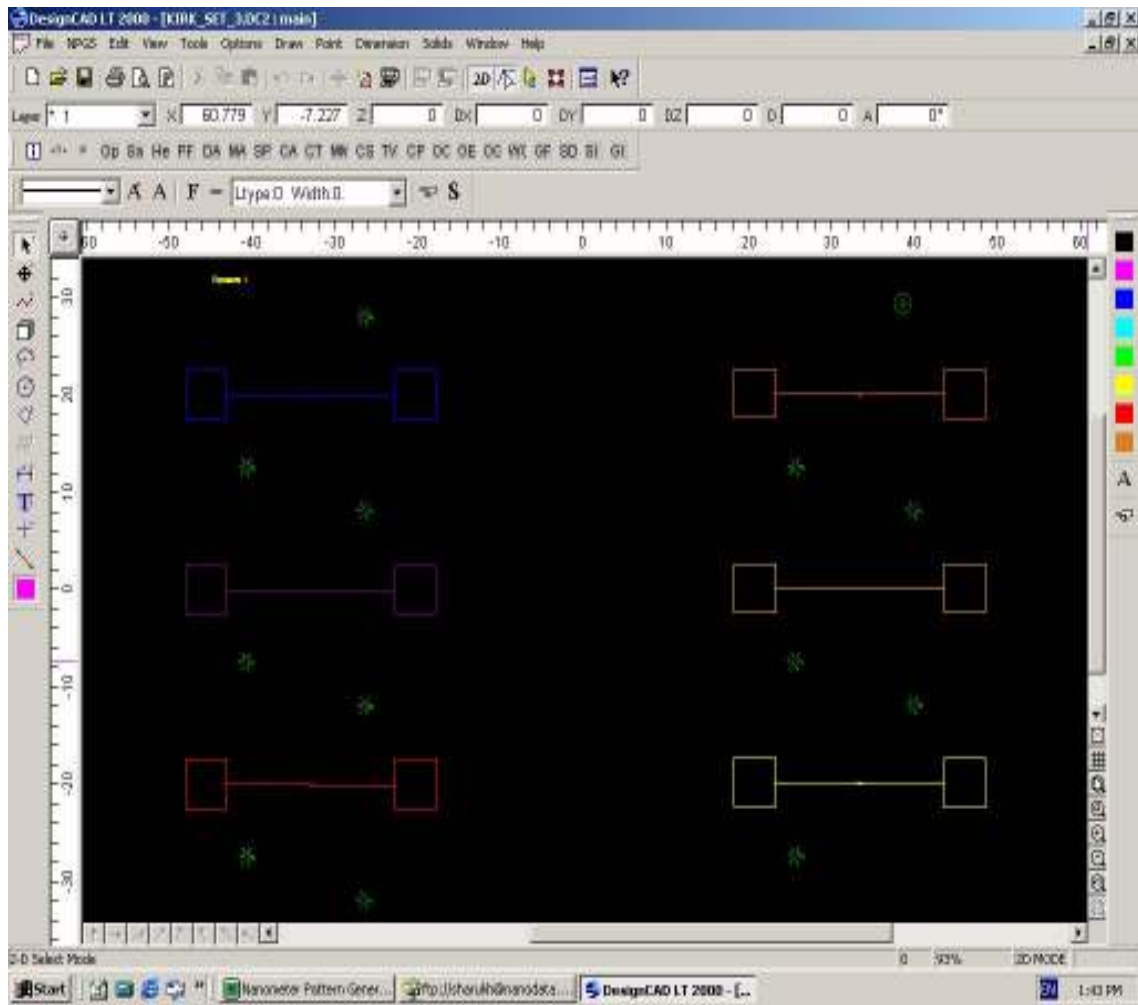
Samples are prebaked at 140°C for 10 minutes on hot plate

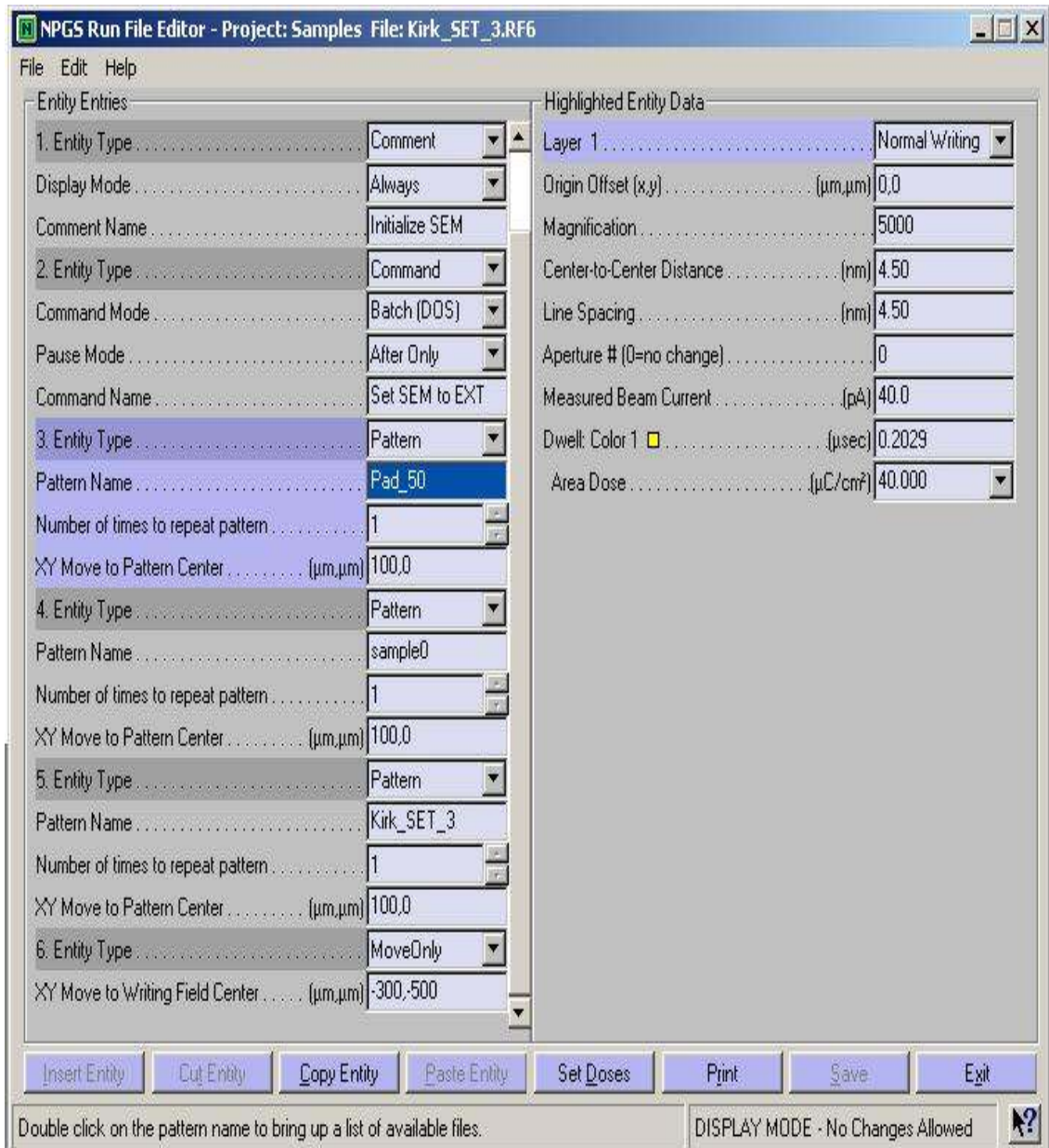
HMDS was spun on at 3000 rpm for 30 seconds

UVN30 was spun on at 5000 rpm for 30 seconds

Pre-exposure bake 140°C for 90 seconds

E-beam parameters





NPGS Run File Editor - Project: Samples File: Kirk_SET_3.RF6

File Edit Help

Entity Entries

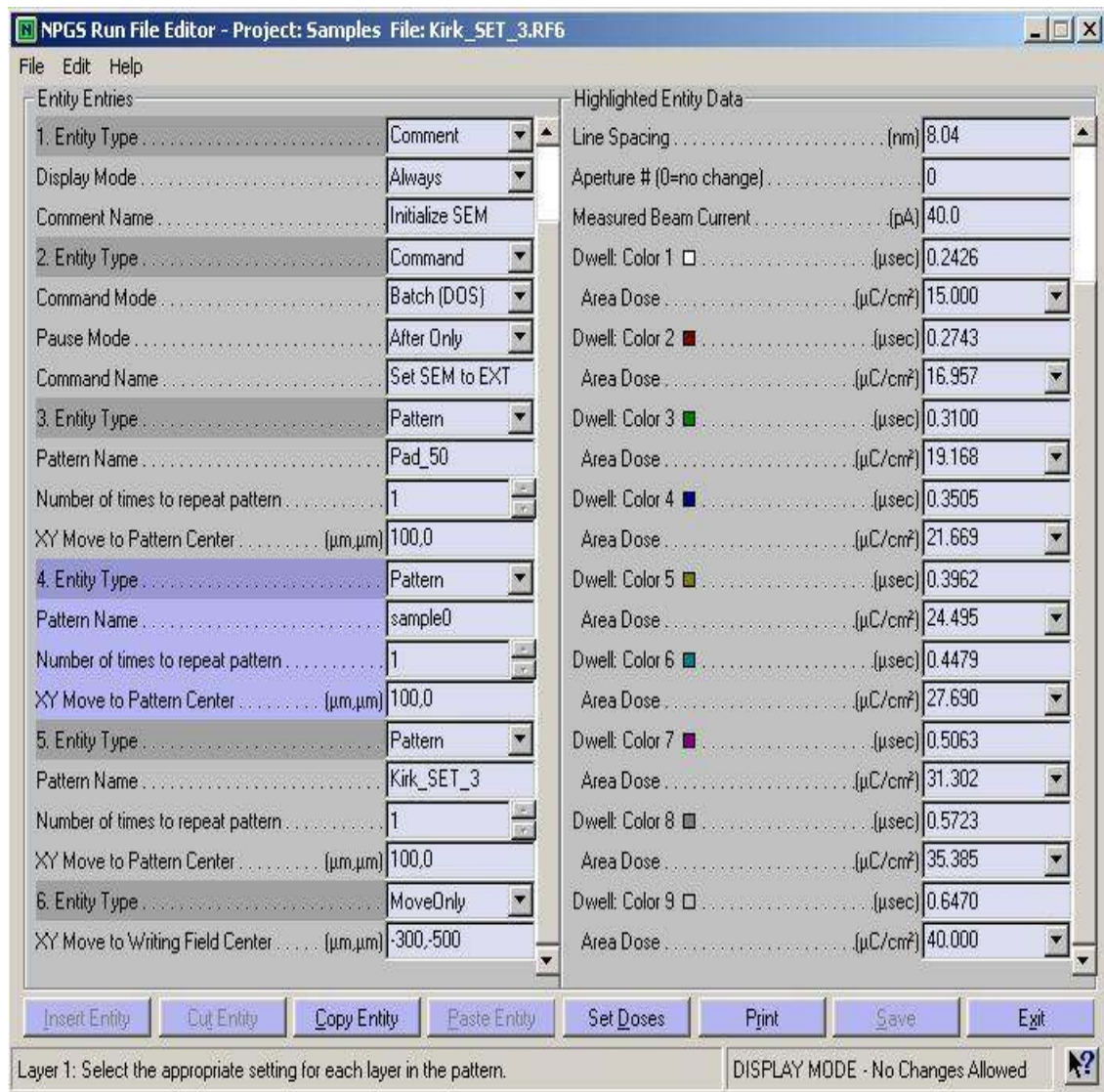
1. Entity Type	Comment
Display Mode	Always
Comment Name	Initialize SEM
2. Entity Type	Command
Command Mode	Batch (DOS)
Pause Mode	After Only
Command Name	Set SEM to EXT
3. Entity Type	Pattern
Pattern Name	Pad_50
Number of times to repeat pattern	1
XY Move to Pattern Center (μm,μm)	100,0
4. Entity Type	Pattern
Pattern Name	sample0
Number of times to repeat pattern	1
XY Move to Pattern Center (μm,μm)	100,0
5. Entity Type	Pattern
Pattern Name	Kirk_SET_3
Number of times to repeat pattern	1
XY Move to Pattern Center (μm,μm)	100,0
6. Entity Type	MoveOnly
XY Move to Writing Field Center (μm,μm)	-300,500

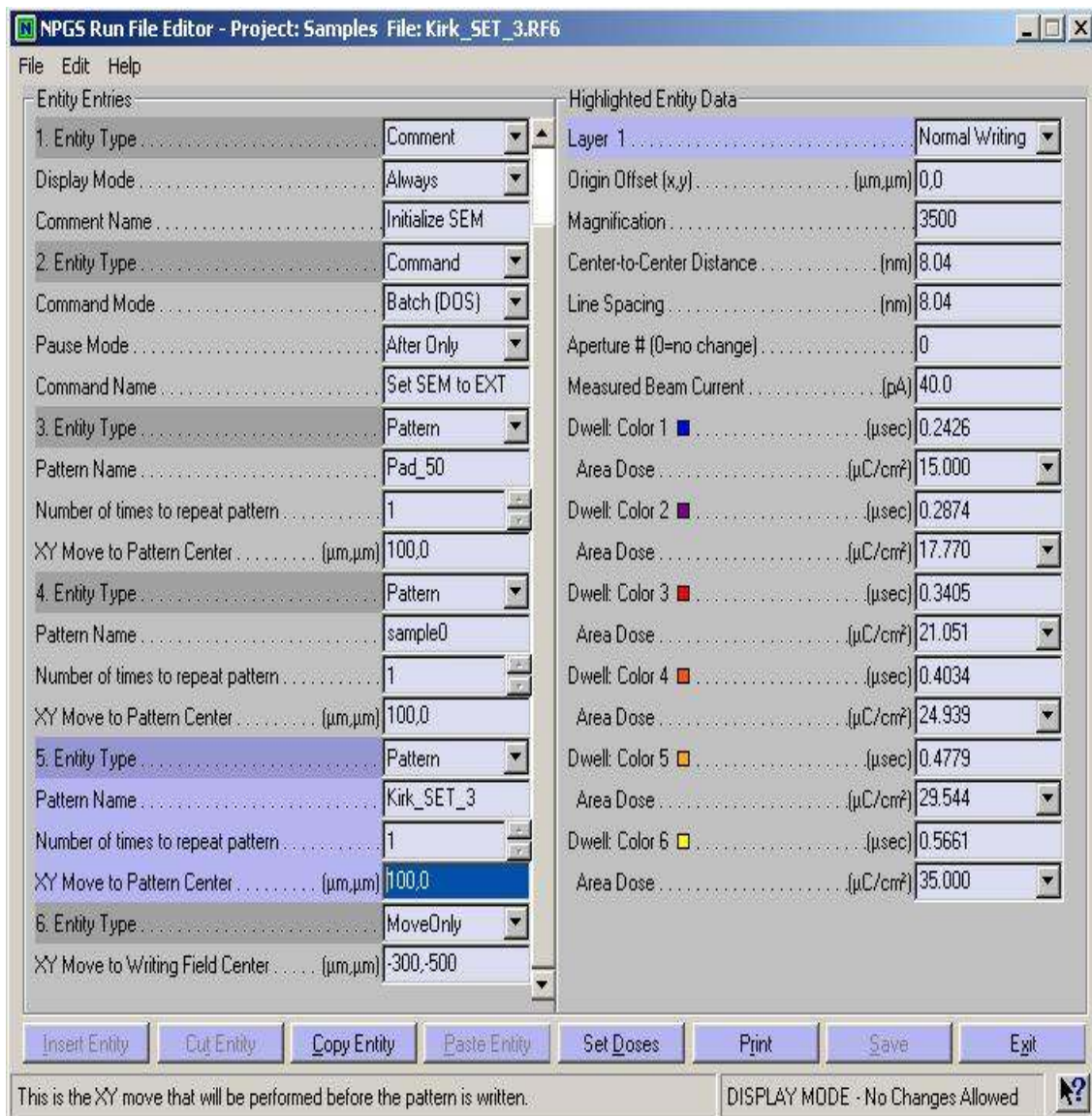
Highlighted Entity Data

Layer 1	Normal Writing
Origin Offset (x,y) (μm,μm)	0,0
Magnification	3500
Center-to-Center Distance (nm)	8.04
Line Spacing (nm)	8.04
Aperture # (0=no change)	0
Measured Beam Current (pA)	40.0
Dwell: Color 1 <input type="checkbox"/> (μsec)	0.2426
Area Dose (μC/cm ²)	15.000
Dwell: Color 2 <input checked="" type="checkbox"/> (μsec)	0.2743
Area Dose (μC/cm ²)	16.957
Dwell: Color 3 <input checked="" type="checkbox"/> (μsec)	0.3100
Area Dose (μC/cm ²)	19.168
Dwell: Color 4 <input checked="" type="checkbox"/> (μsec)	0.3505
Area Dose (μC/cm ²)	21.669
Dwell: Color 5 <input checked="" type="checkbox"/> (μsec)	0.3962
Area Dose (μC/cm ²)	24.495
Dwell: Color 6 <input checked="" type="checkbox"/> (μsec)	0.4479
Area Dose (μC/cm ²)	27.690
Dwell: Color 7 <input checked="" type="checkbox"/> (μsec)	0.5063
Area Dose (μC/cm ²)	31.302

Insert Entity
Cut Entity
Copy Entity
Paste Entity
Set Doses
Print
Save
Exit

Up to 100 can be entered, but in Alignment mode, this should be left at one. DISPLAY MODE - No Changes Allowed





Development procedure

Post exposure bake for 130°C for 40seconds.

MF702 dip for 90 seconds

DI water dip

Blow dry with Nitrogen

Fourth UVN30 wafer

Wafer specifications

1 cm x 1 cm piece from a poly crystalline silicon wafer, p-type doping

Samples are prebaked at 140 °C for 10 minutes on hot plate

HMDS was spun on at 3000 rpm for 10 seconds

UVN30 was spun on at 5000 rpm for 30 seconds

Pre-exposure bake 110 °C for 120 seconds

Development procedure

Large time gap between exposure and the post exposure bake

Post exposure bake for 110°C for 40seconds.

MF702 dip for 90 seconds

DI water dip

Blow dry with Nitrogen

Fifth UVN30 wafer

Wafer specifications

1cm x 1cm piece from a poly crystalline silicon wafer, p-type doping

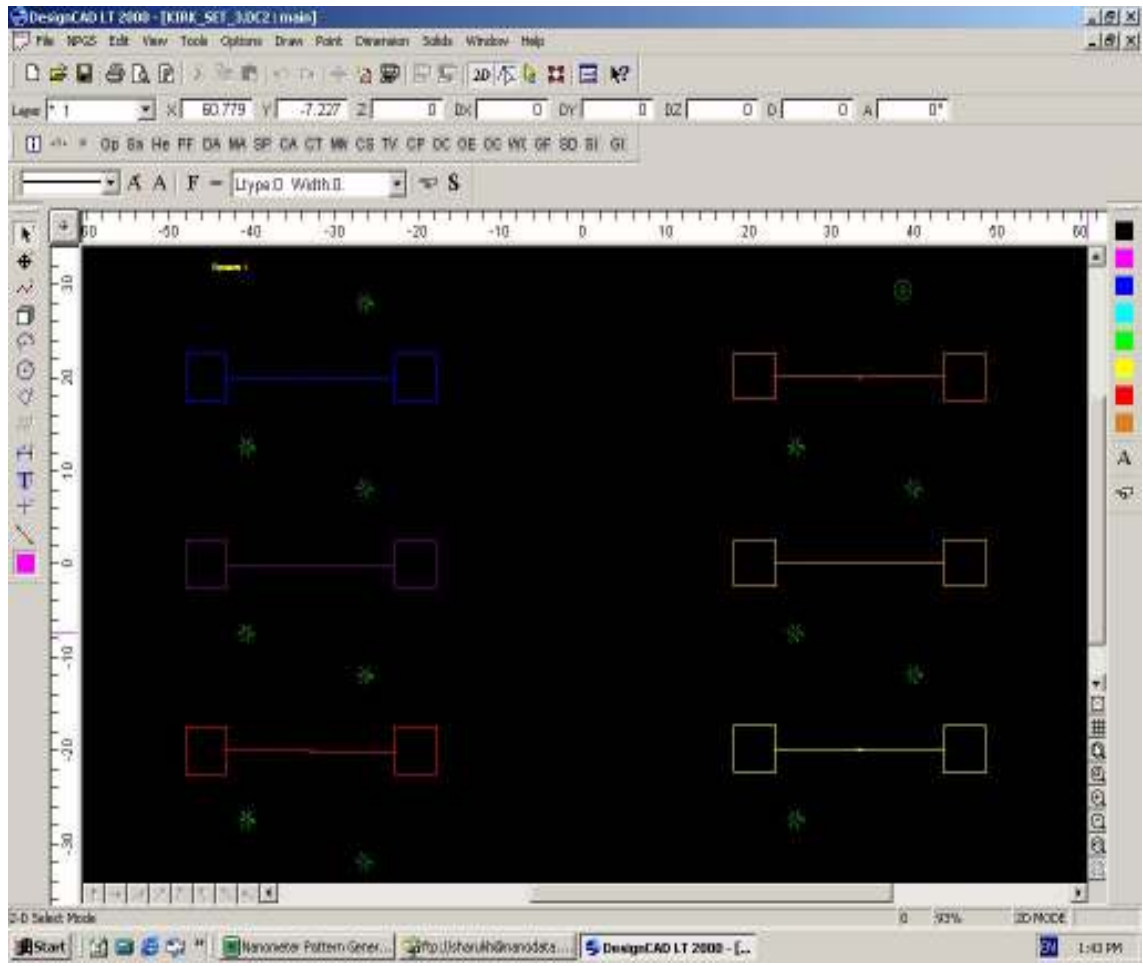
Samples are prebaked at 140°C for 10 minutes on hot plate

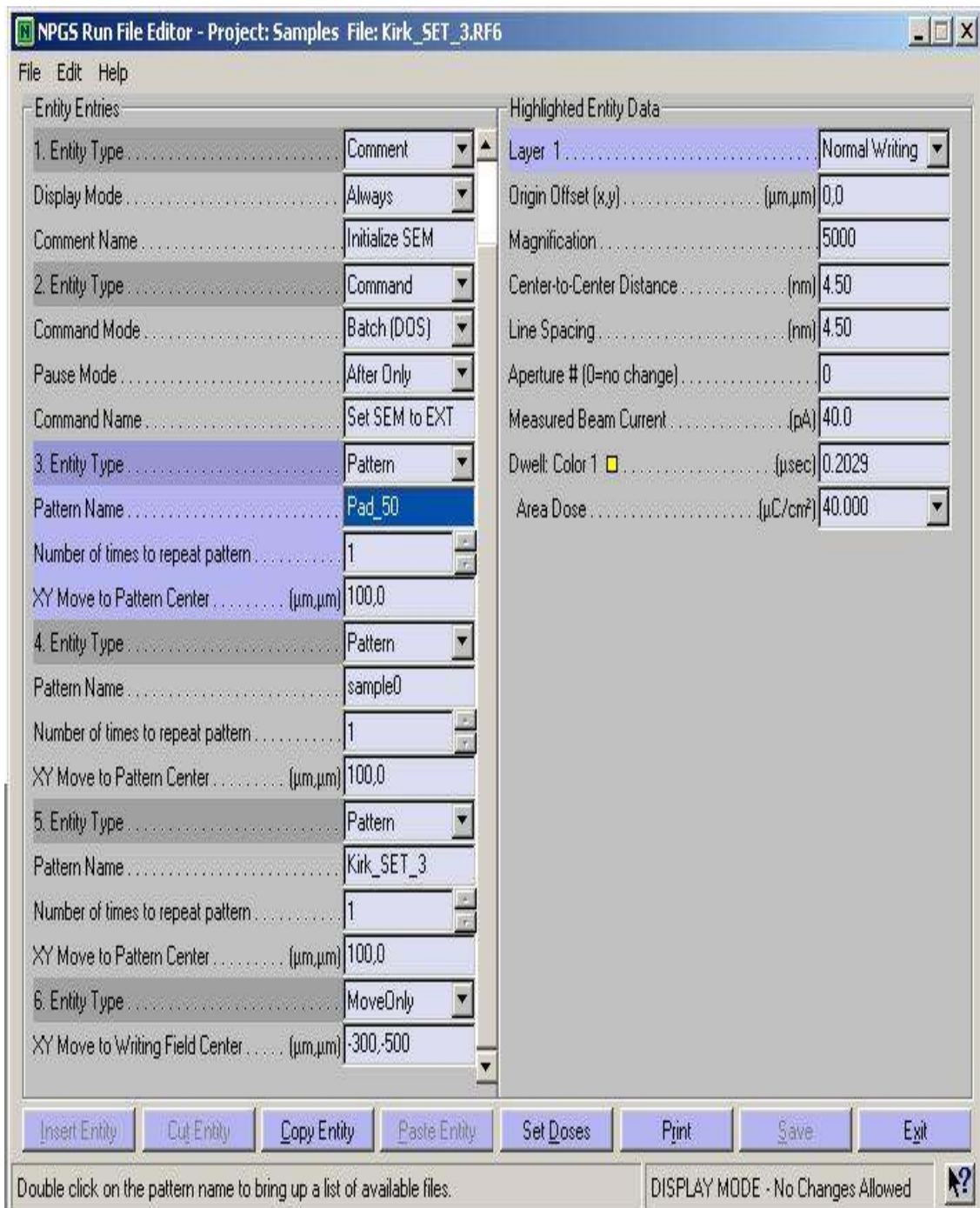
HMDS was spun on at 3000 rpm for 30 seconds

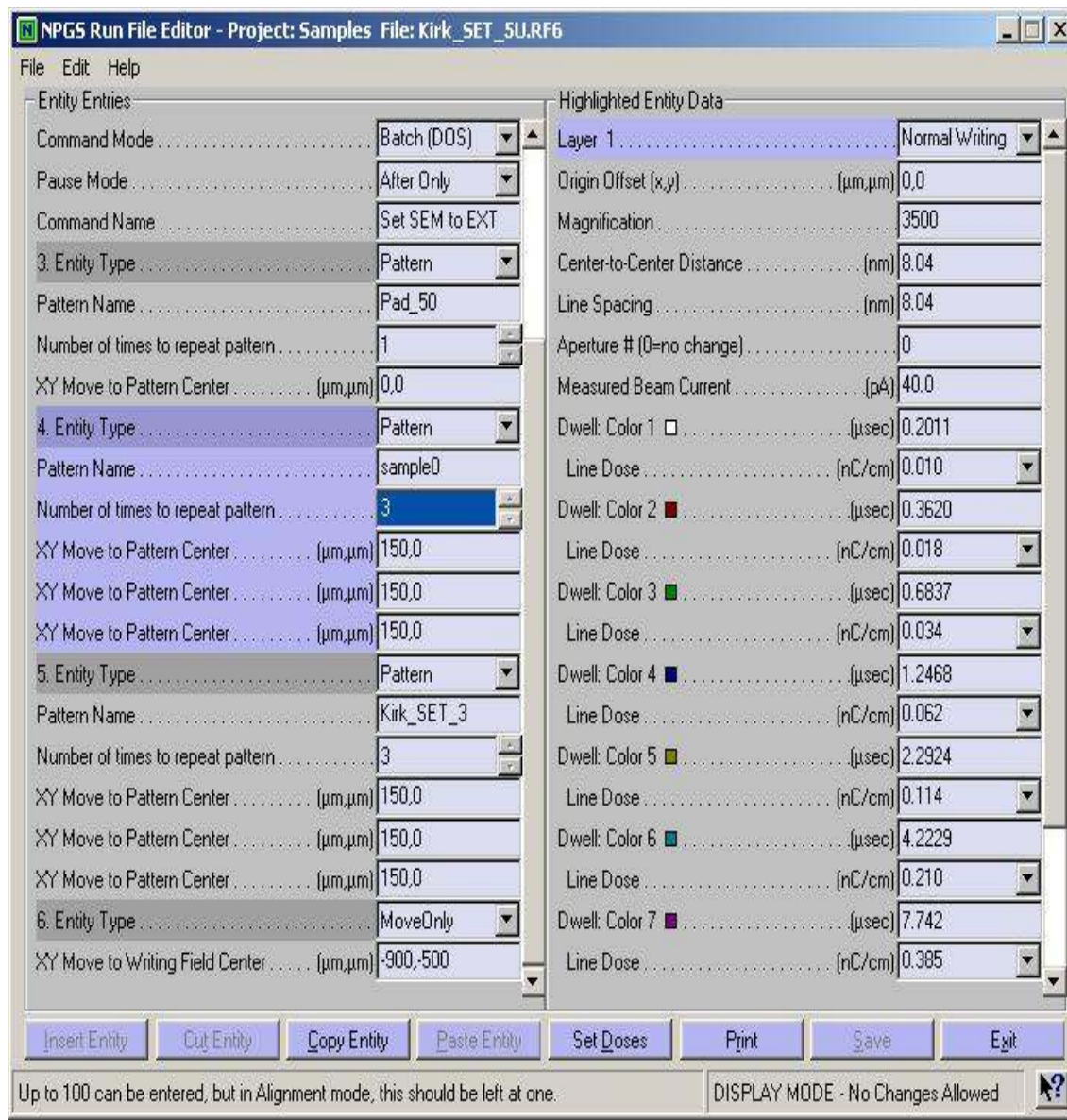
UVN30 was spun on at 5000 rpm for 30 seconds

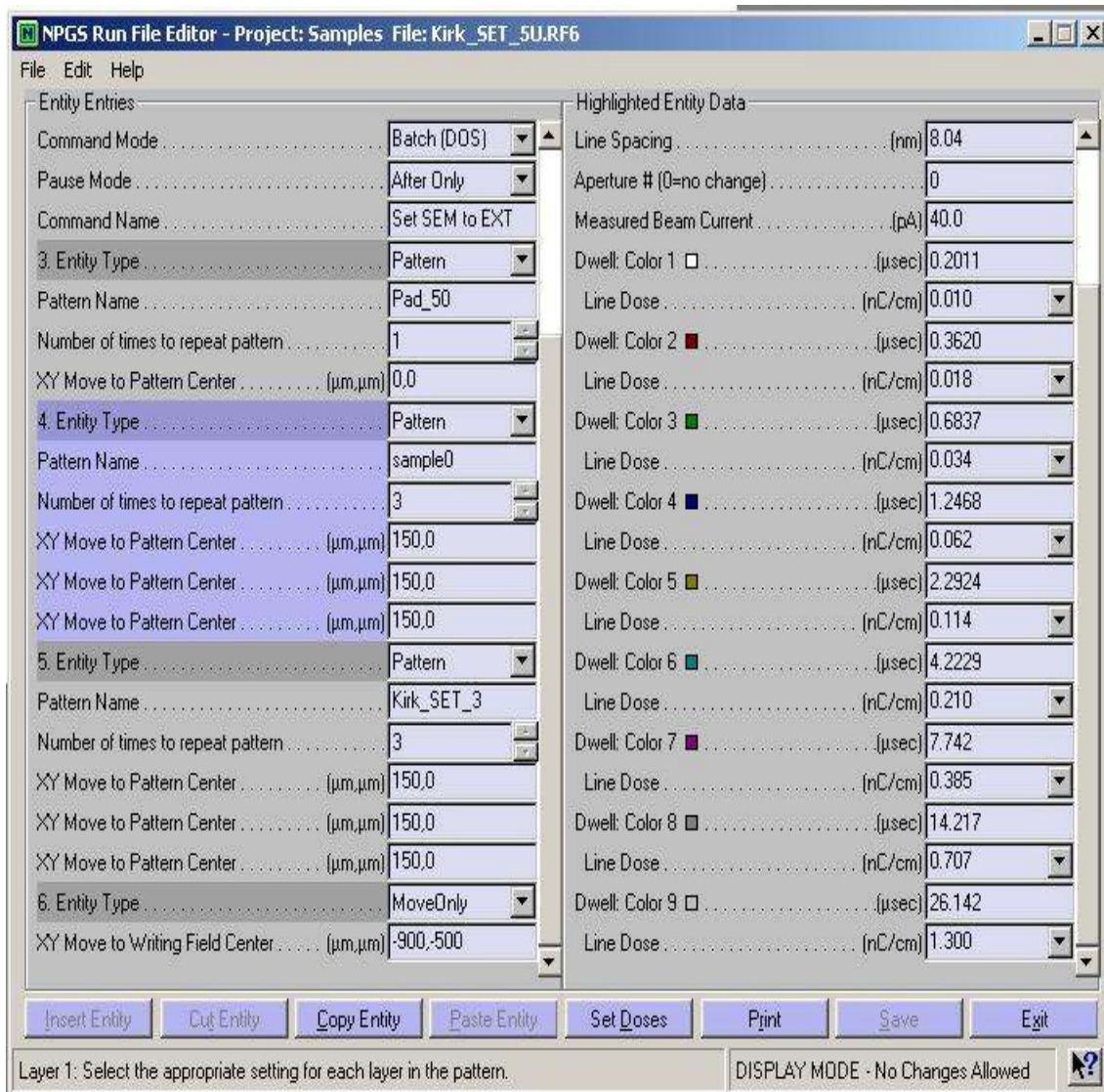
Pre-exposure bake 110°C for 120 seconds

E-beam parameters











Development procedure

Post exposure bake for 140°C for 40seconds.

MF702 dip for 90 seconds

DI water dip

Blow dry with Nitrogen

Sixth UVN30 wafer

Wafer specifications

1cm x 1cm piece from a poly crystalline silicon wafer, p-type doping

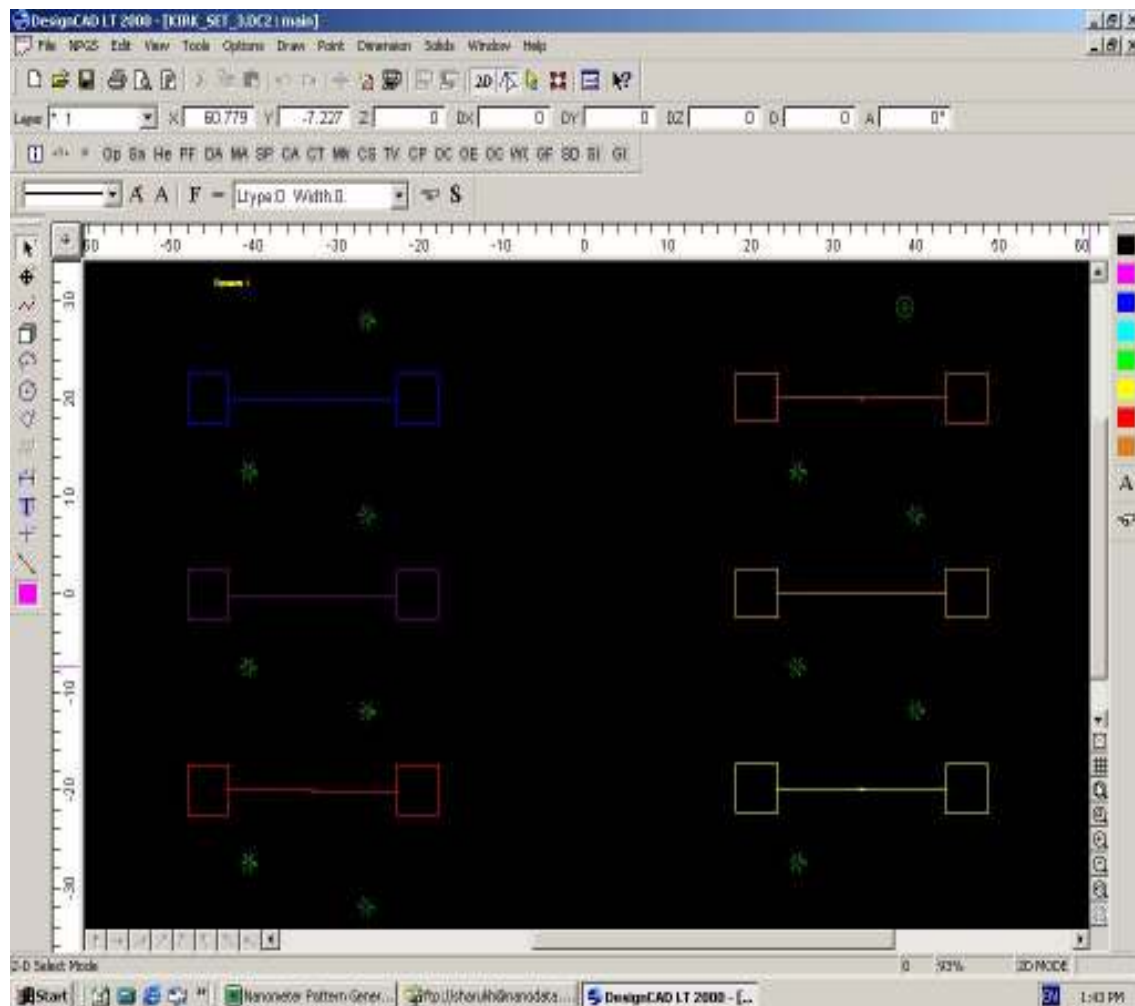
Samples are prebaked at 140°C for 10 minutes on hot plate

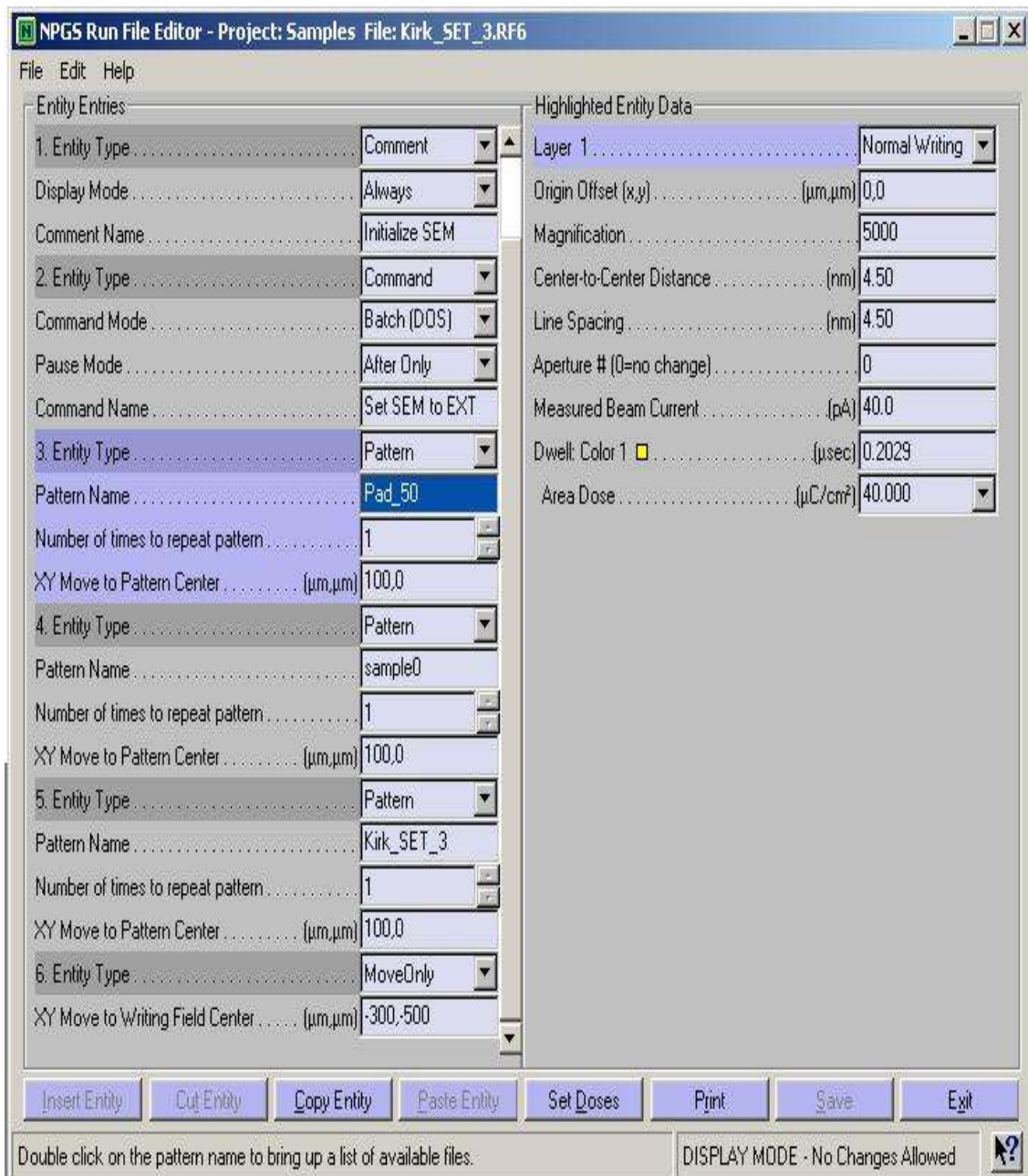
HMDS was spun on at 3000 rpm for 30 seconds

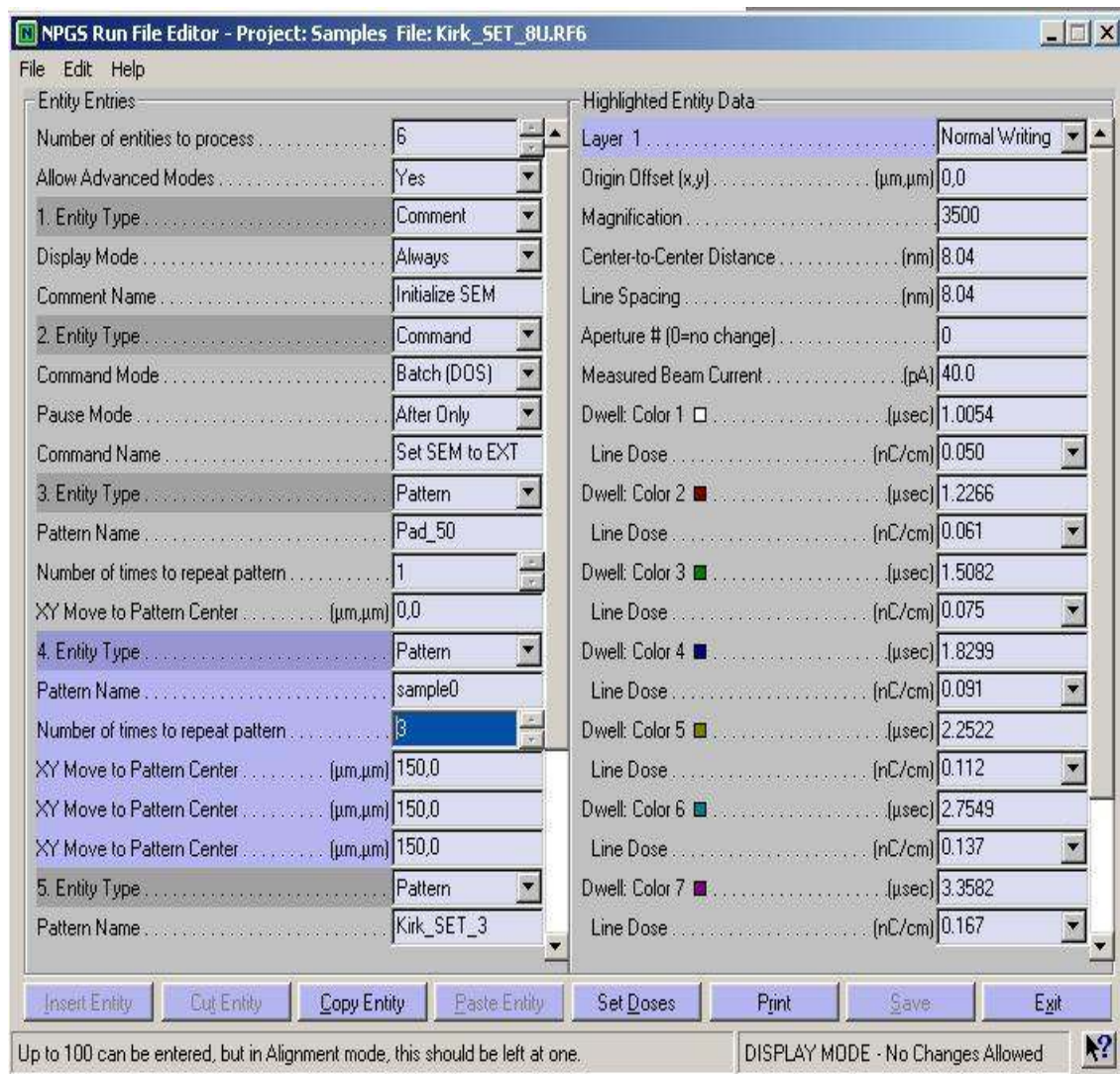
UVN30 was spun on at 5000 rpm for 30 seconds

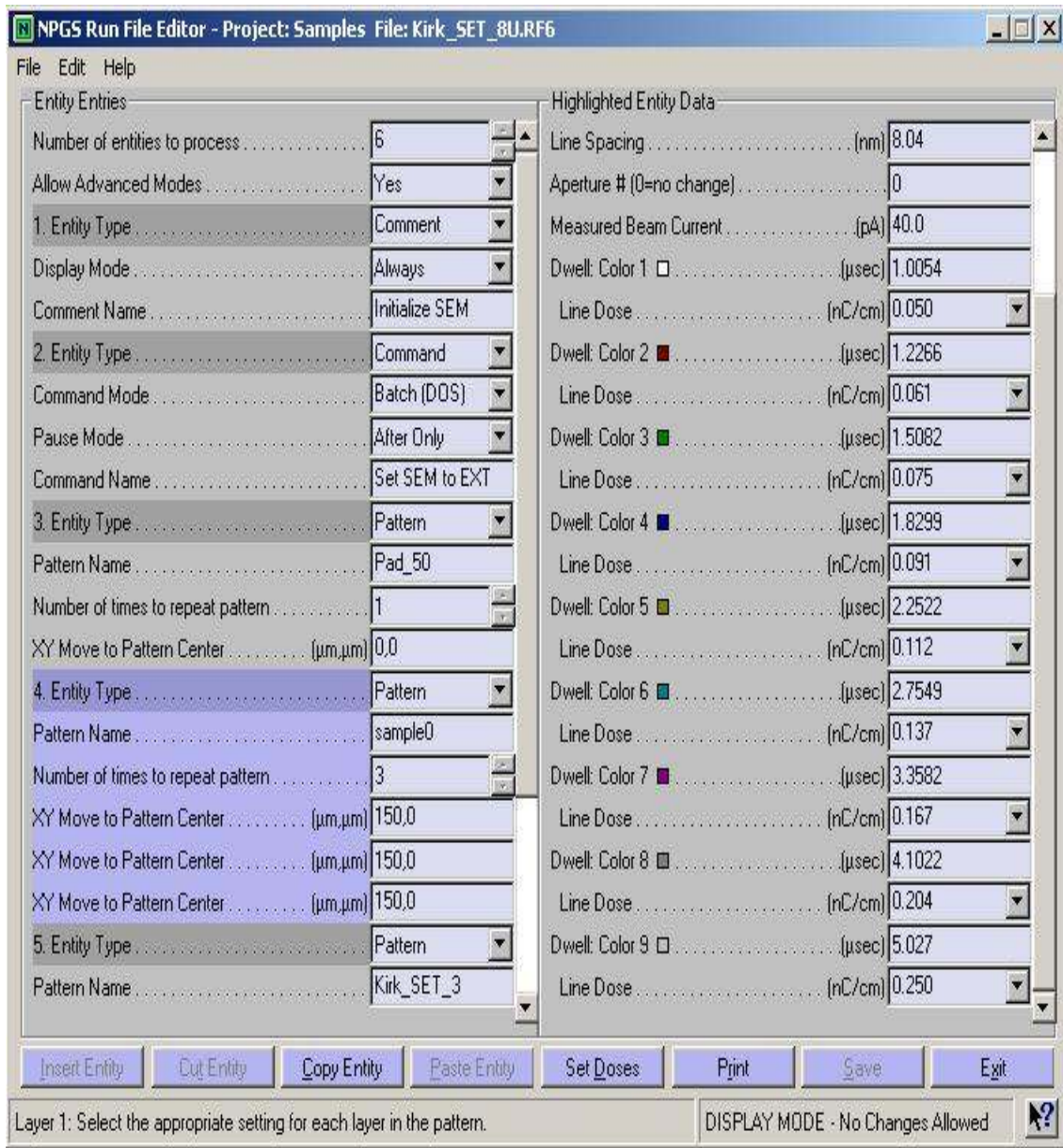
Pre-exposure bake 110°C for 120 seconds

E-beam parameters











Development procedure

Post exposure bake for 140°C for 40seconds.

MF702 dip for 90 seconds

DI water dip

Blow dry with Nitrogen

APPENDIX B

PMMA RECIPES

First PMMA wafer

Wafer specifications

1cm x 1cm piece from a poly crystalline silicon wafer, p-type doping

950K molecular weight PMMA is used

2% PMMA is prepared by mixing 11ml of PMMA and 51ml Anisole

PMMA was spun on at 4000 rpm for 60 seconds yielding a thickness of approximately 50nm

Pre-exposure bake 180°C for 90 seconds

E-beam parameters

Aperture designations

Aperture #1.....30 microns

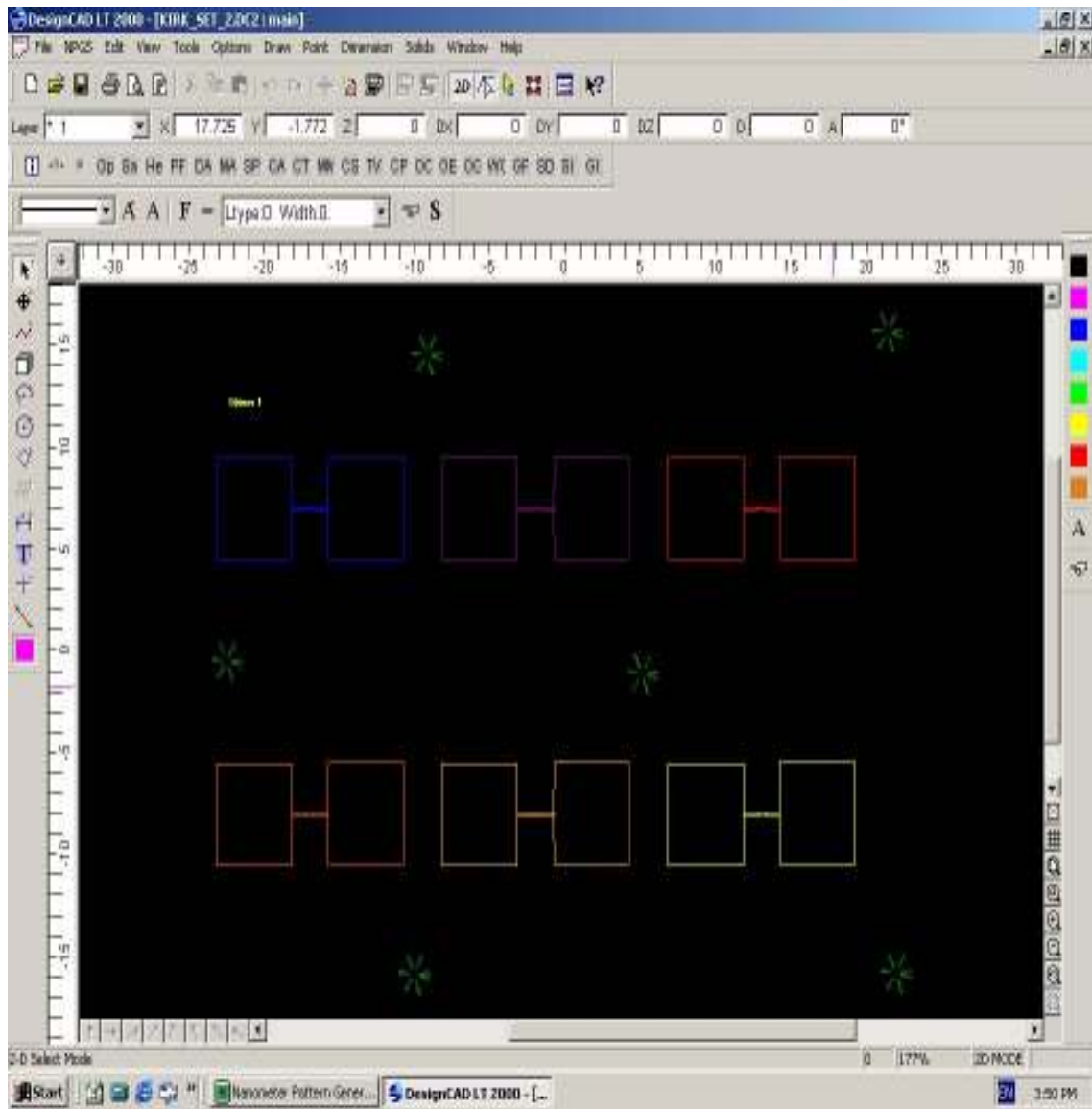
Aperture #2.....7.5 microns

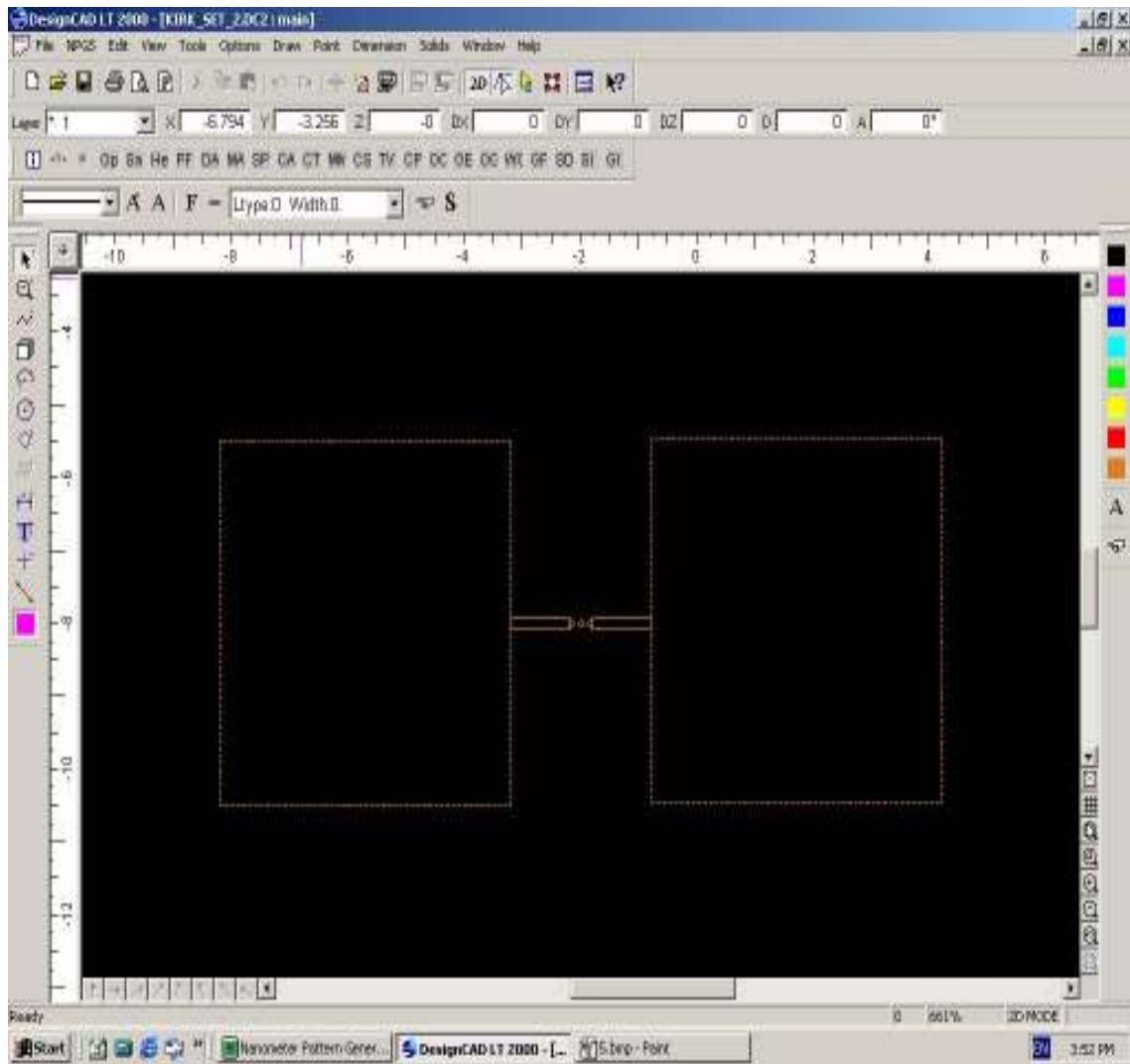
Aperture #3.....10 microns

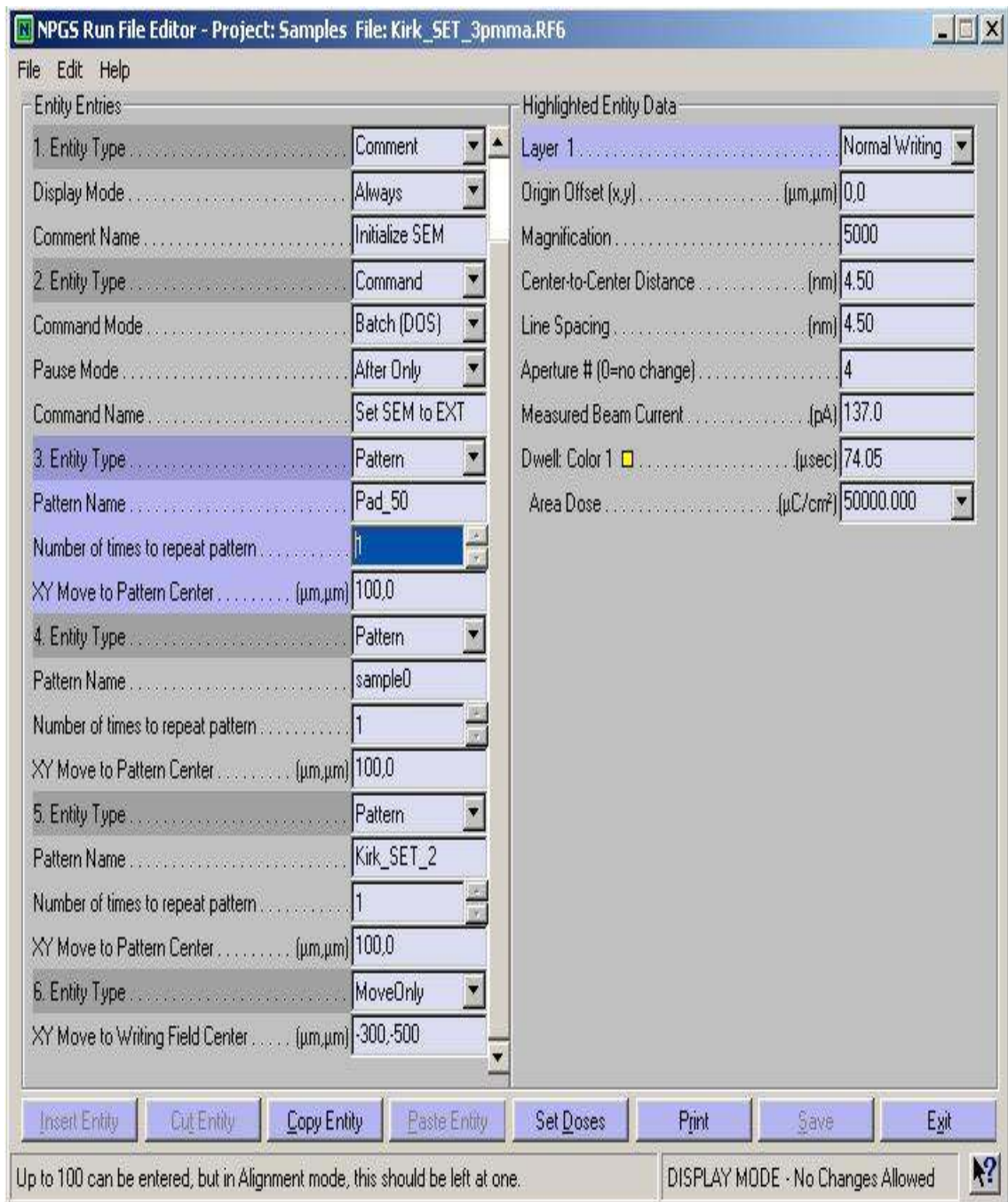
Aperture #4.....20 microns

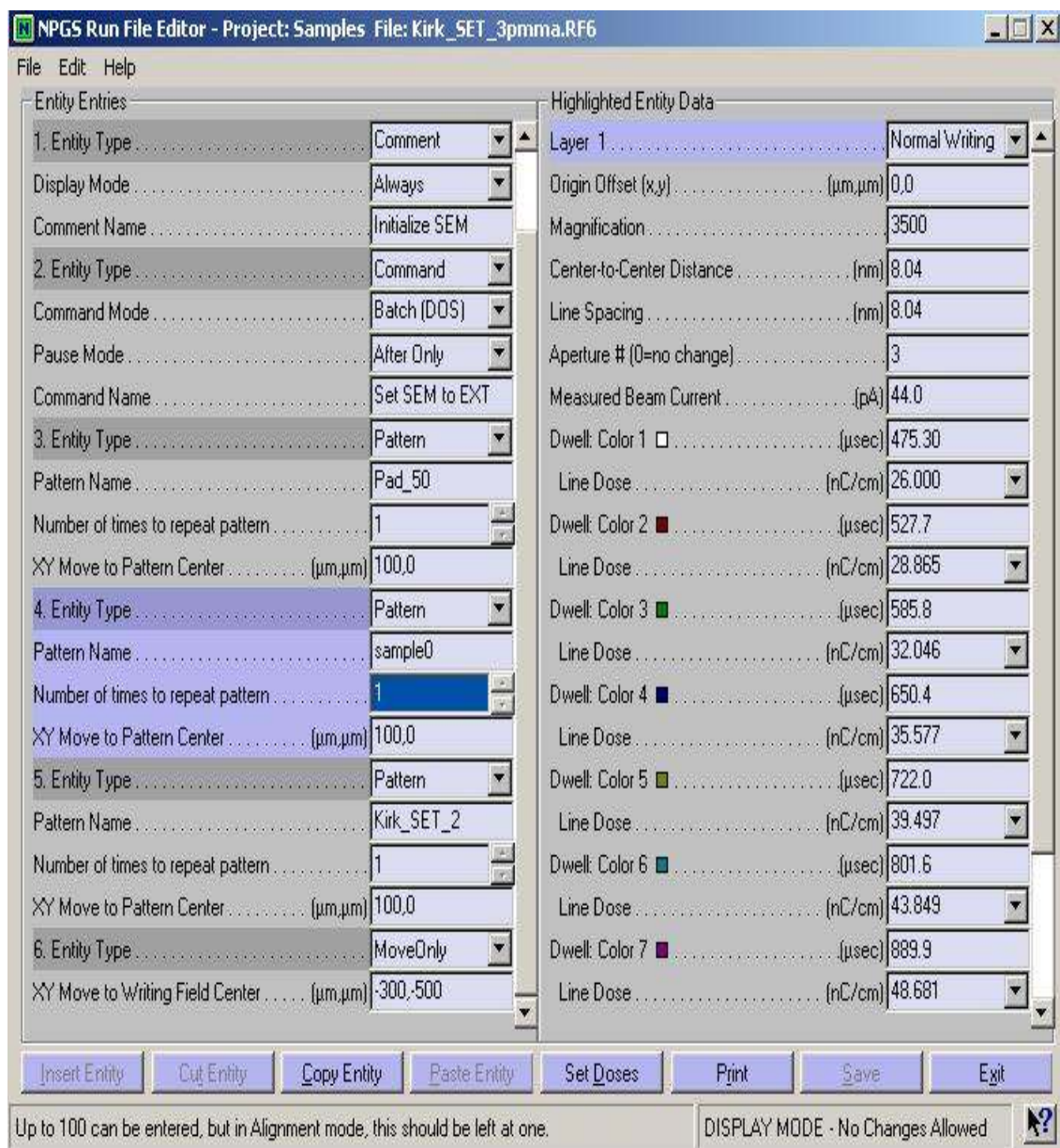
Aperture #5.....60 microns

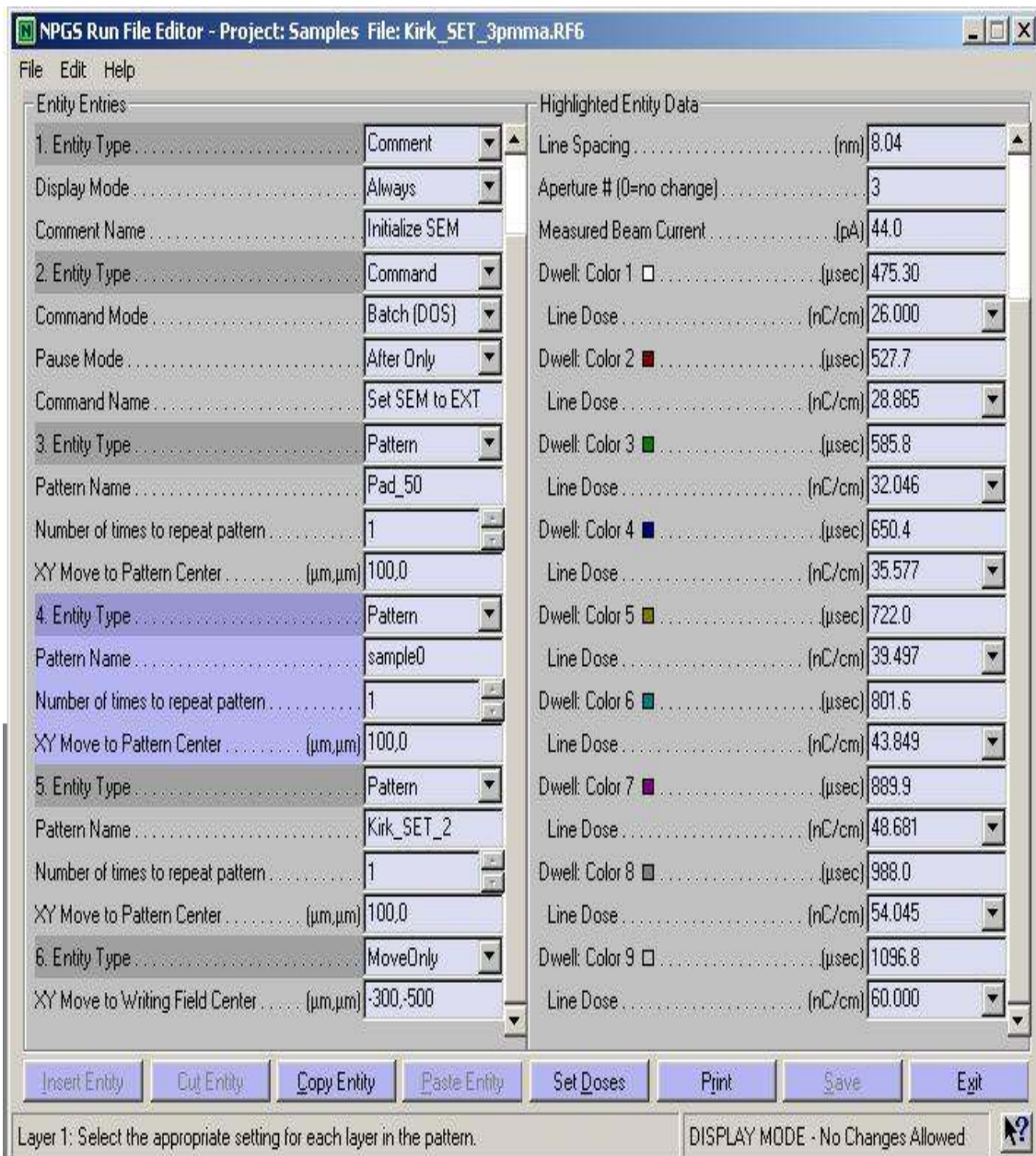
Aperture #6.....120 microns

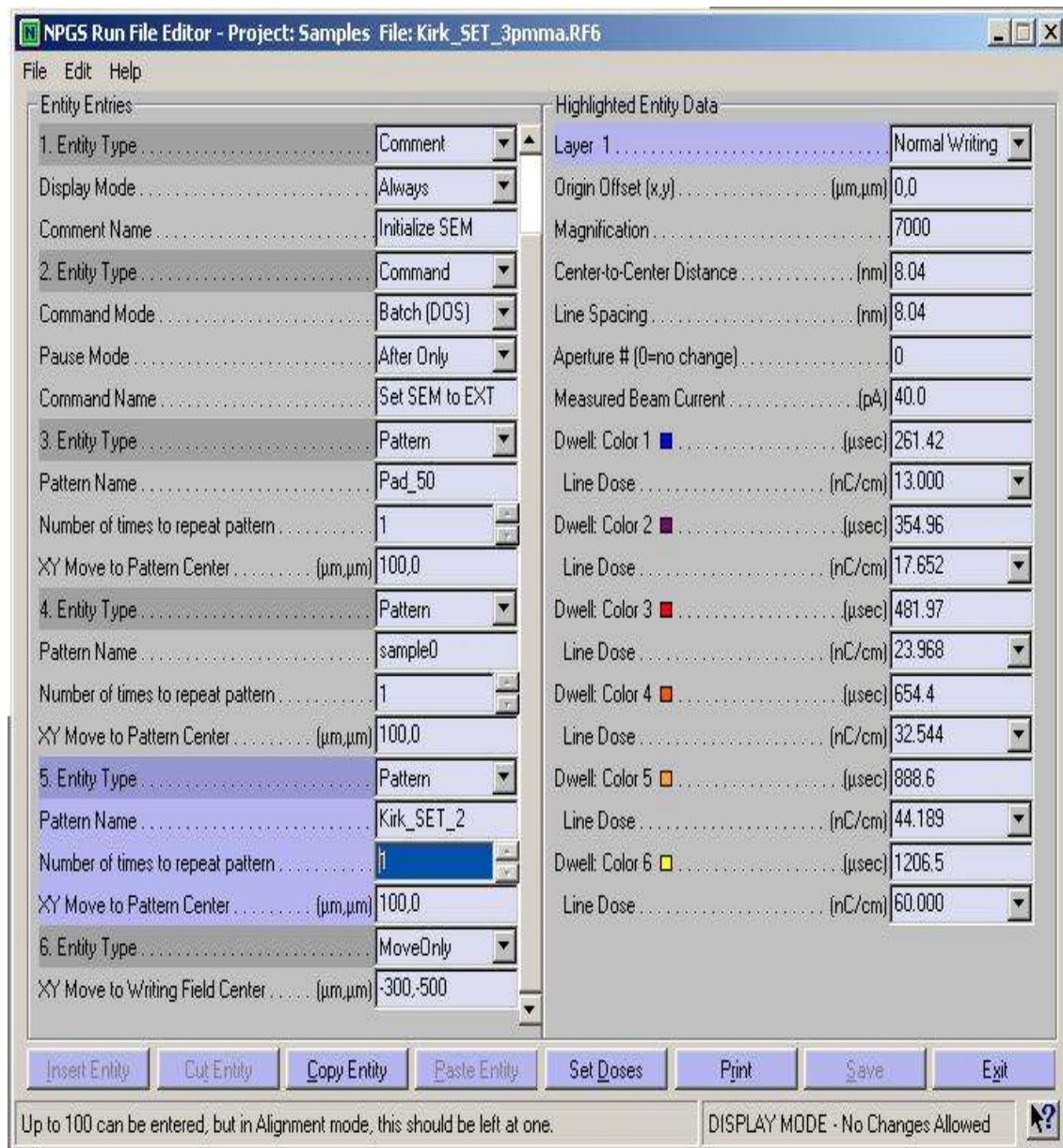












Development procedure

Post exposure bake for 180°C for 90seconds.

Acetone dip for 60 seconds

Rinsed in Isopropanol

Blow dry with Nitrogen

Second PMMA wafer

Wafer specifications

1cm x 1cm piece from a poly crystalline silicon wafer, p-type doping

950K molecular weight PMMA is used

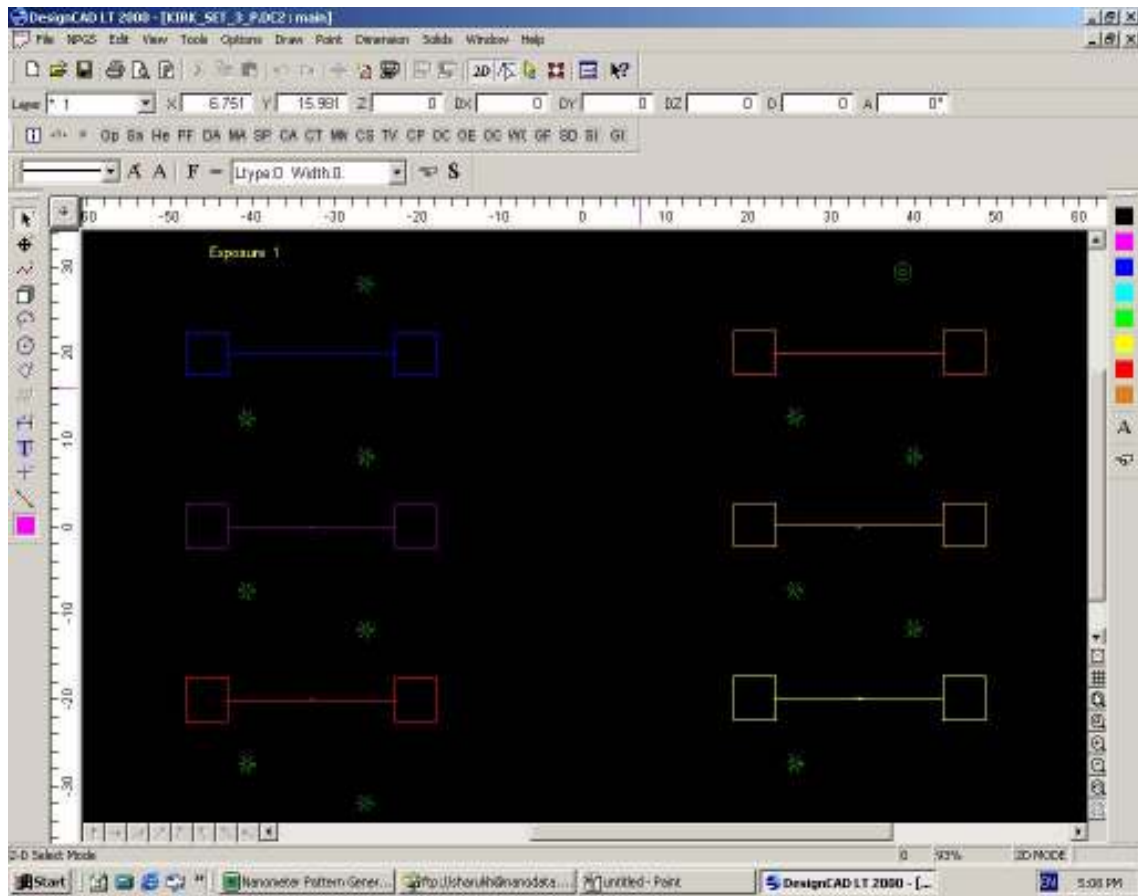
2% PMMA is prepared by mixing 11ml of PMMA and 51ml Anisole

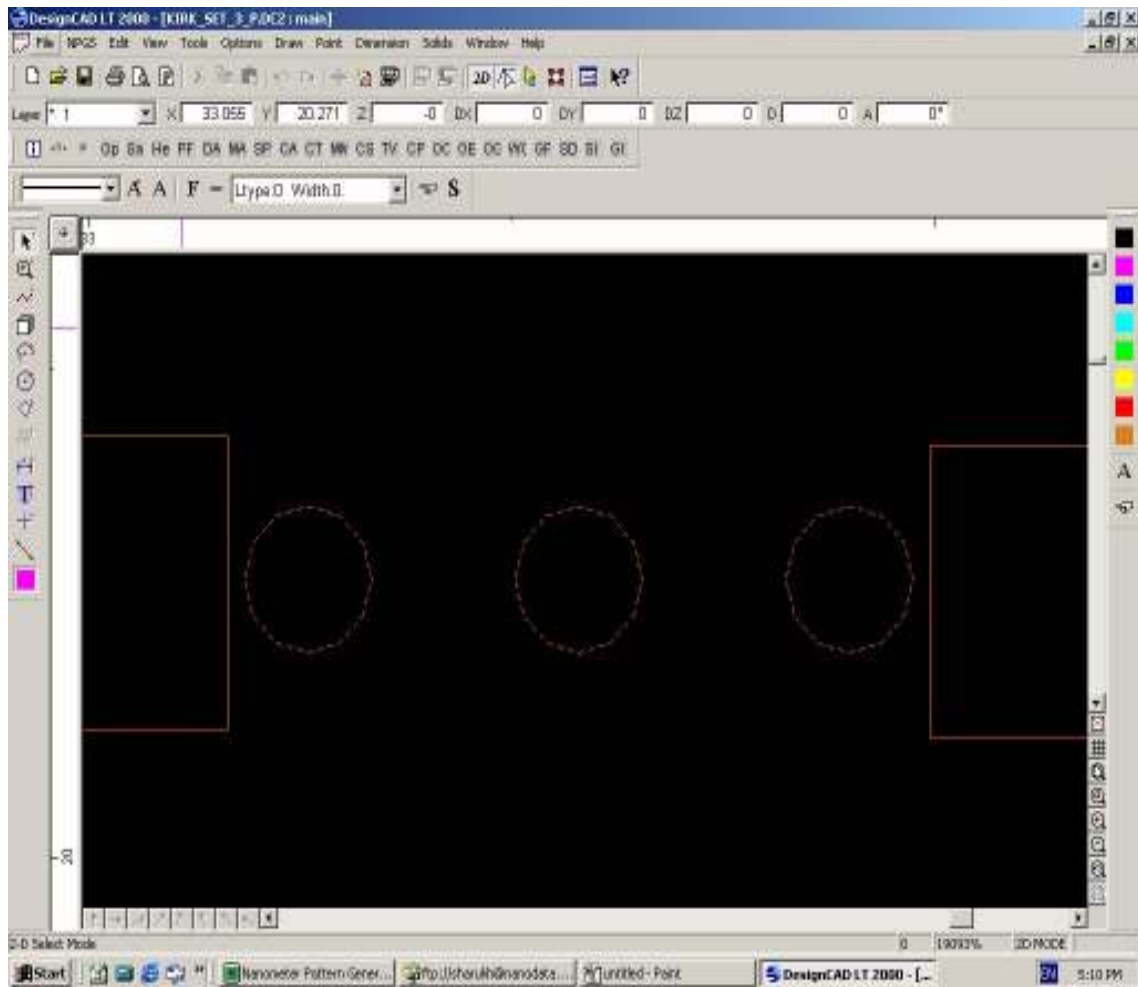
PMMA was spun on at 4000 rpm for 60 seconds yielding a thickness of approximately

50nm

Pre-exposure bake 180°C for 60 seconds

E-beam parameters




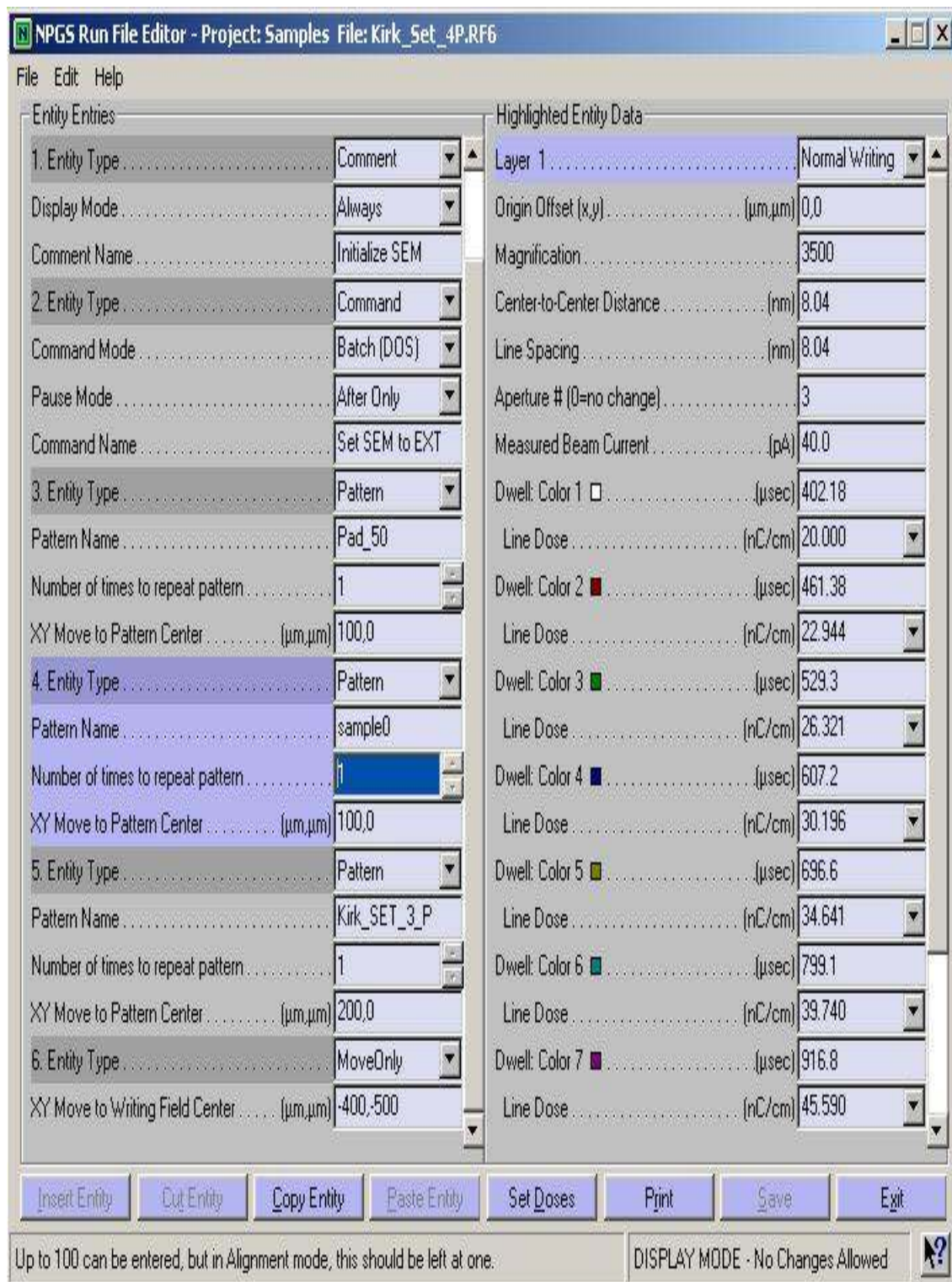


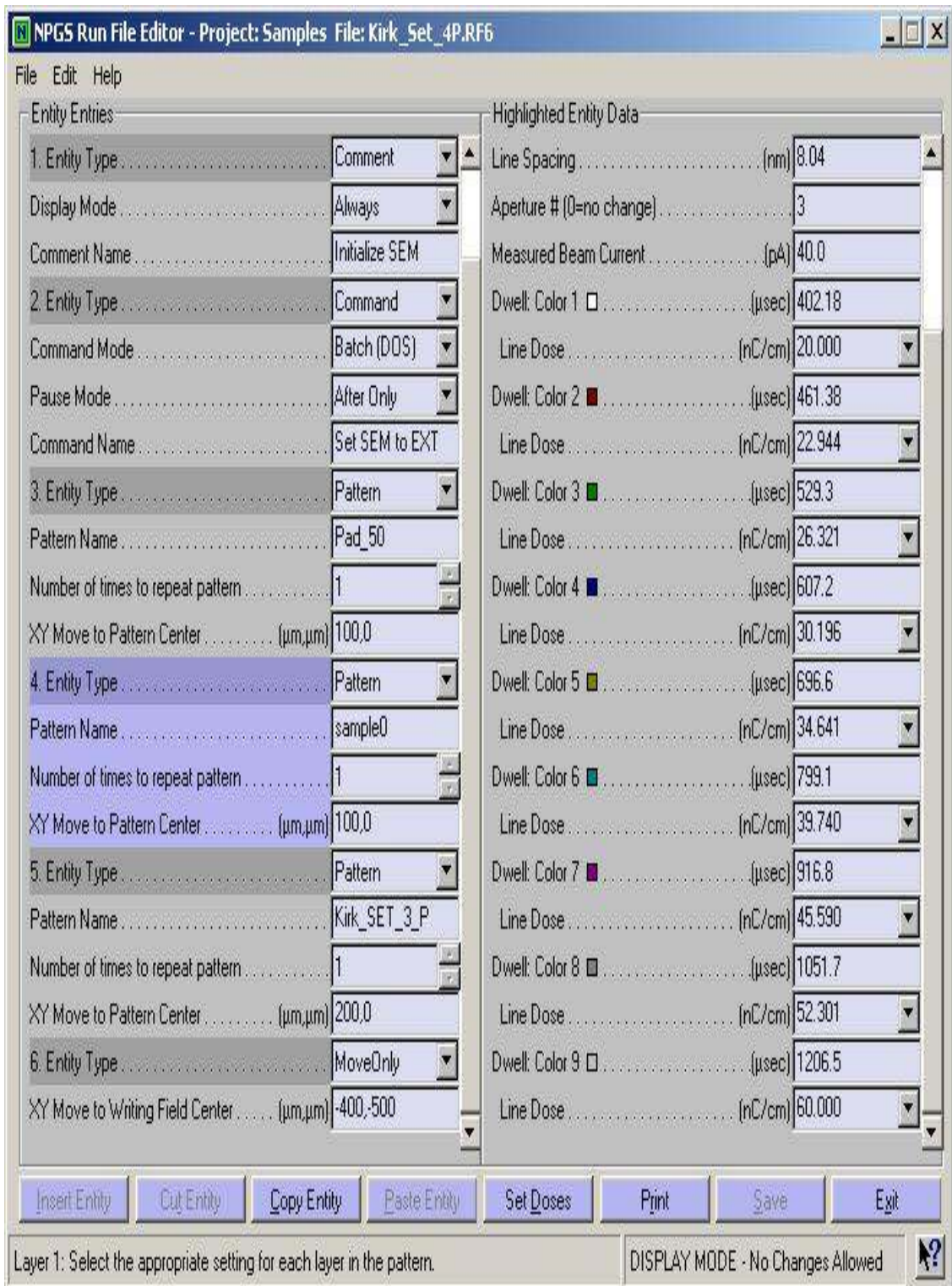
NPG5 Run File Editor - Project: Samples File: Kirk_Set_4P.RF6

File Edit Help

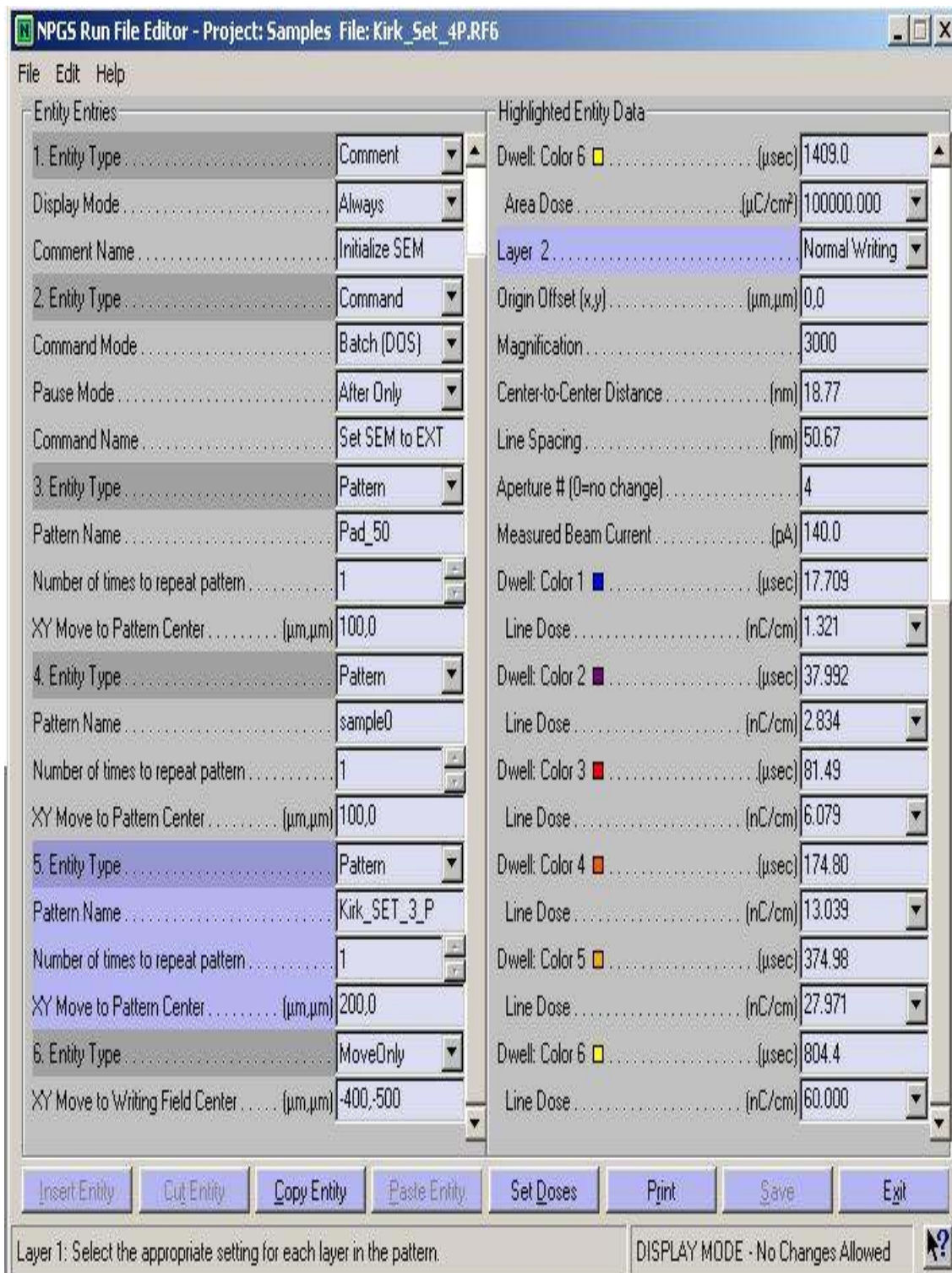
Entity Entries		Highlighted Entity Data	
1. Entity Type	Comment	Layer 1	Normal Writing
Display Mode	Always	Origin Offset (x,y)	($\mu\text{m}, \mu\text{m}$) 0,0
Comment Name	Initialize SEM	Magnification	5000
2. Entity Type	Command	Center-to-Center Distance	(nm) 4.50
Command Mode	Batch (DOS)	Line Spacing	(nm) 4.50
Pause Mode	After Only	Aperture # (0=no change)	4
Command Name	Set SEM to EXT	Measured Beam Current	(pA) 137.0
3. Entity Type	Pattern	Dwell: Color 1 <input type="checkbox"/>	(μsec) 74.05
Pattern Name	Pad_50	Area Dose	($\mu\text{C}/\text{cm}^2$) 50000.000
Number of times to repeat pattern	1		
XY Move to Pattern Center	($\mu\text{m}, \mu\text{m}$) 100,0		
4. Entity Type	Pattern		
Pattern Name	sample0		
Number of times to repeat pattern	1		
XY Move to Pattern Center	($\mu\text{m}, \mu\text{m}$) 100,0		
5. Entity Type	Pattern		
Pattern Name	Kirk_SET_3_P		
Number of times to repeat pattern	1		
XY Move to Pattern Center	($\mu\text{m}, \mu\text{m}$) 200,0		
6. Entity Type	MoveOnly		
XY Move to Writing Field Center	($\mu\text{m}, \mu\text{m}$) -400,500		

Double click on the pattern name to bring up a list of available files. DISPLAY MODE - No Changes Allowed 









Development procedure

Acetone dip for 120 seconds

Rinsed in Isopropanol

Blow dry with Nitrogen

Third PMMA wafer

Wafer specifications

1cm x 1cm piece from a poly crystalline silicon wafer, p-type doping

950K molecular weight PMMA is used

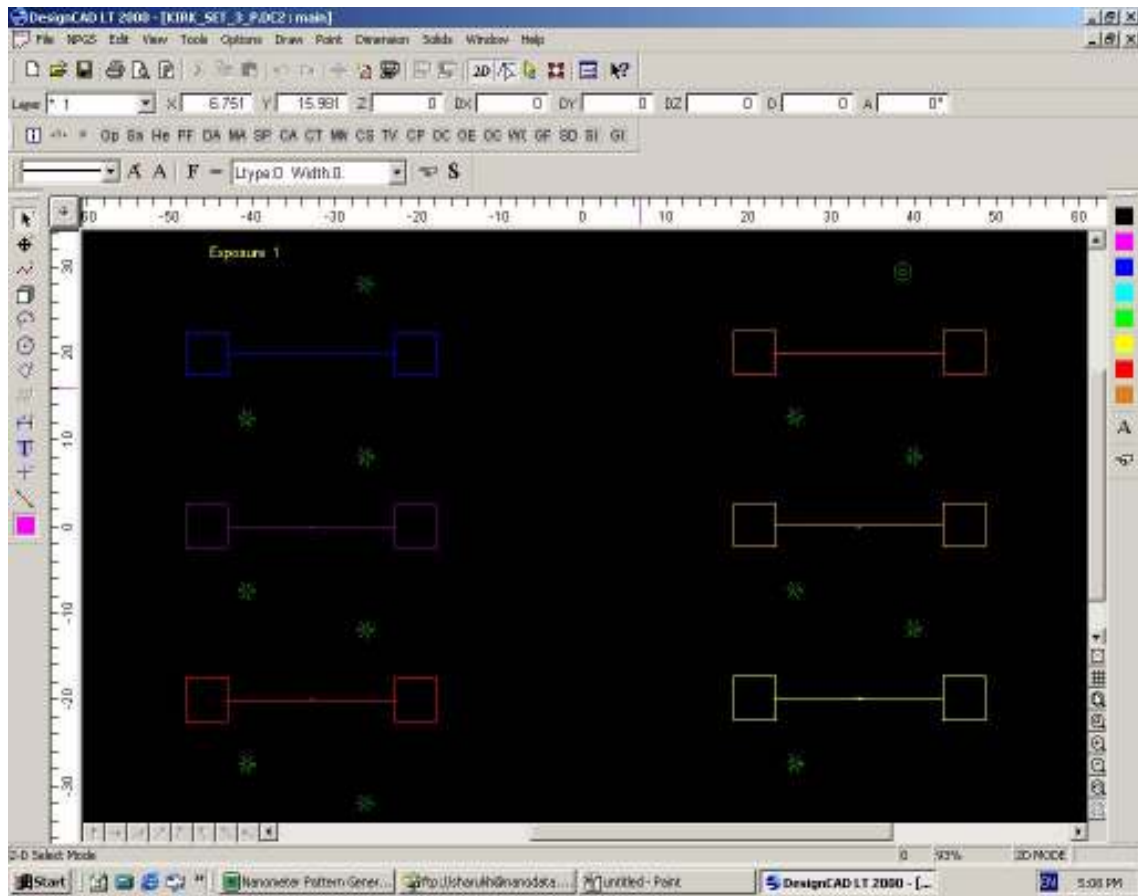
2% PMMA is prepared by mixing 11ml of PMMA and 51ml Anisole

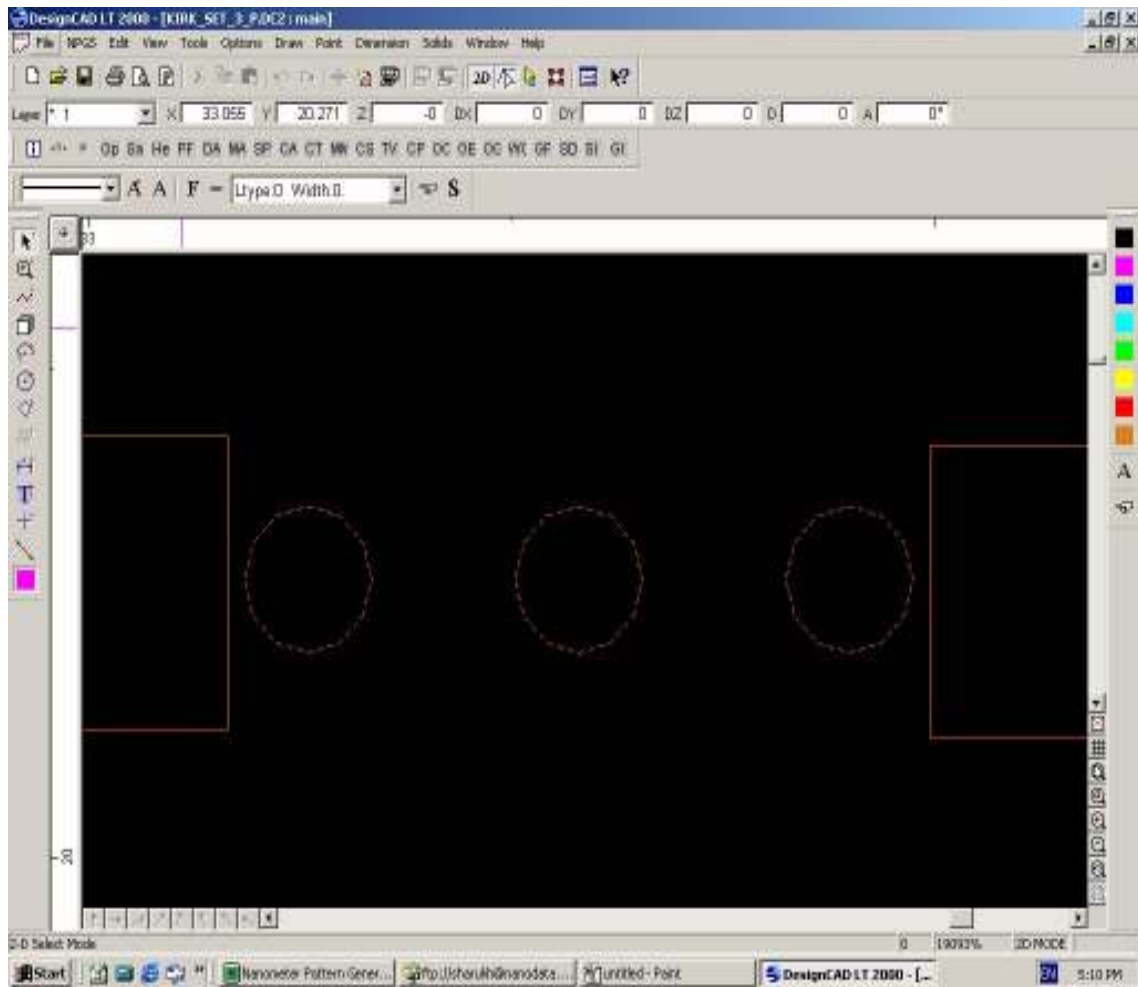
PMMA was spun on at 3000 rpm for 60 seconds yielding a thickness of approximately

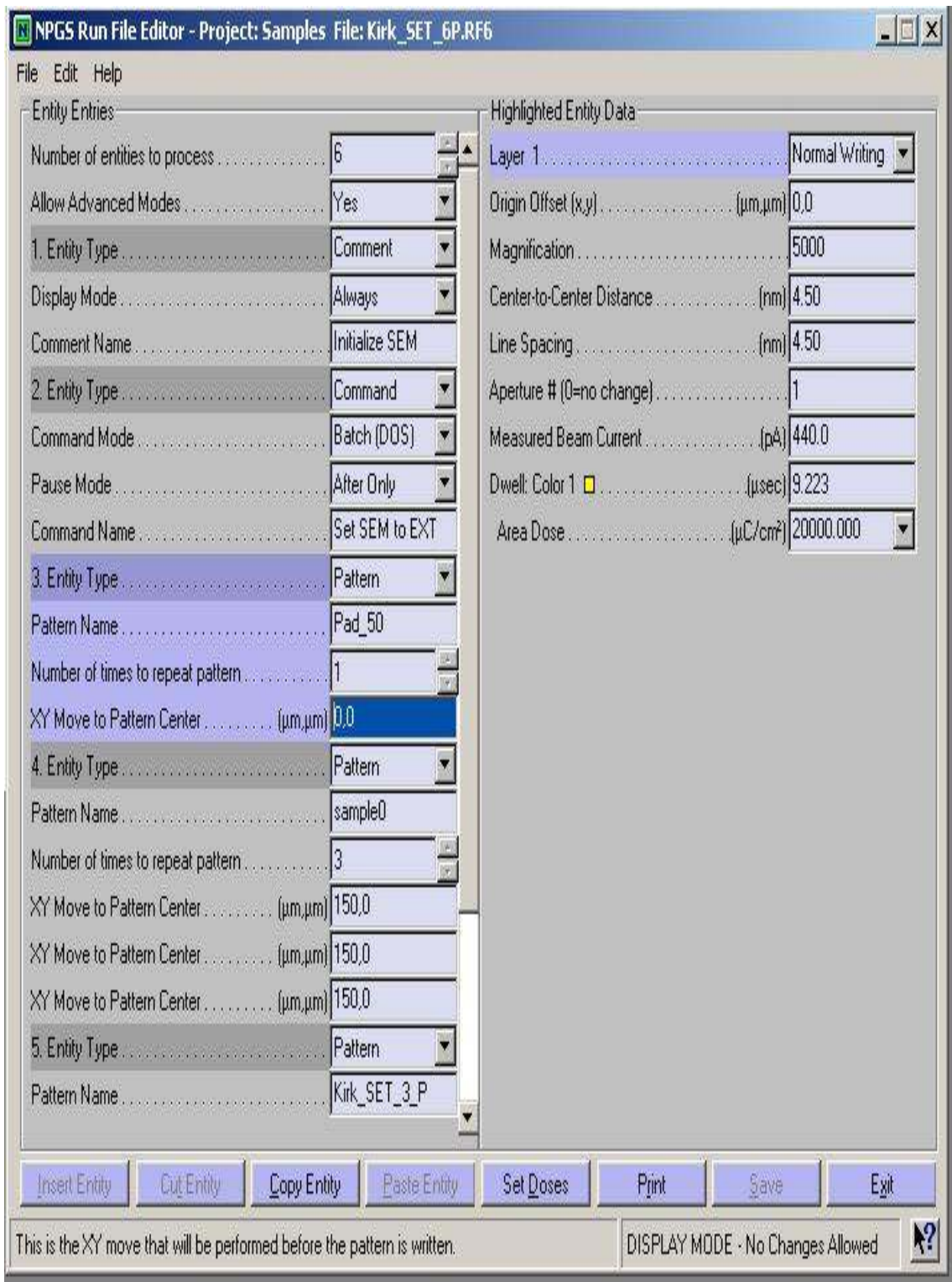
50nm

Pre-exposure bake 180°C for 60 seconds

E-beam parameters







NPGS Run File Editor - Project: Samples File: Kirk_SET_6P.RF6

File Edit Help

Entity Entries

Number of entities to process	6
Allow Advanced Modes	Yes
1. Entity Type	Comment
Display Mode	Always
Comment Name	Initialize SEM
2. Entity Type	Command
Command Mode	Batch (DOS)
Pause Mode	After Only
Command Name	Set SEM to EXT
3. Entity Type	Pattern
Pattern Name	Pad_50
Number of times to repeat pattern	1
XY Move to Pattern Center (μm,μm)	0,0
4. Entity Type	Pattern
Pattern Name	sample0
Number of times to repeat pattern	3
XY Move to Pattern Center (μm,μm)	150,0
XY Move to Pattern Center (μm,μm)	150,0
XY Move to Pattern Center (μm,μm)	150,0
5. Entity Type	Pattern
Pattern Name	Kirk_SET_3_P

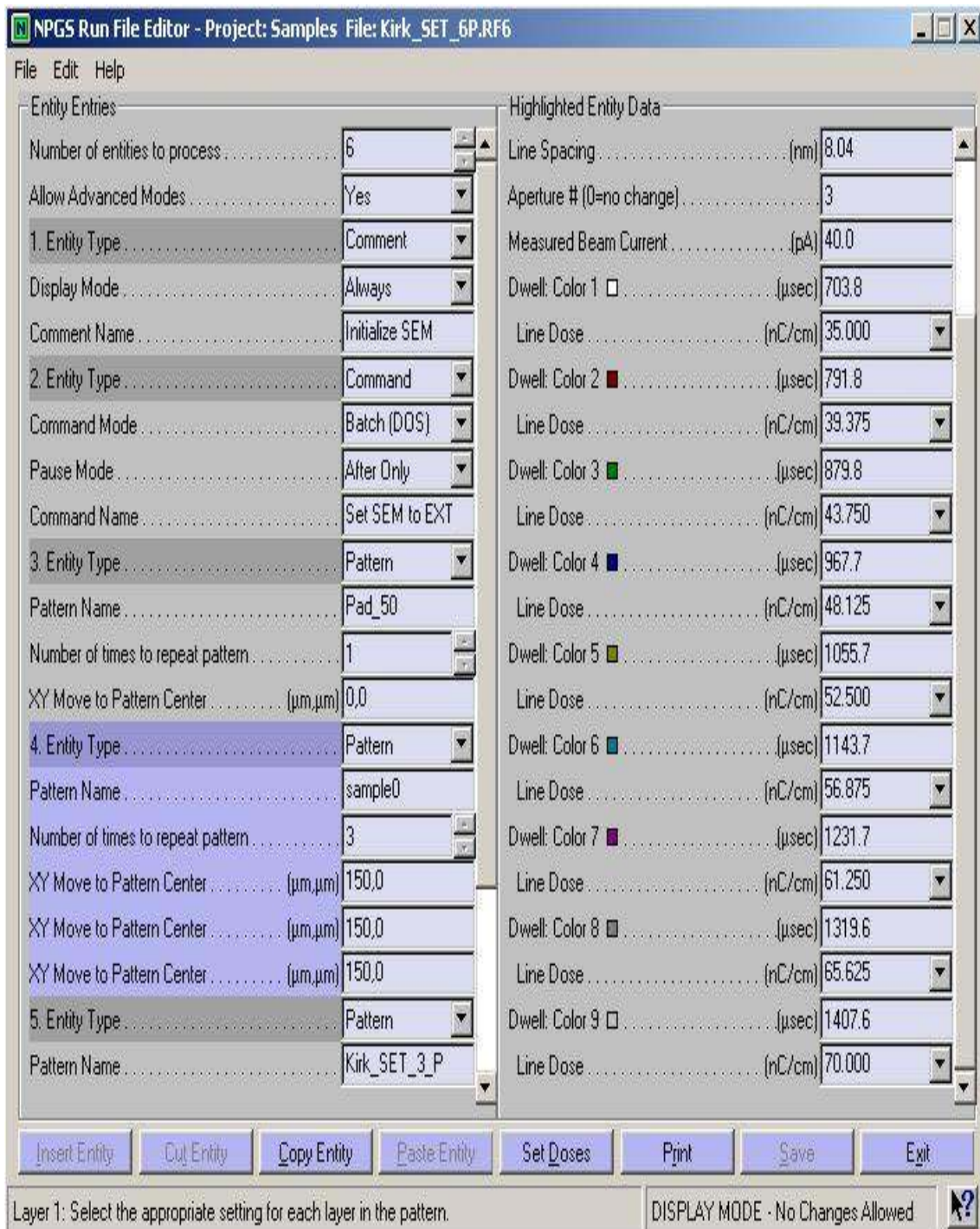
Highlighted Entity Data

Layer 1	Normal Writing
Origin Offset (x,y) (μm,μm)	0,0
Magnification	3500
Center-to-Center Distance (nm)	8,04
Line Spacing (nm)	8,04
Aperture # (0=no change)	3
Measured Beam Current (pA)	40,0
Dwell: Color 1 (μsec)	703,8
Line Dose (nC/cm)	35,000
Dwell: Color 2 (μsec)	791,8
Line Dose (nC/cm)	39,375
Dwell: Color 3 (μsec)	879,8
Line Dose (nC/cm)	43,750
Dwell: Color 4 (μsec)	967,7
Line Dose (nC/cm)	48,125
Dwell: Color 5 (μsec)	1055,7
Line Dose (nC/cm)	52,500
Dwell: Color 6 (μsec)	1143,7
Line Dose (nC/cm)	56,875
Dwell: Color 7 (μsec)	1231,7
Line Dose (nC/cm)	61,250

Insert Entity
Cut Entity
Copy Entity
Paste Entity
Set Doses
Print
Save
Exit

Up to 100 can be entered, but in Alignment mode, this should be left at one.


DISPLAY MODE - No Changes Allowed



NPGS Run File Editor - Project: Samples File: Kirk_SET_6P.RF6

File Edit Help

Entity Entries		Highlighted Entity Data	
Comment Name	Initialize SEM	Layer 1	Normal Writing
2. Entity Type	Command	Origin Offset (x,y)	($\mu\text{m},\mu\text{m}$) 0,0
Command Mode	Batch (DOS)	Magnification	3000
Pause Mode	After Only	Center-to-Center Distance	(nm) 7.51
Command Name	Set SEM to EXT	Line Spacing	(nm) 7.51
3. Entity Type	Pattern	Aperture # (0=no change)	3
Pattern Name	Pad_50	Measured Beam Current	(pA) 40.0
Number of times to repeat pattern	1	Dwell: Color 1	(μsec) 750.7
XY Move to Pattern Center	($\mu\text{m},\mu\text{m}$) 0,0	Line Dose	(nC/cm) 40.000
4. Entity Type	Pattern	Dwell: Color 2	(μsec) 900.9
Pattern Name	sample0	Line Dose	(nC/cm) 48.000
Number of times to repeat pattern	3	Dwell: Color 3	(μsec) 1051.0
XY Move to Pattern Center	($\mu\text{m},\mu\text{m}$) 150,0	Line Dose	(nC/cm) 56.000
XY Move to Pattern Center	($\mu\text{m},\mu\text{m}$) 150,0	Dwell: Color 4	(μsec) 1201.2
XY Move to Pattern Center	($\mu\text{m},\mu\text{m}$) 150,0	Line Dose	(nC/cm) 64.000
5. Entity Type	Pattern	Dwell: Color 5	(μsec) 1351.3
Pattern Name	Kirk_SET_3_P	Line Dose	(nC/cm) 72.000
Number of times to repeat pattern	2	Dwell: Color 6	(μsec) 1501.5
XY Move to Pattern Center	($\mu\text{m},\mu\text{m}$) 100,0	Line Dose	(nC/cm) 80.000
XY Move to Pattern Center	($\mu\text{m},\mu\text{m}$) 100,0	Layer 2	Normal Writing
6. Entity Type	MoveOnly	Origin Offset (x,y)	($\mu\text{m},\mu\text{m}$) 0,0

Double click on the pattern name to bring up a list of available files. DISPLAY MODE - No Changes Allowed 

NPG5 Run File Editor - Project: Samples File: Kirk_SET_6P.RF6

File Edit Help

Entity Entries		Highlighted Entity Data	
Comment Name	Initialize SEM	Dwell: Color 6	1501.5 (μsec)
2. Entity Type	Command	Line Dose	80.000 (nC/cm)
Command Mode	Batch (DOS)	Layer 2	Normal Writing
Pause Mode	After Only	Origin Offset (x,y)	0,0 (μm,μm)
Command Name	Set SEM to EXT	Magnification	3000
3. Entity Type	Pattern	Center-to-Center Distance	16.89 (nm)
Pattern Name	Pad_50	Line Spacing	50.67 (nm)
Number of times to repeat pattern	1	Aperture # (0=no change)	4
XY Move to Pattern Center (μm,μm)	0,0	Measured Beam Current	140.0 (pA)
4. Entity Type	Pattern	Dwell: Color 1	427.98 (μsec)
Pattern Name	sample0	Area Dose	7000.000 (μC/cm²)
Number of times to repeat pattern	3	Dwell: Color 2	501.4 (μsec)
XY Move to Pattern Center (μm,μm)	150,0	Area Dose	8200.000 (μC/cm²)
XY Move to Pattern Center (μm,μm)	150,0	Dwell: Color 3	574.7 (μsec)
XY Move to Pattern Center (μm,μm)	150,0	Area Dose	9400.000 (μC/cm²)
5. Entity Type	Pattern	Dwell: Color 4	648.1 (μsec)
Pattern Name	Kirk_SET_3_P	Area Dose	10600.000 (μC/cm²)
Number of times to repeat pattern	2	Dwell: Color 5	721.5 (μsec)
XY Move to Pattern Center (μm,μm)	100,0	Area Dose	11800.000 (μC/cm²)
XY Move to Pattern Center (μm,μm)	100,0	Dwell: Color 6	794.8 (μsec)
6. Entity Type	MoveOnly	Area Dose	13000.000 (μC/cm²)

Layer 1: Select the appropriate setting for each layer in the pattern. DISPLAY MODE - No Changes Allowed

Development procedure

Acetone dip for 150 seconds

Rinsed in Isopropanol

Blow dry with Nitrogen

Fourth PMMA wafer

Wafer specifications

1cm x 1cm piece from a poly crystalline silicon wafer, p-type doping

950K molecular weight PMMA is used

2% PMMA is prepared by mixing 11ml of PMMA and 51ml Anisole

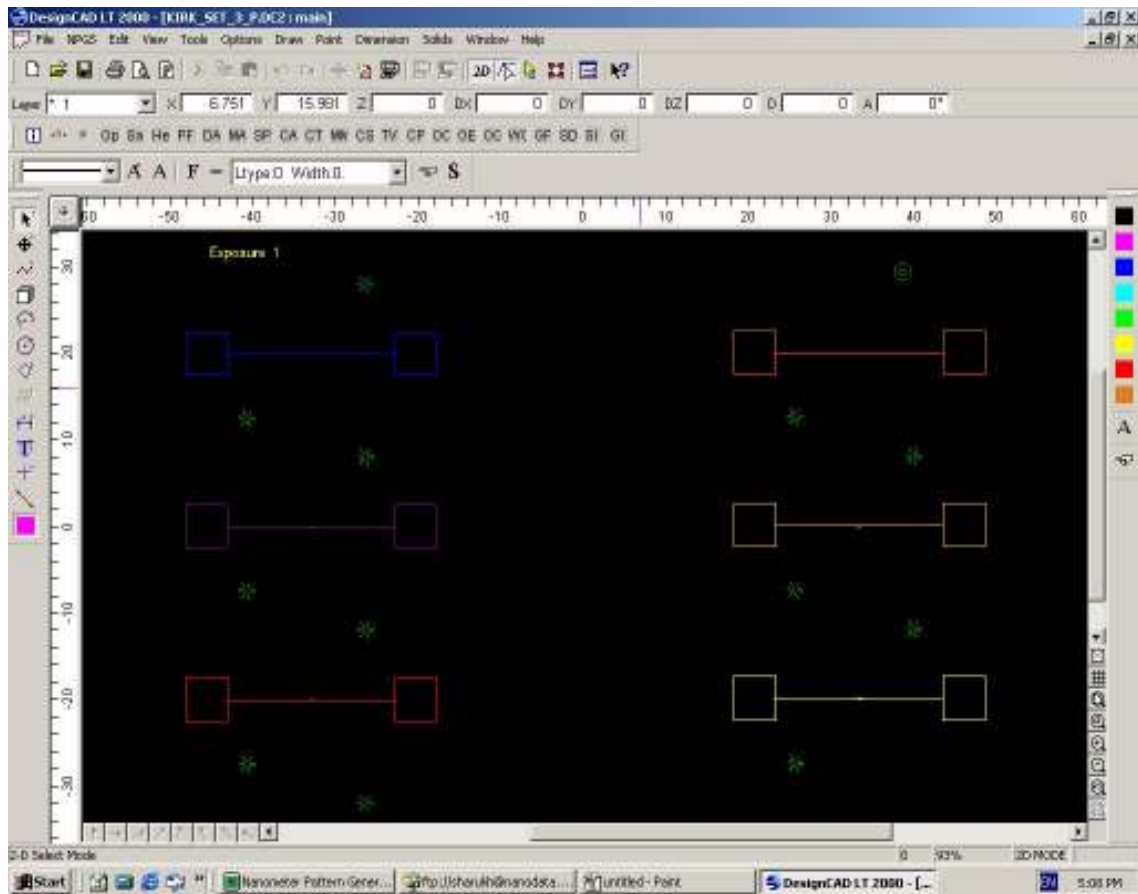
PMMA was spun on at 4000 rpm for 60 seconds for wafer 1

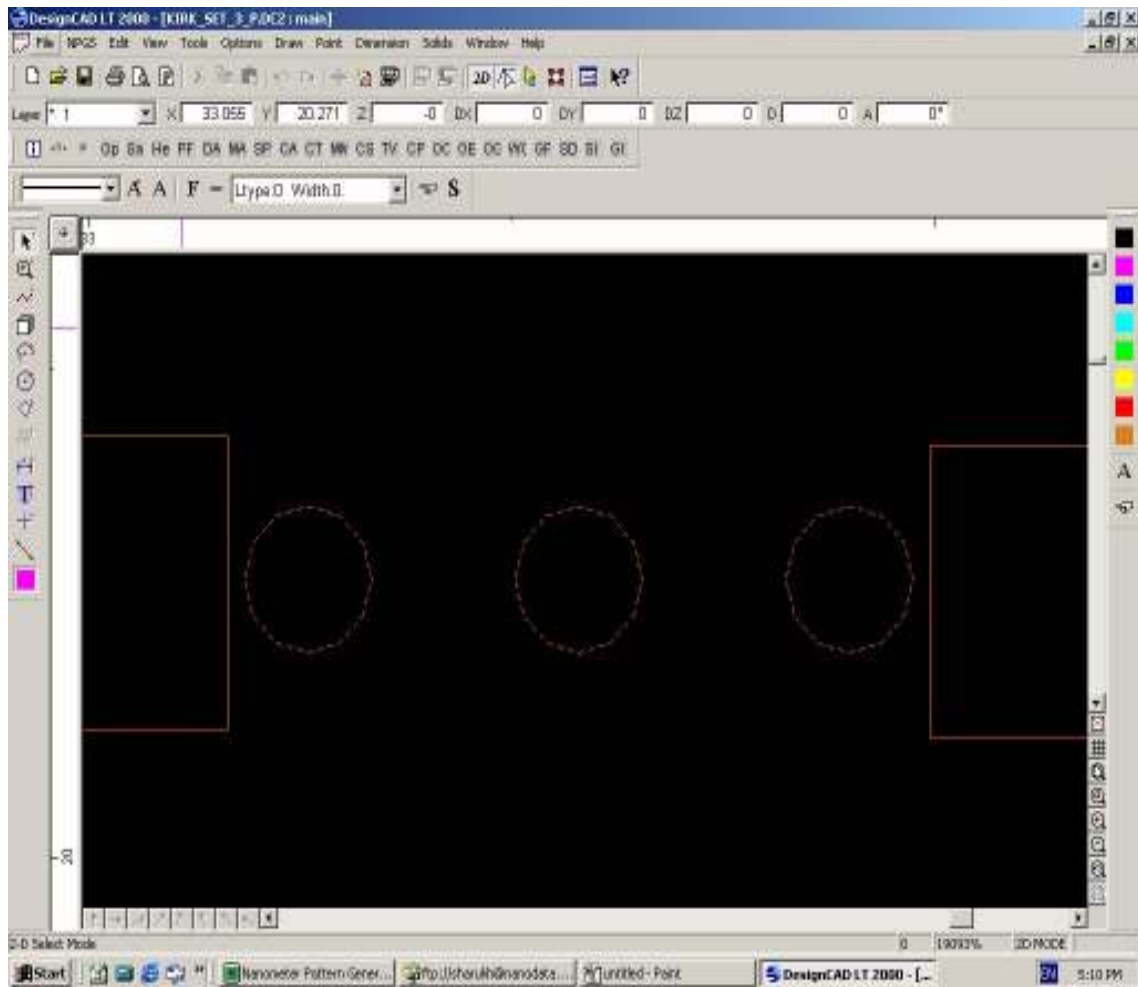
PMMA was spun on at 2500 rpm for 60 seconds for wafer 2

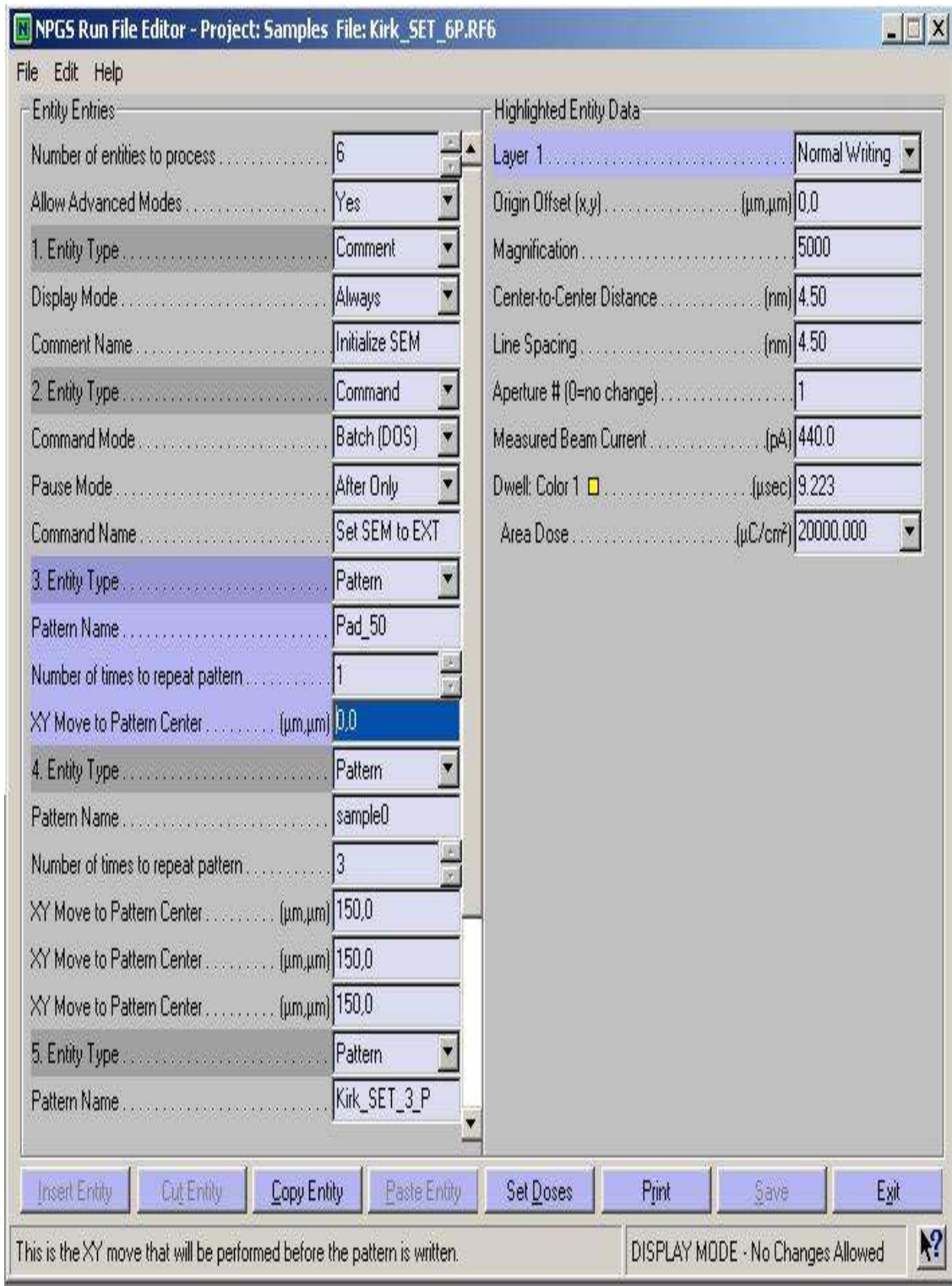
50nm

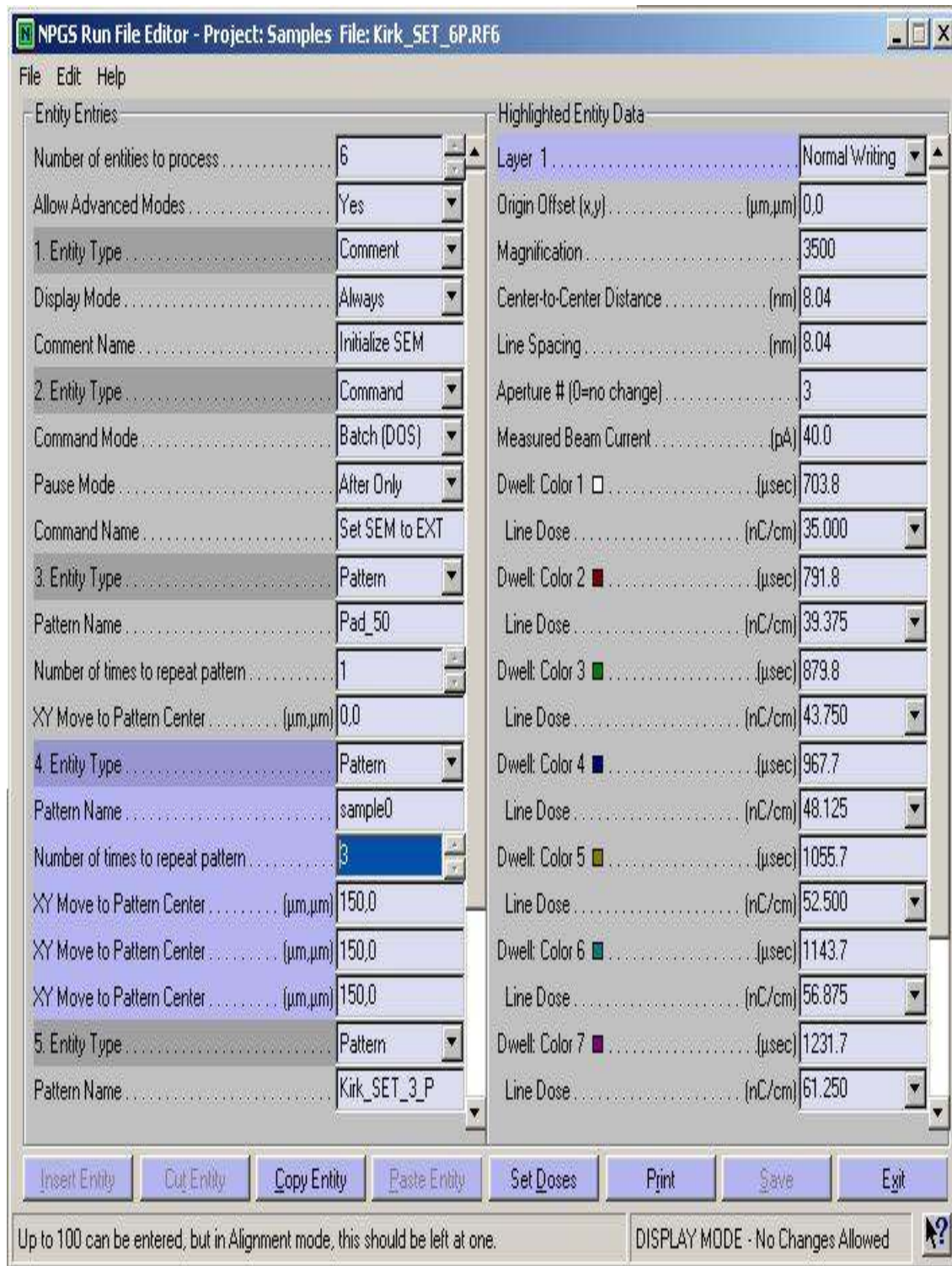
Pre-exposure bake 180°C for 60 seconds

E-beam parameters (for both wafers)









NPGS Run File Editor - Project: Samples File: Kirk_SET_6P.RF6

File Edit Help

Entity Entries

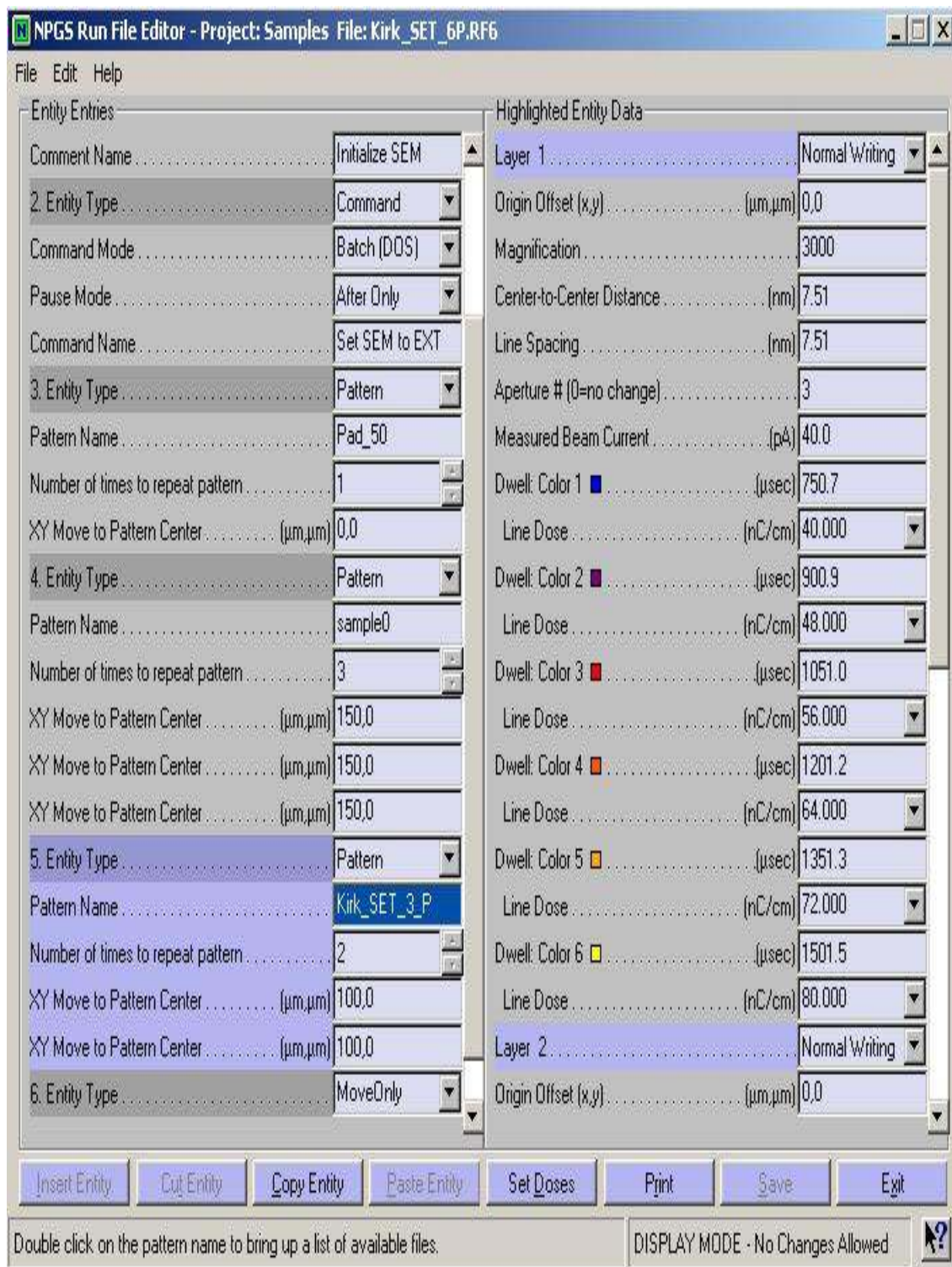
Number of entities to process	6
Allow Advanced Modes	Yes
1. Entity Type	Comment
Display Mode	Always
Comment Name	Initialize SEM
2. Entity Type	Command
Command Mode	Batch (DOS)
Pause Mode	After Only
Command Name	Set SEM to EXT
3. Entity Type	Pattern
Pattern Name	Pad_50
Number of times to repeat pattern	1
XY Move to Pattern Center (μm,μm)	0,0
4. Entity Type	Pattern
Pattern Name	sample0
Number of times to repeat pattern	3
XY Move to Pattern Center (μm,μm)	150,0
XY Move to Pattern Center (μm,μm)	150,0
XY Move to Pattern Center (μm,μm)	150,0
5. Entity Type	Pattern
Pattern Name	Kirk_SET_3_P

Highlighted Entity Data

Line Spacing (nm)	8.04
Aperture # (0=no change)	3
Measured Beam Current (pA)	40.0
Dwell: Color 1 (μsec)	703.8
Line Dose (nC/cm)	35.000
Dwell: Color 2 (μsec)	791.8
Line Dose (nC/cm)	39.375
Dwell: Color 3 (μsec)	879.8
Line Dose (nC/cm)	43.750
Dwell: Color 4 (μsec)	967.7
Line Dose (nC/cm)	48.125
Dwell: Color 5 (μsec)	1055.7
Line Dose (nC/cm)	52.500
Dwell: Color 6 (μsec)	1143.7
Line Dose (nC/cm)	56.875
Dwell: Color 7 (μsec)	1231.7
Line Dose (nC/cm)	61.250
Dwell: Color 8 (μsec)	1319.6
Line Dose (nC/cm)	65.625
Dwell: Color 9 (μsec)	1407.6
Line Dose (nC/cm)	70.000

Insert Entity Cut Entity Copy Entity Paste Entity Set Doses Print Save Exit

Layer 1: Select the appropriate setting for each layer in the pattern. DISPLAY MODE - No Changes Allowed





Development procedure (for both wafers)

Acetone dip for 150 seconds

Rinsed in Isopropanol

Blow dry with Nitrogen

APPENDIX C

HSQ RECIPES

First HSQ wafer

Wafer specifications

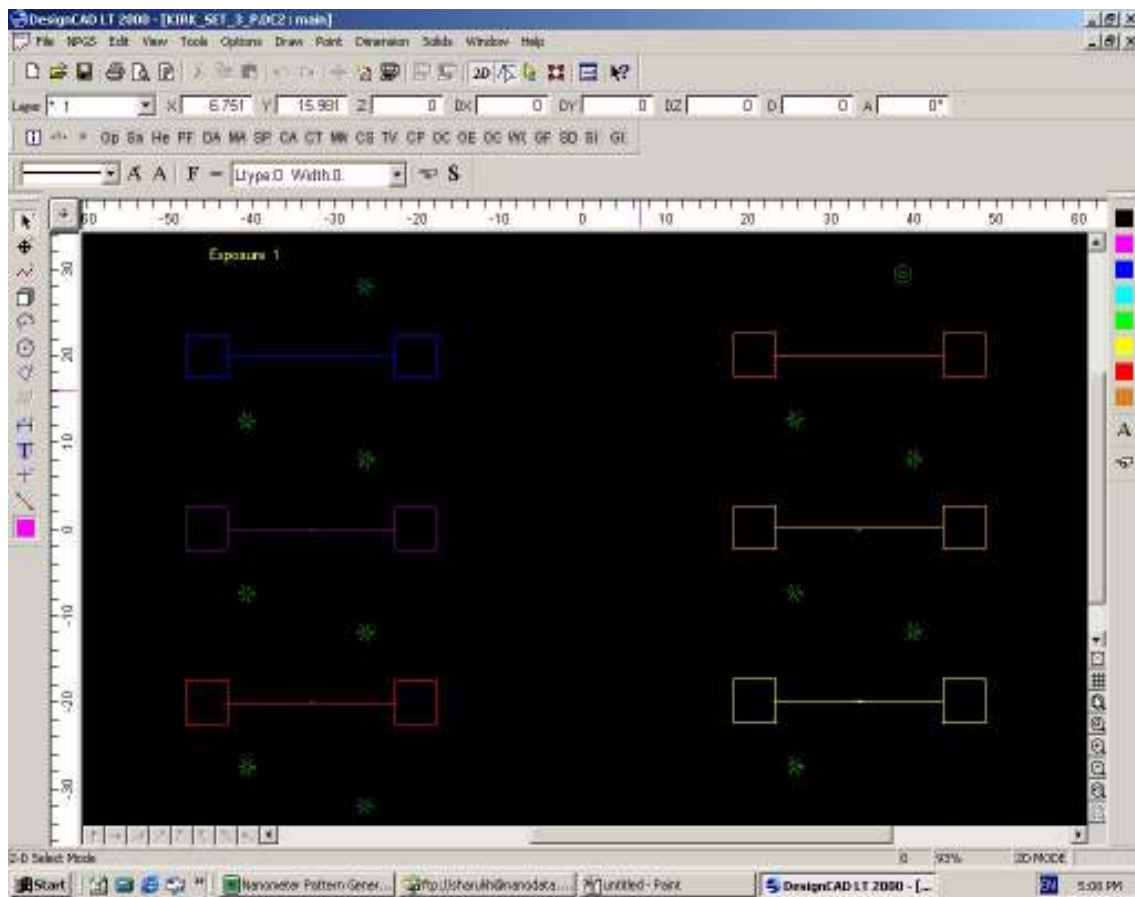
1cm x 1cm piece from a poly crystalline silicon wafer, p-type doping

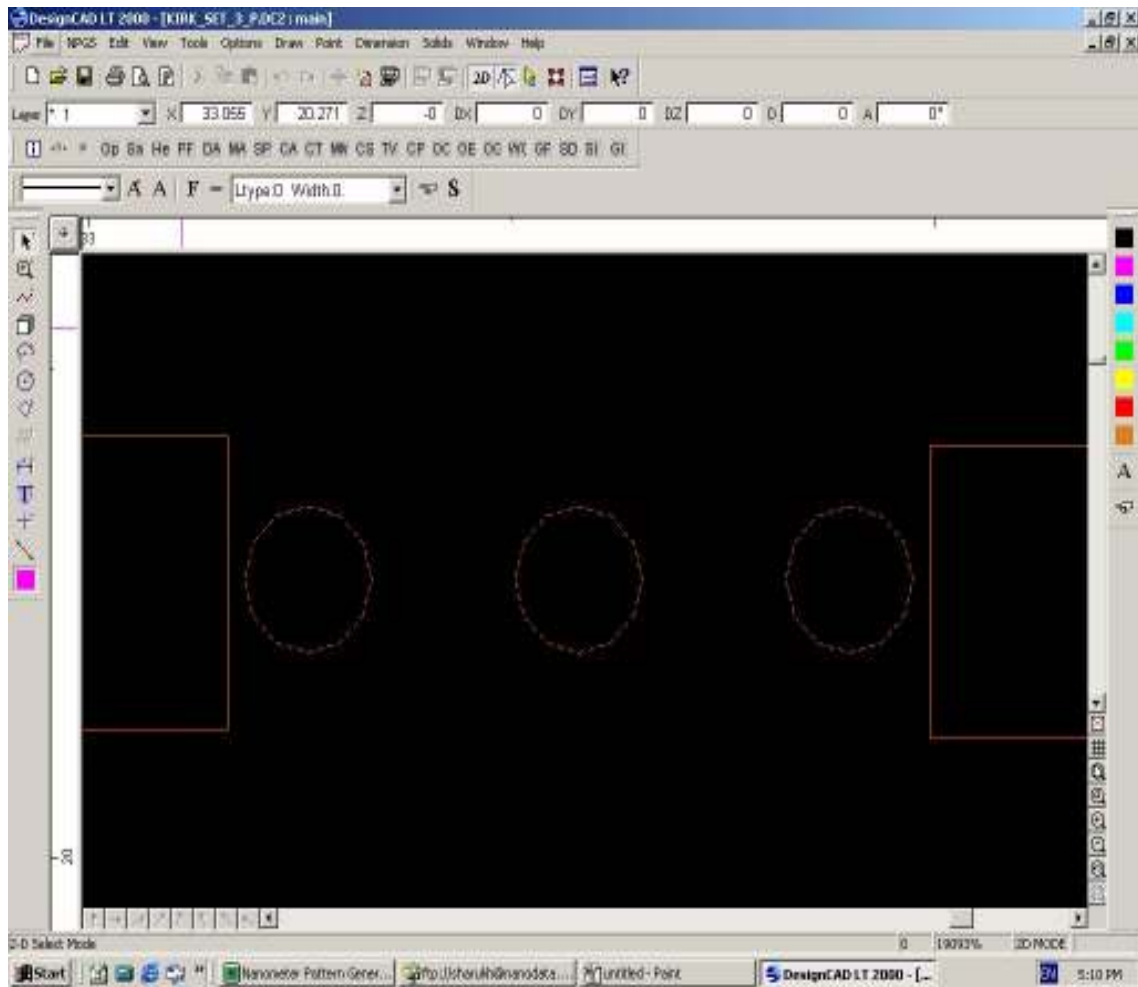
XR-1541 (containing 4% solids of HSQ) was used

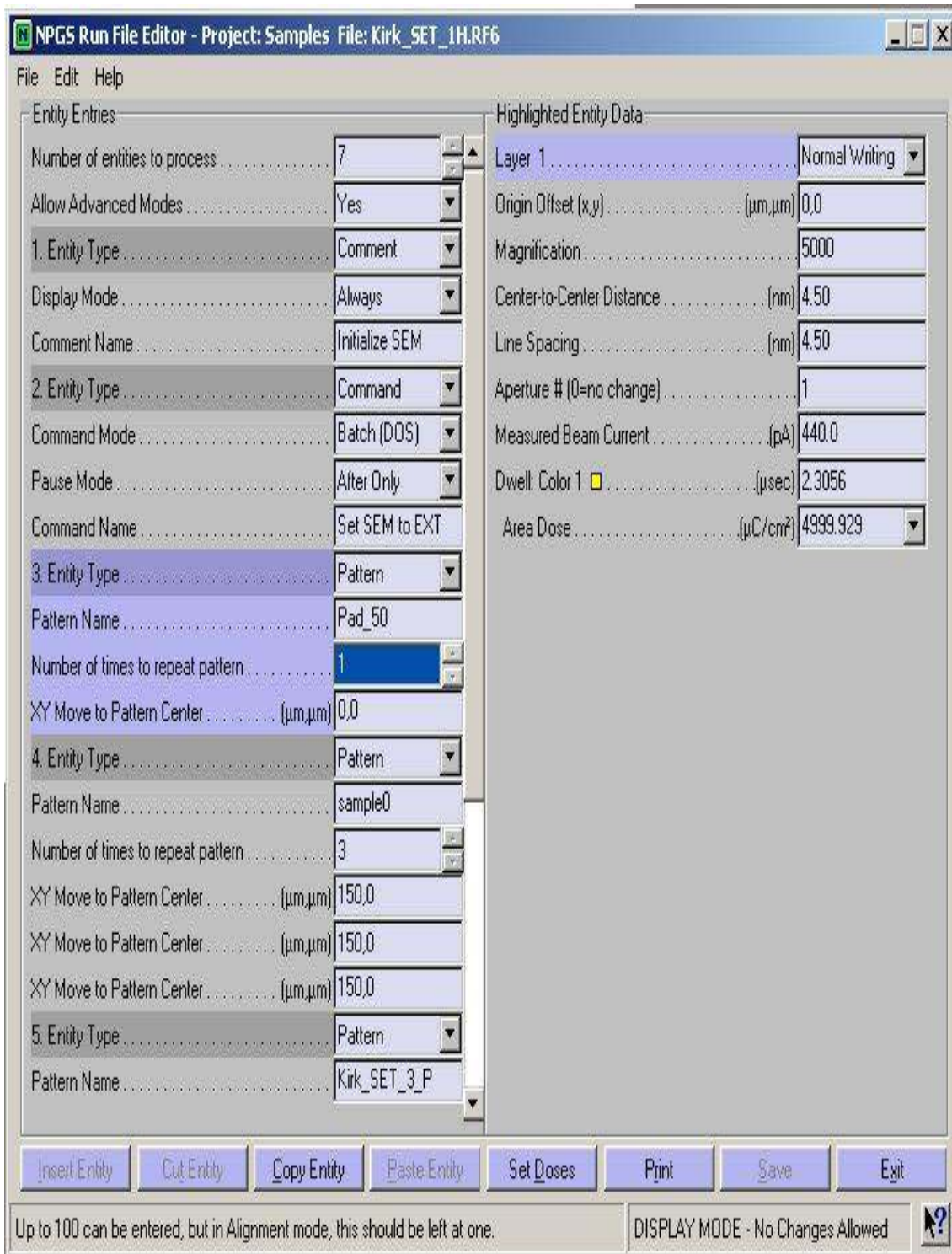
HSQ was spun on at 2000 rpm for 60 seconds

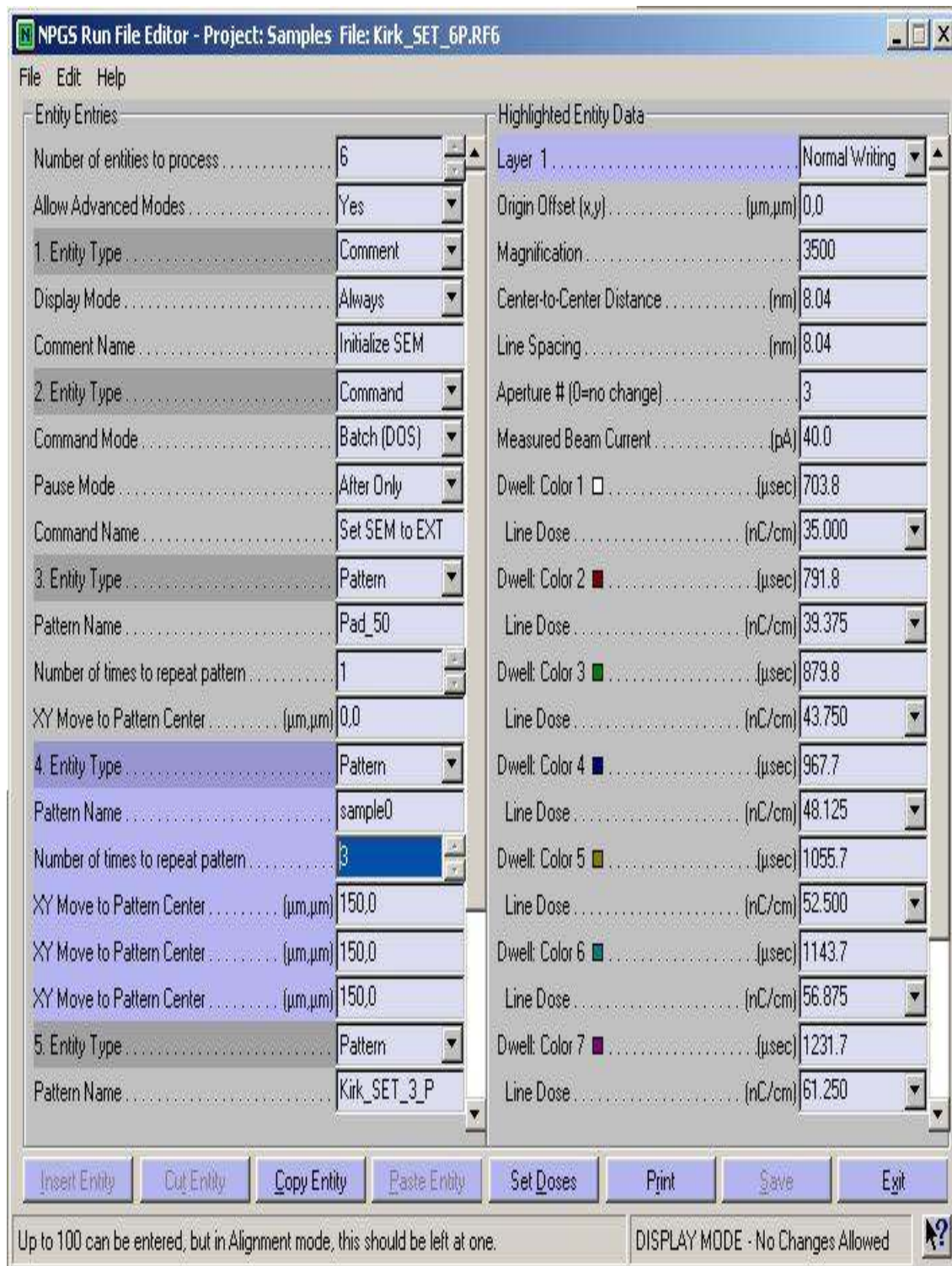
Pre-exposure bake 120°C for 60 seconds

E-beam parameters (for both wafers)









NPGS Run File Editor - Project: Samples File: Kirk_SET_6P.RF6

File Edit Help

Entity Entries

Number of entities to process	6
Allow Advanced Modes	Yes
1. Entity Type	Comment
Display Mode	Always
Comment Name	Initialize SEM
2. Entity Type	Command
Command Mode	Batch (DOS)
Pause Mode	After Only
Command Name	Set SEM to EXT
3. Entity Type	Pattern
Pattern Name	Pad_50
Number of times to repeat pattern	1
XY Move to Pattern Center (μm,μm)	0,0
4. Entity Type	Pattern
Pattern Name	sample0
Number of times to repeat pattern	3
XY Move to Pattern Center (μm,μm)	150,0
XY Move to Pattern Center (μm,μm)	150,0
XY Move to Pattern Center (μm,μm)	150,0
5. Entity Type	Pattern
Pattern Name	Kirk_SET_3_P

Highlighted Entity Data

Line Spacing (nm)	8.04
Aperture # (0=no change)	3
Measured Beam Current (pA)	40.0
Dwell: Color 1 (μsec)	703.8
Line Dose (nC/cm)	35.000
Dwell: Color 2 (μsec)	791.8
Line Dose (nC/cm)	39.375
Dwell: Color 3 (μsec)	879.8
Line Dose (nC/cm)	43.750
Dwell: Color 4 (μsec)	967.7
Line Dose (nC/cm)	48.125
Dwell: Color 5 (μsec)	1055.7
Line Dose (nC/cm)	52.500
Dwell: Color 6 (μsec)	1143.7
Line Dose (nC/cm)	56.875
Dwell: Color 7 (μsec)	1231.7
Line Dose (nC/cm)	61.250
Dwell: Color 8 (μsec)	1319.6
Line Dose (nC/cm)	65.625
Dwell: Color 9 (μsec)	1407.6
Line Dose (nC/cm)	70.000

Insert Entity Cut Entity Copy Entity Paste Entity Set Doses Print Save Exit

Layer 1: Select the appropriate setting for each layer in the pattern. DISPLAY MODE - No Changes Allowed

NPGS Run File Editor - Project: Samples File: Kirk_SET_1H.RF6

File Edit Help

Entity Entries

3. Entity Type	Pattern
Pattern Name	Pad_50
Number of times to repeat pattern	1
XY Move to Pattern Center (μm,μm)	0,0
4. Entity Type	Pattern
Pattern Name	sample0
Number of times to repeat pattern	3
XY Move to Pattern Center (μm,μm)	150,0
XY Move to Pattern Center (μm,μm)	150,0
XY Move to Pattern Center (μm,μm)	150,0
5. Entity Type	Pattern
Pattern Name	Kirk_SET_3_P
Number of times to repeat pattern	2
XY Move to Pattern Center (μm,μm)	150,0
XY Move to Pattern Center (μm,μm)	150,0
6. Entity Type	Pattern
Pattern Name	P_Young_50um
Number of times to repeat pattern	1
XY Move to Pattern Center (μm,μm)	150,0
7. Entity Type	MoveOnly
XY Move to Writing Field Center (μm,μm)	-900,-500

Highlighted Entity Data

Layer 1	Normal Writing
Origin Offset (x,y) (μm,μm)	0,0
Magnification	3000
Center-to-Center Distance (nm)	7.51
Line Spacing (nm)	7.51
Aperture # (0=no change)	3
Measured Beam Current (pA)	40.0
Dwell: Color 1 (μsec)	750.7
Line Dose (nC/cm)	40.000
Dwell: Color 2 (μsec)	938.4
Line Dose (nC/cm)	50.000
Dwell: Color 3 (μsec)	1126.1
Line Dose (nC/cm)	60.000
Dwell: Color 4 (μsec)	1313.8
Line Dose (nC/cm)	70.000
Dwell: Color 5 (μsec)	1501.5
Line Dose (nC/cm)	80.000
Dwell: Color 6 (μsec)	1689.1
Line Dose (nC/cm)	90.000
Layer 2	Pause First
Origin Offset (x,y) (μm,μm)	0,0

Insert Entity
Cut Entity
Copy Entity
Paste Entity
Set Doses
Print
Save
Exit

Double click on the pattern name to bring up a list of available files. DISPLAY MODE - No Changes Allowed



Development procedure

No post exposure bake.

MF322 dip for 60 seconds

DI water rinse

Blow dry with Nitrogen

Second HSQ wafer

Wafer specifications

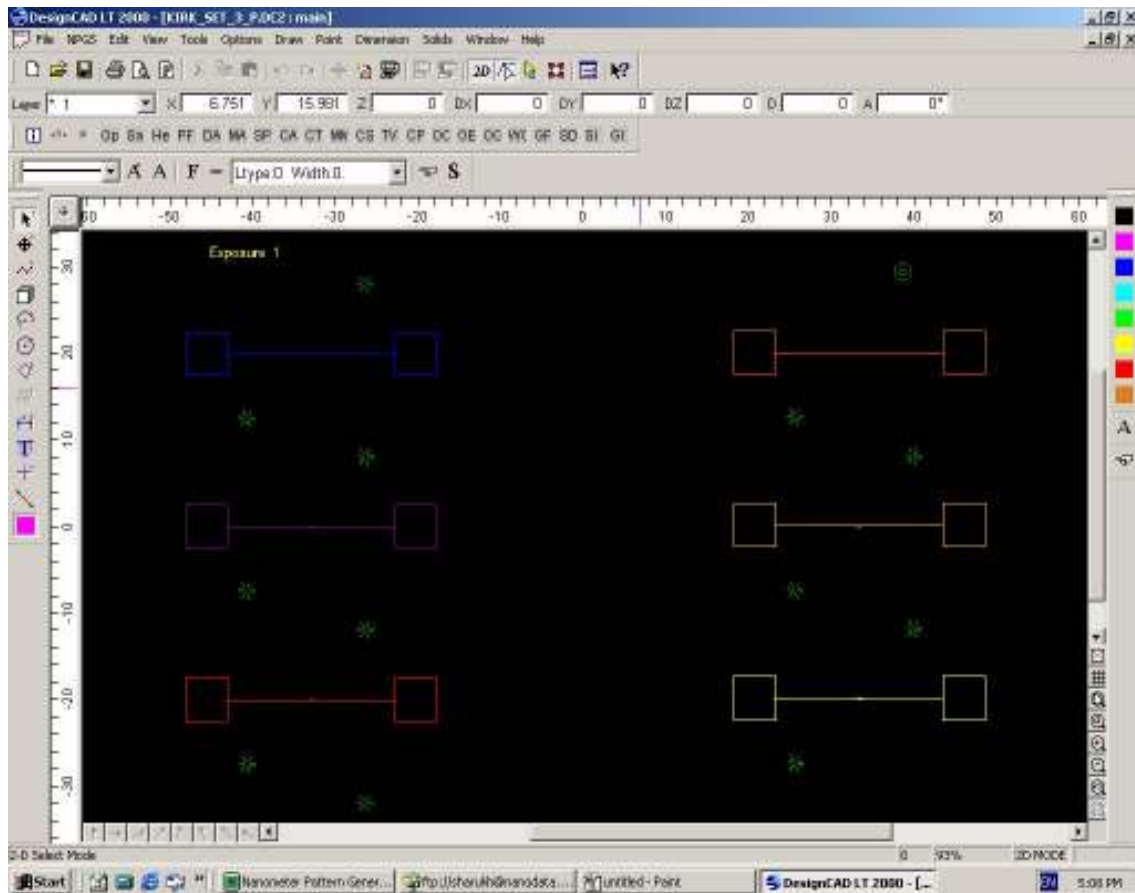
1cm x 1cm piece from a poly crystalline silicon wafer, p-type doping

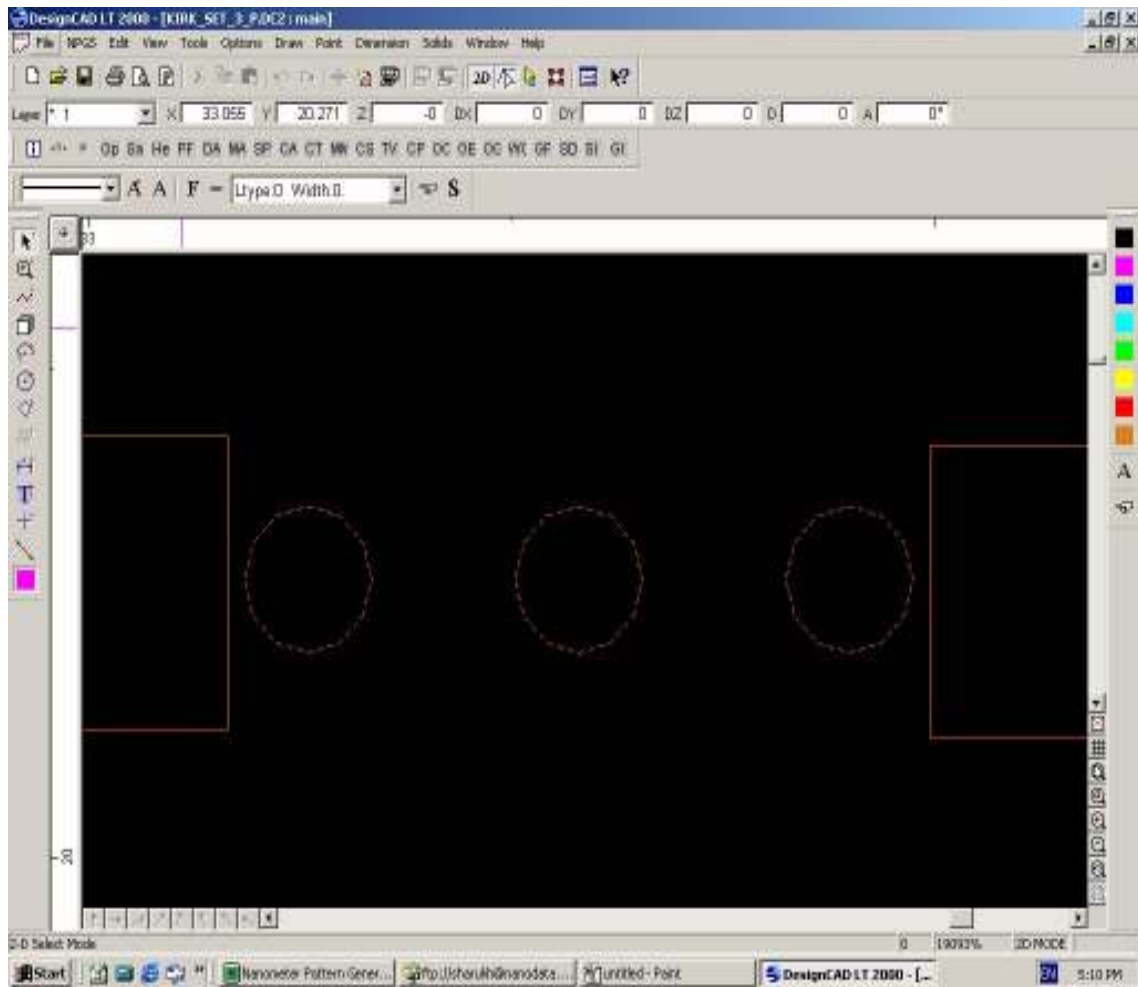
XR-1541 (containing 4% solids of HSQ) was used

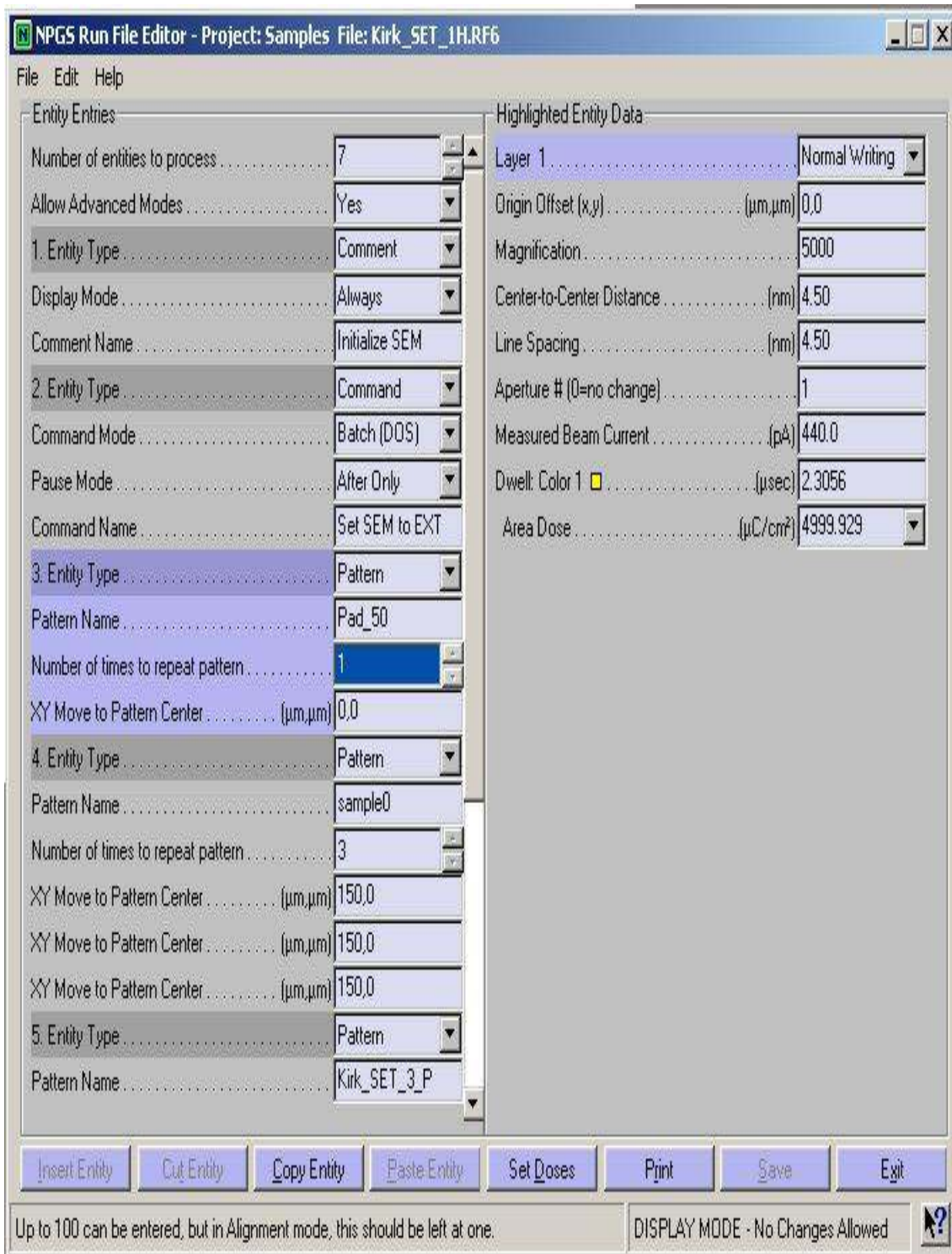
HSQ was spun on at 4000 rpm for 60 seconds

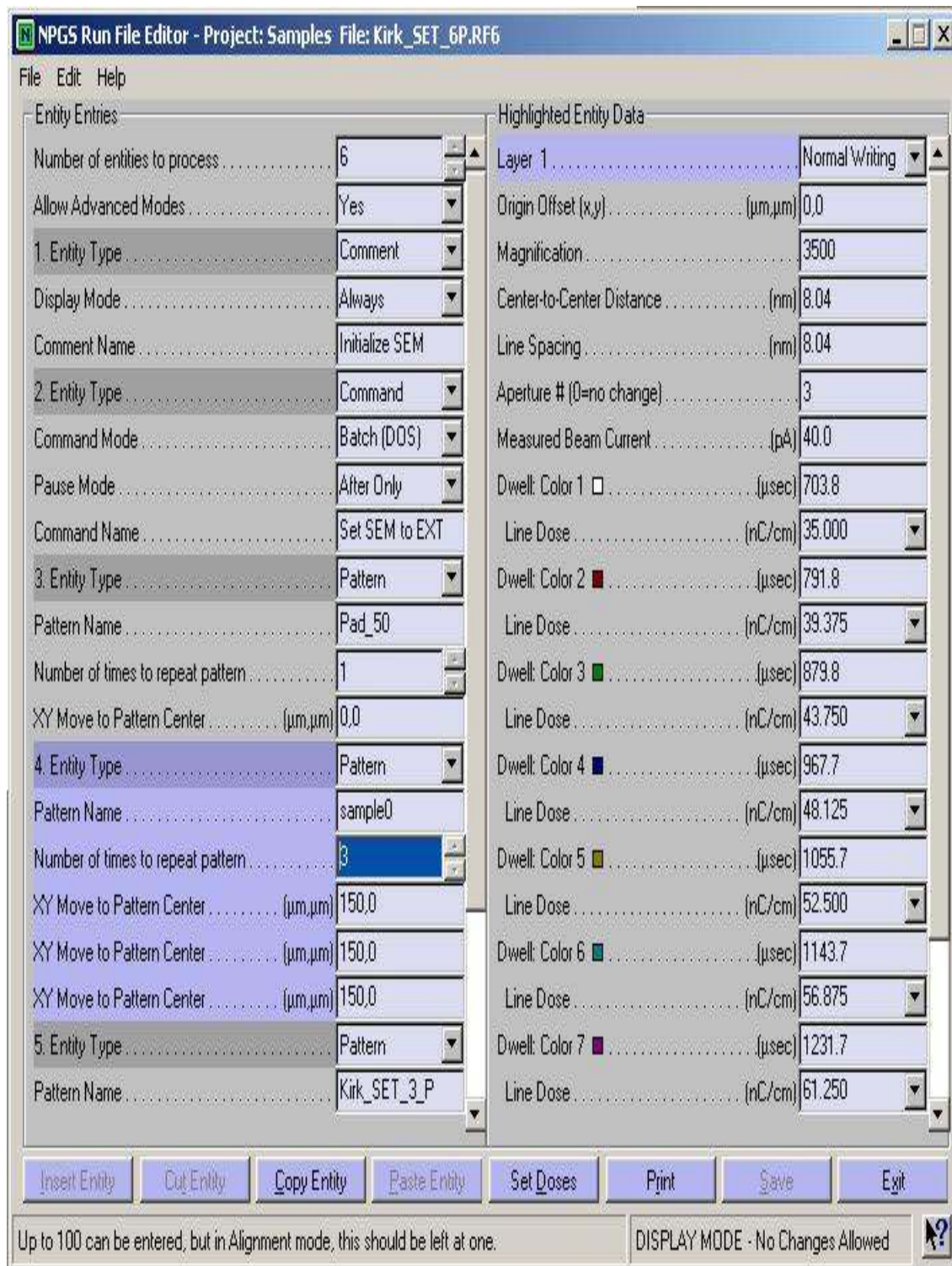
Pre-exposure bake 225°C for 120 seconds

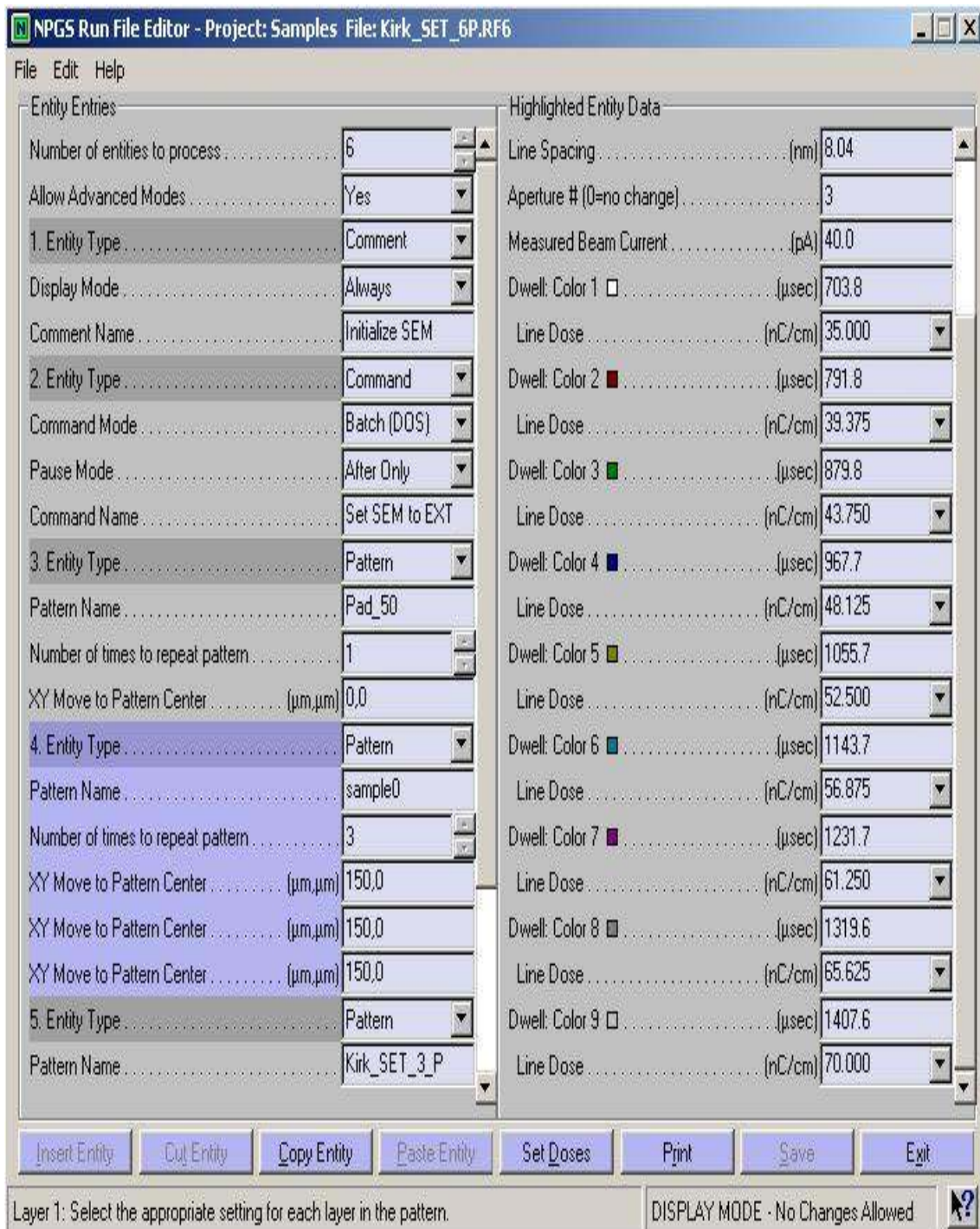
E-beam parameters















Development procedure

Post exposure bake at 225°C for 120 seconds.

300 MIF dip for 120 seconds

1:9 300 MIF and DI water rinse for 10 seconds

DI water dip for 10 seconds

Blow dry with Nitrogen

First HSQ and Al wafer

Wafer specifications

1cm x 1cm piece from a poly crystalline silicon wafer, p-type doping

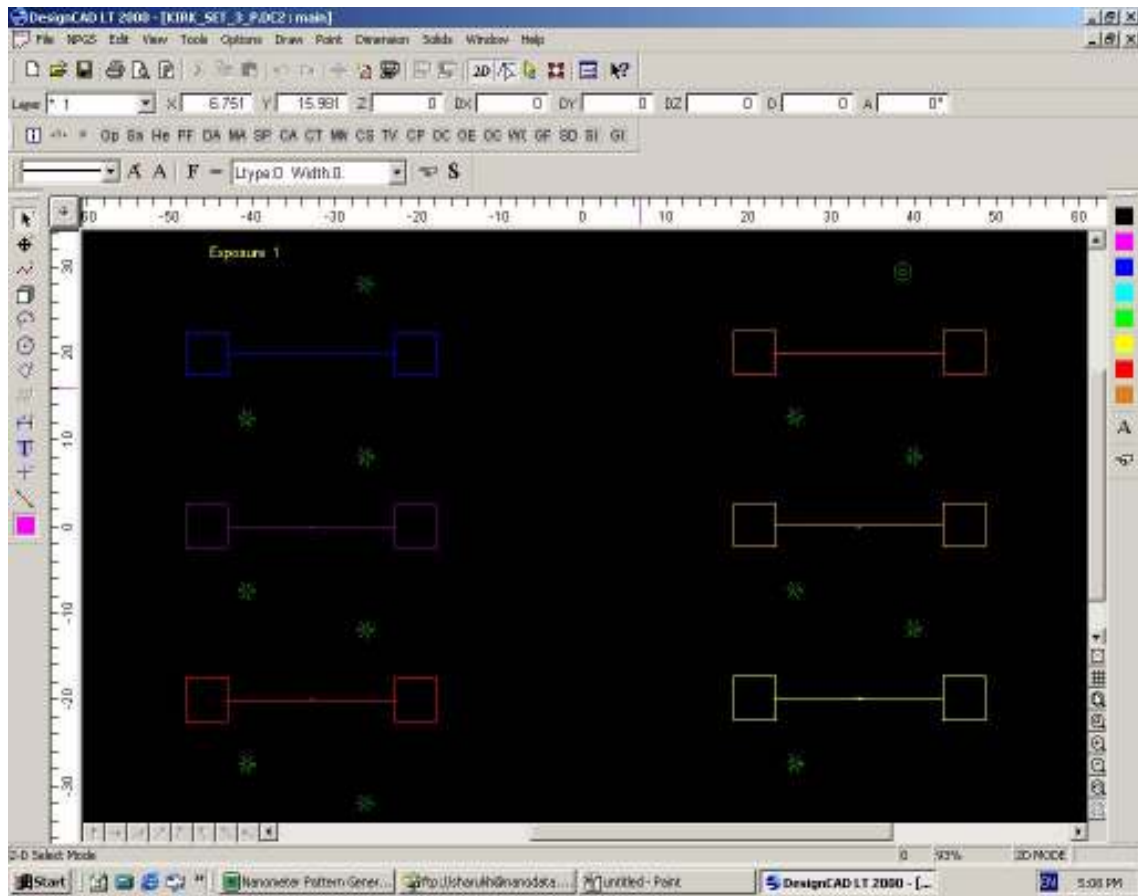
62.3nm of Aluminum evaporated

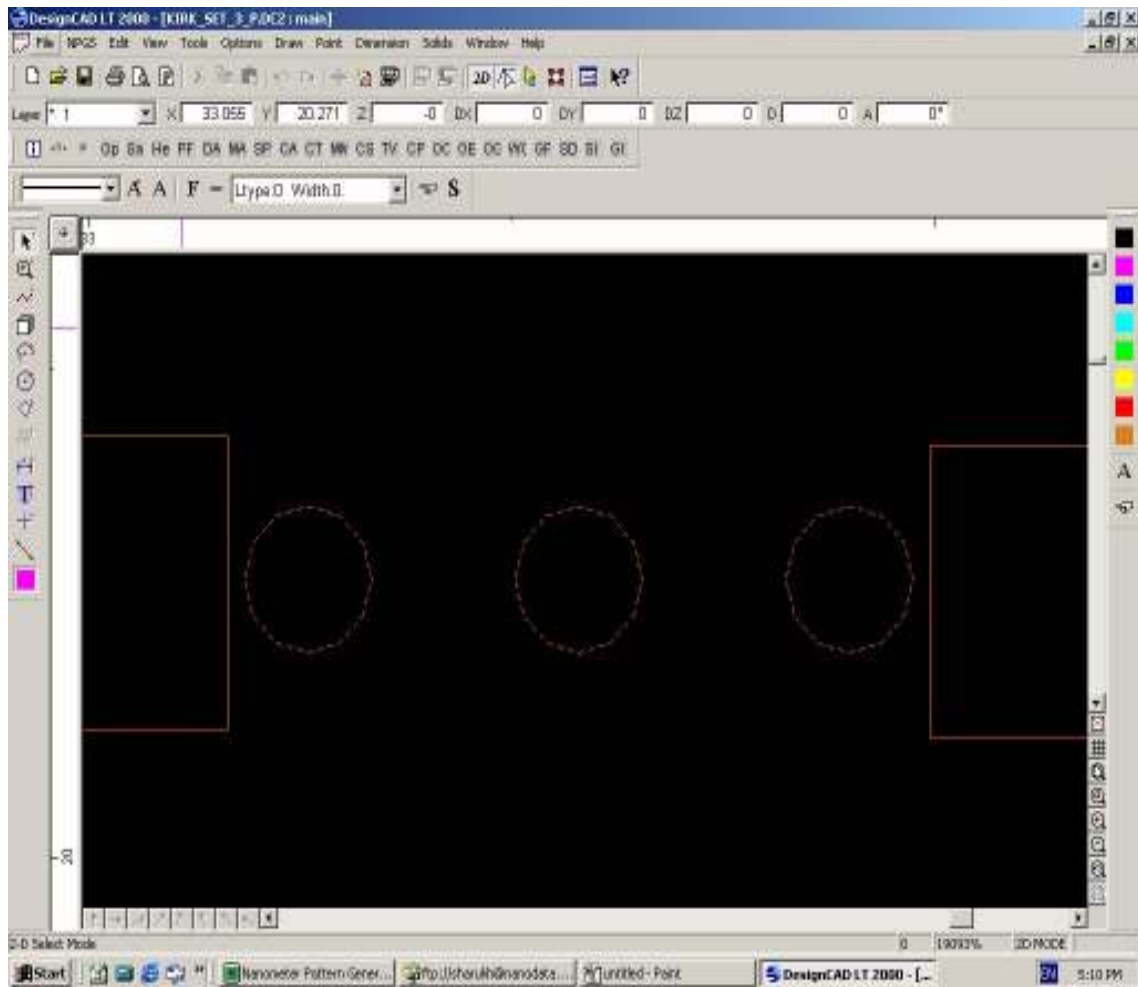
XR-1541 (containing 4% solids of HSQ) was used

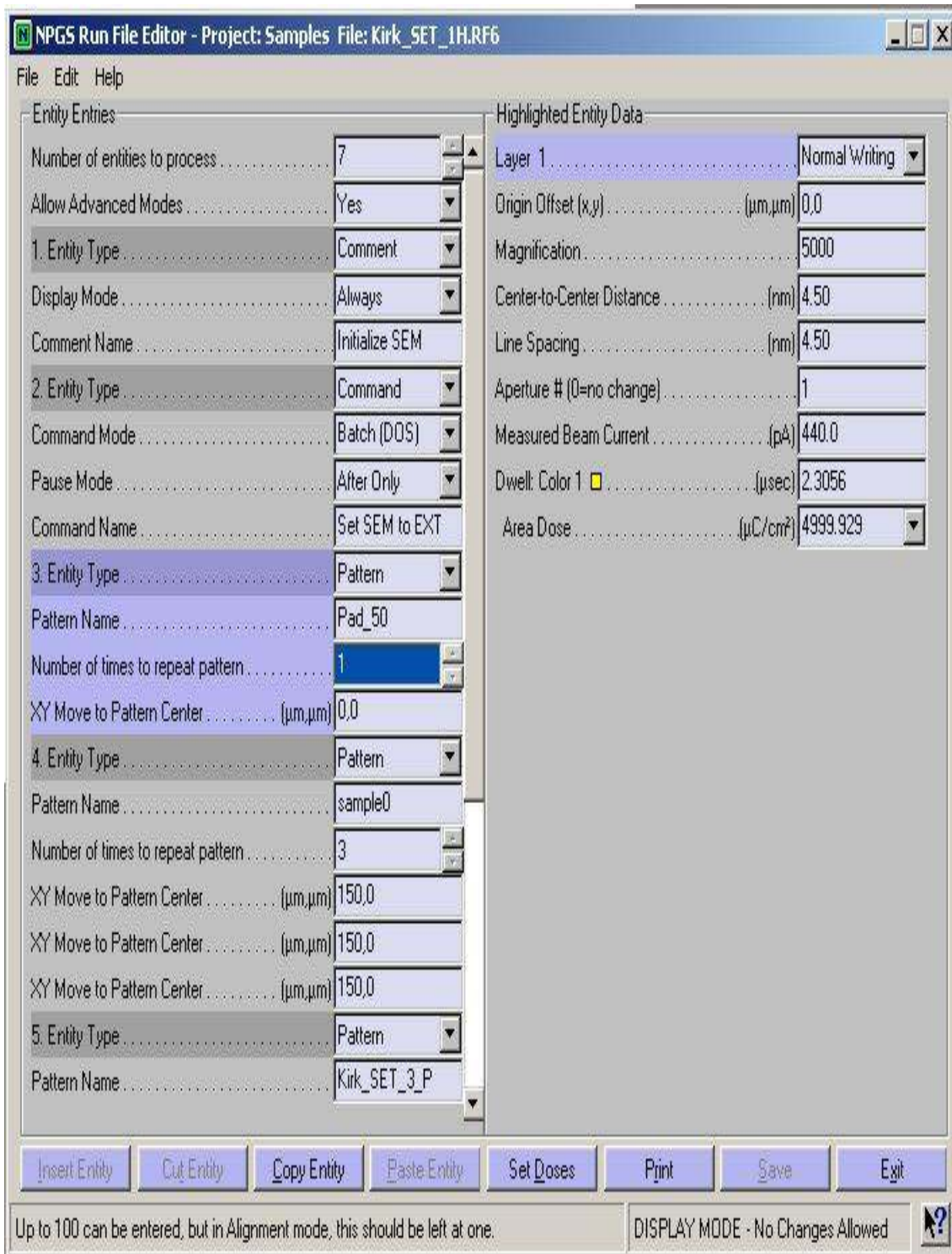
HSQ was spun on at 4000 rpm for 60 seconds

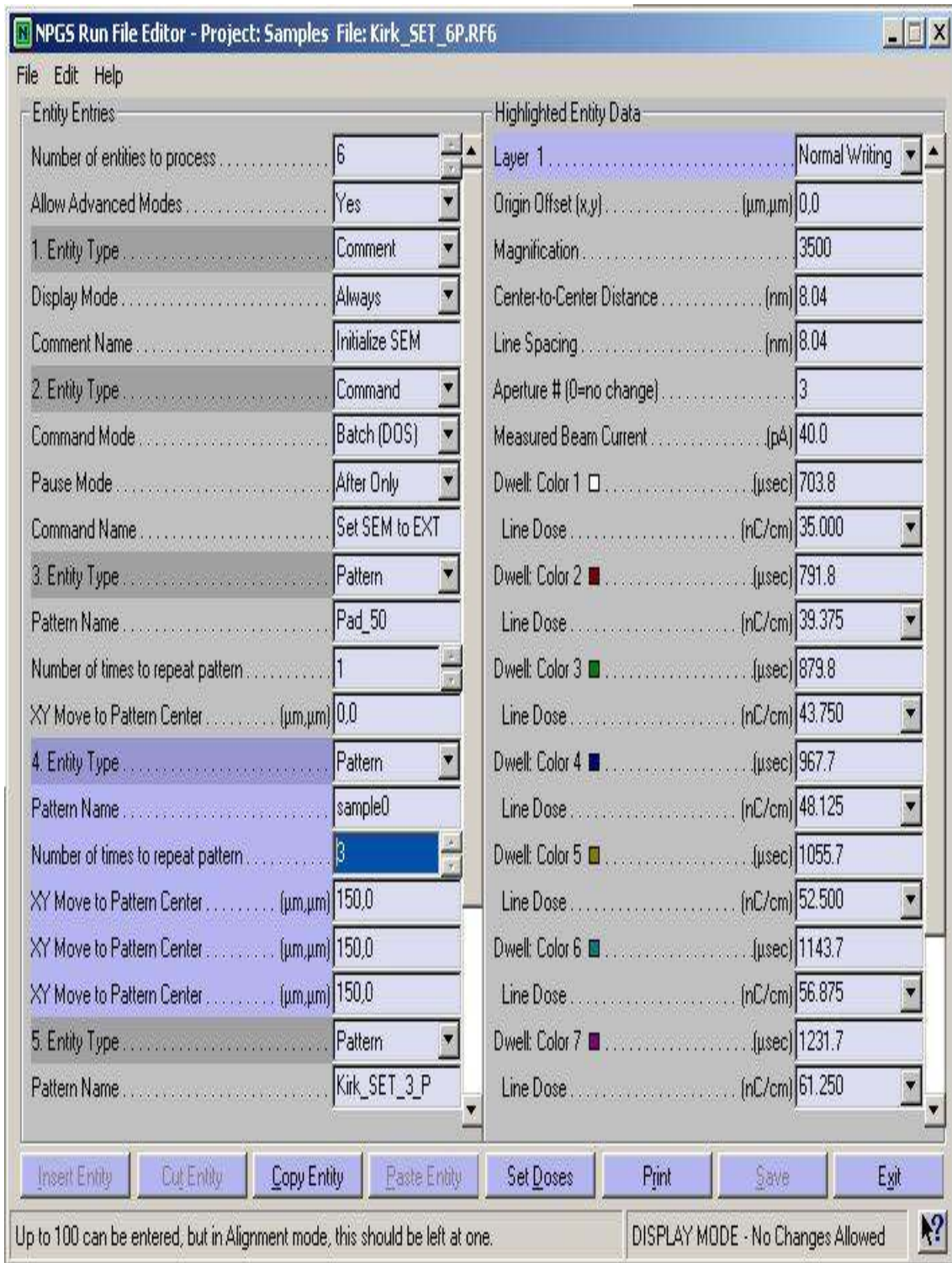
Pre-exposure bake 225°C for 120 seconds

E-beam parameters









NPGS Run File Editor - Project: Samples File: Kirk_SET_6P.RF6

File Edit Help

Entity Entries

Number of entities to process	6
Allow Advanced Modes	Yes
1. Entity Type	Comment
Display Mode	Always
Comment Name	Initialize SEM
2. Entity Type	Command
Command Mode	Batch (DOS)
Pause Mode	After Only
Command Name	Set SEM to EXT
3. Entity Type	Pattern
Pattern Name	Pad_50
Number of times to repeat pattern	1
XY Move to Pattern Center (μm,μm)	0,0
4. Entity Type	Pattern
Pattern Name	sample0
Number of times to repeat pattern	3
XY Move to Pattern Center (μm,μm)	150,0
XY Move to Pattern Center (μm,μm)	150,0
XY Move to Pattern Center (μm,μm)	150,0
5. Entity Type	Pattern
Pattern Name	Kirk_SET_3_P

Highlighted Entity Data

Line Spacing (nm)	8.04
Aperture # (0=no change)	3
Measured Beam Current (pA)	40.0
Dwell: Color 1 (μsec)	703.8
Line Dose (nC/cm)	35.000
Dwell: Color 2 (μsec)	791.8
Line Dose (nC/cm)	39.375
Dwell: Color 3 (μsec)	879.8
Line Dose (nC/cm)	43.750
Dwell: Color 4 (μsec)	967.7
Line Dose (nC/cm)	48.125
Dwell: Color 5 (μsec)	1055.7
Line Dose (nC/cm)	52.500
Dwell: Color 6 (μsec)	1143.7
Line Dose (nC/cm)	56.875
Dwell: Color 7 (μsec)	1231.7
Line Dose (nC/cm)	61.250
Dwell: Color 8 (μsec)	1319.6
Line Dose (nC/cm)	65.625
Dwell: Color 9 (μsec)	1407.6
Line Dose (nC/cm)	70.000

Insert Entity Cut Entity Copy Entity Paste Entity Set Doses Print Save Exit

Layer 1: Select the appropriate setting for each layer in the pattern. DISPLAY MODE - No Changes Allowed





Development procedure

Post exposure bake at 225°C for 120 seconds.

300 MIF dip for 120 seconds

1:9 300 MIF and DI water rinse for 10 seconds

DI water dip for 10 seconds

Blow dry with Nitrogen

Unwanted Al was removed using a aluminum etchant dip

Third HSQ wafer

Wafer specifications

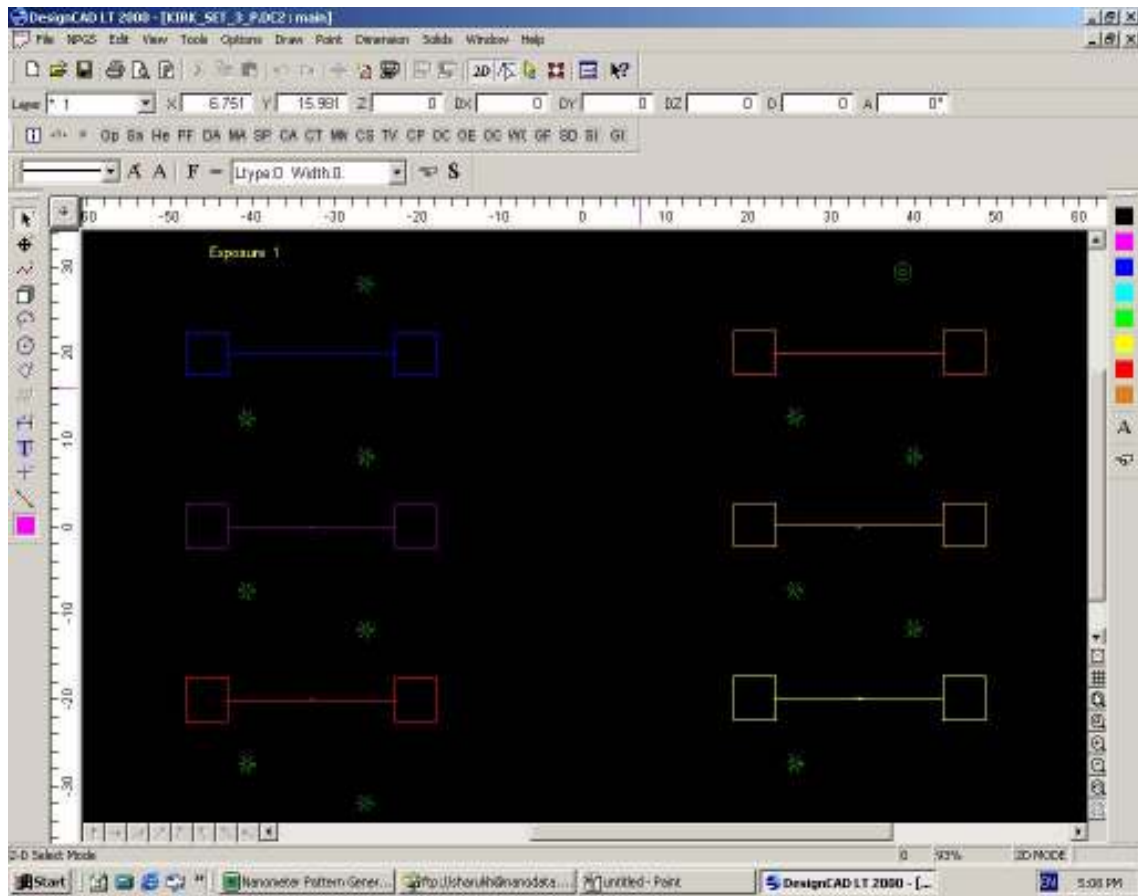
1cm x 1cm piece from a poly crystalline silicon wafer, p-type doping

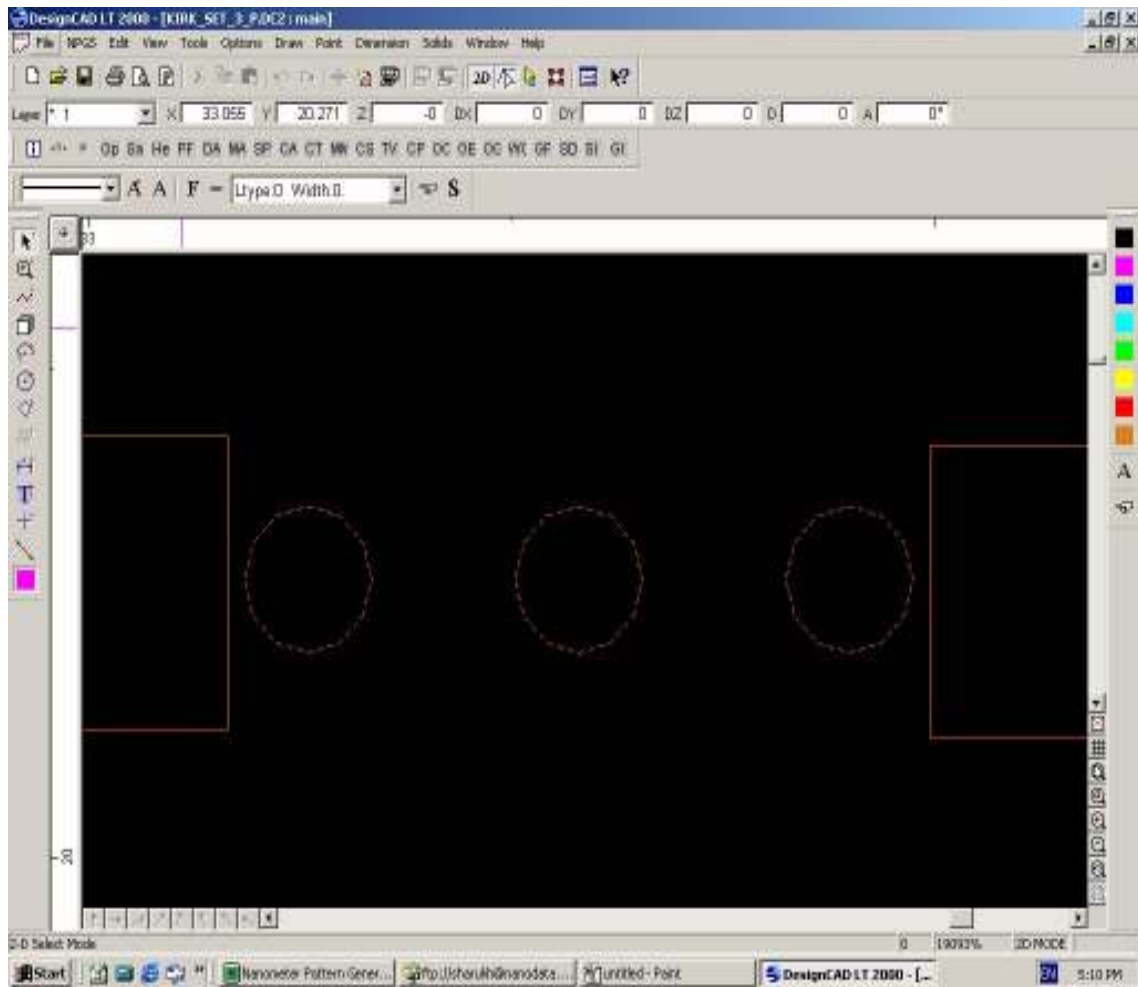
XR-1541 (containing 4% solids of HSQ) was used

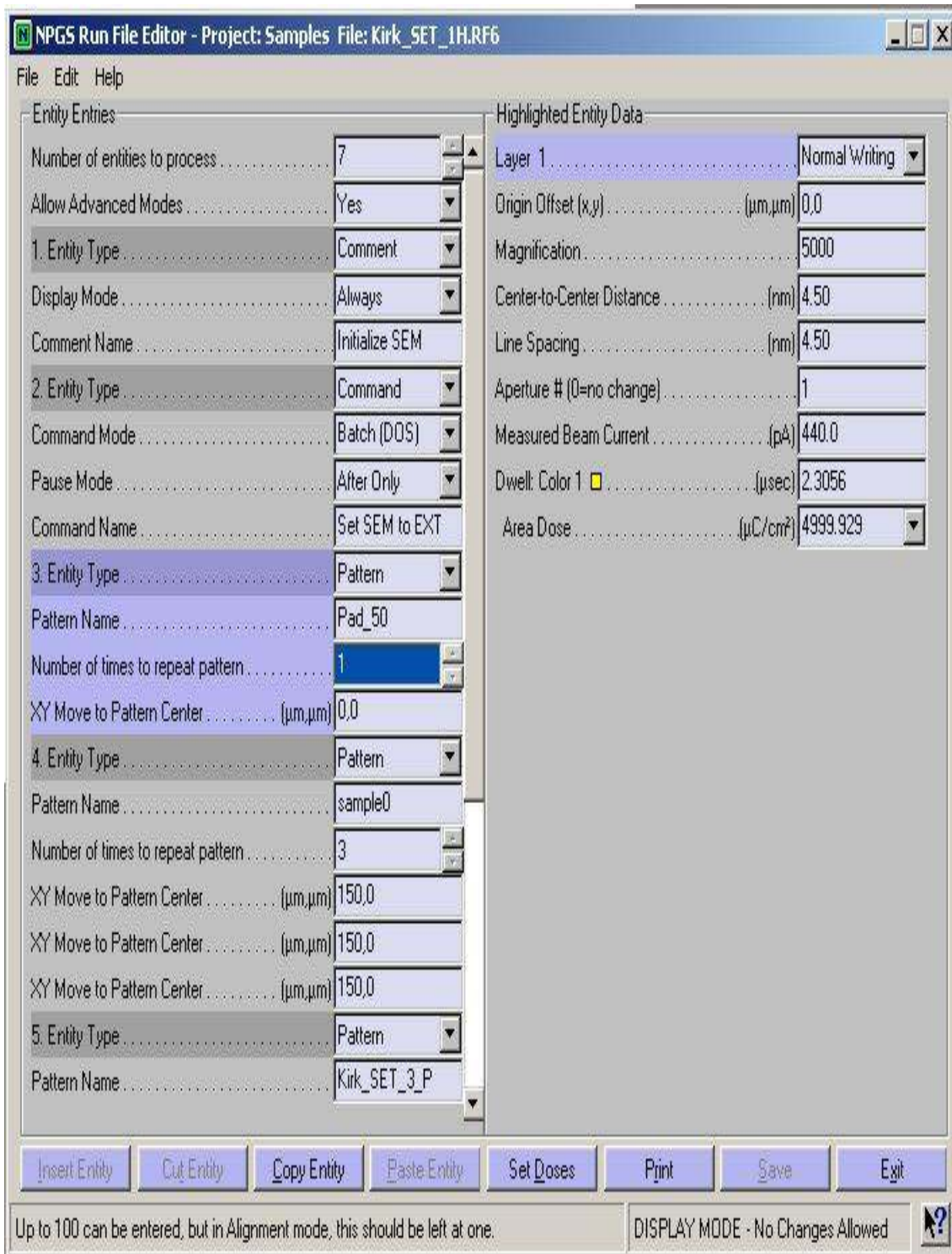
HSQ was spun on at 4000 rpm for 60 seconds

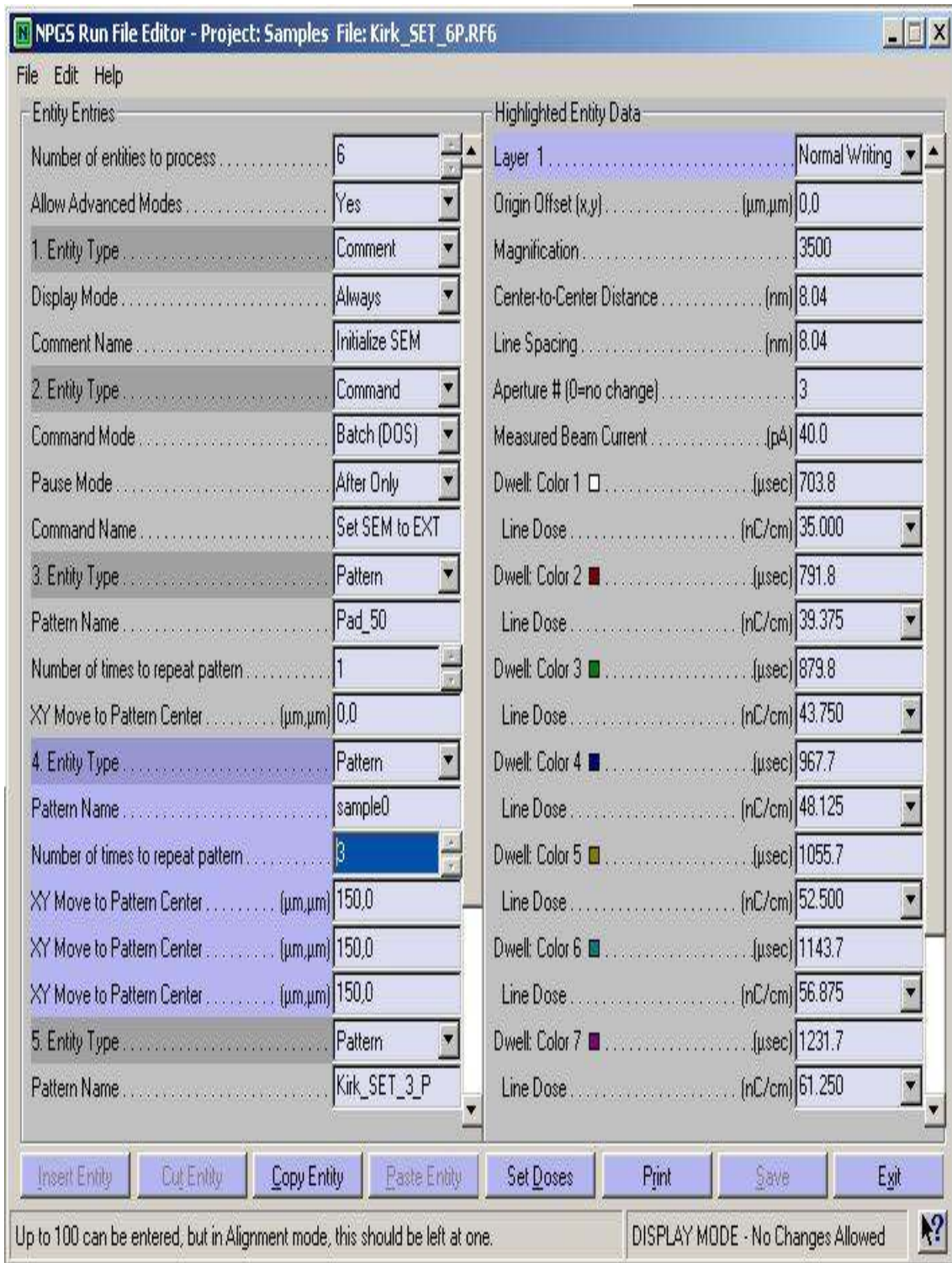
Pre-exposure bake 225°C for 120 seconds

E-beam parameters









NPGS Run File Editor - Project: Samples File: Kirk_SET_6P.RF6

File Edit Help

Entity Entries

Number of entities to process	6
Allow Advanced Modes	Yes
1. Entity Type	Comment
Display Mode	Always
Comment Name	Initialize SEM
2. Entity Type	Command
Command Mode	Batch (DOS)
Pause Mode	After Only
Command Name	Set SEM to EXT
3. Entity Type	Pattern
Pattern Name	Pad_50
Number of times to repeat pattern	1
XY Move to Pattern Center (μm,μm)	0,0
4. Entity Type	Pattern
Pattern Name	sample0
Number of times to repeat pattern	3
XY Move to Pattern Center (μm,μm)	150,0
XY Move to Pattern Center (μm,μm)	150,0
XY Move to Pattern Center (μm,μm)	150,0
5. Entity Type	Pattern
Pattern Name	Kirk_SET_3_P

Highlighted Entity Data

Line Spacing (nm)	8.04
Aperture # (0=no change)	3
Measured Beam Current (pA)	40.0
Dwell: Color 1 (μsec)	703.8
Line Dose (nC/cm)	35.000
Dwell: Color 2 (μsec)	791.8
Line Dose (nC/cm)	39.375
Dwell: Color 3 (μsec)	879.8
Line Dose (nC/cm)	43.750
Dwell: Color 4 (μsec)	967.7
Line Dose (nC/cm)	48.125
Dwell: Color 5 (μsec)	1055.7
Line Dose (nC/cm)	52.500
Dwell: Color 6 (μsec)	1143.7
Line Dose (nC/cm)	56.875
Dwell: Color 7 (μsec)	1231.7
Line Dose (nC/cm)	61.250
Dwell: Color 8 (μsec)	1319.6
Line Dose (nC/cm)	65.625
Dwell: Color 9 (μsec)	1407.6
Line Dose (nC/cm)	70.000

Insert Entity Cut Entity Copy Entity Paste Entity Set Doses Print Save Exit

Layer 1: Select the appropriate setting for each layer in the pattern. DISPLAY MODE - No Changes Allowed

NPGS Run File Editor - Project: Samples File: Kirk_SET_1H.RF6

File Edit Help

Entity Entries

3. Entity Type	Pattern
Pattern Name	Pad_50
Number of times to repeat pattern	1
XY Move to Pattern Center (μm,μm)	0,0
4. Entity Type	Pattern
Pattern Name	sample0
Number of times to repeat pattern	3
XY Move to Pattern Center (μm,μm)	150,0
XY Move to Pattern Center (μm,μm)	150,0
XY Move to Pattern Center (μm,μm)	150,0
5. Entity Type	Pattern
Pattern Name	Kirk_SET_3_P
Number of times to repeat pattern	2
XY Move to Pattern Center (μm,μm)	150,0
XY Move to Pattern Center (μm,μm)	150,0
6. Entity Type	Pattern
Pattern Name	P_Young_50um
Number of times to repeat pattern	1
XY Move to Pattern Center (μm,μm)	150,0
7. Entity Type	MoveOnly
XY Move to Writing Field Center (μm,μm)	-900,-500

Highlighted Entity Data

Layer 1	Normal Writing
Origin Offset (x,y) (μm,μm)	0,0
Magnification	3000
Center-to-Center Distance (nm)	7.51
Line Spacing (nm)	7.51
Aperture # (0=no change)	3
Measured Beam Current (pA)	40.0
Dwell: Color 1 (μsec)	750.7
Line Dose (nC/cm)	40.000
Dwell: Color 2 (μsec)	938.4
Line Dose (nC/cm)	50.000
Dwell: Color 3 (μsec)	1126.1
Line Dose (nC/cm)	60.000
Dwell: Color 4 (μsec)	1313.8
Line Dose (nC/cm)	70.000
Dwell: Color 5 (μsec)	1501.5
Line Dose (nC/cm)	80.000
Dwell: Color 6 (μsec)	1689.1
Line Dose (nC/cm)	90.000
Layer 2	Pause First
Origin Offset (x,y) (μm,μm)	0,0

Insert Entity
Cut Entity
Copy Entity
Paste Entity
Set Doses
Print
Save
Exit

Double click on the pattern name to bring up a list of available files. DISPLAY MODE - No Changes Allowed



Development procedure

Post exposure bake at 225°C for 120 seconds.

300 MIF dip for 120 seconds

1:9 300 MIF and DI water rinse for 10 seconds

DI water dip for 10 seconds

Blow dry with Nitrogen

Fourth HSQ wafer

Wafer specifications

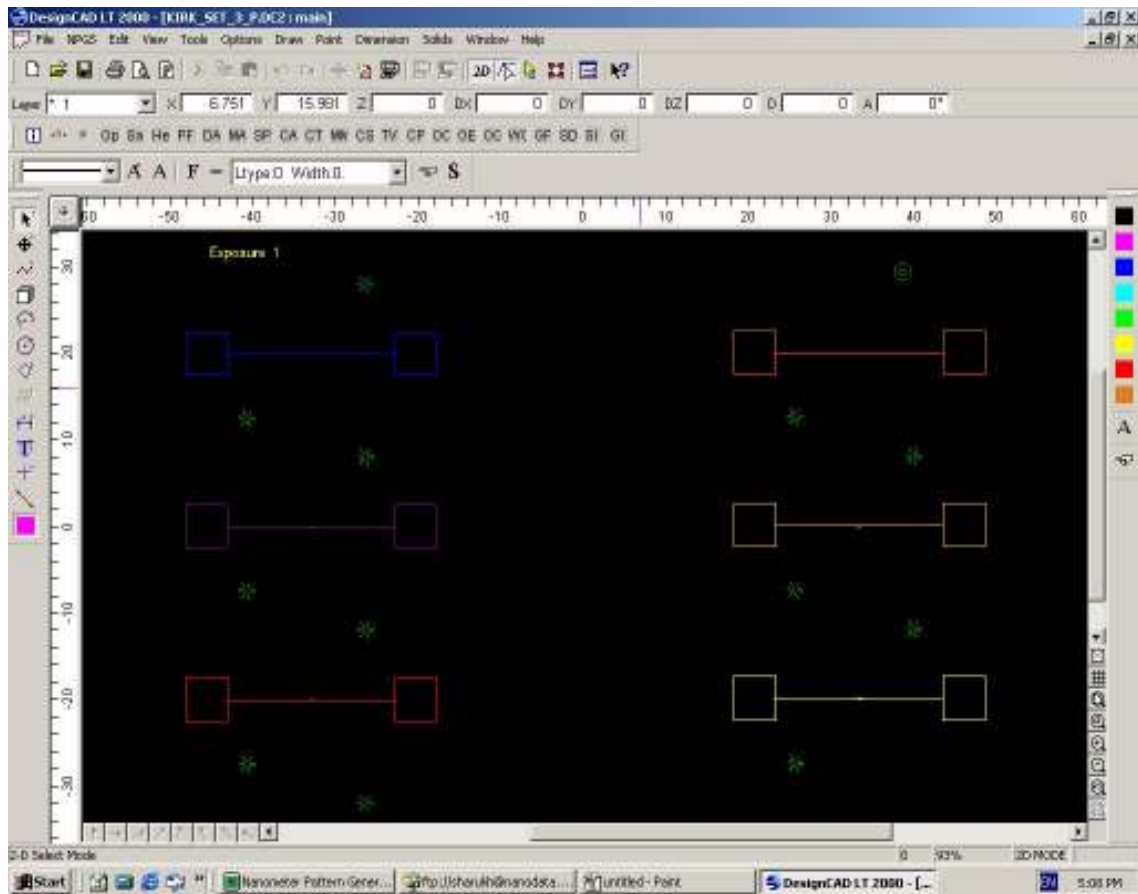
1cm x 1cm piece from a poly crystalline silicon wafer, p-type doping

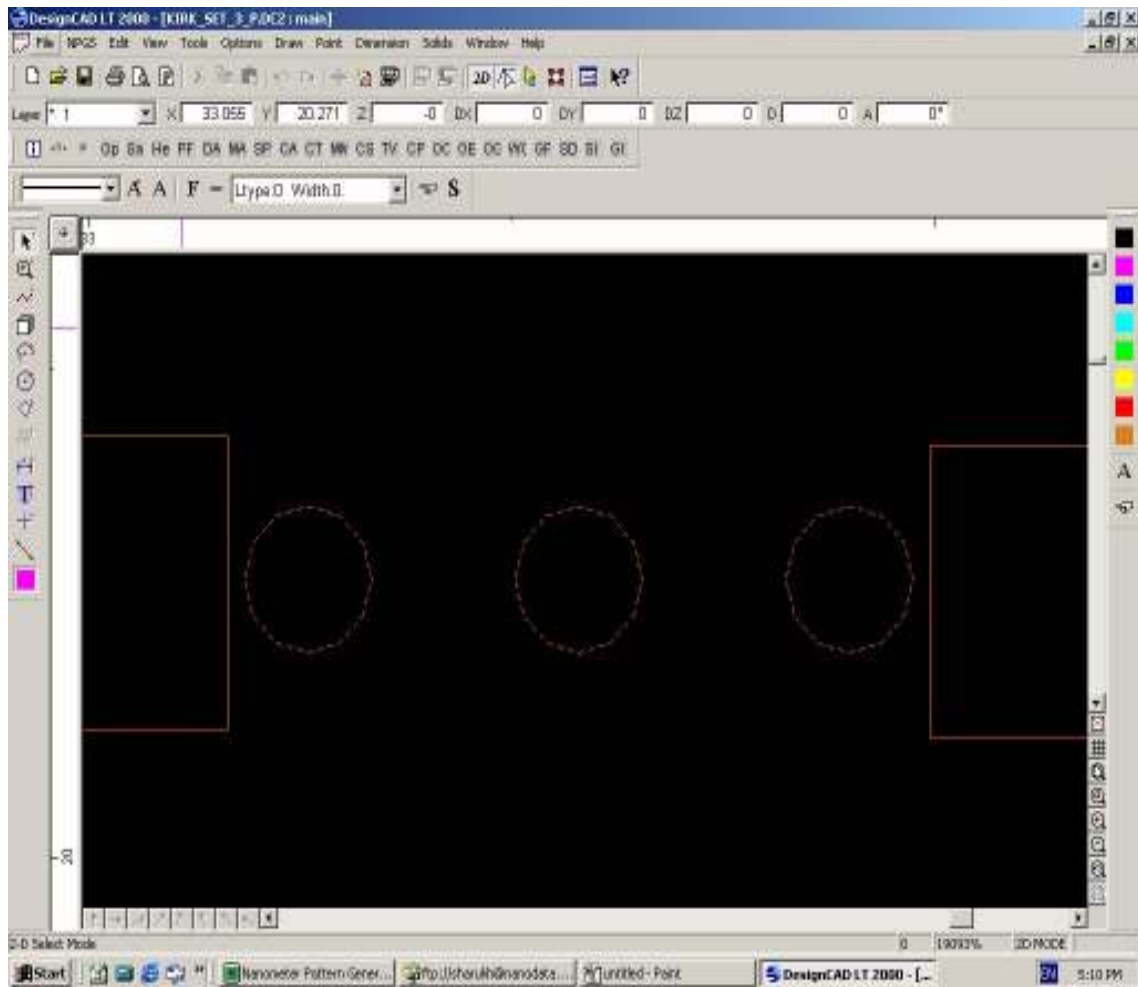
XR-1541 (containing 4% solids of HSQ) was used

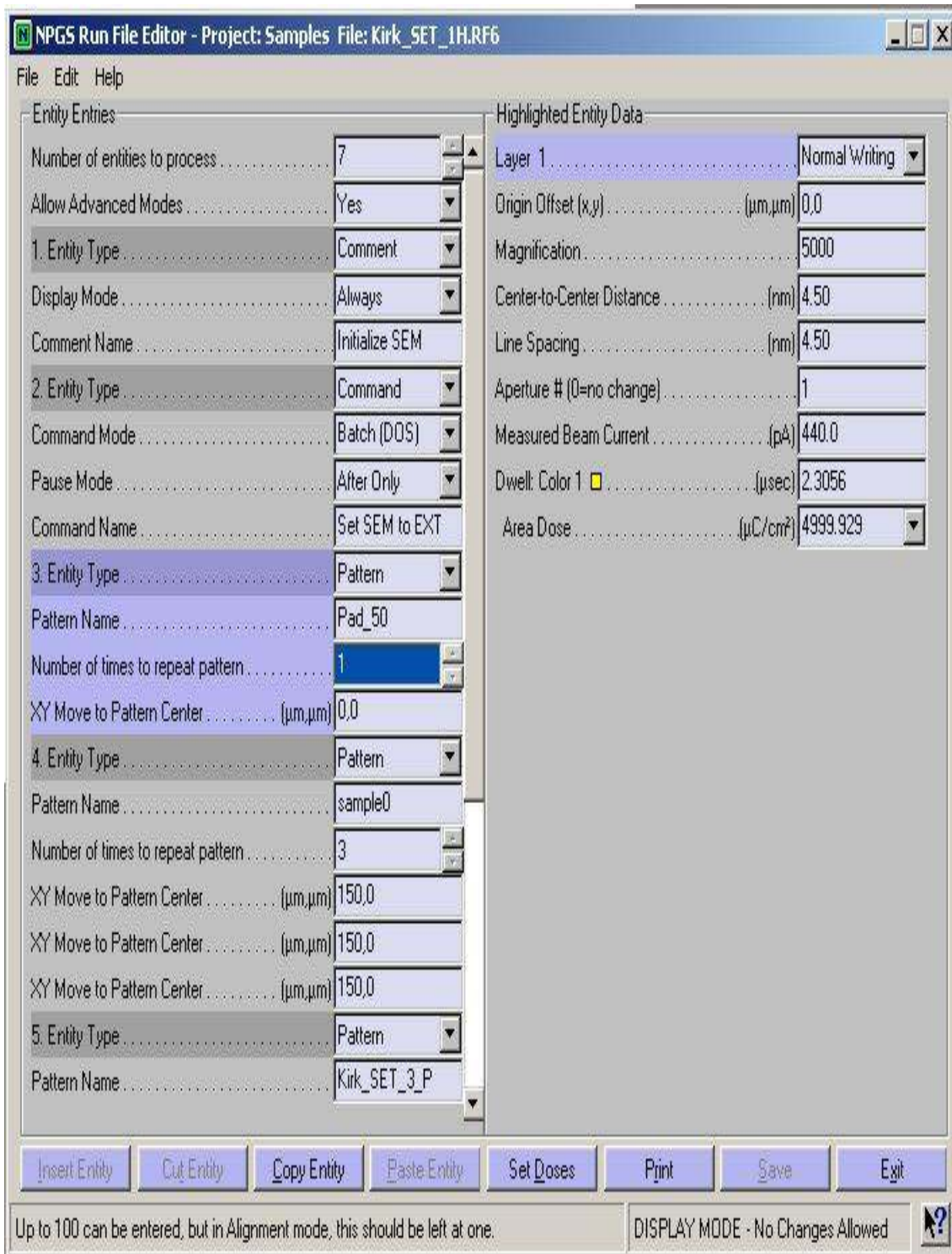
HSQ was spun on at 4000 rpm for 60 seconds

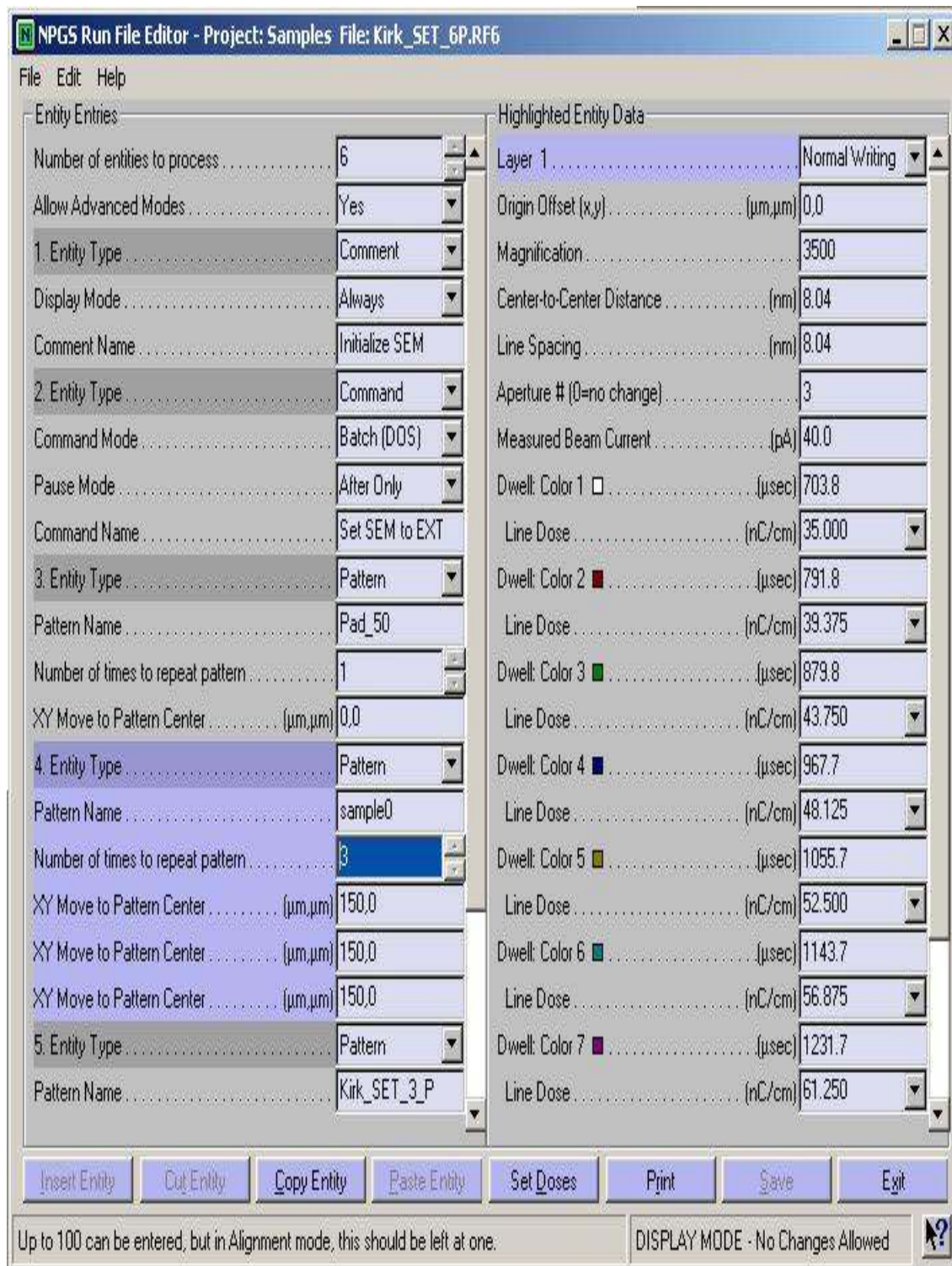
Pre-exposure bake 225°C for 120 seconds

E-beam parameters









NPGS Run File Editor - Project: Samples File: Kirk_SET_6P.RF6

File Edit Help

Entity Entries

Number of entities to process 6

Allow Advanced Modes Yes

1. Entity Type Comment

Display Mode Always

Comment Name Initialize SEM

2. Entity Type Command

Command Mode Batch (DOS)

Pause Mode After Only

Command Name Set SEM to EXT

3. Entity Type Pattern

Pattern Name Pad_50

Number of times to repeat pattern 1

XY Move to Pattern Center (μm,μm) 0,0

4. Entity Type Pattern

Pattern Name sample0

Number of times to repeat pattern 3

XY Move to Pattern Center (μm,μm) 150,0

XY Move to Pattern Center (μm,μm) 150,0

XY Move to Pattern Center (μm,μm) 150,0

5. Entity Type Pattern

Pattern Name Kirk_SET_3_P

Highlighted Entity Data

Line Spacing (nm) 8.04

Aperture # (0=no change) 3

Measured Beam Current (pA) 40.0

Dwell: Color 1 (μsec) 703.8

Line Dose (nC/cm) 35.000

Dwell: Color 2 (μsec) 791.8

Line Dose (nC/cm) 39.375

Dwell: Color 3 (μsec) 879.8

Line Dose (nC/cm) 43.750

Dwell: Color 4 (μsec) 967.7

Line Dose (nC/cm) 48.125

Dwell: Color 5 (μsec) 1055.7

Line Dose (nC/cm) 52.500

Dwell: Color 6 (μsec) 1143.7

Line Dose (nC/cm) 56.875

Dwell: Color 7 (μsec) 1231.7

Line Dose (nC/cm) 61.250

Dwell: Color 8 (μsec) 1319.6

Line Dose (nC/cm) 65.625

Dwell: Color 9 (μsec) 1407.6

Line Dose (nC/cm) 70.000

Insert Entity Cut Entity Copy Entity Paste Entity Set Doses Print Save Exit

Layer 1: Select the appropriate setting for each layer in the pattern. DISPLAY MODE - No Changes Allowed

NPGS Run File Editor - Project: Samples File: Kirk_SET_2H.RF6

File Edit Help

Entity Entries

Pause Mode	Alter Only
Command Name	Set SEM to EXT
3. Entity Type	Pattern
Pattern Name	Pad_50
Number of times to repeat pattern	1
XY Move to Pattern Center (μm,μm)	0,0
4. Entity Type	Pattern
Pattern Name	sample0
Number of times to repeat pattern	1
XY Move to Pattern Center (μm,μm)	150,0
5. Entity Type	Pattern
Pattern Name	Kirk_SET_3_P
Number of times to repeat pattern	2
XY Move to Pattern Center (μm,μm)	150,0
XY Move to Pattern Center (μm,μm)	150,0
6. Entity Type	Pattern
Pattern Name	P_Young_50um
Number of times to repeat pattern	1
XY Move to Pattern Center (μm,μm)	150,0
7. Entity Type	MoveOnly
XY Move to Writing Field Center (μm,μm)	-900,-500

Highlighted Entity Data

Layer 1	Normal Writing
Origin Offset (x,y) (μm,μm)	0,0
Magnification	3000
Center-to-Center Distance (nm)	7.51
Line Spacing (nm)	7.51
Aperture # (0=no change)	3
Measured Beam Current (pA)	40.0
Dwell: Color 1 (μsec)	93.84
Line Dose (nC/cm)	5.000
Dwell: Color 2 (μsec)	142.25
Line Dose (nC/cm)	7.579
Dwell: Color 3 (μsec)	215.59
Line Dose (nC/cm)	11.487
Dwell: Color 4 (μsec)	326.78
Line Dose (nC/cm)	17.411
Dwell: Color 5 (μsec)	495.30
Line Dose (nC/cm)	26.390
Dwell: Color 6 (μsec)	750.7
Line Dose (nC/cm)	40.000
Layer 2	Normal Writing
Origin Offset (x,y) (μm,μm)	0,0

Insert Entity Cut Entity Copy Entity Paste Entity Set Doses Print Save Exit

This is the XY move that will be performed before the pattern is written. DISPLAY MODE - No Changes Allowed



Development procedure

Post exposure bake at 225°C for 120 seconds.

300 MIF dip for 120 seconds

1:9 300 MIF and DI water rinse for 10 seconds

DI water dip for 10 seconds

Blow dry with Nitrogen

Fifth HSQ wafer

Wafer specifications

1cm x 1cm piece from a SOI wafer with 55nm single crystal silicon, 140nm silicon

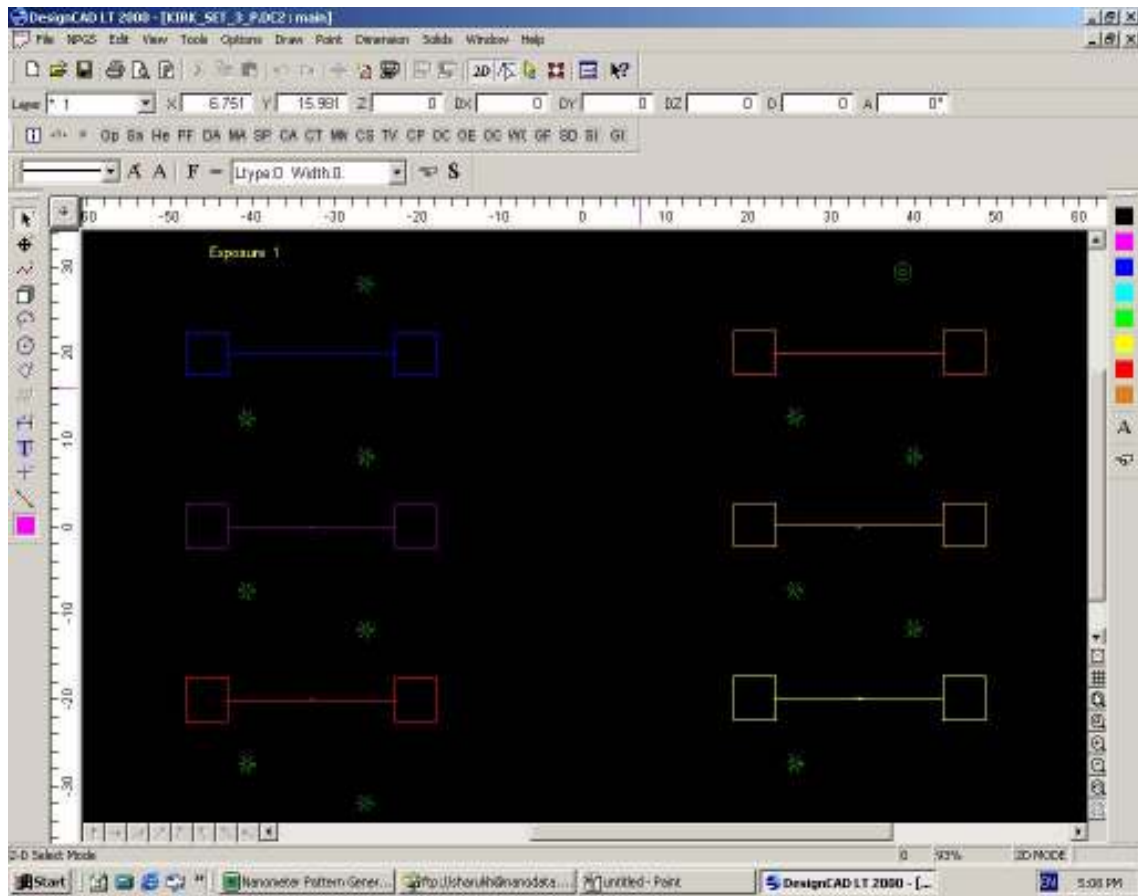
dioxide wafer, 2 microns of poly-crystalline silicon

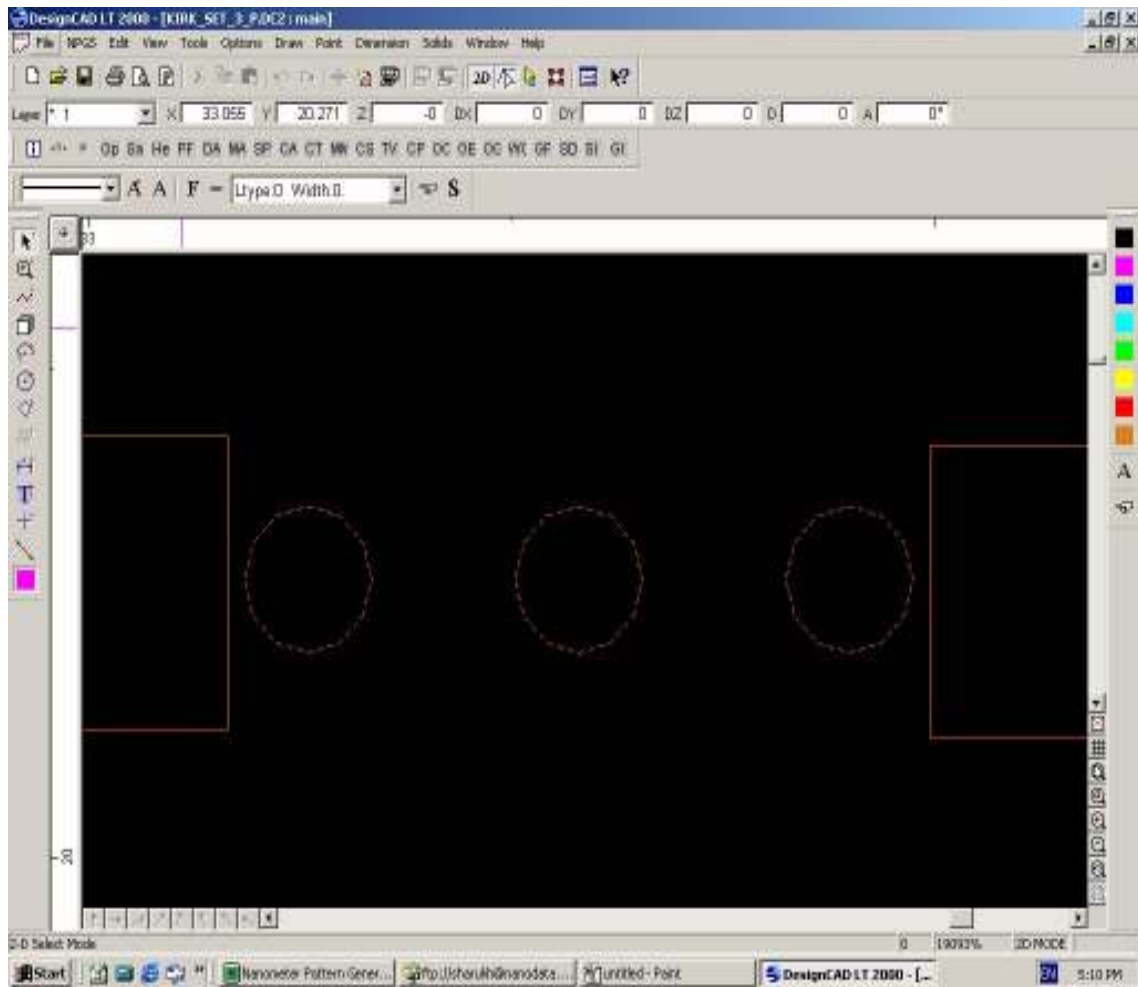
XR-1541 (containing 4% solids of HSQ) was used

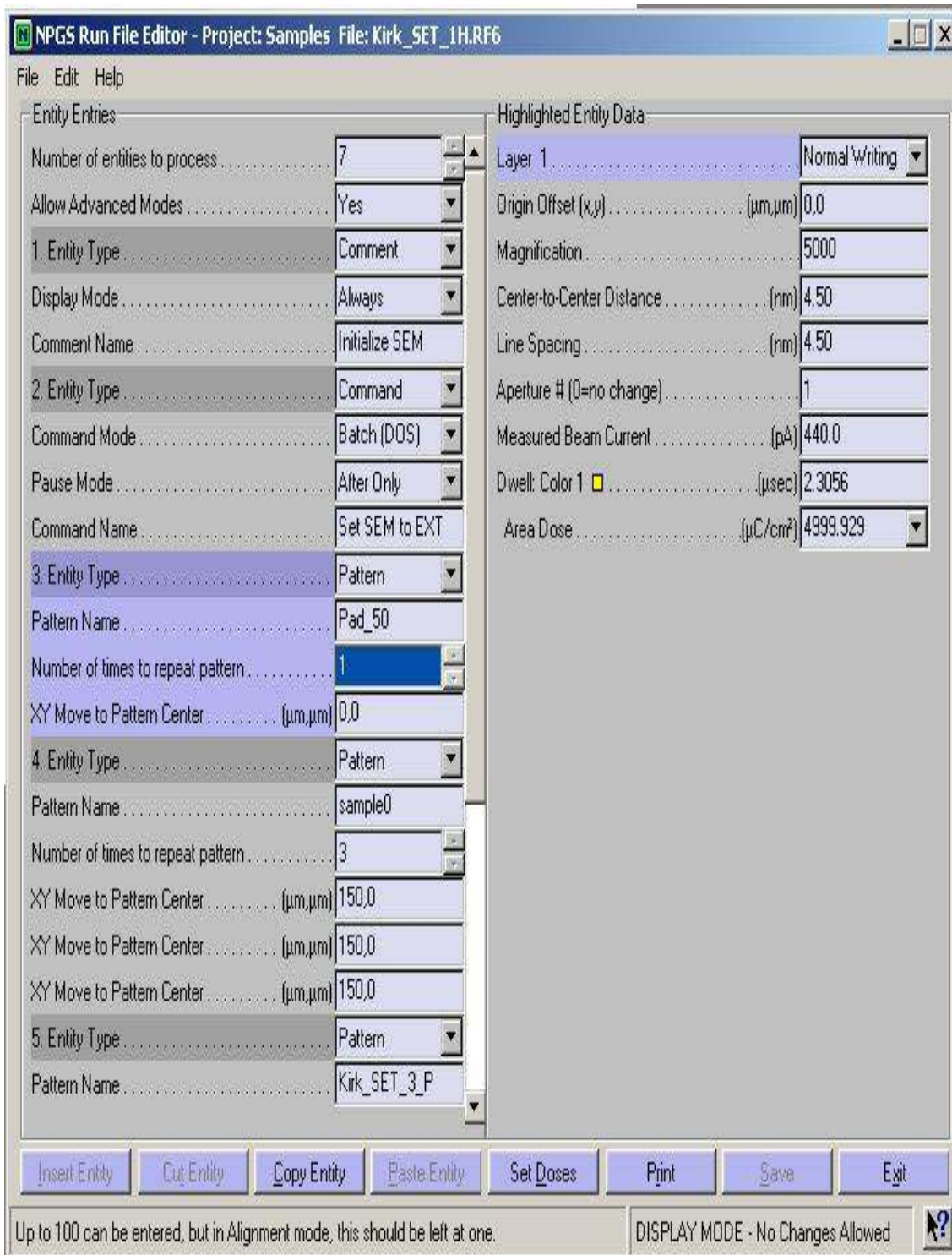
HSQ was spun on at 4000 rpm for 60 seconds

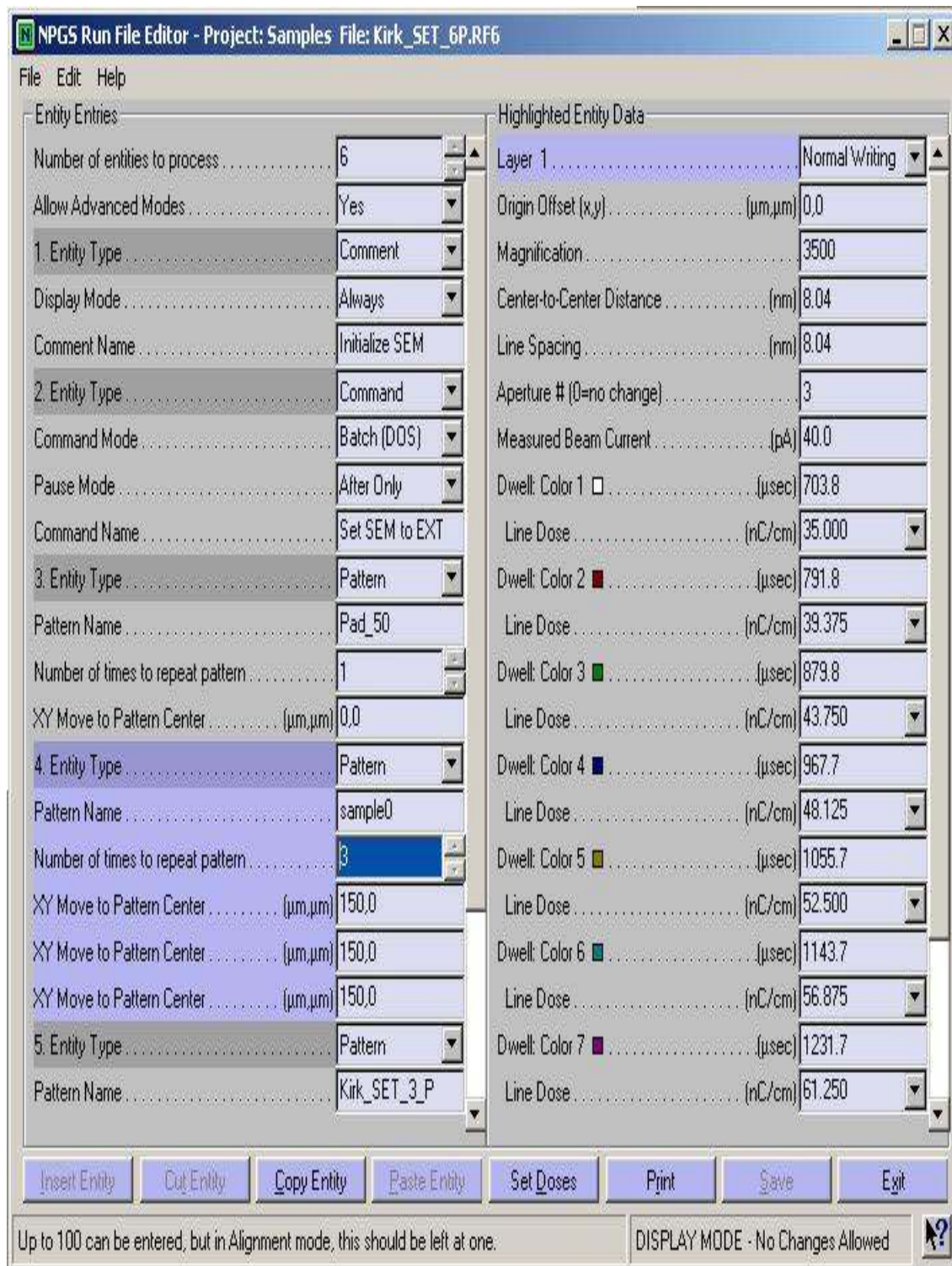
Pre-exposure bake 225°C for 120 seconds

E-beam parameters









NPGS Run File Editor - Project: Samples File: Kirk_SET_6P.RF6

File Edit Help

Entity Entries

Number of entities to process	6
Allow Advanced Modes	Yes
1. Entity Type	Comment
Display Mode	Always
Comment Name	Initialize SEM
2. Entity Type	Command
Command Mode	Batch (DOS)
Pause Mode	After Only
Command Name	Set SEM to EXT
3. Entity Type	Pattern
Pattern Name	Pad_50
Number of times to repeat pattern	1
XY Move to Pattern Center (μm,μm)	0,0
4. Entity Type	Pattern
Pattern Name	sample0
Number of times to repeat pattern	3
XY Move to Pattern Center (μm,μm)	150,0
XY Move to Pattern Center (μm,μm)	150,0
XY Move to Pattern Center (μm,μm)	150,0
5. Entity Type	Pattern
Pattern Name	Kirk_SET_3_P

Highlighted Entity Data

Line Spacing (nm)	8.04
Aperture # (0=no change)	3
Measured Beam Current (pA)	40.0
Dwell: Color 1 (μsec)	703.8
Line Dose (nC/cm)	35.000
Dwell: Color 2 (μsec)	791.8
Line Dose (nC/cm)	39.375
Dwell: Color 3 (μsec)	879.8
Line Dose (nC/cm)	43.750
Dwell: Color 4 (μsec)	967.7
Line Dose (nC/cm)	48.125
Dwell: Color 5 (μsec)	1055.7
Line Dose (nC/cm)	52.500
Dwell: Color 6 (μsec)	1143.7
Line Dose (nC/cm)	56.875
Dwell: Color 7 (μsec)	1231.7
Line Dose (nC/cm)	61.250
Dwell: Color 8 (μsec)	1319.6
Line Dose (nC/cm)	65.625
Dwell: Color 9 (μsec)	1407.6
Line Dose (nC/cm)	70.000

Insert Entity Cut Entity Copy Entity Paste Entity Set Doses Print Save Exit

Layer 1: Select the appropriate setting for each layer in the pattern. DISPLAY MODE - No Changes Allowed

NPGS Run File Editor - Project: Samples File: Kirk_SET_2H.RF6

File Edit Help

Entity Entries

Pause Mode	Alter Only
Command Name	Set SEM to EXT
3. Entity Type	Pattern
Pattern Name	Pad_50
Number of times to repeat pattern	1
XY Move to Pattern Center (μm,μm)	0,0
4. Entity Type	Pattern
Pattern Name	sample0
Number of times to repeat pattern	1
XY Move to Pattern Center (μm,μm)	150,0
5. Entity Type	Pattern
Pattern Name	Kirk_SET_3_P
Number of times to repeat pattern	2
XY Move to Pattern Center (μm,μm)	150,0
XY Move to Pattern Center (μm,μm)	150,0
6. Entity Type	Pattern
Pattern Name	P_Young_50um
Number of times to repeat pattern	1
XY Move to Pattern Center (μm,μm)	150,0
7. Entity Type	MoveOnly
XY Move to Writing Field Center (μm,μm)	-900,-500

Highlighted Entity Data

Layer 1	Normal Writing
Origin Offset (x,y) (μm,μm)	0,0
Magnification	3000
Center-to-Center Distance (nm)	7.51
Line Spacing (nm)	7.51
Aperture # (0=no change)	3
Measured Beam Current (pA)	40.0
Dwell: Color 1 (μsec)	93.84
Line Dose (nC/cm)	5.000
Dwell: Color 2 (μsec)	142.25
Line Dose (nC/cm)	7.579
Dwell: Color 3 (μsec)	215.59
Line Dose (nC/cm)	11.487
Dwell: Color 4 (μsec)	326.78
Line Dose (nC/cm)	17.411
Dwell: Color 5 (μsec)	495.30
Line Dose (nC/cm)	26.390
Dwell: Color 6 (μsec)	750.7
Line Dose (nC/cm)	40.000
Layer 2	Normal Writing
Origin Offset (x,y) (μm,μm)	0,0

Insert Entity Cut Entity Copy Entity Paste Entity Set Doses Print Save Exit

This is the XY move that will be performed before the pattern is written. DISPLAY MODE - No Changes Allowed



Development procedure

Post exposure bake at 225°C for 120 seconds.

300 MIF dip for 70 seconds

1:9 300 MIF and DI water rinse for 10 seconds

DI water dip for 10 seconds

Blow dry with Nitrogen

Baking conditions

Sample was baked in an inert atmosphere using the Blue M oven

Start at 25°C

Ramp from 25°C to 125°C in 15 minutes

Ramp from 125°C to 400°C in 15 minutes

Steady at 400°C for 30 minutes

From 400°C to 25°C at its own pace usually takes 2 hours 15 minutes

Sixth HSQ wafer

Wafer specifications

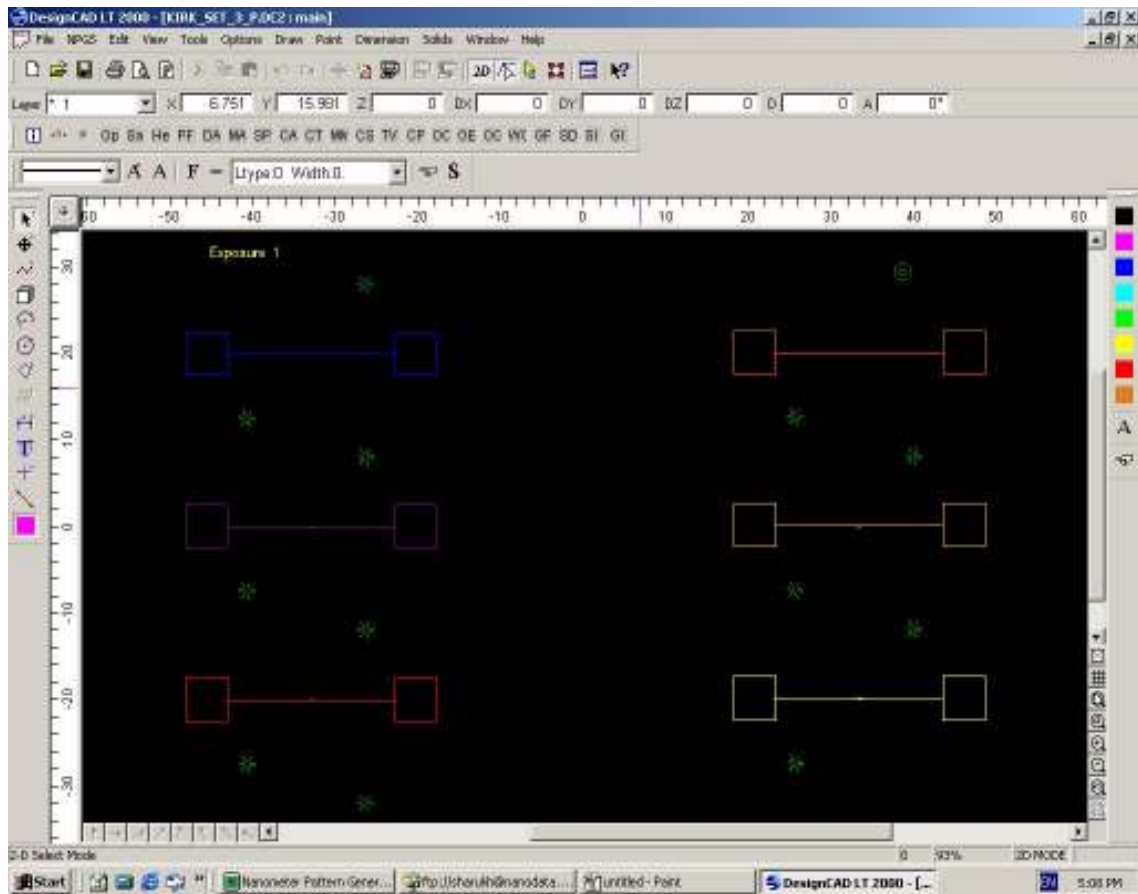
1cm x 1cm piece from a SOI wafer with 55nm single crystal silicon, 140nm silicon dioxide wafer, 2 microns of poly-crystalline silicon

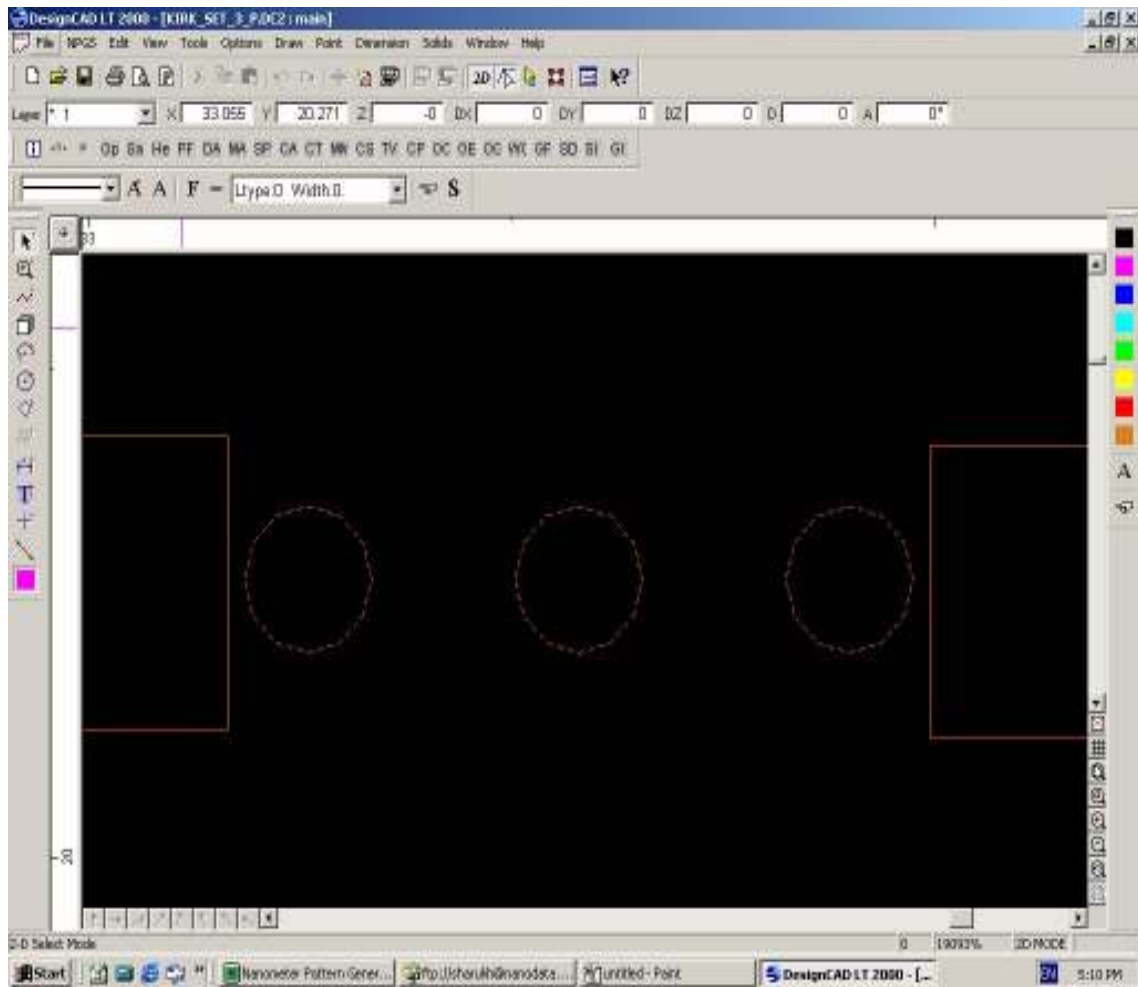
XR-1541 (containing 4% solids of HSQ) was used

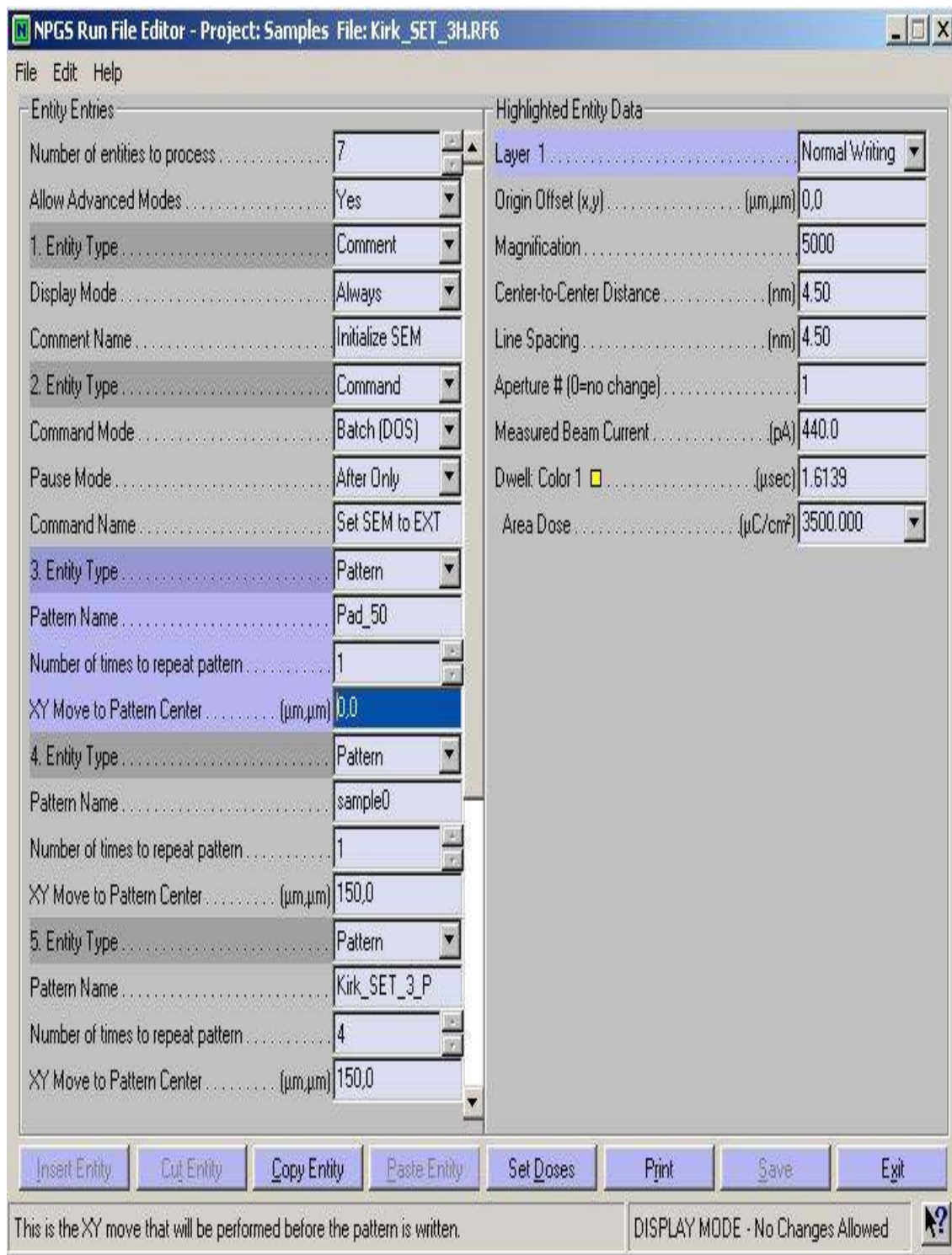
HSQ was spun on at 2000 rpm for 60 seconds

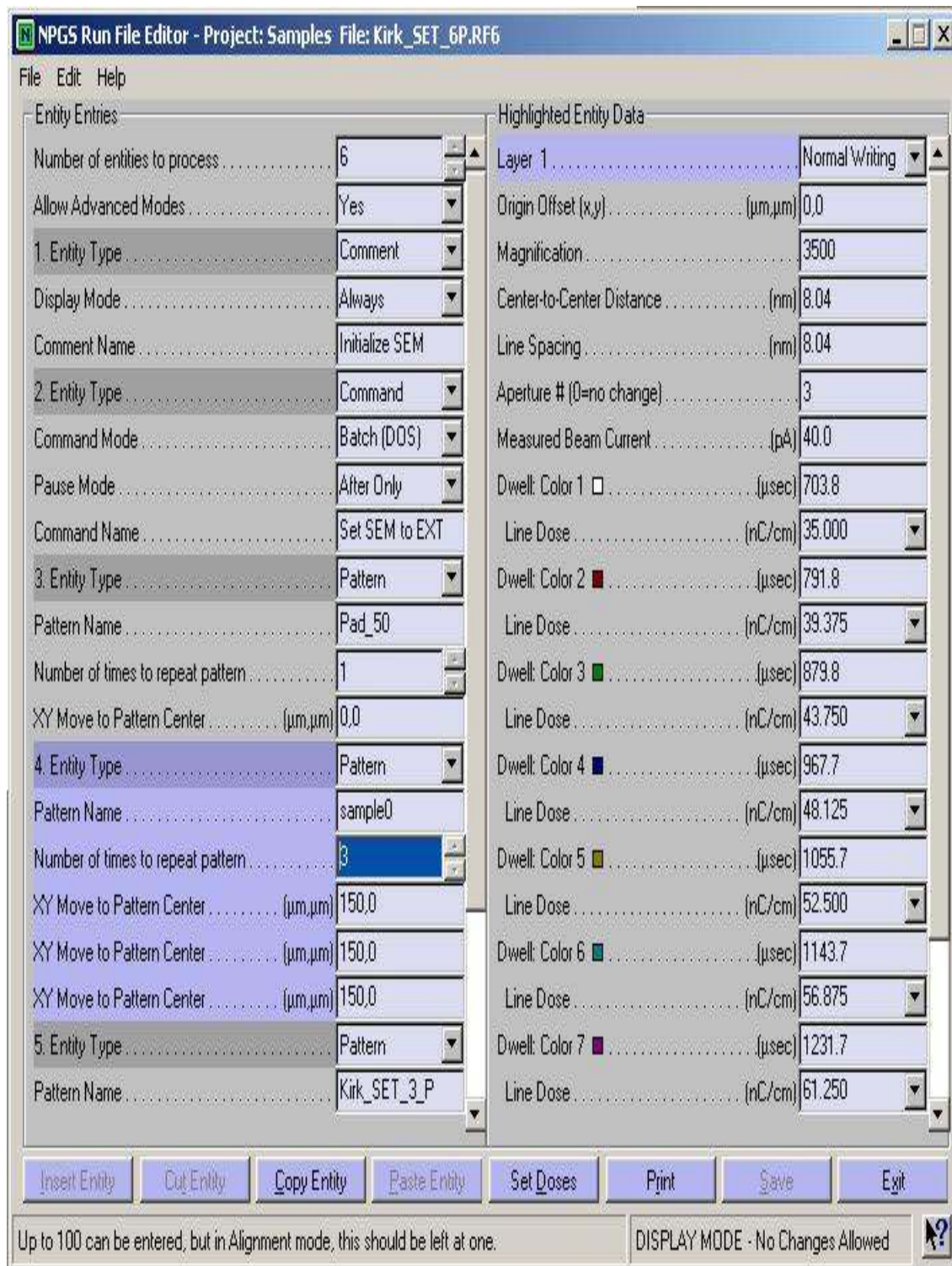
Pre-exposure bake 225°C for 120 seconds

E-beam parameters









NPGS Run File Editor - Project: Samples File: Kirk_SET_6P.RF6

File Edit Help

Entity Entries

Number of entities to process 6

Allow Advanced Modes Yes

1. Entity Type Comment

Display Mode Always

Comment Name Initialize SEM

2. Entity Type Command

Command Mode Batch (DOS)

Pause Mode After Only

Command Name Set SEM to EXT

3. Entity Type Pattern

Pattern Name Pad_50

Number of times to repeat pattern 1

XY Move to Pattern Center ($\mu\text{m}, \mu\text{m}$) 0,0

4. Entity Type Pattern

Pattern Name sample0

Number of times to repeat pattern 3

XY Move to Pattern Center ($\mu\text{m}, \mu\text{m}$) 150,0

XY Move to Pattern Center ($\mu\text{m}, \mu\text{m}$) 150,0

XY Move to Pattern Center ($\mu\text{m}, \mu\text{m}$) 150,0

5. Entity Type Pattern

Pattern Name Kirk_SET_3_P

Highlighted Entity Data

Line Spacing (nm) 8.04

Aperture # (0=no change) 3

Measured Beam Current (pA) 40.0

Dwell: Color 1 (μsec) 703.8

Line Dose (nC/cm) 35.000

Dwell: Color 2 (μsec) 791.8

Line Dose (nC/cm) 39.375

Dwell: Color 3 (μsec) 879.8

Line Dose (nC/cm) 43.750

Dwell: Color 4 (μsec) 967.7

Line Dose (nC/cm) 48.125

Dwell: Color 5 (μsec) 1055.7

Line Dose (nC/cm) 52.500

Dwell: Color 6 (μsec) 1143.7

Line Dose (nC/cm) 56.875

Dwell: Color 7 (μsec) 1231.7

Line Dose (nC/cm) 61.250

Dwell: Color 8 (μsec) 1319.6

Line Dose (nC/cm) 65.625

Dwell: Color 9 (μsec) 1407.6

Line Dose (nC/cm) 70.000

Insert Entity Cut Entity Copy Entity Paste Entity Set Doses Print Save Exit

Layer 1: Select the appropriate setting for each layer in the pattern. DISPLAY MODE - No Changes Allowed

NPGS Run File Editor - Project: Samples File: Kirk_SET_3H.RF6

File Edit Help

Entity Entries		Highlighted Entity Data	
3. Entity Type	Pattern	Layer 1	Normal Writing
Pattern Name	Pad_50	Origin Offset (x,y)	($\mu\text{m}, \mu\text{m}$) 0,0
Number of times to repeat pattern	1	Magnification	3000
XY Move to Pattern Center ($\mu\text{m}, \mu\text{m}$)	0,0	Center-to-Center Distance	(nm) 7.51
4. Entity Type	Pattern	Line Spacing	(nm) 7.51
Pattern Name	sample0	Aperture # (0=no change)	3
Number of times to repeat pattern	1	Measured Beam Current	(pA) 40.0
XY Move to Pattern Center ($\mu\text{m}, \mu\text{m}$)	150,0	Dwell: Color 1	(μsec) 93.84
5. Entity Type	Pattern	Line Dose	(nC/cm) 5,000
Pattern Name	Kirk_SET_3_P	Dwell: Color 2	(μsec) 93.84
Number of times to repeat pattern	4	Line Dose	(nC/cm) 5,000
XY Move to Pattern Center ($\mu\text{m}, \mu\text{m}$)	150,0	Dwell: Color 3	(μsec) 93.84
XY Move to Pattern Center ($\mu\text{m}, \mu\text{m}$)	150,0	Line Dose	(nC/cm) 5,000
XY Move to Pattern Center ($\mu\text{m}, \mu\text{m}$)	150,0	Dwell: Color 4	(μsec) 93.84
XY Move to Pattern Center ($\mu\text{m}, \mu\text{m}$)	150,0	Line Dose	(nC/cm) 5,000
6. Entity Type	Pattern	Dwell: Color 5	(μsec) 93.84
Pattern Name	P_Young_50um	Line Dose	(nC/cm) 5,000
Number of times to repeat pattern	1	Dwell: Color 6	(μsec) 93.84
XY Move to Pattern Center ($\mu\text{m}, \mu\text{m}$)	150,0	Line Dose	(nC/cm) 5,000
7. Entity Type	MoveOnly	Layer 2	Normal Writing
XY Move to Writing Field Center ($\mu\text{m}, \mu\text{m}$)	-900,500	Origin Offset (x,y)	($\mu\text{m}, \mu\text{m}$) 0,0

This is the XY move that will be performed before the pattern is written. DISPLAY MODE · No Changes Allowed



Development procedure

Post exposure bake at 225°C for 120 seconds.

300 MIF dip for 110 seconds

1:9 300 MIF and DI water rinse for 10 seconds

DI water dip for 10 seconds

Blow dry with Nitrogen

Baking conditions

Sample was baked in an inert atmosphere using the Blue M oven

Start at 25°C

Ramp from 25°C to 125°C in 15 minutes

Ramp from 125°C to 400°C in 15 minutes

Steady at 400°C for 30 minutes

From 400°C to 25°C at its own pace usually takes 2 hours 15 minutes

Seventh HSQ wafer

Wafer specifications

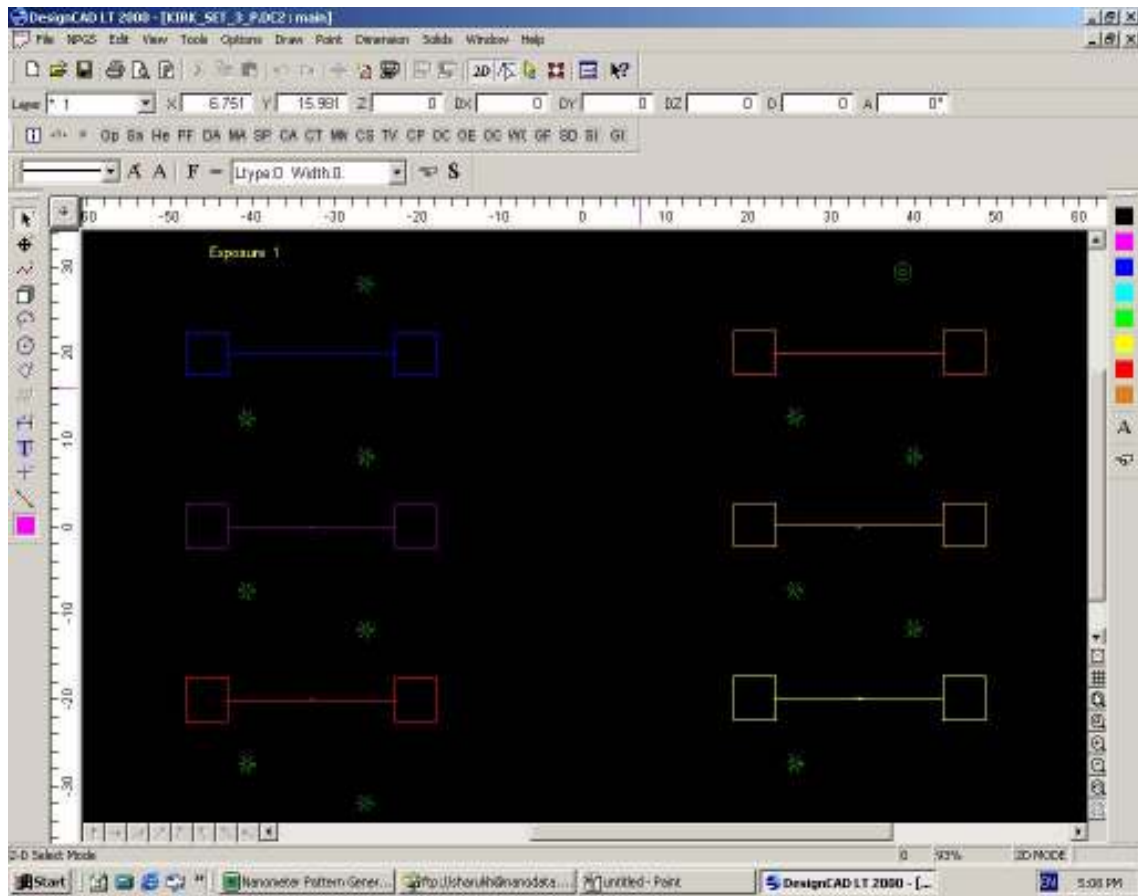
1cm x 1cm piece from a SOI wafer with 55nm single crystal silicon, 140nm silicon dioxide wafer, 2 microns nm of poly-crystalline silicon

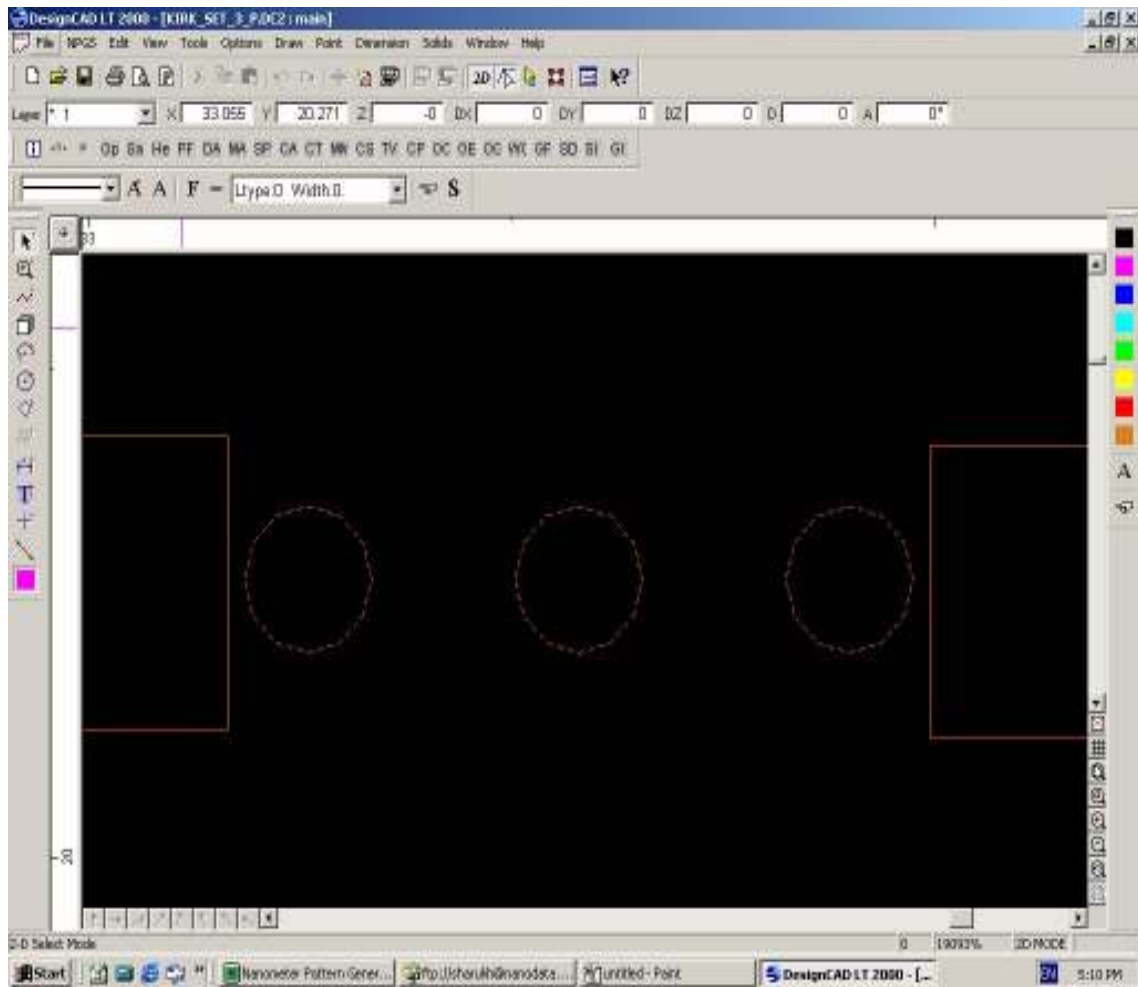
XR-1541 (containing 4% solids of HSQ) was used

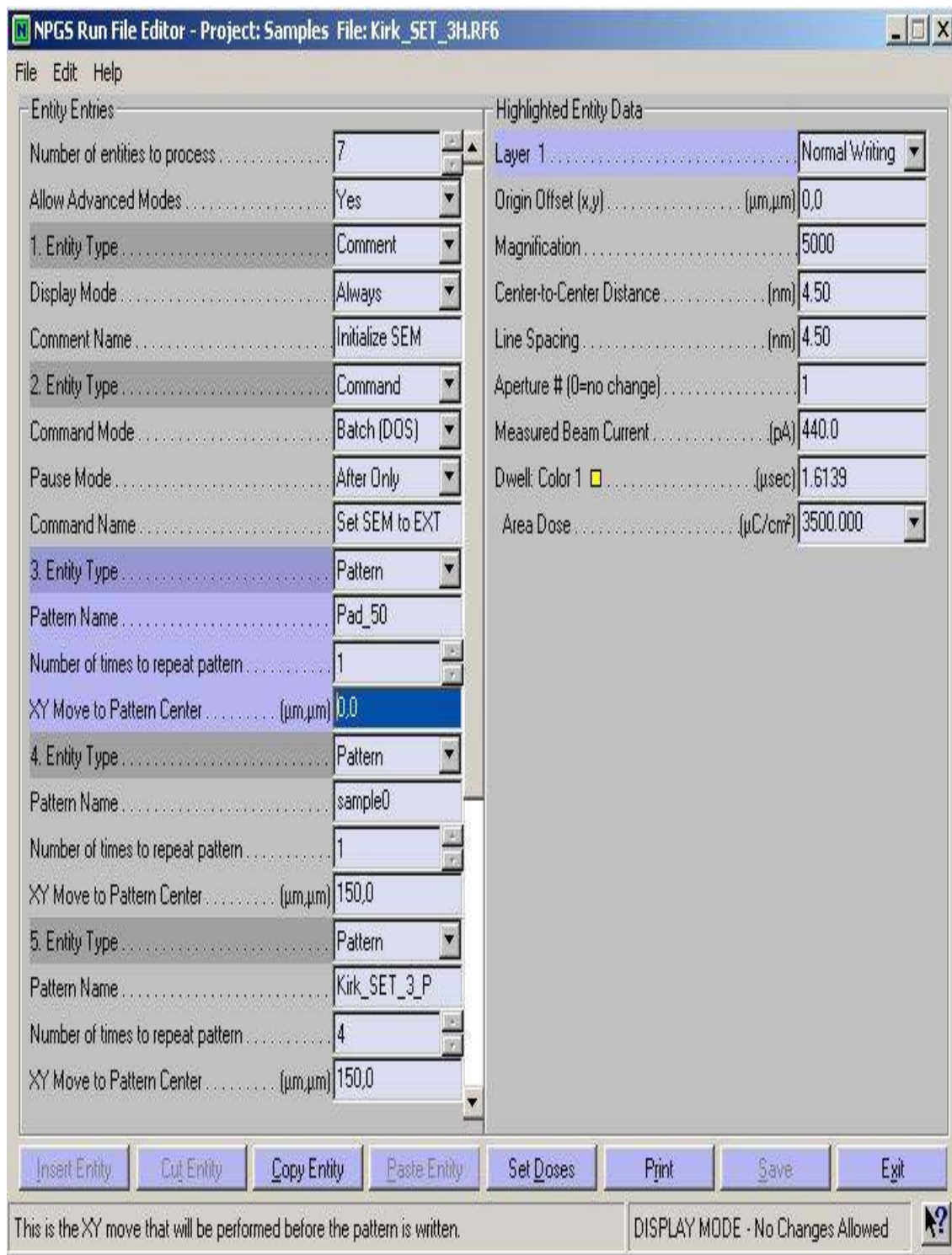
HSQ was spun on at 4000 rpm for 60 seconds

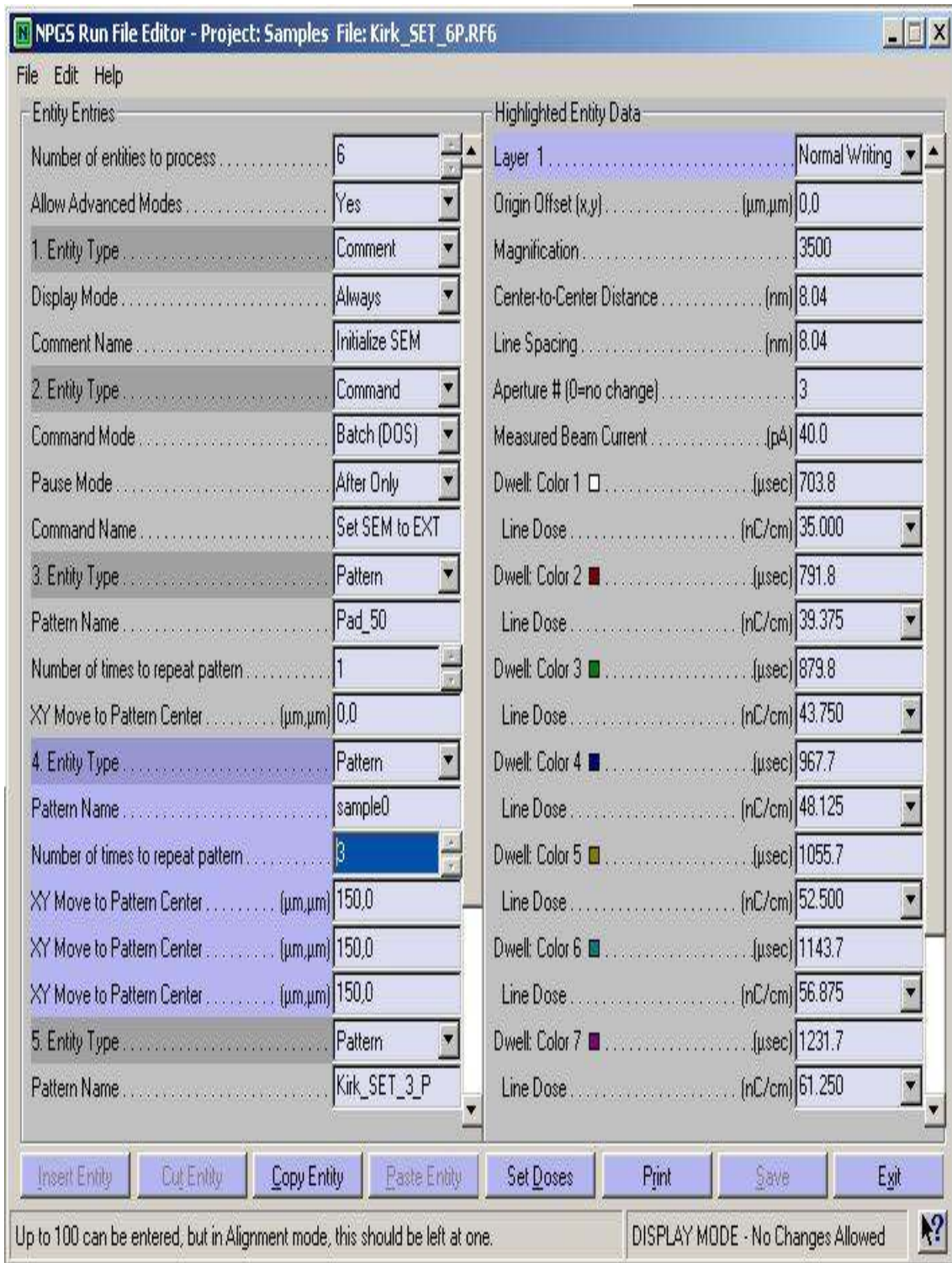
Pre-exposure bake 225°C for 120 seconds

E-beam parameters









NPGS Run File Editor - Project: Samples File: Kirk_SET_6P.RF6

File Edit Help

Entity Entries

Number of entities to process 6

Allow Advanced Modes Yes

1. Entity Type Comment

Display Mode Always

Comment Name Initialize SEM

2. Entity Type Command

Command Mode Batch (DOS)

Pause Mode After Only

Command Name Set SEM to EXT

3. Entity Type Pattern

Pattern Name Pad_50

Number of times to repeat pattern 1

XY Move to Pattern Center (μm,μm) 0,0

4. Entity Type Pattern

Pattern Name sample0

Number of times to repeat pattern 3

XY Move to Pattern Center (μm,μm) 150,0

XY Move to Pattern Center (μm,μm) 150,0

XY Move to Pattern Center (μm,μm) 150,0

5. Entity Type Pattern

Pattern Name Kirk_SET_3_P

Highlighted Entity Data

Line Spacing (nm) 8.04

Aperture # (0=no change) 3

Measured Beam Current (pA) 40.0

Dwell: Color 1 (μsec) 703.8

Line Dose (nC/cm) 35.000

Dwell: Color 2 (μsec) 791.8

Line Dose (nC/cm) 39.375

Dwell: Color 3 (μsec) 879.8

Line Dose (nC/cm) 43.750

Dwell: Color 4 (μsec) 967.7

Line Dose (nC/cm) 48.125

Dwell: Color 5 (μsec) 1055.7

Line Dose (nC/cm) 52.500

Dwell: Color 6 (μsec) 1143.7

Line Dose (nC/cm) 56.875

Dwell: Color 7 (μsec) 1231.7

Line Dose (nC/cm) 61.250

Dwell: Color 8 (μsec) 1319.6

Line Dose (nC/cm) 65.625

Dwell: Color 9 (μsec) 1407.6

Line Dose (nC/cm) 70.000

Insert Entity Cut Entity Copy Entity Paste Entity Set Doses Print Save Exit

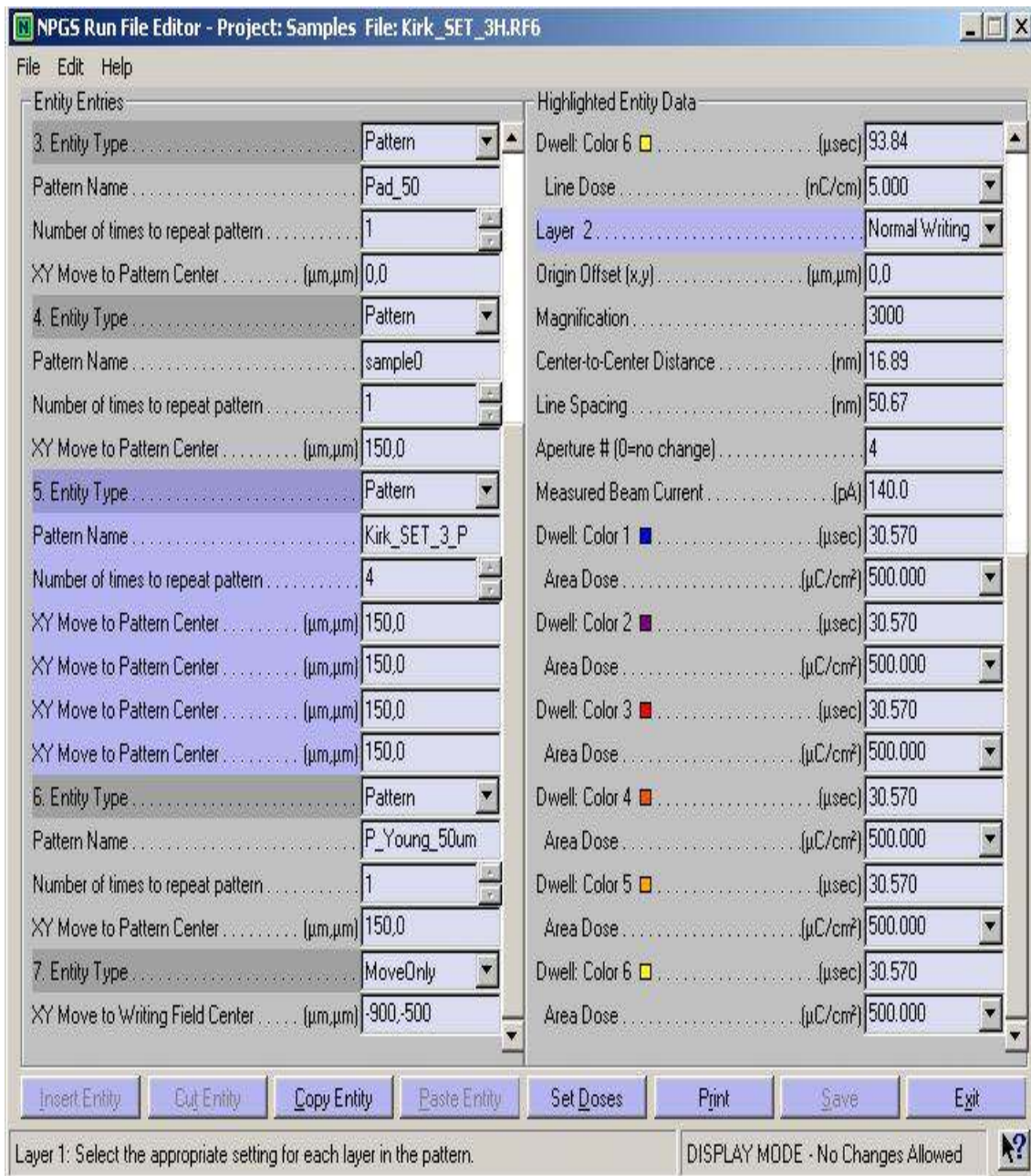
Layer 1: Select the appropriate setting for each layer in the pattern. DISPLAY MODE - No Changes Allowed

NPGS Run File Editor - Project: Samples File: Kirk_SET_3H.RF6

File Edit Help

Entity Entries		Highlighted Entity Data	
3. Entity Type	Pattern	Layer 1	Normal Writing
Pattern Name	Pad_50	Origin Offset (x,y)	($\mu\text{m}, \mu\text{m}$) 0,0
Number of times to repeat pattern	1	Magnification	3000
XY Move to Pattern Center ($\mu\text{m}, \mu\text{m}$)	0,0	Center-to-Center Distance	(nm) 7.51
4. Entity Type	Pattern	Line Spacing	(nm) 7.51
Pattern Name	sample0	Aperture # (0=no change)	3
Number of times to repeat pattern	1	Measured Beam Current	(pA) 40.0
XY Move to Pattern Center ($\mu\text{m}, \mu\text{m}$)	150,0	Dwell: Color 1	(μsec) 93.84
5. Entity Type	Pattern	Line Dose	(nC/cm) 5,000
Pattern Name	Kirk_SET_3_P	Dwell: Color 2	(μsec) 93.84
Number of times to repeat pattern	4	Line Dose	(nC/cm) 5,000
XY Move to Pattern Center ($\mu\text{m}, \mu\text{m}$)	150,0	Dwell: Color 3	(μsec) 93.84
XY Move to Pattern Center ($\mu\text{m}, \mu\text{m}$)	150,0	Line Dose	(nC/cm) 5,000
XY Move to Pattern Center ($\mu\text{m}, \mu\text{m}$)	150,0	Dwell: Color 4	(μsec) 93.84
XY Move to Pattern Center ($\mu\text{m}, \mu\text{m}$)	150,0	Line Dose	(nC/cm) 5,000
6. Entity Type	Pattern	Dwell: Color 5	(μsec) 93.84
Pattern Name	P_Young_50um	Line Dose	(nC/cm) 5,000
Number of times to repeat pattern	1	Dwell: Color 6	(μsec) 93.84
XY Move to Pattern Center ($\mu\text{m}, \mu\text{m}$)	150,0	Line Dose	(nC/cm) 5,000
7. Entity Type	MoveOnly	Layer 2	Normal Writing
XY Move to Writing Field Center ($\mu\text{m}, \mu\text{m}$)	-900,500	Origin Offset (x,y)	($\mu\text{m}, \mu\text{m}$) 0,0

This is the XY move that will be performed before the pattern is written. DISPLAY MODE · No Changes Allowed



Development procedure

Post exposure bake at 225°C for 120 seconds.

300 MIF dip for 90 seconds

1:9 300 MIF and DI water rinse for 10 seconds

DI water dip for 10 seconds

Blow dry with Nitrogen

Eighth HSQ wafer (first one with the new pattern)

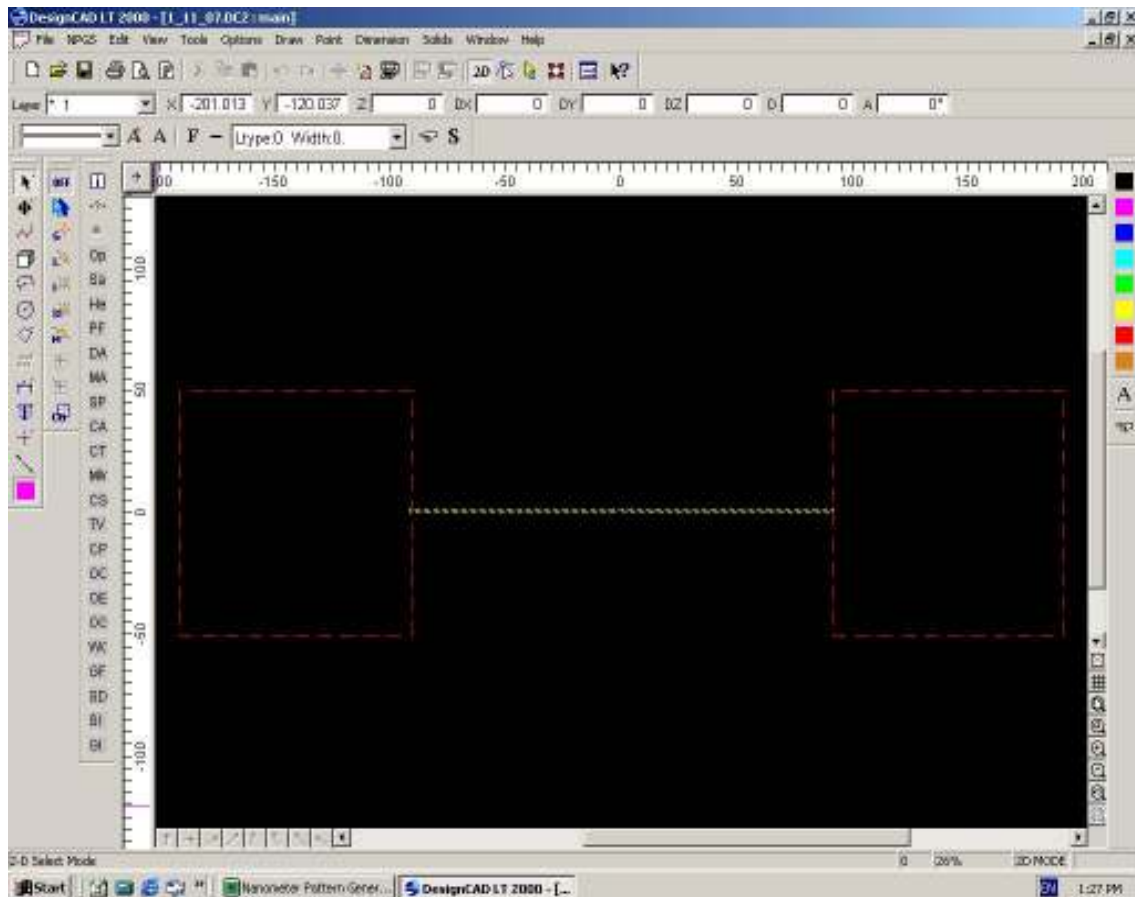
Wafer specifications

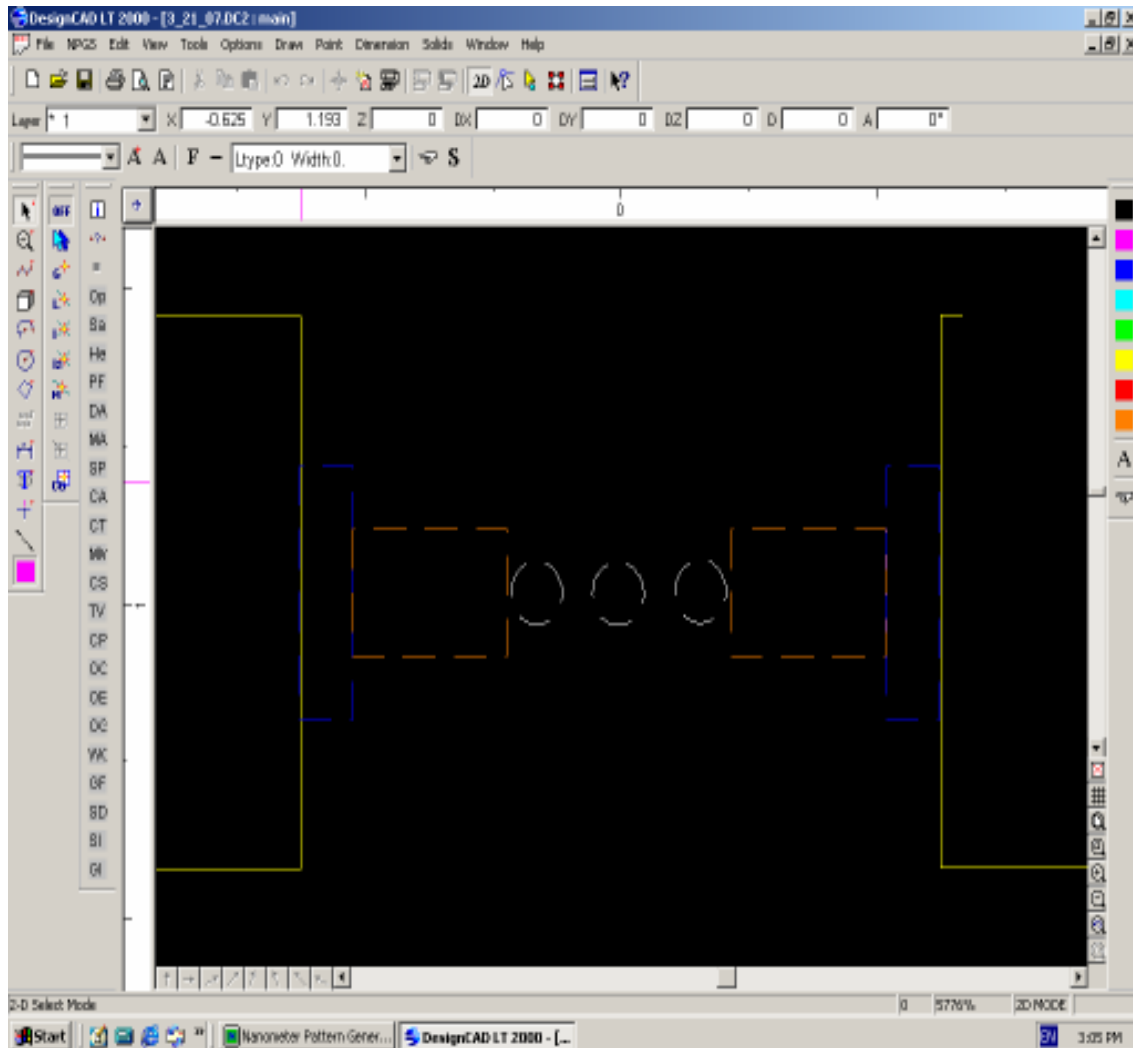
1cm x 1cm piece from a SOI wafer with 55nm single crystal silicon, 140nm silicon dioxide wafer, 2 microns of poly-crystalline silicon

HSQ was spun on at 2000 rpm for 60 seconds

Pre-exposure bake 225°C for 2 minutes

E-beam parameters (the design file remains the same for all exposures henceforth)





For all the patterns the layer 2 (100 micron pads) parameters were constant

Layer 2

Magnification.....850

Center-to-centre distance.....46.37nm

Line spacing.....46.37nm

Aperture #.....4(20 micron)

Measured beam current.....140pA

Dwell (red).....46.073 μ sec

Area dose.....3000 μ C/cm²

Pattern #1

Layer 1

Magnification.....1800

Center-to-centre distance.....6.26nm

Line spacing.....6.26nm

Aperture #.....3(10 micron)

Measured beam current.....41.3pA

Area dose.....3000 μ C/cm² for every element of the layer

Development procedure

Post exposure bake for 225°C for 2 minutes.

300 MIF dip for 120 seconds

1:9 300 MIF and DI water dip for 10 seconds

DI water dip for 10 seconds

Blow dry with Nitrogen

Ninth HSQ wafer

Wafer specifications

1cm x 1cm piece from a SOI wafer with 55nm single crystal silicon, 140nm silicon

dioxide wafer, 2 microns of poly-crystalline silicon

HSQ was spun on at 3000 rpm for 30 seconds

Pre-exposure bake 150°C for 1 minute

E-beam parameters

For all the patterns the layer 2 (100 micron pads) parameters were constant

Layer 2

Magnification.....850

Center-to-centre distance.....46.37nm

Line spacing.....46.37nm

Aperture #.....4(20 micron)

Measured beam current.....140pA

Dwell (red).....46.073μsec

Area dose.....300μC/cm²

Pattern #1

Layer 1

Magnification.....1800

Center-to-centre distance.....6.26nm

Line spacing.....6.26nm

Aperture #.....3(10 micron)

Measured beam current.....41.3pA

Area dose.....50μC/cm² for every element of the layer

Pattern #2

Layer 1

Magnification.....1800

Center-to-centre distance.....6.26nm

Line spacing.....6.26nm

Aperture #.....3(10 micron)

Measured beam current.....41.3pA

Area dose.....200 $\mu\text{C}/\text{cm}^2$ for every element of the layer

Pattern #3

Layer 1

Magnification.....1800

Center-to-centre distance.....6.26nm

Line spacing.....6.26nm

Aperture #.....3(10 micron)

Measured beam current.....41.3pA

Area dose.....600 $\mu\text{C}/\text{cm}^2$ for every element of the layer

Pattern #4

Layer 1

Magnification.....1800

Center-to-centre distance.....6.26nm

Line spacing.....6.26nm

Aperture #.....3(10 micron)

Measured beam current.....41.3pA

Area dose.....2000 $\mu\text{C}/\text{cm}^2$ for every element of the layer

Development procedure

No post exposure bake

Developed roughly 21 hours after exposure.

MIF300 dip for 70 seconds

1:9 MIF300 and DI water dip for 10 seconds

DI water dip for 10 seconds

Blow dry with Nitrogen

Tenth HSQ wafer

Wafer specifications

1cm x 1cm piece from a SOI wafer with 55nm single crystal silicon, 140nm silicon dioxide wafer, 2 microns of poly-crystalline silicon

HSQ was spun on at 3000 rpm for 30 seconds

Pre-exposure bake 125°C for 1 minute

E-beam parameters

For all the patterns the layer 2 (100 micron pads) parameters were constant

Layer 2

Magnification.....850

Center-to-centre distance.....46.37nm

Line spacing.....46.37nm

Aperture #.....4(20 micron)

Measured beam current.....140pA

Dwell (red).....46.073μsec

Area dose.....300μC/cm²

Pattern #1

Layer 1

Magnification.....1800

Center-to-centre distance.....6.26nm

Line spacing.....6.26nm

Aperture #.....3(10 micron)

Measured beam current.....41.3pA

Dwell (white).....2.834μsec

Area dose.....300μC/cm²

Dwell (blue).....2.834μsec

Area dose.....300μC/cm²

Dwell (yellow).....2.834μsec

Area dose.....300μC/cm²

Dwell (orange).....2.834μsec

Area dose.....300μC/cm²

Pattern #2

Layer 1

Magnification.....1800

Center-to-centre distance.....6.26nm

Line spacing.....6.26nm

Aperture #.....3(10 micron)

Measured beam current.....41.3pA

Dwell (white).....4.7384μsec

Area dose.....500 μ C/cm²

Dwell (blue).....4.7384 μ sec

Area dose.....500 μ C/cm²

Dwell (yellow).....4.7384 μ sec

Area dose.....500 μ C/cm²

Dwell (orange).....4.7384 μ sec

Area dose.....500 μ C/cm²

Development procedure

No post exposure bake

Spin developed with the wafer spinning at 1000 rpm for 60 seconds.

Eleventh HSQ wafer

Wafer specifications

1cm x 1cm piece from a SOI wafer with 55nm single crystal silicon, 140nm silicon dioxide wafer, 2 microns of poly-crystalline silicon

HSQ was spun on at 3000 rpm for 30 seconds

Pre-exposure bake 125°C for 1 minute

E-beam parameters

For all the patterns the layer 2 (100 micron pads) parameters were constant

Layer 2

Magnification.....850

Center-to-centre distance.....46.37nm

Line spacing.....46.37nm

Aperture #.....4(20 micron)

Measured beam current.....140pA

Dwell (red).....46.073μsec

Area dose.....300μC/cm²

Pattern #1

Layer 1

Magnification.....1800

Center-to-centre distance.....6.26nm

Line spacing.....6.26nm

Aperture #.....3(10 micron)

Measured beam current.....41.3pA

Dwell (white).....5.686μsec

Area dose.....600μC/cm²

Dwell (blue).....4.7384μsec

Area dose.....500μC/cm²

Dwell (yellow).....2.843μsec

Area dose.....300μC/cm²

Dwell (orange).....4.7384μsec

Area dose.....500μC/cm²

Development procedure

Post exposure bake 128°C for 1 minute

Spin developed with the wafer spinning at 1000 rpm for 35 seconds and a constant

spray of MIF300. Allowed to spin at 1000 rpm for another 25 seconds without MIF300.

Baking procedure

Start at 25°C

Ramp from 25°C to 125°C in 15 minutes

Ramp from 125°C to 400°C in 15 minutes

Steady at 400°C for 1 hour

From 400°C to 25°C at its own pace usually takes 2 hours 15 minutes

Twelfth HSQ wafer

Wafer specifications

1cm x 1cm piece from a SOI wafer with 55nm single crystal silicon, 140nm silicon dioxide wafer, 2 microns of poly-crystalline silicon

HSQ was spun on at 3000 rpm for 30 seconds

Pre-exposure bake 125°C for 1 minute

E-beam parameters

For all the patterns the layer 2 (100 micron pads) parameters were constant

Layer 2

Magnification.....850

Center-to-centre distance.....46.37nm

Line spacing.....46.37nm

Aperture #.....4(20 micron)

Measured beam current.....140pA

Dwell (red).....46.073 μ sec
Area dose.....300 μ C/cm²
Pattern #1
Layer 1
Magnification.....1800
Center-to-centre distance.....6.26nm
Line spacing.....6.26nm
Aperture #.....3(10 micron)
Measured beam current.....41.3pA
Dwell (white).....3.7097 μ sec
Area dose.....400 μ C/cm²
Dwell (blue).....3.7097 μ sec
Area dose.....400 μ C/cm²
Dwell (yellow).....3.7097 μ sec
Area dose.....400 μ C/cm²
Dwell (orange).....3.7097 μ sec
Area dose.....400 μ C/cm²
Pattern #2
Layer 1
Magnification.....1800
Center-to-centre distance.....6.26nm
Line spacing.....6.26nm

Aperture #.....3(10 micron)
Measured beam current.....41.3pA
Dwell (white).....5.7097μsec
Area dose.....610μC/cm²
Dwell (blue).....4.7567μsec
Area dose.....510μC/cm²
Dwell (yellow).....2.8570μsec
Area dose.....310μC/cm²
Dwell (orange).....4.7567μsec
Area dose.....510μC/cm²
Pattern #3
Layer 1
Magnification.....1800
Center-to-centre distance.....6.26nm
Line spacing.....6.26nm
Aperture #.....3(10 micron)
Measured beam current.....41.3pA
Dwell (white).....5.7097μsec
Area dose.....610μC/cm²
Dwell (blue).....4.7567μsec
Area dose.....510μC/cm²
Dwell (yellow).....2.8570μsec

Area dose.....310 $\mu\text{C}/\text{cm}^2$
Dwell (orange).....4.7567 μsec
Area dose.....510 $\mu\text{C}/\text{cm}^2$
Pattern #4
Layer 1
Magnification.....1800
Center-to-centre distance.....6.26nm
Line spacing.....6.26nm
Aperture #.....3(10 micron)
Measured beam current.....41.3pA
Dwell (white).....7.581 μsec
Area dose.....800 $\mu\text{C}/\text{cm}^2$
Dwell (blue).....7.581 μsec
Area dose.....800 $\mu\text{C}/\text{cm}^2$
Dwell (yellow).....7.581 μsec
Area dose.....800 $\mu\text{C}/\text{cm}^2$
Dwell (orange).....7.581 μsec
Area dose.....800 $\mu\text{C}/\text{cm}^2$
Pattern #5
Layer 1
Magnification.....1800
Center-to-centre distance.....6.26nm

Line spacing.....6.26nm

Aperture #.....3(10 micron)

Measured beam current.....41.3pA

Dwell (white).....4.7384 μ sec

Area dose.....500 μ C/cm²

Dwell (blue).....4.265 μ sec

Area dose.....450 μ C/cm²

Dwell (yellow).....2.8430 μ sec

Area dose.....300 μ C/cm²

Dwell (orange).....4.265 μ sec

Area dose.....500 μ C/cm²

Development procedure

Post exposure bake 150°c for 1 minute

Spin developed with the wafer spinning at 1000 rpm for 40 seconds and a constant spray of MIF300. Allowed to spin at 1000 rpm for another 20 seconds without MIF300.

Baking procedure

Start at 25°C

Ramp from 25°C to 125°C in 15 minutes

Ramp from 125°C to 400°C in 15 minutes

Steady at 400°C for 4 hours

From 400°C to 25°C at its own pace usually takes 2 hours 15 minutes

APPENDIX D

ETCHING RECEIPES

First PMMA test

Wafer specifications

A wafer with PMMA spun on at 4000 rpm and patterned with the same parameters mentioned under the fifth PMMA wafer in Appendix B.

Etching equipment

Technics Micro-RIE

Test conditions

Flow rates

$CF_4 = 30$ sccm

$O_2 = 6$ sccm

Power = 100 Watts

Base Pressure = 27 mTorr

Pressure with gas flow = 197 mTorr

Pressure during etch = 247 mTorr

Etch time = 30 minutes

Second PMMA test

Wafer specifications

A wafer with PMMA spun on at 4000 rpm and only a 50 micron pad patterned with an exposure dose of 50000 nC/cm²

Etching equipment

Technics Micro-RIE

Test conditions

Flow rates

$\text{CF}_4 = 30 \text{ sccm}$

$\text{O}_2 = \text{Not used}$

Power = 50 Watts

Base Pressure = 28 mTorr

Pressure with gas flow = 151 mTorr

Pressure during etch = 191 mTorr

Etch time = 30 seconds

Third PMMA test

Wafer specifications

A wafer with PMMA spun on at 4000 rpm and only a 50 micron pad patterned with an exposure dose of 50000 nC/cm^2

Etching equipment

Technics Micro-RIE

Test conditions

Flow rates

$\text{CF}_4 = 30 \text{ sccm}$

$\text{O}_2 = 3 \text{ sccm}$

Power = 50 Watts

Base Pressure = 27 mTorr

Pressure with gas flow = 189 mTorr

Pressure during etch = 225 mTorr

Etch time = 30 seconds

PMMA and Al test

Wafer specifications

A poly-Si wafer with p-type doping was chosen

62.8 nm of Aluminum was evaporated on the top surface of the wafer

PMMA spun on at 2000 rpm for 60 seconds

Only a 50 micron pad patterned with an exposure dose of $50000\text{nC}/\text{cm}^2$

Developed in acetone for 2.5 minutes and then an Isopropyl alcohol rinse for 60 seconds

A wet etch was conducted for Aluminum using an Aluminum etchant dip at 40°C for 10 seconds

Etching equipment

Technics Micro-RIE

Test conditions

Flow rates

$\text{CF}_4 = 10 \text{ sccm}$

$\text{O}_2 = \text{Not used}$

Power = 100 Watts

Base Pressure = 27 mTorr

Pressure with gas flow = varied around 110 mTorr

Pressure during etch = varied around 125 mTorr

Etch time = 2 minutes + 5 minutes + 5 minutes

Remaining Al was then removed by another dip in the Aluminum etchant

UVN30 test

Wafer specifications

The wafer named sixth UVN30 wafer in Appendix A was used

Etching equipment

Technics Micro-RIE

Test conditions

Flow rates

$CF_4 = 30$ sccm

$O_2 = 6$ sccm

Power = 100 Watts

Base Pressure = 29 mTorr

Pressure with gas flow = 204 mTorr

Pressure during etch = 257 mTorr

Etch time = 3 minutes

First HSQ test

Wafer specifications

The wafer named second HSQ wafer in Appendix C was used

Etching equipment

Technics Micro-RIE

Test conditions

Flow rates

CF₄ = 10 sccm

O₂ = not used

Power = 100 Watts

Base Pressure = 27 mTorr

Pressure with gas flow = 134 mTorr

Pressure during etch = 153 mTorr

Etch time = 1 minute

First HSQ and Al test

Wafer specifications

The wafer named first HSQ and Al wafer in Appendix C was used

Etching equipment

Technics Micro-RIE

Test conditions

Flow rates

CF₄ = 10 sccm

O₂ = Not used

Power = 100 Watts

Base Pressure = 27 mTorr

Pressure with gas flow = 138 mTorr

Pressure during etch = 155 mTorr

Etch time = 1 minute

Second HSQ test

Wafer specifications

The wafer named third HSQ wafer in Appendix C was used

Etching equipment

Technics Micro-RIE

Test conditions

Flow rates

$\text{CF}_4 = 7 \text{ sccm}$

$\text{O}_2 = \text{not used}$

Power = 75 Watts

Base Pressure = 25 mTorr

Pressure with gas flow = 126 mTorr

Pressure during etch = 141 mTorr

Etch time = 1 minute

Third HSQ test

Wafer specifications

The wafer named sixth HSQ wafer in Appendix C was used

Etching equipment

Technics Micro-RIE

Test conditions

Flow rates

$\text{CF}_4 = 10 \text{ sccm}$

$\text{O}_2 = \text{not used}$

Power = 100 Watts

Base Pressure = 50 mTorr

Pressure with gas flow = 164 mTorr

Pressure during etch = 222 mTorr

Etch time = 1 minute

Fourth HSQ test

Wafer specifications

The wafer named twelfth HSQ wafer in Appendix C was used

Etching equipment

Trion Technology DRIE

Test conditions

Etch #1

This is a three step process

Step #1 (This is to introduce gasses and then equalize the pressure)

Flow rates

$\text{CF}_4 = 0$ sccm

$\text{O}_2 = 10$ sccm

$\text{SF}_6 = 20$ sccm

Ar = 200 sccm

He = 200 sccm

Pressure = 50 mtorr

He Pressure = 5 mtorr

ICP power = 0 Watts

Power given to the bottom electrode = 0 Watts

Time = 10 secs

Step #2 (The etching step)

Flow rates

$\text{CF}_4 = 0$ sccm

$\text{O}_2 = 10$ sccm

$\text{SF}_6 = 20$ sccm

Ar = 200 sccm

He = 200 sccm

Pressure = 50 mtorr

He Pressure = 5 mtorr

ICP power = 0 Watts

Power given to the bottom electrode = 100 Watts

Time = 60 secs

Step #3 (The gasses are removed from the chamber)

Flow rates

$\text{CF}_4 = 0$ sccm

$\text{O}_2 = 0$ sccm

$\text{SF}_6 = 0$ sccm

Ar = 0 sccm

He = 100 sccm

Pressure = 0 mtorr

He Pressure = 5 mtorr

ICP power = 0 Watts

Power given to the bottom electrode = 0 Watts

Time = 20 secs

Etch #2

Step #1 (This is to introduce gasses and then equalize the pressure)

Flow rates

$\text{CF}_4 = 0$ sccm

$\text{O}_2 = 10$ sccm

$\text{SF}_6 = 20$ sccm

Ar = 200 sccm

He = 200 sccm

Pressure = 50 mtorr

He Pressure = 5 mtorr

ICP power = 0 Watts

Power given to the bottom electrode = 0 Watts

Time = 10 secs

Step #2 (The etching step)

Flow rates

$\text{CF}_4 = 0$ sccm

$\text{O}_2 = 10$ sccm

SF₆ = 20 sccm

Ar = 200 sccm

He = 200 sccm

Pressure = 50 mtorr

He Pressure = 5 mtorr

ICP power = 0 Watts

Power given to the bottom electrode = 100 Watts

Time = 20 secs

Step #3 (The gasses are removed from the chamber)

Flow rates

CF₄ = 0 sccm

O₂ = 0 sccm

SF₆ = 0 sccm

Ar = 0 sccm

He = 100 sccm

Pressure = 0 mtorr

He Pressure = 5 mtorr

ICP power = 0 Watts

Power given to the bottom electrode = 0 Watts

Time = 20 secs

REFERENCES

- [1] G. E. Moore, "Cramming More Components onto Integrated Circuits", Proceedings of the IEEE, Vol. 86, No. 1, January 1998, pp. 82-85.
- [2] K. K. Likharev, "Single-electron devices and Their Applications", Proceedings of the IEEE, Vol. 87, No. 4, April 1999, pp. 606-632.
- [3] L. Esaki, "New phenomenon in Narrow Germanium p-n Junctions", Physical Review, Vol. 109, Issue 2, January 1958, pp. 602-603.
- [4] K. Okhura, T. Kitade and A. Nakajima, "Periodic Coulomb oscillations in Si single-electron transistor based on multiple islands", Journal of Applied Physics, Vol. 98, Issue 12, December 2005, pp. 124503 (6 pages).
- [5] R. Waser, "Nanoelectronics and Information Technology", Wiley-VCH, Second edition, 2005.
- [6] D. J. Thouless, "Maximum Metallic Resistance in Thin Wires", Physical Review Letters, Vol. 39, No. 18, October 1977, pp. 1167-1169.
- [7] L. P. Kouwenhoven, T. H. Oosterkamp, M. W. S. Danoesastro, M. Eto, D. G. Austing, T. Honda and S. Tarucha "Excitation Spectra of Circular, Few-Electron Quantum Dots", Science, Vol. 278, No. 5344, December 1997, pp. 1788-1792.
- [8] H. R. Zeller and I. Giaver, "Tunneling, Zero-Bias Anamolies, and Small Superconductors", Physical Review , Vol. 181, No. 2, May 1969, pp. 789-800.

- [9] K. K. Likharev, "Correlated Discrete Transfer of Single Electrons in Ultrasmall Tunnel Junctions", IBM Journal of Research and Development, Vol. 32, No. 1, January 1988, pp. 144-158.
- [10] T. A. Fulton and G. J. Dolan, "Observation of Single-electron Charging effects in Small Tunnel Junctions", Physical Review Letters, Vol. 59, No. 1, July 1987, pp. 109-112.
- [11] J. H. F. Scott-Thomas, S. B. Field, M. A. Kastner, H. I. Smith and D. A. Antoniadis, "Conductance Oscillations Periodic in the Density of a One-Dimensional Electron Gas", Physical Review Letters, Vol. 62, No. 5, January 1989, pp. 583-586.
- [12] <http://jcnabity.com/sysdec.htm>
- [13] UVN30 datasheet
- [14] A. C. F. Hoole, M. E. Welland and A. N. Broers, "Negative PMMA as a high-resolution-the limits and possibilities", Semiconductor Science and Technology, Vol. 12, June 1997, pp. 1166-1170.
- [15] H. Namatsu, T. Yamaguchi, M. Nagase, K. Yamakazi and K. Kurihara, "Nano-Patterning of a Hydrogen Silsesquioxane Resist with Reduced Linewidth Fluctuations", Microelectronic Engineering, Vol. 41-42, March 1998, pp. 331-334.
- [16] H. Namatsu, T. Yamaguchi, M. Nagase, K. Yamakazi and K. Kurihara, "Three-dimensional Siloxane Resist for the Formation of Nanopatterns with Minimum Linewidth Fluctuations", Journal of Vacuum Science and Technology B, Vol. 16, Issue 1, January 1998, pp. 69-76.

- [17] H. Namatsu, "Supercritical Resist Drying for Isolated Nanoline Formation", *Journal of Vacuum Science and Technology B*, Vol. 19, Issue 6, September 2001, pp. 2709-2712.
- [18] L. O'Faolain, M. V. Kotlyar, N. Tripathi, R. Wilson and T. F. Krauss, "Fabrication of Photonic Crystals using a spin-coated silsesquioxane hard mask", *Journal of Vacuum Science and Technology B*, Vol. 24, Issue 1, January 2006, pp. 336-339.
- [19] J. K. W. Yang, V. Anant and K. K. Berggren, "Enhancing Etch Resistance of Hydrogen Silsesquioxane via Postdevelop Electron Curing", *Journal of Vacuum Science and Technology B*, Vol. 24, Issue 6, November 2006, pp. 3157-3161.
- [20] F. C. M. J. M. van Delft, "Delay-time and Aging Effects on Contrast and Sensitivity of Hydrogen Silsesquioxane", *Journal of Vacuum Science and Technology B*, Vol. 20, Issue 6, November 2002, pp. 2932-2936.
- [21] W.-C. Liu, C.-C. Yang, W.-C. Chen, B.-T. Dai and M.-S. Tsai, "The Structural Transformation and Properties of Spin-on Poly(silsesquioxane) Films by Thermal Curing", *Journal of Non-Crystalline Solids*, Vol. 311, 2002, pp. 233-240.
- [22] H.-C. Liou, J. Pretzer, "Effect of curing temperature on the mechanical properties of hydrogen silsesquioxane thin films", *Thin Solid Films*, Vol. 335, 1998, pp. 186-191.
- [23] S.-J. Park, J. A. Liddle, A. Persaud, F.I. Allen, T. Schenkel and J. Bokor, "Formation of 15 nm scale Coulomb Blockade Oscillation Structures by Electron Beam Lithography with a Bilayer Resist Process", *Journal of Vacuum Science and Technology B*, Vol. 22, Issue 6, November 2004, pp. 3115-3118.

- [24] S. F. Hu, G. J. Hwang, Y. P. Fang, Z. Y. Pan and Y. C. Chou, "A simple method for Fabricating a Si-based Single Electron Transistor", Chinese Journal of Physics, Vol. 42, No. 5, October 2004, pp. 636-642.
- [25] J. R. Tucker, "Complementary Digital Logic based on the Coulomb Blockade", Journal of Applied Physics, Vol. 72, Issue 9, November 1992, pp. 4399-4413.
- [26] K. Nakazato, R. J. Blaikie and H. Ahmed, "Single-electron Memory", Journal of Applied Physics, Vol. 75, Issue 10, May 1995, pp. 5123-5134.
- [27] Y. Takahashi, M. Nagase, H. Namatsu, K. Kurihara, K. Iwdate, Y. Nakajima, s. Horiguchi, K. Murase and M. Tabe, "Fabrication Technique for Si Single-electron Transistor Operating at Room Temperature", Electronics Letters, Vol. 31, No. 2, January 1995, pp. 136-137.

BIOGRAPHICAL INFORMATION

Sharukh Roomy Chinoy was born on December 21, 1982 in Mumbai, India. He completed his Bachelors in Electronics Engineering from the University of Mumbai. He is pursuing a Masters in Electrical Engineering with an emphasis of nanoelectronics and quantum electronic devices at the University of Texas at Arlington. His plans are to pursue a career in the semiconductor industry.